

The effects of alpha-synuclein gain-of-function on synaptic plasticity

Dissertation
zur Erlangung des Doktorgrades
der Naturwissenschaften

vorgelegt beim Fachbereich Biowissenschaften
der Johann Wolfgang Goethe-Universität
in Frankfurt am Main

von

Nadine Brehm

*01.12.1985 Wiesbaden

Frankfurt 2015

(D 30)

vom Fachbereich Biowissenschaften der
Johann Wolfgang Goethe-Universität als Dissertation angenommen.

Dekan: Prof. Dr. Meike Piepenbring

Gutachter: Prof. Dr. A. Starzinski-Powitz
Prof. Dr. G. Auburger

Datum der Disputation: 16.09.2015

Scientific publications and presentations from this thesis

Publications

Brehm N, Bez F, Carlsson T, Kern B, Gispert S, Auburger G[§], Cenci MA[§] (2014)

„A genetic mouse model of Parkinson’s disease shows involuntary movements and increased post-synaptic sensitivity to apomorphine.” Mol Neurobiol. Oct 12. [Epub ahead of print]

Gispert S[§], Brehm N[§], Weil J, Seidel K, Rüb U, Kern B, Walter M, Roeper J, Auburger G (2014)

„Potentiation of neurotoxicity in double mutant mice with Pink1 ablation and A53T-SNCA overexpression.” Hum Mol Genet, 24(4):1061-76.

§ shared first author

Poster Presentations

N. Brehm, F. Bez, S. Gispert, M. A. Cenci, G. Auburger (2014)

„Striatal post-synaptic supersensitivity in a genetic mouse model of Parkinson’s disease.”
Parkinson’s Disease: Genetics, Mechanisms and Therapeutics (Keystone Symposium, Colorado)

Nadine Brehm, Alexander Kurz, Suzana Gispert, Georg Auburger (2013)

„Identification of molecular markers for early pathology and progression of Parkinson’s disease.”

AD/PD Conference, Florence

N. Brehm, A. Kurz, S. Gispert, G. Auburger (2013)

„*Homer1* and *Nurr77* are possible biomarkers for early nigrostriatal pathology in Parkinson’s disease (PD).” New Frontiers in Neurodegenerative Disease Research (Santa Fe, New Mexico)

Oral Presentation

“Mouse Models of Parkinson’s Disease” (18.11.2014)

Educational program of IMPRS “Modern Topics in neuroscience”

Max-Planck Institute for Brain Research, Frankfurt

„A genetic mouse model of Parkinson’s disease shows involuntary movements and increased post-synaptic sensitivity to apomorphine.” (11.9.2014)

52. Wissenschaftliche Tagung der Gesellschaft für Versuchstierkunde in Frankfurt am Main

„A genetic mouse model of Parkinson’s disease shows involuntary movements and increased post-synaptic sensitivity to apomorphine.” (10.07.2014)

Young Investigators Colloquium, Neuroscience Center Frankfurt am Main

“Mouse Models of Parkinson’s Disease” (11.11.2013)

Educational program of IMPRS “Modern Topics in neuroscience”

Max-Planck Institut for Brain Research, Frankfurt

Scientific publications and presentations outside this thesis

Publications

Gispert S, Kurz A, Brehm N, Rau K, Walter M, Riess O, Auburger G (2014)

“Complexin-1 and Foxp1 Expression Changes Are Novel Brain Effects of Alpha-Synuclein Pathology.” Mol Neurobiol. Aug 12. [Epub ahead of print]

Dominguez-Bautista JA, Klinkenberg M, Brehm N, Subramaniam M, Kern B, Roeper J, Auburger G, Jendrach M (2015)

„Loss of lysosome-associated membrane protein 3 (LAMP3) enhances cellular vulnerability against proteasomal inhibition.” European Journal of Cell Biology. Jan 30 [Epub ahead of print]

Manuscripts in Revision or Submission

Mai S, Brehm N, Auburger G, Bereiter-Hahn J, Jendrach M:

„Age-induced dysfunction of the autophago-lysosomal pathway in human endothelial cells“

In revision at Journal of Biological Chemistry

N. Brehm[§], K. Rau[§], A. Kurz, S. Gispert, G. Auburger:

„Age-related changes of 14-3-3 isoforms in midbrain of A53T-SNCA overexpressing mice“

[§] shared first author

In revision at Journal of Molecular Neuroscience

Lahut S^s, Gispert S^s, Ömür Ö, Depboylu C, Seidel K, Domínguez-Bautista J, Brehm N, Tireli H, Hackmann K, Pirkevi C, Leube B, Ries V, Reim K, Brose N, Den Dunnen W, Johnson M, Wolf Z, Schindewolf M, Frangakis AS, Schröck E, Steinmetz H, Jendrach M, Rüb U, Oertel W, Başak AN, Auburger G.:

“Blood biomarkers of risk for synucleinopathy, a variant of Parkinson’s disease”

In submission at Proc. Natl. Acad. Sci. USA.

1. INTRODUCTION	1
1.1 PARKINSON'S DISEASE.....	1
1.1.1 <i>Symptoms and Diagnosis</i>	1
1.2 PHYSIOLOGY AND NEUROPATHOLOGY OF PARKINSON'S DISEASE	3
1.2.1 <i>Anatomy and Physiology of the Basal Ganglia and Dopamine Networks</i>	3
1.2.1.1 The Direct and Indirect Pathway	5
1.2.1.2 The Role of Dopamine in the Basal Ganglia.....	6
1.2.2 <i>Lewy Body Pathology</i>	7
1.2.3 <i>Protein Degradation in Healthy Aging and Parkinson's Disease</i>	10
1.3 GENETICS OF PARKINSON'S DISEASE.....	10
1.3.1 <i>Genes and Loci Associated with Parkinson's Disease</i>	11
1.3.2 <i>Autosomal Dominant Forms of PD</i>	12
1.3.2.1 Alpha-Synuclein (Park1/4).....	13
1.3.2.1.1 Protein Family and Function of Alpha-Synuclein	14
1.3.3 <i>Autosomal recessive forms of PD</i>	18
1.3.3.1 PTEN-induced Kinase 1 (Park6).....	18
1.3.3.1.1 PINK1 Function and Role for Parkinson's Disease.....	19
1.4 THERAPY OF PARKINSON'S DISEASE.....	21
1.4.1 <i>Therapeutic Side Effects - Levodopa Induced Dyskinesia</i>	23
1.4.1.1 Molecular Basis of Levodopa Induced Dyskinesia.....	26
1.5 MOUSE MODELS OF PARKINSON'S DISEASE.....	28
1.5.1 <i>Genetically Engineered Mouse Models of PD</i>	28
1.5.1.1 The A53T-SNCA Overexpressing Mouse Model	29
1.5.1.2 The <i>Pink1</i> KO Mouse Model	29
1.5.1.3 The A53T-SNCA + <i>Pink1</i> KO Mouse Model	30
1.5.2 <i>The 6-OHDA Lesioned Mouse Model</i>	30
1.6 AIM OF THE THESIS.....	32
2. MATERIAL AND METHODS.....	33
2.1 MATERIAL.....	33
2.1.1 <i>General Laboratory Equipment</i>	33
2.1.2 <i>Behavioral Analysis and Perfusion</i>	34
2.1.2.1 Instruments	34
2.1.2.2 Expendable Materials	35
2.1.2.3 Chemicals.....	36
2.1.2.4 Buffers and Solutions	36
2.1.2.5 Pharmaceuticals	36
2.1.3 <i>RNA Purification and qPCR</i>	37
2.1.3.1 Laboratory Instruments	37
2.1.3.2 Expendable Materials	37

2.1.3.3 Chemicals	37
2.1.3.4 Kits	38
2.1.3.5 TaqMan Gene Expression Assays (Applied Biosystems)	38
2.1.4 <i>Western Blot</i>	41
2.1.4.1 Instruments	41
2.1.4.2 Material	41
2.1.4.3 Reagents	42
2.1.4.4 Buffers and Solutions	43
2.1.4.5 Primary Antibodies	44
2.1.4.6 Secondary Antibodies	44
2.1.5 <i>Immunohistochemistry</i>	44
2.1.5.1 Instruments	44
2.1.5.2 Material	45
2.1.5.3 Chemicals	46
2.1.5.4 Buffers and Solutions	46
2.1.5.5 Primary Antibodies	47
2.1.5.6 Secondary Antibodies	48
2.1.6 <i>Online Databases</i>	48
2.1.7 <i>Software</i>	49
2.2 METHODS	50
2.2.1 <i>Animals</i>	50
2.2.1.1 Animal Housing and Welfare	50
2.2.1.2 Generation and Breeding of A53T-SNCA Overexpressing Mice	50
2.2.1.3 Generation and Breeding of <i>Pink1</i> KO Mice	51
2.2.1.4 Generation and Breeding of A53T-SNCA + <i>Pink1</i> KO Mice	51
2.2.2 <i>Genotyping</i>	51
2.2.2.1 DNA Extraction from Tail	51
2.2.2.2 Polymerase Chain Reaction (PCR)	52
2.2.2.3 Genotyping of A53T-SNCA overexpressing mice	52
2.2.2.4 Genotyping of <i>Pink1</i> KO mice	53
2.2.2.5 Genotyping of A53T-SNCA + <i>Pink1</i> KO mice	53
2.2.2.6 Agarose Gel Electrophoresis	53
2.2.3 <i>Apomorphine Treatment</i>	53
2.2.4 <i>Stereotyped Movement Scoring</i>	54
2.2.4.1 Statistic of Behavioral Analysis	55
2.2.5 <i>Dissection of Mouse Brain</i>	55
2.2.6 <i>Quantitative Reverse Transcriptase Real-Time PCR (qPCR)</i>	55
2.2.6.1 RNA Isolation	55
2.2.6.2 Determination of RNA Concentration	56
2.2.6.3 DNase I Treatment and cDNA-Synthesis	56
2.2.6.4 Quantitative Real-Time PCR using TaqMan® Assays	57
2.2.6.5 Statistics	57

2.2.7 Western Blot.....	57
2.2.7.1 Protein Isolation.....	57
2.2.7.2 Determination of Protein Concentration.....	58
2.2.7.3 SDS-Polyacrylamide-Gelelectrophoresis (SDS-PAGE).....	58
2.2.7.4 Western Blotting.....	59
2.2.7.5 Immunodetection.....	59
2.2.7.6 Densitometric Analysis of Target Proteins.....	59
2.2.7.7 Statistics.....	60
2.2.8 Immunohistochemistry.....	60
2.2.8.1 Perfusion and Dissection of Mouse Brain and Spinal Cord.....	60
2.2.8.2 Immunohistochemistry – Free-Floating.....	60
<i>Apomorphine project</i>	60
2.2.8.3 Immunohistochemistry – Paraffin Embedded.....	62
2.2.8.4 Immunohistochemistry – Double Immunofluorescence Paraffin Embedded.....	62
2.2.8.5 Immunohistochemistry – Double Immunofluorescence Free-Floating.....	63
2.2.8.6 Microscopy.....	64
2.2.8.7 Quantitative Densitometric Analysis of Target Proteins.....	64
2.2.8.8 Statistics.....	65
3. RESULTS.....	66
3.1 PROJECT I: ALPHA-SYNUCLEIN GAIN-OF-FUNCTION EFFECTS ON CANDIDATE GENES POSSIBLY INVOLVED IN SYNAPTIC PLASTICITY.....	66
3.1.1 <i>Pre- and Post-Synaptic Expression Changes of Glutamate Receptor Subunits in 6-Month-Old Mice</i>	66
3.1.1.1 PrPmtA Mice Show an Increased Glutamate Receptor Subunit Expression.....	68
3.1.1.2 Additional <i>Pink1</i> Ablation (A53T-SNCA + <i>Pink1</i> KO Mice) Leads to Reduced Expression Levels.....	70
3.1.1.3 Exclusive <i>Pink1</i> Ablation has Only Minor Effects on Glutamate Receptor Subunit Expression.....	72
3.1.2 <i>Pre- and Post-Synaptic Expression Changes of Scaffolding Proteins in 6-Month-Old Mice</i>	74
3.1.2.1 PrPmtA Mice Show an Reduced <i>Homer1</i> and Increased <i>Psd95</i> Expression.....	75
3.1.2.2 Additional <i>Pink1</i> Ablation (A53T-SNCA + <i>Pink1</i> KO Mice) Maintains Reduced <i>Homer1</i> Expression but not <i>Psd95</i>	76
3.1.2.3 Exclusive <i>Pink1</i> Ablation Affects <i>Homer1</i> Expression only in the Striatum.....	76
3.1.3 <i>Pre- and Post-Synaptic Expression Changes of Immediate-Early-Genes and Transcription Factors in 6-Month-Old Mice</i>	77
3.1.3.1 PrPmtA Mice Show a Reduced Expression of Immediate-Early-Genes and Transcription Factors.....	78
3.1.3.2 Additional <i>Pink1</i> Ablation (A53T-SNCA + <i>Pink1</i> KO Mice) Maintains a Reduced Expression of Immediate-Early-Genes and Transcription Factors.....	80
3.1.3.3 Exclusive <i>Pink1</i> Ablation has only Minor Effects on the Expression of Immediate-Early-Genes and Transcription Factors.....	81
3.1.4 <i>Pre- and Post-Synaptic Expression Changes of Additional Candidate Genes in 6-Month-Old Mice</i> ... 83	
3.1.4.1 PrPmtA Mice Show an Increased Expression of <i>Pcbd1</i> , <i>Bad</i> , <i>Tac1</i> , <i>Sqstm1</i> , <i>IP3R</i> and <i>RGS2</i>	84

3.1.4.2 Additional <i>Pink1</i> Ablation (A53T-SNCA + <i>Pink1</i> KO Mice) Leads to Reduced Expression Level for <i>Sqstm1</i>	86
3.1.4.3 Exclusive <i>Pink1</i> Ablation has no Effect on the Expression of <i>Pcbd1</i> , <i>Bad</i> , <i>Tac1</i> and <i>Sqstm1</i>	87
3.1.5 Analysis of 3-Month-Old <i>PrPmtA</i> Mice to Depict the Earliest Effects of Alpha-Synuclein Gain-of-Function	87
3.1.5.1 The Regulation of Glutamate Receptor Subunits Appears with Age Progression and is not Present in Young Mice.....	87
3.1.5.2 Among the Earliest Effects of Alpha-Synuclein Gain-of-Function are Expression Alterations for <i>Homer1</i> , <i>cFos</i> , <i>NOR1</i> , <i>Nurr1</i> and <i>Nur77</i>	88
3.2 PROJECT II: THE IMPACT OF ALPHA-SYNUCLEIN GAIN-OF-FUNCTION ON THE BEHAVIORAL AND MOLECULAR RESPONSE TO APOMORPHINE TREATMENT.....	91
3.2.1 <i>PrPmtA</i> Mice Show Increased Involuntary Movements with Stereotypic and Dystonic Features after Apomorphine Treatment	91
3.2.2 Immunohistochemical Analysis of <i>PrPmtA</i> mice Reveals Alpha-Synuclein Overexpression without Dopaminergic Cell Loss.....	94
3.2.3 Alpha-Synuclein Dependent Alterations of Striatal <i>Erk1/2</i> Phosphorylation in Response to Apomorphine – Analysis via Quantitative Immunoblots.....	96
3.2.3.1 Analysis of Striatal Tissue 30 min after Apomorphine Treatment Reveals no Genotype Dependent Differences.....	97
3.2.3.2 Analysis of Striatal Tissue 100 min after Apomorphine Treatment Reveals Reduced pERK1/2 Level in <i>PrPmtA</i> Mice.....	98
3.2.4 Alpha-Synuclein Dependent Alterations of Striatal Histone H3 Phosphorylation in Response to Apomorphine - Analysis via IHC.....	100
3.2.5 Alpha-Synuclein Gain-of-Function Affects the Expression of ERK Pathway Elements in Response to Apomorphine Treatment	102
3.2.5.1 Analysis of Striatal Tissue 30 min after Apomorphine Treatment Reveals Genotype Dependent Differences for <i>cFos</i>	103
3.2.5.2 Analysis of Striatal Tissue 100 min after Apomorphine Treatment Reveals Increased <i>cFos</i> , <i>Dusp1</i> , <i>Dusp6</i> and <i>Nur77</i> Levels.....	104
3.2.5.3 Analysis of Additional <i>Dusp</i> Family Members Reveals Increased Apomorphine Dependent mRNA levels but no Genotype Dependent Differences	105
3.2.5.4 Apomorphine and Genotype Dependent Increases of <i>cFos</i> , <i>Dusp1</i> , <i>Dusp6</i> and <i>Nur77</i> Levels are Predominantly but not Exclusively Found in Striatal Tissue.....	106
3.2.6 Alpha-Synuclein Gain-of-Function Effects on <i>DUSP6</i> Abundance in Response to Apomorphine Treatment – Analysis on Protein Level.....	108
3.3 PROJECT III: POTENTIATION OF ALPHA-SYNUCLEIN GAIN-OF-FUNCTION EFFECTS IN DOUBLE-MUTANT MICE WITH <i>PINK1</i> ABLATION	110
3.3.1 The Spinal Cord of A53T-SNCA + <i>Pink1</i> KO Mice Shows pSer129-SNCA, p62/SQSTM1 and Ubiquitin Positive Cells	111
3.3.2 The Midbrain of A53T-SNCA + <i>Pink1</i> KO Mice Shows pSer129-SNCA, p62/SQSTM1 and Ubiquitin Positive Cells.....	113

3.3.3 <i>pSer129-SNCA, p62/SQSTM1 and Ubiquitin Positive Cells of A53T-SNCA + Pink1KO Midbrain Slices are not TH Positive</i>	116
3.3.4 <i>pSer129-SNCA, p62/SQSTM1 and Ubiquitin Positive Cells of A53T-SNCA + Pink1KO Midbrain Slices are Positive for Interneuron Specific Markers</i>	118
4. DISCUSSION	120
4.1 PROJECT I: ALPHA-SYNUCLEIN GAIN-OF-FUNCTION EFFECTS ON CANDIDATE GENES POSSIBLY INVOLVED IN SYNAPTIC PLASTICITY	120
4.1.1 <i>Alpha-Synuclein Gain-of-Function Increases the Expression of Candidate Genes Involved in Synaptic Signaling Efforts and Decreases the Expression of Candidate Genes Downstream of Synaptic Signaling Cascades in A53T-SNCA Mice</i>	121
4.1.2 <i>Alpha-Synuclein Gain-of-Function and Additional Pink1 Ablation Decreases the Expression of Candidate Genes Involved in Synaptic Signaling Efforts and Decreases the Expression of Candidate Genes Downstream of Synaptic Signaling Cascades</i>	130
4.1.3 <i>Exclusive Pink1 Ablation has Only Minor Effects on the Expression of Candidate Genes Involved in Synaptic Plasticity</i>	132
4.2 PROJECT II: THE IMPACT OF ALPHA-SYNUCLEIN GAIN-OF-FUNCTION ON THE BEHAVIORAL AND MOLECULAR RESPONSE TO APOMORPHINE TREATMENT	134
4.2.1 <i>Alpha-Synuclein Gain-of-Function Increases Involuntary Movements with Stereotypic and Dystonic Features after Apomorphine Treatment</i>	135
4.2.2 <i>Alpha-Synuclein Gain-of-Function Changes the Temporal Dynamics of Striatal Signaling Responses to Apomorphine Treatment</i>	137
4.3 PROJECT III: POTENTIATION OF ALPHA-SYNUCLEIN GAIN-OF-FUNCTION EFFECTS IN DOUBLE MUTANT MICE WITH PINK1 ABLATION	145
4.3.1 <i>PINK1 Deficiency is a Relevant Modulator of Alpha-Synuclein Aggregation</i>	145
5. PERSPECTIVES	150
6. SUMMARY	151
7. ZUSAMMENFASSUNG	156
8. REFERENCES	162
9. ABBREVIATIONS	190
10. LIST OF TABLES AND FIGURES	193
10.1 LIST OF TABLES.....	193
10.2 LIST OF FIGURES	194
11. WRITTEN DECLARATION	197
12. ACKNOWLEDGEMENTS	FEHLER! TEXTMARKE NICHT DEFINIERT.
13. CURRICULUM VITAE	FEHLER! TEXTMARKE NICHT DEFINIERT.

1. INTRODUCTION

1.1 Parkinson's Disease

In 1817, based on six patients, the London surgeon and Member of Parliament James Parkinson first described the characteristic symptoms of Parkinson's disease (PD) in "an essay of the shaking palsy". His work remained unnoticed until 1877 when the French neurologist Jean Martin Charcot recognized the importance of James Parkinson's work and named the disorder "maladie de Parkinson" (Parkinson's disease) (Lees, 2007).

Today, Parkinson's disease is the second most frequent neurodegenerative disorder after Alzheimer's disease, affecting 0.3% of the population in industrialized countries. The probability of developing PD increases with age, leading to a prevalence of 1-2% in people over the age of 60 in western countries, and 3-4% in those over 80 years (Tanner and Goldman, 1996, Nussbaum and Ellis, 2003). In addition to age, several studies have reported a gender effect, which shows a greater probability of males developing PD (Mayeux et al., 1995, Fall et al., 1996, de Lau and Breteler, 2006). However this effect remains contentious as other studies have failed to find the same effect (Tison et al., 1994, de Rijk et al., 1995, de Rijk et al., 1997).

1.1.1 Symptoms and Diagnosis

The cardinal motor symptoms of PD, illustrated in figure 1, are clinically characterized by rigidity, postural instability, bradykinesia/akinesia (slowness/absence of motor activity), flexed posture, freezing and low-frequency resting tremor (Fahn, 2003). The onset of PD motor symptoms is typically mild and asymmetrical and responsive to adequate levodopa therapy, but nevertheless symptoms worsen as the disease progresses (Fahn, 2003). The development of symptoms is variable and patient specific, therefore not all of the six cardinal features need to be present for a clinical diagnosis (Morrish et al., 1996). However a definitive confirmation of the disease requires *post mortem* analysis showing neuronal cell loss, depigmentation of the substantia nigra and evidence of proteinaceous intracellular inclusions, the so-called Lewy bodies. With respect to the motor symptoms, resting tremor is often the first symptom recognized, due to its obvious appearance, but bradykinesia is often the first symptom to develop. Bradykinesia is characterized by slower and smaller handwriting, decreased arm swing and leg stride when walking, decreased facial expression as well as an de-

creased amplitude of voice (Fahn, 2003). The earliest symptoms of PD, resting tremor, bradykinesia and rigidity, are associated with a progressive loss of nigrostriatal dopamine, whereas flexed posture, freezing and postural instability are non-dopamine-related symptoms of PD. In addition to these widely recognized motor symptoms, many PD patients develop non-motor symptoms such as depression, cognitive impairment, olfactory dysfunction, anxiety, REM sleep disturbance, fatigue or dementia among others (Owen et al., 1992, Martignoni et al., 1995, Aarsland et al., 1999, Fahn, 2003, Owen, 2004). The non-motor symptoms of PD are predominantly associated with the degeneration of serotonergic neurons of the raphe nucleus, noradrenergic neurons of the locus ceruleus or cholinergic neurons of the nucleus basalis of Meynert, rather than dopaminergic neurons (Corti et al., 2011).

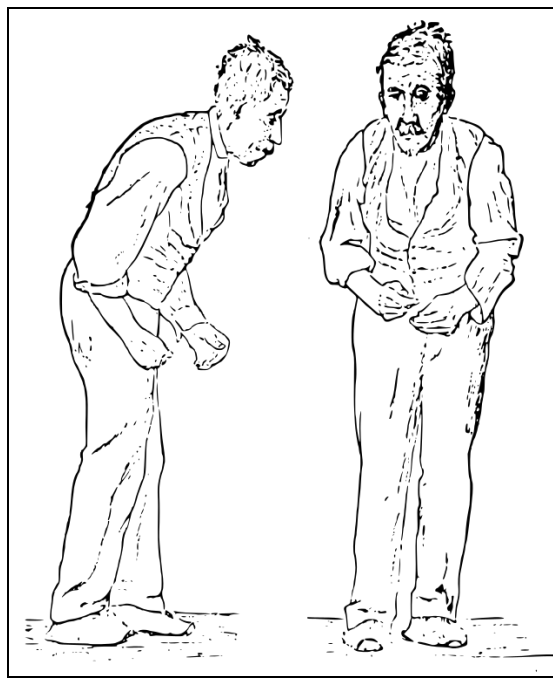


Fig. 1 Illustration of the cardinal motor symptoms in Parkinson's disease. Gowers, W. R. (1886), *A Manual of Diseases of the Nervous System*.

To date, there are no conclusive pre-mortem diagnostic tests for PD, instead a clinical diagnosis relies on the stereotypical motor and non-motor symptoms of PD. This means there exists the possibility of misdiagnosis as clinicians may confuse PD with other disorders such as postencephalic, drug-induced and arteriosclerotic parkinsonism until a post mortem analysis confirms the diagnosis (Hughes et al., 1992). The most helpful tool in diagnosing PD is the substantial response to levodopa, a typical feature of PD, illustrating the presynaptic dopamine deficiency in parallel to the preservation of postsynaptic receptors.

1.2 Physiology and Neuropathology of Parkinson's Disease

The pathological process leading to the described motor symptoms of PD is the degeneration of dopaminergic neurons of the substantia nigra pars compacta (SNc) and their striatal projections. Motor symptoms typically appear after approximately 50% of dopaminergic neurons of the SNc, and 70% of striatal dopamine content are lost (Bernheimer et al., 1973, Fearnley and Lees, 1991). Healthy individuals, depending on their age as well as on the counting method used, hold between 250 000 to 550 000 dopaminergic neurons located in the SNc (Hirsch et al., 1988, Fearnley and Lees, 1991). In healthy aging, approximately 5% of SNc dopaminergic neurons are lost per decade, thus 33-48% of dopaminergic cell loss occurs between the age of 20 and 90 years (McGeer et al., 1977, Fearnley and Lees, 1991). In PD patients, dopaminergic cell loss is increased up to 10-fold (Fearnley and Lees, 1991, Vingerhoets et al., 1994, Morrish et al., 1996), and the magnitude of dopaminergic cell death is strongly correlated with severity of PD motor symptoms (Foley and Riederer, 1999). Beyond the SNc, the ventral tegmental area (VTA) of the midbrain which projects to the caudate nucleus and the nucleus accumbens is also affected by dopaminergic cell loss in PD, albeit to a lesser extent than the SNc. As mentioned previously, besides the degeneration of dopaminergic neurons, the serotonergic and noradrenergic systems are also affected leading to the non-motor symptoms of PD (Scatton et al., 1983, Braak et al., 2003).

1.2.1 Anatomy and Physiology of the Basal Ganglia and Dopamine Networks

The progressive loss of dopaminergic neurons of the SNc and their striatal projections results in reduced dopamine content within the striatum. The striatum is the largest and main input step of the basal ganglia, receiving glutamatergic excitatory inputs from cortical areas, thalamic nuclei and from the cerebellum (Hoshi et al., 2005) as well as dopaminergic inputs from the SNc (Pickel et al., 1992). The basal ganglia are an important brain region for goal-directed behavior and habit formation. The general anatomical structure of the basal ganglia circuitry is shown in figure 2 that was adapted from "pathophysiology of parkinsonism" (Galvan and Wichmann, 2008). The basal ganglia of humans comprises the striatum that is further divided into the sub-regions caudate nucleus and putamen, the external and internal segments of the globus pallidus (GPe, GPi), the subthalamic nucleus (STN), the substantia nigra pars compacta (SNc) as well as the substantia nigra pars reticulata (SNr). In contrast to humans, rodents do not show this further segmentation of the striatum and the GP, which is referred to as en-

topeduncular nucleus in rodents. The basal ganglia circuitry can be described as a closed feed-forward loop connecting all cortical areas sequentially through the striatum and thalamus with the frontal cortex, using glutamatergic excitatory afferents (Elias S., 2008). The frontal cortex thereafter projects to the brainstem and spinal cord. Besides excitatory glutamatergic input from the cortex, the striatum also receives regulatory dopaminergic input from the substantia nigra pars compacta (Pickel et al., 1992). The dopaminergic and glutamatergic afferents project onto striatal GABAergic medium spiny neurons that represent 95% of the striatal neurons as well as onto GABAergic and cholinergic interneurons (Dube et al., 1988, Lapper and Bolam, 1992). The striatal GABAergic medium spiny neurons in turn project via the direct pathway to the GPi and via the indirect pathway to the STN. The glutamatergic STN neurons then project to the SNr and GPi. The feed-forward loop is closed by these GABAergic neurons of the GPi and SNr projecting to the thalamus, which then send glutamatergic projections to the cortex (Obeso et al., 2000b).

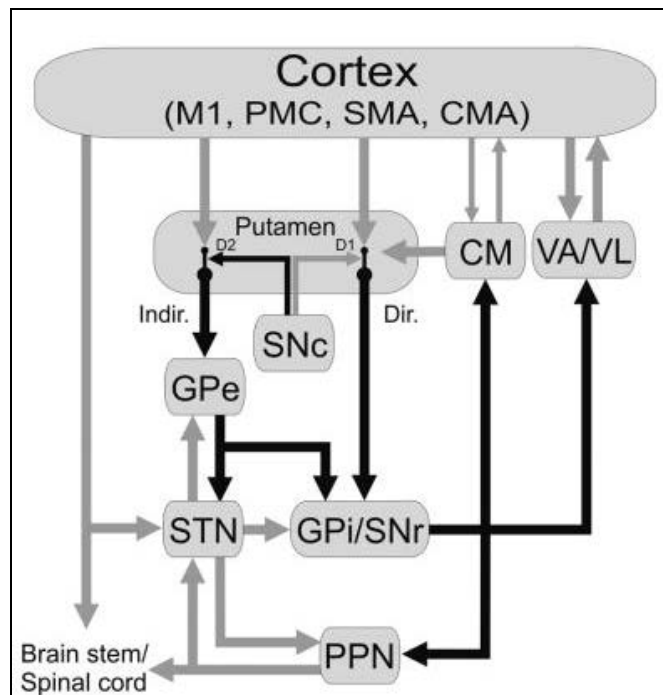


Fig. 2 Anatomical structure of the basal ganglia circuitry adapted from Galvan and Wichmann, 2008. Gray arrows show excitatory glutamatergic connections and black arrows show inhibitory GABAergic connections. Areas illustrated: external pallidal segment (Gpe); subthalamic nucleus (STN); internal pallidal segment (GPi); substantia nigra pars reticulata (SNr); substantia nigra pars compacta (SNc); pedunculo pontine nucleus (PPN); centromedian nucleus of the thalamus (CM); ventral anterior and ventrolateral nucleus of the thalamus (VA/VL).

1.2.1.1 The Direct and Indirect Pathway

The anatomical description of the basal ganglia circuitry depicted two major projection systems between input and output structures, the direct and the indirect pathway (illustrated in figure 3). Both pathways are concurrently activated and act in a coordinated way in order to support or suppress actions (Cui et al., 2013). Cortical glutamatergic activation of the direct pathway medium spiny neurons (MSNs) leads to an inhibition of the GPi that has inhibitory GABAergic connections to the thalamus. The inhibition of the GPi therefore, leads to an disinhibition of glutamatergic thalamic neurons, which in turn sends excitatory (glutamatergic) input to the cortex resulting in locomotor activity (reviewed in (Calabresi et al., 2014)). In contrast, cortical glutamatergic activation of the indirect pathway MSNs inhibits the GABAergic neurons of the GPe leading to a disinhibition of the STN. In turn the STN sends excitatory (glutamatergic) input to GABAergic neurons of the SNr, which project to the thalamus and results in a reduction of locomotor activity (for review see (Calabresi et al., 2014)).

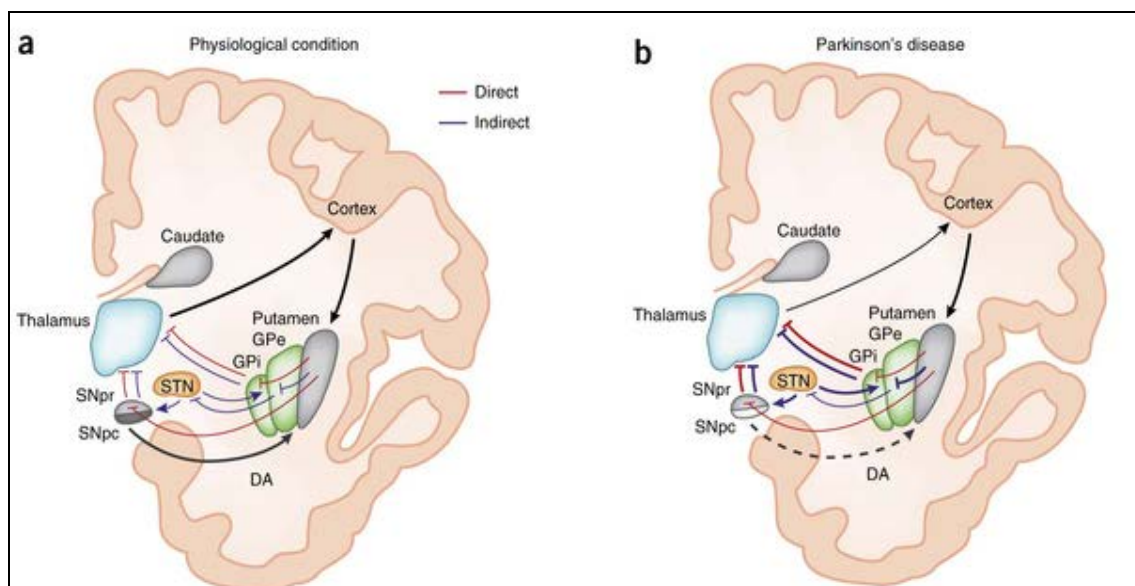


Fig. 3 Illustration of the direct and indirect pathway in physiological conditions (a) and in Parkinson's disease (b). Red lines highlight the direct pathway, where dopamine arising from the SNc (here SNpc) activates D1-expressing MSNs and in blue the indirect pathway, where dopamine arising from the SNc inhibits D2-expressing MSNs. In PD dopaminergic neurons degenerate, therefore the imbalance between direct and indirect pathway leads to abnormal activation of basal ganglia output nuclei and hence overinhibition of thalamic neurons that project to the cortex. Abbreviations: GPe, external pallidal segment; STN, subthalamic nucleus; GPi, internal pallidal segment; SNpr, substantia nigra pars reticulata; SNpc, substantia nigra pars compacta; DA, dopamine. Figure adapted from (Calabresi et al., 2014).

In addition to these differences in projection targets, GABAergic neurons that constitute the direct and indirect pathway also differ neurochemically. GABAergic MSNs of the direct pathway express substance P, dynorphin and the dopamine receptor D1 leading to increased in-

trinsic excitability, therefore promoting long-term potentiation (LTP). Whereas GABAergic MSNs of the indirect pathway express primarily enkephalin and the dopamine receptor D2 leading to decreased intrinsic excitability, and therefore promoting long-term depression (LTD) (Surmeier et al., 2014). Electrophysiological approaches could additionally show a different excitability as well as differences in resting membrane potentials in striatal MSNs containing D1 receptors compared to those containing primarily D2 receptors, with D2 containing MSNs firing at a higher frequency (Kreitzer and Malenka, 2007, Cepeda et al., 2008).

1.2.1.2 The Role of Dopamine in the Basal Ganglia

Striatal GABAergic medium spiny neurons receive cortical and thalamic glutamatergic activation and are further modulated by dopamine. The dopaminergic input terminates at the neck of MSNs, which enables the dopaminergic input to regulate corticostriatal transmission (Galvan and Wichmann, 2008). There is experimental evidence that dopamine released from terminals of the nigrostriatal projection differentially modulates the direct and indirect pathway. Dopaminergic activation of dopamine receptor D1 excites MSNs of the direct pathway leading to an activation of corticostriatal transmission, whereas dopaminergic activation of dopamine receptor D2 inhibits MSNs of the indirect pathway (Albin et al., 1989). The opposing effect of striatal dopamine release on the direct and indirect pathway impacts the balance of activity between indirect and direct pathway. In this model an increased dopamine release would activate direct pathway neurons and inactivate indirect pathway neurons, both leading to a reduced output from GPi/SNr to the thalamus and therefore resulting in locomotor activity and movement as described in 1.2.1.1. In PD the progressive loss of dopaminergic neurons in the substantia nigra leads to reduced dopamine levels in the striatum resulting in disinhibition of the indirect pathway and reduced activation of the direct pathway that in turn results in increased basal ganglia output to the thalamus and therefore reduction of locomotor activity (Galvan and Wichmann, 2008). The loss of dopaminergic input into the basal ganglia also provokes morphological alterations, for instance reduced density of dendritic spines on MSNs in the putamen (Ingham et al., 1989, Zaja-Milatovic et al., 2005) and changes in density and sensitivity of dopamine receptors.

1.2.2 Lewy Body Pathology

In 1912 Fritz Heinrich Lewy was the first to describe intraneuronal proteinaceous cytoplasmic inclusions in the dorsal vagal nucleus (Lewy, 1912). Seven years later Konstantin Nikolaevich Tretiakoff found similar aggregates while analyzing the substantia nigra of 54 *post mortem* brains with nine of them having paralysis agitans and three postencephalitic Parkinsonism. In recognition to Fritz Heinrich Lewy, Konstantin Nikolaevich Tretiakoff called these aggregates “corps de Lewy” (Lees et al., 2008). Parkinson’s disease is neuropathologically defined on one hand by the progressive loss of dopaminergic neurons in the substantia nigra and on the other hand by the presence of Lewy bodies and Lewy neurites in this region. There have been two types of Lewy bodies described, the brainstem-type which is considered the classical type, and the cortical type (Wakabayashi et al., 2007). Both types of Lewy bodies are composed of filamentous structures but under light microscopy (Hematoxylin-Eosin-staining) show two distinct morphologies: the brainstem-type appear as intracytoplasmic eosinophilic structures with a dense core and a peripheral halo, whereas the cortical-type (also eosinophilic) does not show a peripheral halo or a central core (Okazaki et al., 1961, Kosaka et al., 1976, Wakabayashi et al., 2007). Lewy bodies and Lewy neurites are not exclusive to the substantia nigra, they can be found in the dorsal motor nucleus of the vagus (Forno, 1996), nucleus basalis of the Meynert (Forno, 1996), locus coeruleus, hypothalamus, hippocampus (Dickson et al., 1991), amygdala (Braak et al., 1994), neocortex (Irizarry et al., 1998), olfactory bulb (Del Tredici et al., 2002) and spinal cord (Del Tredici and Braak, 2012). However, neurons susceptible to Lewy body pathology share some common features: they all belong to the class of projection neurons that develop a long and thin axon (Braak et al., 2006), and they have unmyelinated or poorly myelinated axons (Braak and Del Tredici, 2004, Braak et al., 2004). This suggests myelin has a neuroprotective role, which could be the result of reduced oxidative stress during impulse transmission (Beal, 1995, Sohal, 2002, Jenner, 2003, Ahlskog, 2005), as well as a stabilizing role, making myelinated neurons less susceptible to pathological sprouting (Kapfhammer and Schwab, 1994). Because PD is a progressive neurodegenerative disorder, Braak and colleagues proposed that the pathological processes associated with PD, such as Lewy body pathology, will exacerbate with disease duration and therefore they developed a system of disease progression stages (shown in figure 4).

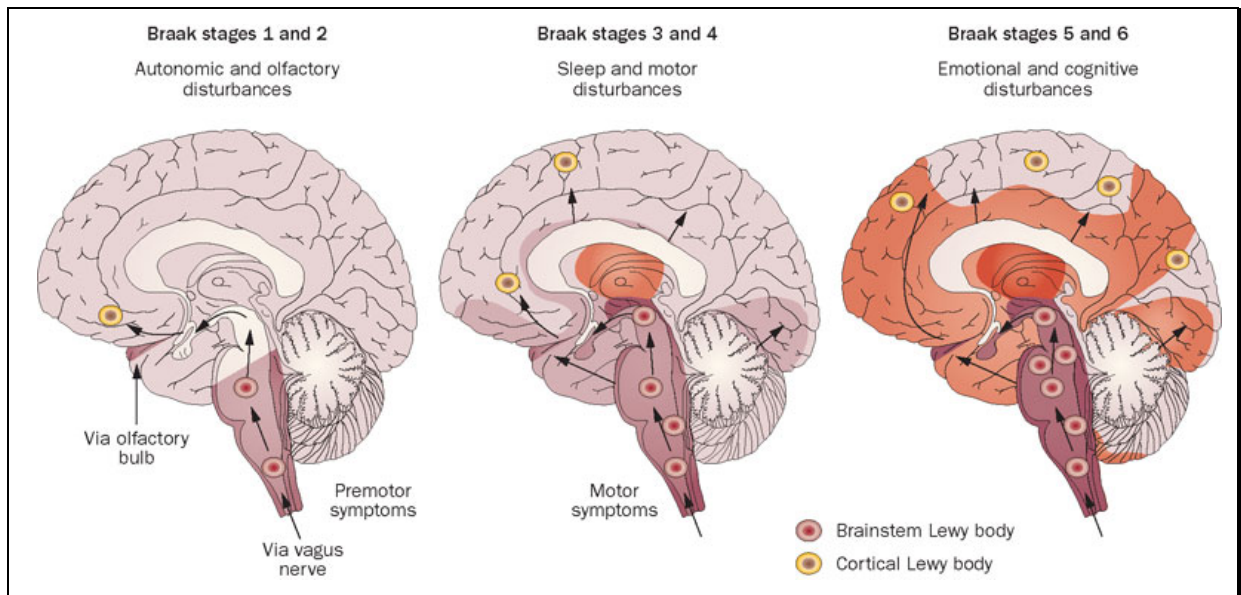


Fig. 4 Illustration of Braak's staging system adapted from (Doty, 2012). The red color grading represents the pattern of PD pathology.

The main protein found in Lewy bodies is alpha-synuclein; therefore alpha-synuclein immunoreactivity was used for staging of 110 clinically diagnosed PD brains as well as 58 age- and sex-matched controls. The earliest alpha-synuclein immunoreactivity was found in the dorsal motor nucleus of the vagus nerve as well as in the anterior olfactory structure, representing Braak stage 1 (Lewy, 1912, Eadie, 1963, Forno, 1969, Daniel and Hawkes, 1992). In stage 2, lesions in the dorsal motor nucleus are more severe than in stage 1 and additional Lewy body pathology is found in brainstem nuclei as well as in the noradrenergic locus coeruleus (Saper et al., 1991, Braak et al., 2000). Stage 3 is characterized by pathology of the central subnucleus of the amygdala (Bohus et al., 1996) and the basal forebrain including Meynert's nucleus (Perry et al., 1999, Pahapill and Lozano, 2000). Also of importance is the first appearance of Lewy neurites in the substantia nigra, followed by punctuate structures, pale bodies and Lewy bodies but without neuronal loss (Braak and Braak, 1986, Gibb and Lees, 1991, Braak et al., 2004). In stage 4 Lewy bodies for the first time appear in the mesocortex (Braak, 1980). This mesocortex pathology is more severe in stage 5 where also the related insular and cingulate mesocortex are involved. Stage 6 represents the complete pathological dimension, with the substantia nigra and cortical structures being severely affected and even the neocortex showing Lewy body pathology. Clinical symptoms of PD become visible mostly at stage 4 in some cases already at stage 3. Stage 5 and 6 represent the complete clinical picture of symptoms associated with PD (Apaydin et al., 2002, Braak et al., 2005, Braak et al., 2006). Even if it is widely accepted, that Lewy body pathology worsens with PD progression (Braak et al.,

2003) and is associated with neuronal loss, it is still a matter of debate if these inclusions actually cause cell death (Terry, 2000). As mentioned previously, the main protein found in Lewy bodies is alpha-synuclein, therefore immunoreactivity of alpha-synuclein was used to illustrate that Lewy body formation consists of several stages shown in figure 5 (Wakabayashi et al., 1998, Kuusisto et al., 2003). However there are many other proteins and molecules composing Lewy bodies. Among these molecules are structural elements, alpha-synuclein-binding proteins, synphilin-1-binding proteins, components of the ubiquitin-proteasome system, proteins of the cellular response machinery, phosphorylation and signal transduction elements, cytoskeletal proteins, cell cycle proteins and many others (for review see (Wakabayashi et al., 2007). Most interesting for this work is the presence of conformational and posttranslational modified alpha-synuclein (Beyer, 2006), such as alpha-synuclein phosphorylated at serine 129 (pSer129-SNCA) as well as the presence of sequestosome 1 (SQSTM1/p62) and ubiquitin.

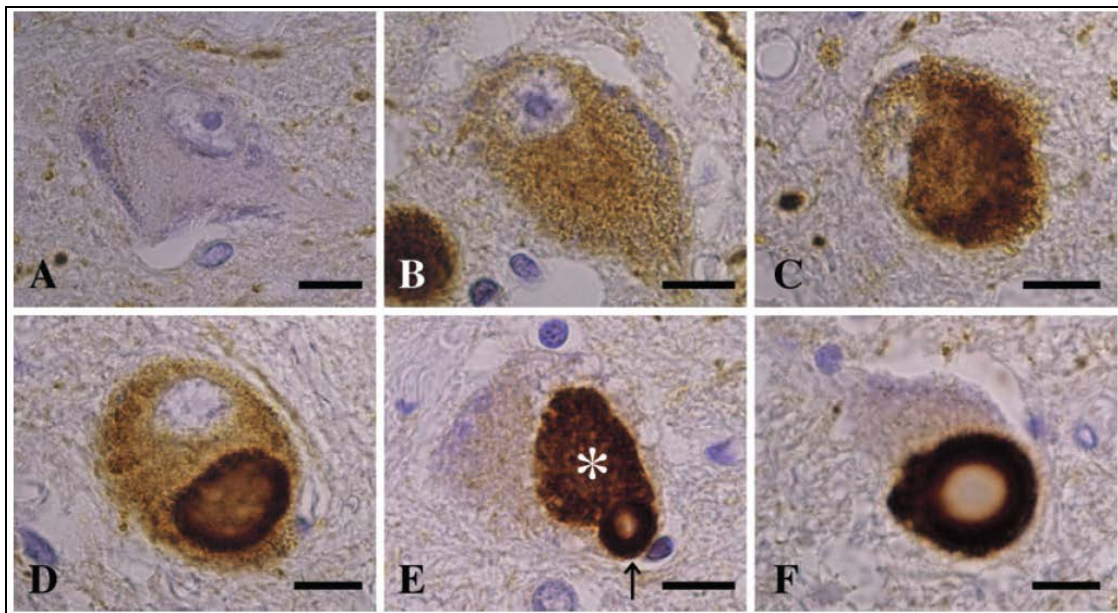


Fig. 5 Different maturation stages of substantia nigra Lewy bodies visualized by alpha-synuclein immunoreactivity. (A) Alpha-synuclein immunoreactivity is absent in the cytoplasm of a healthy neuron. (B) Light alpha-synuclein immunoreactivity in the cytoplasm. (C) Stronger staining, irregular shaped. (D) Pale body staining. (E) Alpha-synuclein aggregate with pale body indicated by asterisk and Lewy body indicated by arrow. (F) Doughnut-shaped Lewy body. Bar (A-F) 10 μ m, picture adapted from (Wakabayashi et al., 2007).

1.2.3 Protein Degradation in Healthy Aging and Parkinson`s Disease

In PD patients, Lewy bodies are found in remaining dopaminergic cells of the SNc giving evidence that protein degradation might be a crucial factor for the pathogenesis of PD (Pollanen et al., 1993, Forno, 1996). Lewy bodies, as described in 1.2.2, consist of a variety of proteins including ubiquitin and proteasomal elements (Ii et al., 1997), such as 20/20s, an enzyme responsible for the degradation of ubiquitinated proteins (Craiu et al., 1997, Ii et al., 1997) pointing to an involvement of proteasomal function to PD pathology. Protein misfolding and accumulation occurs in every organism. In healthy individuals, misfolded proteins are degraded by the ubiquitin-proteasome system (UPS) (Sherman and Goldberg, 2001). In brief, this process involves the identification of abnormal proteins and their labeling with ubiquitin molecules by several enzymes. Ubiquitin labeled proteins are then recognized by a multi-subunit proteases (the 26S proteasome) (DeMartino and Slaughter, 1999) and degraded into short peptides and amino acids that can be recycled. This proteasomal activity is particularly important for neurons since they are postmitotic and would otherwise accumulate damaged organelles and misfolded proteins (He and Klionsky, 2009). The composition of Lewy bodies indicates that their proteins were originally tagged for degradation, but possibly due to an UPS impairment, were compartmentalized into insoluble aggregates potentially to protect neurons against protein-mediated neurotoxicity (reviewed in (McNaught et al., 2001b)). In line with this hypothesis is the finding that proteasomal function is lower in the SNc of aged humans compared to other brain regions, as well as in PD patients compared to healthy age-matched controls, highlighting dopaminergic neurons to be more vulnerable (McNaught et al., 2001b, McNaught et al., 2003). There is also evidence that damage of the proteasomal system is a common feature in both sporadic and familial forms of PD. Mutations in Parkin impairing normal ubiquitination, in PINK1 impairing mitochondrial quality control and degradation as well as in UCHL1 controlling de-ubiquitination, are associated with familial forms of PD (Halliwell and Jenner, 1998, McNaught et al., 2001a).

1.3 Genetics of Parkinson`s Disease

For many years PD, was considered a sporadic disorder until 1880 when Leroux for the first time suggested a heritable factor for PD susceptibility (Leroux, 1880). In 1937, Allen studied familial PD in North Carolina, USA (Allen, 1937) and in 1949 Henry Mjones was the first using a systematic genetic-statistical approach to study a Swedish family of parkinsonism (Mjones, 1949), both suggesting an autosomal dominant inheritance. In spite of these early discoveries

of genetic cases of PD, only in the last decade our understanding of a genetic contribution to PD has evolved. This understanding mainly evolved from studying large families with clear Mendelian inheritance of PD using linkage analysis and more recently through genome-wide association studies (Maraganore et al., 2005, Nalls et al., 2014). Several genes causative for PD were identified within these studies, highlighting mitochondrial or lysosomal dysfunction, protein aggregation, the ubiquitin-proteasome system and therefore protein degradation as well as kinase signaling pathways to contribute to PD pathogenesis (Corti et al., 2011). Although more than 85% of PD cases are sporadic (Thomas and Beal, 2007), and only 5-10% of PD cases can be explained by mutations in any one of the known genes associated with PD, there is evidence that there is a common genetic link between the sporadic and idiopathic forms of PD. Therefore, understanding the function and interactions of those genes can help us broaden our understanding of PD pathology in general, and potentially lead to the development of effective therapies.

1.3.1 Genes and Loci Associated with Parkinson's Disease

In 1996, a genome-wide linkage analysis conducted on an Italian pedigree identified the first gene implicated with idiopathic PD, which was alpha-synuclein (SNCA) (Polymeropoulos et al., 1996). The identification of mutations in the gene encoding SNCA (Polymeropoulos et al., 1997) as well as the identification of SNCA as the major component of Lewy bodies (Spillantini et al., 1997), represents the beginning of a genetic understanding of PD. Since then at least 18 chromosomal loci have been linked to inherited PD and named according to their identification in chronological order from PARK1 to PARK18 (Klein and Westenberger, 2012). This current nomenclature comprises confirmed and un-confirmed loci, additionally not for all loci the causative gene is yet identified. Table 1, that was adapted from (Klein and Westenberger, 2012) summarizes all PARK genes and loci as well as their clinical classification, their inheritance pattern, the gene name and the status of identification.

Tab. 1 Overview of PD-related loci, referred to as PARK. Adapted from (Klein and Westenberger, 2012).

Symbol	Gene locus	Disorder	Inheritance	Gene	Status and remarks	Mode of identification
<i>PARK1</i>	4q21–22	EOPD	AD	<i>SNCA</i>	Confirmed	Linkage analysis
<i>PARK2</i>	6q25.2–q27	EOPD	AR	<i>Parkin</i>	Confirmed	Linkage analysis
<i>PARK3</i>	2p13	Classical PD	AD	Unknown	Unconfirmed; may represent a risk factor; gene not found since first described in 1998	Linkage analysis
<i>PARK4</i>	4q21–q23	EOPD	AD	<i>SNCA</i>	Erroneous locus (identical to <i>PARK1</i>)	Linkage analysis
<i>PARK5</i>	4p13	Classical PD	AD	<i>UCHL1</i>	Unconfirmed (not replicated since described in 1998)	Functional candidate gene approach
<i>PARK6</i>	1p35–p36	EOPD	AR	<i>PINK1</i>	Confirmed	Linkage analysis
<i>PARK7</i>	1p36	EOPD	AR	<i>DJ-1</i>	Confirmed	Linkage analysis
<i>PARK8</i>	12q12	Classical PD	AD	<i>LRRK2</i>	Confirmed; variations in <i>LRRK2</i> gene include risk-conferring variants and disease-causing mutations	Linkage analysis
<i>PARK9</i>	1p36	Kufor-Rakeb syndrome; atypical PD with dementia, spasticity, and supranuclear gaze palsy	AR	<i>ATP13A2</i>	Confirmed; but complex phenotype that would not be mistaken for early-onset or classical parkinsonism	Linkage analysis
<i>PARK10</i>	1p32	Classical PD	Risk factor	Unknown	Confirmed susceptibility locus; gene unknown since first described in 2002	Linkage analysis
<i>PARK11</i>	2q36–27	Late-onset PD	AD	Unknown; not <i>GIGYF2</i>	Not independently confirmed; possibly represents a risk factor; gene not found since first described in 2002	Linkage analysis
<i>PARK12</i>	Xq21–q25	Classical PD	Risk factor	Unknown	Confirmed susceptibility locus; possibly represents a risk factor; gene not found since first described in 2003	Linkage analysis
<i>PARK13</i>	2p12	Classical PD	AD or risk factor	<i>HTRA2</i>	Unconfirmed	Candidate gene approach
<i>PARK14</i>	22q13.1	Early-onset dystonia-parkinsonism	AR	<i>PLA2G6</i>	Confirmed	Linkage analysis (homozygosity mapping)
<i>PARK15</i>	22q12–q13	Early-onset parkinsonian-pyramidal syndrome	AR	<i>FBX07</i>	Confirmed	Linkage analysis
<i>PARK16</i>	1q32	Classical PD	Risk factor	Unknown	Confirmed susceptibility locus	Genome-wide association studies
<i>PARK17</i>	16q11.2	Classical PD	AD	<i>VPS35</i>	Confirmed	Exome sequencing
<i>PARK18</i>	3q27.1	Classical PD	AD	<i>EIF4G1</i>	Unconfirmed; recently published (Chartier-Harlin et al. 2011)	Linkage analysis

AD, autosomal dominant; AR, autosomal recessive.

1.3.2 Autosomal Dominant Forms of PD

The currently known monogenic forms of PD are all either autosomal dominant or autosomal recessive. In autosomal dominant inheritance, the mutation of one allele leads to the development of PD either by haploinsufficiency (i.e., the remaining wildtype gene is not sufficient to provide enough protein for cell function), by a dominant negative effect (i.e., the mutant polypeptide interferes with the normal, and therefore decreases its function), or by gain-of-function (i.e., the mutation modifies the gene function such that new functions are gain or it is abnormal). Presently, two genes, alpha-synuclein (*SNCA*) and Leucin-rich repeat kinase 2 (*LRRK2*), have been strongly linked to the autosomal dominant inheritance of PD, whereas the pathogenic role of the dominant genes ubiquitin COOH-terminal hydrolase 1 (*UCHL1*), GRB10-interacting GYF protein 2 (*GIGYF2*) and the mitochondrial serine protease *HTRA2* are controversial (Corti et al., 2011).

1.3.2.1 Alpha-Synuclein (Park1/4)

As mentioned previously, in 1996 a genome-wide linkage analysis of an Italian pedigree referred to as the Contursi kindred, identified the first gene implicated in familial PD on chromosome 4q21-q23, that contains the gene alpha-synuclein (Polymeropoulos et al., 1996), and named this locus PARK1. Also in this huge Italian family the missense mutation A53T leading to an amino acid substitution (Ala53Thr) was identified and thereafter confirmed in unrelated Greek families of familial PD (Polymeropoulos et al., 1997). SNCA mutations are an extremely rare cause of PD, however since the identification of the missense mutation A53T, six further pathogenic mutations have been found. The missense mutations A30P (Ala30Pro) and E46K (Glu46Lys) have been identified in one pedigree each, the A30P in a small German family (Kruger et al., 1998) and the E46K in a Basque family (Zarranz et al., 2004). Only very recently four additional mutations have been identified, namely the H50Q mutation in 2013 by Proukakis (Proukakis et al., 2013) that has been confirmed in additional studies (Appel-Cresswell et al., 2013, Ghosh et al., 2013, Khalaf et al., 2014), the two mutations A18T and A29S that have been identified in a single patient only by Hoffman-Zacharska in 2013 (Hoffman-Zacharska et al., 2013) as well as the A53E mutation that has been identified in a Finnish patient as well as in two other relatives all showing severe PD symptoms (Pasanen et al., 2014). Besides these missense mutations, also gene multiplications have been linked to familial PD and were referred to as PARK4. A genomic triplication of the complete SNCA gene was identified in the Spellman-Muenter kindred (Singleton et al., 2003) as well as in a Swedish-American family (Farrer et al., 2004). Additionally, a gene duplication was linked to autosomal dominant PD in a French family (Chartier-Harlin et al., 2004, Ibanez et al., 2004). The analysis of families with SNCA multiplication confirmed a direct relationship between SNCA gene dosage and the age of disease onset as well as disease progression and severity (Farrer et al., 2004). Patients carrying a SNCA duplication show the typical symptoms of idiopathic late age PD (Chartier-Harlin et al., 2004, Ibanez et al., 2004), whereas patients carrying a SNCA triplication show a young age of onset as well as fast and aggressive disease progression, severe weight loss, dementia and early death (Muenter et al., 1998, Singleton et al., 2003, Farrer et al., 2004, Fuchs et al., 2007). Even if missense mutations and gene multiplications of SNCA represent only a small number of PD cases, the presence of SNCA in Lewy bodies of sporadic PD cases highlights the importance of this gene and suggests that other modifications such as alternative-splicing, gene expression alterations or interaction with other genes may contribute to PD pathology (Gosal et al., 2006). This assumption is further supported by the identification of Rep1, a polymorphism within the SNCA promoter region that increases the SNCA expression and therefore possibly the prevalence of PD (Maraganore et

al., 2006, Seidel et al., 2010) as well as by the identification of single nucleotide polymorphism (SNP) in the 3'UTR that were recently confirmed by meta-analysis to have an effect on PD risk (Pankratz et al., 2012).

1.3.2.1.1 Protein Family and Function of Alpha-Synuclein

The synuclein protein family consists of three members alpha (α)- beta (β)- and gamma (γ)-synuclein. Synucleins are small proteins that are natively unfolded, show low hydrophathy and do not contain cysteins or tryptophans within their sequence (Surguchov, 2013). All three synuclein family members share a high sequence homology within the N-terminal end, the C-terminal end however is specific for each synuclein member (Surguchov, 2013). The SNCA gene, illustrated in figure 6, has six exons encoding a 140-amino acid and 14 kDa protein (Ueda et al., 1993) that consist of the three described domains, the N-terminus with an amphipathic lysine-rich α -helical domain that can associate with lipids such as membranes of presynaptic vesicles (reviewed in (Farrer, 2006, Lashuel et al., 2013, Ozansoy and Basak, 2013), a central region that was first purified from patients with Alzheimer's disease (AD) (Ueda et al., 1993, Masliah et al., 1996) as well as the specific C-terminal end that contains regions for fibrillization and aggregation (Ozansoy and Basak, 2013). The central region of SNCA is specific to this synuclein family member and contains a highly hydrophobic motif the so-called non-amyloid- β component of AD amyloid plaques (NAC) that is essential for aggregation (El-Agnaf et al., 1998, Giasson et al., 2001b, Luk et al., 2009).

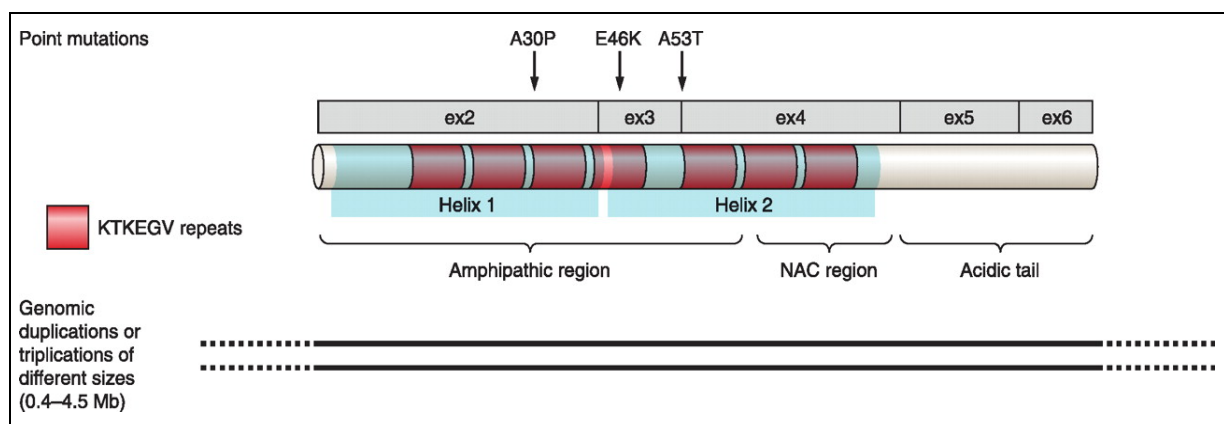


Fig. 6 Illustration of the SNCA gene as well as the protein structure, adapted from (Corti et al., 2011).

The N-terminal domain of SNCA as well as of β - and γ -synuclein contains seven imperfect repeats referred to as KTKEGV that form an amphipathic α -helical domain when the protein

associates with membranes or lipid rafts (Jensen et al., 1997, Fortin et al., 2004). The human SNCA maps to chromosome 4q21.3-q22 (Chen et al., 1995, Shibasaki et al., 1995, Spillantini et al., 1995) and the mouse SNCA maps to chromosome six (Touchman et al., 2001), however the intron/exon structure is highly conserved among human and murine SNCA (Touchman et al., 2001) and the proteins show 95.3% similarity (Lavedan, 1998). Mouse and human SNCA differ at exact seven amino acid sequences, interestingly in mouse the A53T substitution that is associated with familial PD is found naturally (Polymeropoulos et al., 1997, Rochet et al., 2000). For a long time SNCA was known to be a natively unfolded monomer (Weinreb et al., 1996, Eliezer et al., 2001), but recently the discussion about a helical tetrameric state in solution aroused (Bartels et al., 2011, Varkey et al., 2013, Selkoe et al., 2014) and so far remains feasible. However, in compliance with the original opinion the group of 2013 Nobel Prize winner Thomas Südhof confirmed an almost entirely monomeric state (Burre et al., 2013). According to these findings SNCA has the potential to form stable multimers and adopt additional structures in stress-induced conditions such as oxidative stress (Hashimoto et al., 1999), or upon interaction with other proteins, ligands, lipids or membranes (Giasson et al., 2001b, Lashuel et al., 2013), raising the possibility of an equilibrium between different conformational and multimeric stages. The three missense mutations A53T, A30P and E46K amplify the formation of multimers and oligomers, therefore destroying the equilibrium between monomers and oligomers and thus possibly triggering PD (Bertoncini et al., 2005). Already in 1988 SNCA was identified to be associated with synaptic vesicles, hence SNCA shows a presynaptic concentration (Maroteaux et al., 1988). In 1995 George and Iwai showed that SNCA localizes specifically to the nerve terminals and only little to the cell soma, dendrites or extrasynaptic sites along the axon (George et al., 1995, Iwai et al., 1995). SNCA is expressed mainly in the nervous system, however it is also found in red blood cells (Barbour et al., 2008). In order to understand the function of SNCA it is important to analyze its cellular localization and its interactions. It is still enigmatic how SNCA localizes to the nerve terminal, fractioning analysis revealed a very weak association to synaptic vesicles whereas most of the SNCA protein exists in soluble condition (Kahle et al., 2000, Fortin et al., 2004). Besides, it is known that SNCA has a preference to bind membranes with high curvature (Middleton and Rhoades, 2010, Jensen et al., 2011), speaking in favor of its vesicle binding properties. Studies in mice with SNCA knockdown showed impaired synaptic response after high frequency stimulation and impairment in re-filling and trafficking of synaptic vesicles (Abeliovich et al., 2000, Cabin et al., 2002). Transgenic mice that overexpress either human wild-type SNCA or A53T-SNCA, again showed reduced neurotransmitter release as well as impaired vesicle exocytosis (Yavich et al., 2004, Kurz et al., 2010, Nemani et al., 2010, Scott et al., 2010, Platt et al.,

2012, Tozzi et al., 2012). The exact same results were found in studies of rats with SNCA overexpression by unilateral injection of an adeno-associated virus type 6 (AAV6)- α -synuclein vector (Gaugler et al., 2012, Lundblad et al., 2012) as well as in studies of PC12 stable cell lines (Larsen et al., 2006). In a more detailed and general view, the overexpression of SNCA leads to a reduction of releasable vesicles (Gaugler et al., 2012) and due to its impact on endocytosis affects the recycling of vesicles leading to a reduced amount of reserve pool vesicles (Nemani et al., 2010, Scott and Roy, 2012). Besides its interaction with synaptic vesicles, SNCA was also reported to interact with proteins controlling vesicle endocytosis such as phospholipase D2 (Payton et al., 2004) and members of the RAB small GTPases family (Dalfo and Ferrer, 2005). In 2010 the group of the already mentioned Nobel Prize winner Thomas Südhof published a role of SNCA as non-classical chaperone that promotes SNARE-complex assembly and maintenance (Burre et al., 2010). Although the complete cellular function of SNCA is still unknown, the localization to presynaptic terminals as well as its interaction with synaptic vesicles and the observed neurotransmission deficiency in SNCA knockdown or overexpressing mice is in favor for SNCA having a role in the regulation of neurotransmission, especially neurotransmitter release, synaptic function and plasticity (illustrated in figure 7 that was adapted from (Lashuel et al., 2013).

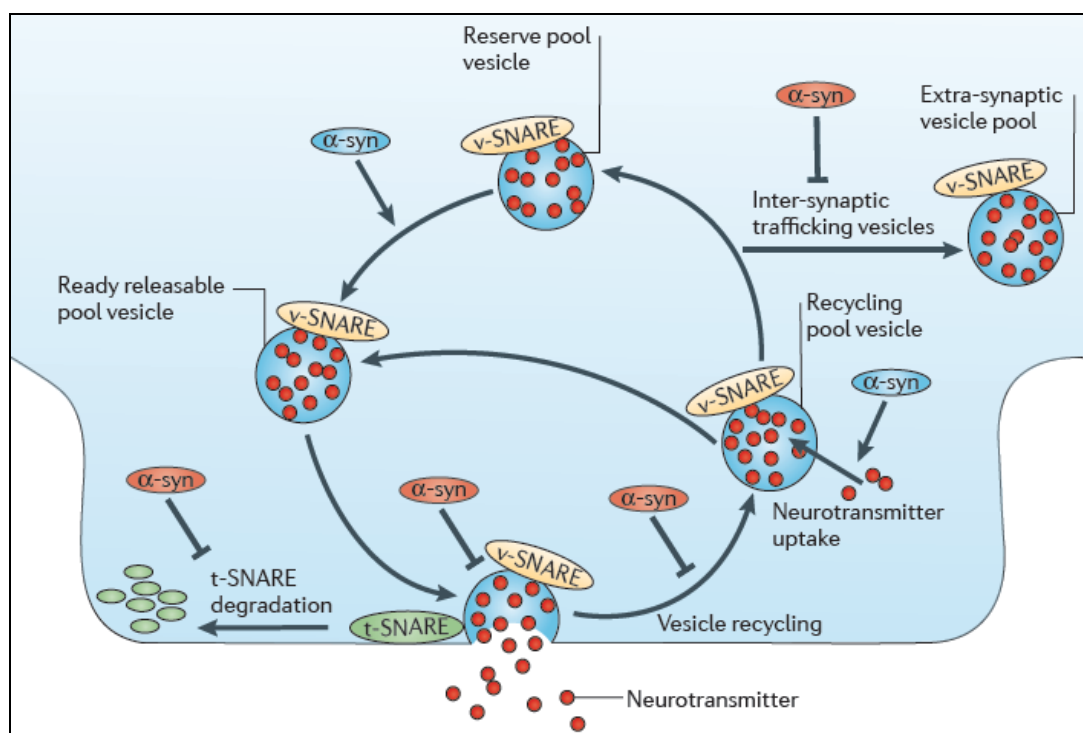


Fig. 7 Illustration of the presynaptic function of SNCA in neurotransmission. The function of SNCA in the regulation of vesicle trafficking and refilling is shown in blue. SNCA in red shows the effects of accumulation with impairment of neurotransmitter release as well as vesicle recycling and trafficking. Abbreviation: SNARE = soluble N-ethylmaleimide-sensitive fusion factor attachment protein receptors; v-SNARE = vesicle-associated SNARE; t-SNARE = target membrane-associated SNARE; Figure adapted from (Lashuel et al., 2013).

The second member of the synuclein family is β -synuclein (SNCB). SNCB is a natively unfolded 134 amino acid containing protein that has a 78% sequence homology with SNCA (Uversky et al., 2002). The human SNCB gene is located on chromosome 5q35 (Spillantini et al., 1995) and is encoded by 7 exons, whereas exon 2 is variably inserted leading to two SNCB transcript variants, both translated into the same protein (Beyer et al., 2010). The mouse SNCB maps to chromosome 13 (Sopher et al., 2001) and encodes a protein of 133 amino acids, therefore the mouse and human SNCB protein share 97.8% identity (Lavedan, 1998). Mutations within the SNCB gene have been associated to dementia with Lewy bodies (Ohtake et al., 2004). The expression level of SNCB is similar to SNCA and both co-localize at presynaptic terminals (Maroteaux et al., 1988). In contrast to SNCA, SNCB lacks 11 amino acid residues in the central region leading to an interruption of the helical structure possibly leading to the non-amyloidogenic characteristics of this synuclein family member (Sung and Eliezer, 2007). Respectively, SNCB was found to inhibit the aggregation of SNCA in vitro (Park and Lansbury, 2003, Tsigelny et al., 2007) and in double transgenic mice (Hashimoto et al., 2001). Additionally, SNCB has been shown to have anti-apoptotic properties (da Costa et al., 2003), cell protective properties (Hashimoto et al., 2004) as well as the ability to restore proteasomal activity that was inhibited by SNCA (Snyder et al., 2005). The third member of the synuclein family is γ -synuclein (SNCG). SNCG was originally termed *breast cancer-specific gene 1* due to its very high abundance in breast cancer (Ji et al., 1997). The human SNCG is a 127-amino acid containing protein that is encoded by 5 exons and has been mapped to chromosome 10q23 (Lavedan et al., 1998), whereas the mouse SNCG is located on chromosome 14 (Alimova-Kost et al., 1999) encoding a 123-amino acid containing protein. Therefore, human and mouse SNCG are 87.7% identical. SNCG is expressed to a much higher extent in human brain, particularly in the substantia nigra and the cortex (Lavedan et al., 1998) whereas the expression in mouse cortex is rather low (Giasson et al., 2001a). Immunohistochemical analysis of SNCG revealed a diffuse distribution through cell bodies and axons of specific peripheral neurons, in particular dopaminergic neurons, and in glia (Buchman et al., 1998, Galvin et al., 2001, Brenz Verca et al., 2003). As mentioned previously, SNCG was originally identified in breast cancer and detailed analysis of its function demonstrated a chaperone activity as well as a role in the stimulation of estrogen receptor (ER)- α signaling, which is important in mammary tumorigenesis (Jiang et al., 2004), therefore SNCB may serve as prognostic tool for the identification of tumorigenesis (Ahmad et al., 2007).

1.3.3 Autosomal recessive forms of PD

In an autosomal recessive inheritance the mutation needs to be present in both copies of the specific gene in order to cause the disease. The identification of recessive loci is done by linkage mapping in nuclear families or by autozygosity mapping in blood related families (Wang et al., 2009). In PD, homozygous or compound heterozygous mutations have been found in three genes that encode Parkin (PARK2), DJ-1 (PARK7) and PTEN-induced kinase 1 (PINK1) (PARK6) (Kitada et al., 1998, Bonifati et al., 2003, Valente et al., 2004). Like most recessive alleles these three mutations result in a loss-of-function leading to an early onset of PD with relatively slow progression and good levodopa-responsiveness (Abou-Sleiman et al., 2004, Mata et al., 2004). Among these three autosomal recessive forms of PD, mutations in the *Parkin* gene represent the most frequent cause of early-onset (<40-50 years) PD (Lucking et al., 2000, Periquet et al., 2003). Mutations in *Parkin* were first identified in Japanese families of juvenile PD with an age of onset frequently before age 20 (Kitada et al., 1998). Since then, more than 170 mutations have been identified within this large gene of 1.35 Mb (Nuytemans et al., 2010). Mutations within *DJ-1* constitute the least common form of autosomal recessive PD representing about 1% of early onset PD (Hedrich et al., 2004, Lockhart et al., 2004). The second most frequent cause among autosomal recessive forms of PD are mutations within *PTEN-induced kinase 1 (PINK1)* (Valente et al., 2001, Valente et al., 2002, Valente et al., 2004).

1.3.3.1 PTEN-induced Kinase 1 (Park6)

PTEN-induced kinase 1 (PINK1) maps to chromosome 1p35-36 (Valente et al., 2001), contains 8 exons and encodes a 581 amino-acid containing protein with a predicted mass of 63 kDa (Valente et al., 2004). The *PINK1* transcript is ubiquitously expressed and encodes a 34 amino-acid mitochondrial target motif (MTS), a putative transmembrane region (TM) as well as a serine-threonine kinase domain that shows a high degree of homology to serine/threonine kinases of the Ca²⁺/calmodulin family (Valente et al., 2004) (Illustration is shown in figure 8).

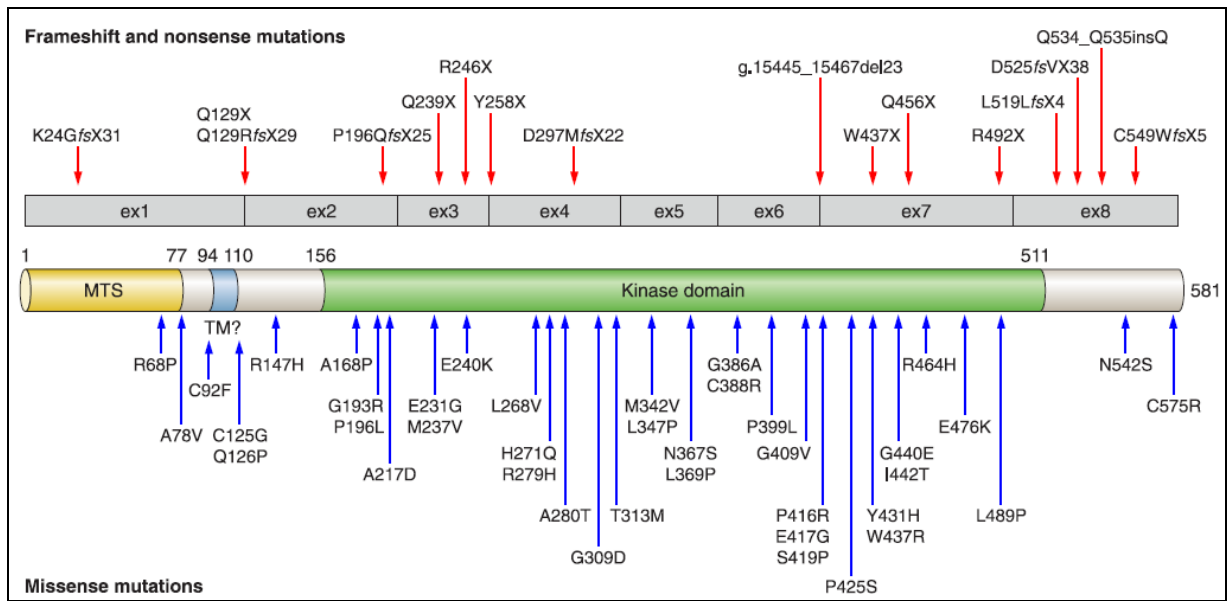


Fig. 8 Illustration of *PINK1* on transcript level and presentation of the functional protein domains. Red arrows above the transcript show frameshift and nonsense mutations and blue arrows below the protein show missense mutations. Abbreviations: MTS = mitochondrial target sequence; TM = transmembrane domain. Figure adapted from (Corti et al., 2011).

Up to now, several homozygous recessive and compound heterozygous mutations in *PINK1* have been found in 1-2% of early-onset PD (Hatano et al., 2004). The first mutation in *Pink1* was identified by Valente and colleagues in 2004 in one Spanish and two Italian families (Valente et al., 2004). Since then mutations in *PINK1* have been described to have effects on the protein stability, the localization and on its kinase activity (Beilina et al., 2005, Petit et al., 2005).

1.3.3.1.1 *PINK1* Function and Role for Parkinson's Disease

The understanding of *PINK1* on a functional level rose within the last years. The first functional evidence suggested a protective role for *PINK1* in neurons from stress-induced mitochondrial dysfunction (Valente et al., 2004). *PINK1* harbors a mitochondrial target sequence, and is recruited to damaged mitochondria (Narendra et al., 2010) where it is mainly placed in the outer mitochondrial membrane with the C-terminus and the kinase domain facing the cytosol (Zhou et al., 2008). In healthy conditions the mitochondrial target sequence of *PINK1* is cleaved by the mitochondrial precursor protease (MPP) in a mitochondrial membrane potential-dependent fashion and immediately degraded by the protease PARL (presenilin-associated rhomboid-like protein) (Whitworth et al., 2008, Deas et al., 2011, Meissner et al.,

2011, Shi et al., 2011). During mitochondrial stress however, the full-length protein of PINK1 is stabilized and accumulates in the damaged and depolarized mitochondria where it recruits the E3 ubiquitin ligase Parkin. Parkin then facilitates the ubiquitination of mitofusin (Tanaka et al., 2010), a mitochondrial fusion-promoting factor, and promotes the degradation of damaged mitochondria through mitophagy, known as the selective degradation of mitochondria by autophagy (Whitworth and Pallanck, 2009, Jones, 2010). Besides, Christofol Vives-Bauza and Serge Przedborski (Vives-Bauza and Przedborski, 2011) discussed a model where p62/SQSTM1 and histone deacetylase 6 (HDAC6) may sequester the ubiquitine targeted mitochondria and link them to autophagosome bound LC3. Thereafter, via retrograde transport potentially mediated by PINK1, autophagosomes fuse to lysosomes where damaged mitochondria will be degraded using lysosomal hydrolases. The model that resulted from these studies is depicted in figure 9 showing the PINK1/Parkin mitochondrial quality control pathway (adapted from (Pallanck, 2010)).

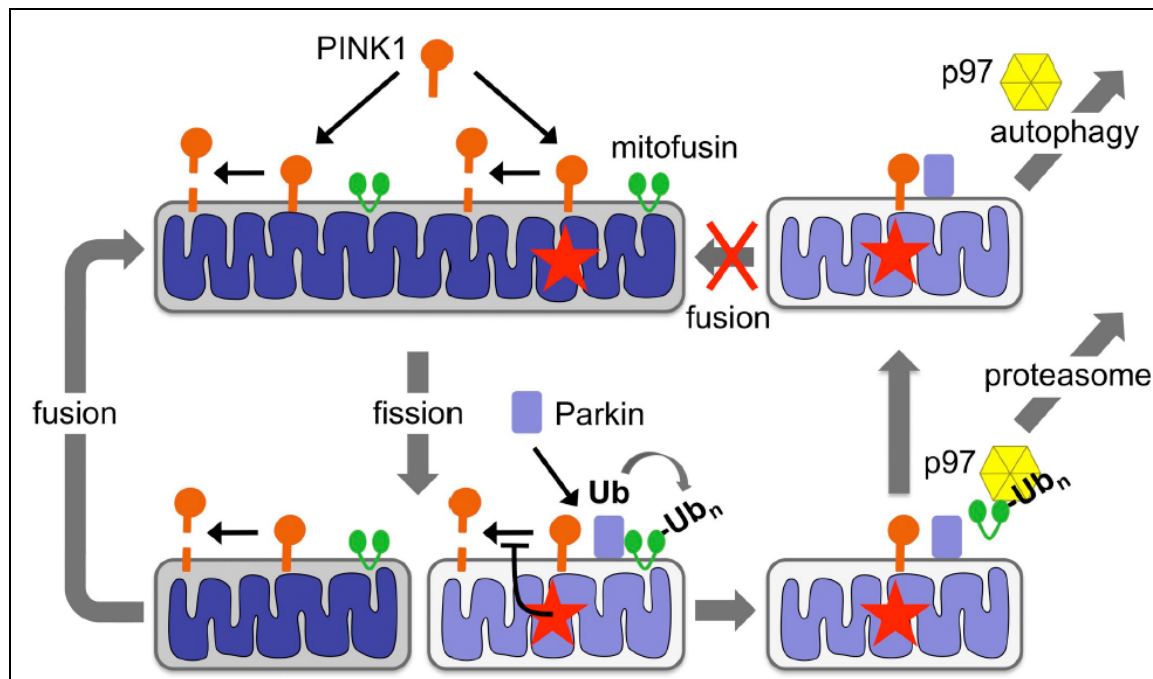


Fig. 9 The PINK1/Parkin mitochondria quality control pathway. Red stars indicate mitochondrial damage. PINK1 harbors a mitochondrial target sequence and is therefore placed in the outer mitochondrial membrane with the C-terminus and the kinase domain facing the cytosol. In healthy conditions, PINK1 is cleaved in a mitochondrial membrane potential-dependent fashion by the mitochondrial precursor protease (MPP) and immediately degraded through the protease PARL (presenilin-associated rhomboid-like protein). Mitochondrial damage stabilizes PINK1, which accumulates and recruits the E3 ubiquitin ligase Parkin. Parkin promotes the degradation of damaged mitochondria through mitophagy by ubiquitination of mitofusin. Figure was taken from (Pallanck, 2010).

As mentioned previously, several homozygous recessive and compound heterozygous mutations in PINK1 have been found in early-onset PD, all leading to a loss of function, therefore

deficits in PINK1 are considered to drive PD pathology. According to the current opinion, deficits in PINK1 or Parkin alter mitochondrial fission and fusion and impair mitochondrial quality control, an essential homeostatic mechanism that provides sufficient amounts of functional mitochondria to maintain the energy demands of a cell. In this respect it has been shown, that loss of PINK1 impairs mitophagy after stress and leads to accumulation of damaged mitochondria (Geisler et al., 2010, Narendra et al., 2010, Vives-Bauza et al., 2010). Studies in our lab documented the involvement of PINK1 in the cellular stress response to starvation (Mei et al., 2009, Klinkenberg et al., 2012), showing PINK1 transcription activation in parallel to general autophagy. Furthermore, our lab could demonstrate that reduced *PINK1* expression level in combination with additional stress compromises the autophago-lysosomal pathway and results in increased cell death (Parganlija et al., 2014). In addition to its function for mitochondrial quality control, PINK1 is also involved in the Ca^{2+} -efflux regulation within neurons as well as in the protection against oxidative stress (Hoepken et al., 2007, Gautier et al., 2008, Wood-Kaczmar et al., 2008, Gandhi et al., 2009). In this respect, the study of Hoepken analyzed skin fibroblasts of a Spanish PARK6 family, where PINK1 loss-of-function resulted in mitochondrial dysfunction, peroxidation damage and changes in the ROS defending glutathione system (Hoepken et al., 2007). This human PARK6 skin fibroblasts also showed increased *SNCA* mRNA levels (Hoepken et al., 2008), giving the very first evidence of a shared pathophysiology of autosomal dominant and autosomal recessive inherited PD.

1.4 Therapy of Parkinson's Disease

There are three major modalities of PD therapy, medications, surgery (deep brain stimulation) and physical therapy. Up to this day, there is no PD treatment available that interferes with the neurodegenerative process, but pharmacological therapies with strong beneficial impact on the motor symptomatic of PD are available and there are several exciting drugs that are only evolving (see overview in figure 10 adapted from (Schapira et al., 2014)). The current gold standard treatment of PD motor symptoms is the dopamine replacement therapy using the DA precursor 3,4-dihydroxyphenyl-L-alanine (L-DOPA or levodopa). L-DOPA is an immediate precursor of dopamine that, in contrast do dopamine itself can cross the blood-brain barrier using the large amino-acid transporter (Wade and Katzman, 1975, Oldendorf and Szabo, 1976, Hardebo and Owman, 1980, Kageyama et al., 2000). As soon as L-DOPA crossed the blood-brain barrier it enters the remaining dopaminergic and serotonergic neurons and is converted into dopamine by an enzyme called L-aromatic amino-acid decarbox-

ylase (AADC) (Hokfelt et al., 1973, Arai et al., 1994, Arai et al., 1995, Arai et al., 1996, Tanaka et al., 1999). Generally, L-DOPA is administered in combination with a peripheral decarboxylase inhibitor such as carbidopa or benserazide that do not significantly cross the blood-brain barrier, in order to prevent the formation of dopamine in peripheral tissues allowing a higher amount of L-DOPA to enter the brain (Bertler et al., 1966, Constantinidis et al., 1968, Duvoisin and Mytilineou, 1978). Oral administration of L-DOPA is the most effective treatment of PD motor symptoms, however the majority of PD patients treated with L-DOPA develop severe side effects including both motor complications, such as dyskinesia (abnormal involuntary movements) and “wearing off fluctuations”(Obeso et al., 2000a, Ahlskog and Muentner, 2001) as well as non-motor complications, such as hallucination and psychosis (Moskowitz et al., 1978, Nausieda et al., 1984, Aarsland et al., 1999, Ahlskog and Muentner, 2001). These side effects occur in about 40% of PD patients after 4-6 years of L-DOPA treatment and in 90% of patients after 10 years of treatment (Ahlskog and Muentner, 2001, Obeso et al., 2004, Mazzella et al., 2005, Manson et al., 2012).

The most powerful drugs in treating PD motor symptoms after L-DOPA are dopamine agonists such as bromocriptine, pergolide, pramipexole and apomorphine which seem to be the most effective. Apomorphine is a non-selective dopamine receptor agonist with a slightly higher preference for D2 receptors (Millan et al., 2002). Apomorphine is very well tolerated with a low frequency of side effects, but since it needs to be injected subcutaneously it provides some risk for infections. Already in 1951 Schwab and colleagues showed that apomorphine is effective in treating tremor and rigidity of PD patients (Schwab et al., 1951). Furthermore, in 1979 Corsini demonstrated the beneficial use of subcutaneous apomorphine in combination with domperidone to relieve vomiting (Corsini et al., 1979) and Hardie confirmed these findings in 1984 (Hardie et al., 1984). In 1990 Kempster and colleagues compared the effect of a single dose of subcutaneous apomorphine with a single oral dose of L-DOPA in 14 PD patients and showed an indistinguishable response pattern regarding the quality of motor response after drug administration but with a shorter motor response after apomorphine (Kempster et al., 1990). Importantly, apomorphine has some advantages compared to L-DOPA. Studies show, that apomorphine monotherapy can reset peak-dose dyskinesia in L-DOPA treated patients and there have been reports about beneficial effects on PD non-motor symptoms (Manson et al., 2002).

Glutamate inhibitors and antimuscarine drugs such as amantadine are also used in PD treatment and have shown potential neuroprotective properties in animal models of PD (Turski et al., 1991, Greenamyre et al., 1994, Doble, 1999, Schapira et al., 2006). Very recently the effect

of inflammation on the pathogenesis of PD, which includes microglia activation and the expression of proinflammatory cytokines, was studied (McGeer et al., 1988, Boka et al., 1994, Hunot et al., 1999). There is evidence that the suppression of reactive astrocytes or the reduced expression of proinflammatory cytokines has neuroprotective properties (Chung et al., 2010a, Chung et al., 2010b). The role of inflammation in PD pathogenesis is furthermore supported by the finding of Chen et al., showing a lower risk of developing PD when using anti-inflammatory drugs (Chen et al., 2003).

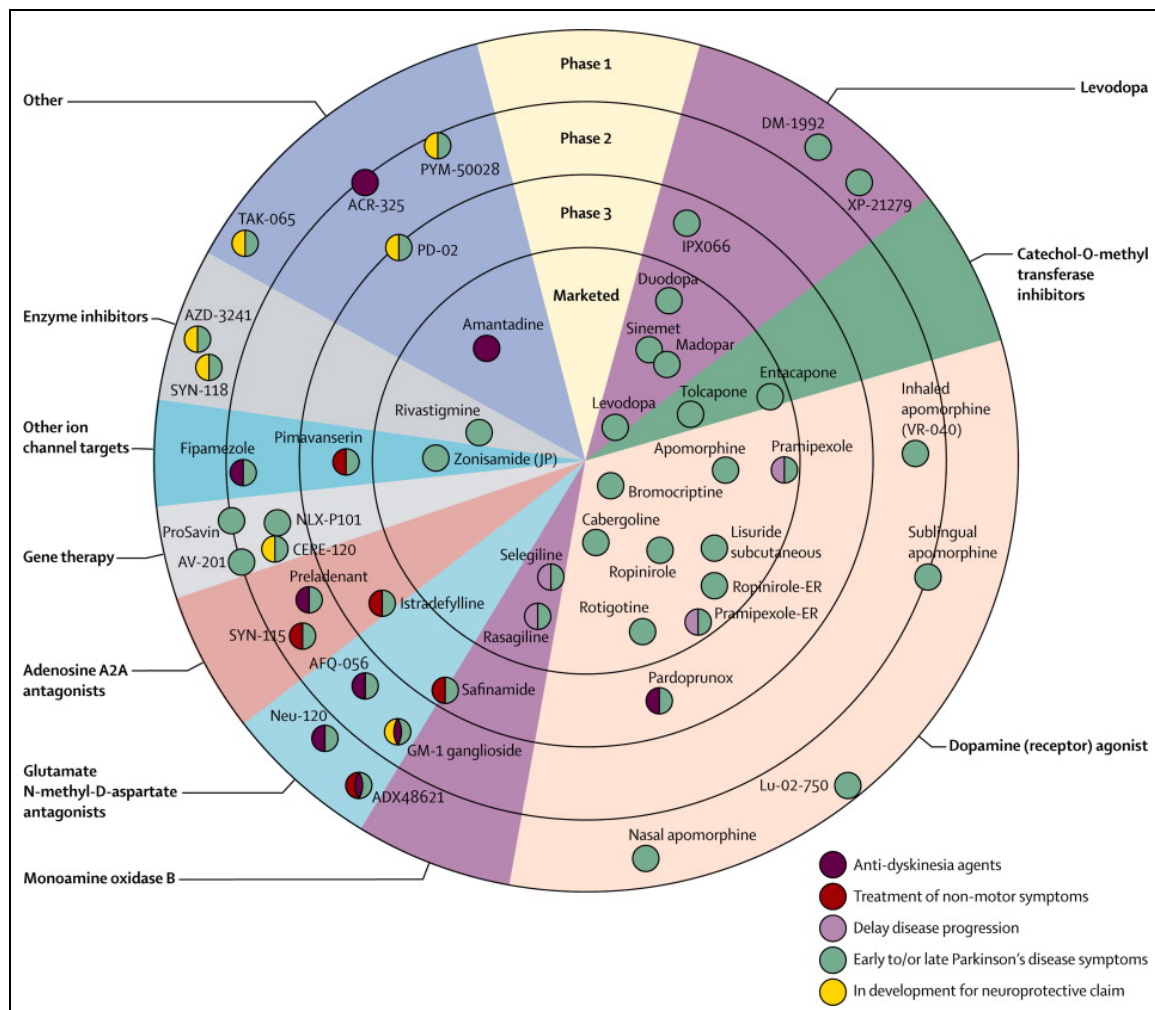


Fig. 10 Overview of available drugs for PD motor and non-motor symptoms as well as exciting new drugs that are in development. Each pharmacological agent is shown according to its mechanism of action, target indication, and phase of development. Figure was taken from (Schapira et al., 2014).

1.4.1 Therapeutic Side Effects - Levodopa Induced Dyskinesia

PD motor symptoms are only recognized when more than 50% of dopaminergic neurons are dead, indicating that there are strong compensatory mechanisms that buffer deficits that

come along with the neuronal loss. This example illustrates a very important ability of the brain known as neuroplasticity. Already in 1893 Tanzi stated that changes in existing connections rather than actual neuronal growth underlie the storage of information in the brain (Tanzi, 1893) and in the same year Cajal speculated that the mechanism of learning requires growth of neuronal processes and not the development of new neurons (Ramón y Cajal, 1893). These two ideas were combined in the well-known proposal of Hebb, explaining the basic principle of synaptic plasticity where he stated that alterations in synaptic strength, as well as the formation of new synapses can mediate the formation of memory (Hebb, 1949). Under physiological conditions, synaptic plasticity occurs at dendritic spines (Desmond and Levy, 1990) and in the striatum the majority of neuronal cells are medium spiny neurons (MSNs) that are characterized by a huge number of spines. It is well established that MSNs show both principal forms of synaptic plasticity events namely long-term-potentialiation (LTP) (Calabresi et al., 1992c, 1996, Centonze et al., 1999) and long-term-depression (LTD) (Calabresi et al., 1992b, Lovinger et al., 1993). Striatal LTP is characterized by a long-term increase of glutamatergic synaptic efficiency (Calabresi et al., 1992c, Charpier and Deniau, 1997), while LTD is characterized by a long-term decrease of synaptic efficiency (Calabresi et al., 1992a, Calabresi et al., 1992b, Calabresi et al., 1994, Choi and Lovinger, 1997b, a). The induction of striatal synaptic plasticity (illustrated in figure 11) occurs in interaction with dopamine, which plays a critical role in the development of striatal LTP and LTD by acting on D1 and D2 receptors with other neurotransmitters such as glutamate, acetylcholine, nitric oxide and endogenous cannabinoids. The requirement of endogenous dopamine for the induction of synaptic plasticity is unique to the striatum and is not found in other brain areas (reviewed in (Calabresi et al., 2007)). In brief, there is experimental evidence that dopamine acting on D1 receptors induces LTP, whereas the induction of LTD requires both D1 and D2 receptor activation (Calabresi et al., 1992a, Calabresi et al., 2000, Picconi et al., 2003). The direction of synaptic plasticity, resulting either in LTP or LTD, critically depends on the level of membrane depolarization as well as on the involvement of different subtypes of ionotropic glutamate receptor subunits (Bagetta et al., 2010). The induction of striatal LTP requires high frequency stimulation in Mg^{2+} -free medium that allows the activation of NMDA receptors which is mandatory for LTP induction (Calabresi et al., 1992c). NMDA receptor activation itself requires the presynaptic glutamate release and a strong postsynaptic membrane depolarization at the same time to enable the relieve of the Mg^{2+} block within the channel (Calabresi et al., 1992c). LTD in contrast, does not require the activation of NMDA receptors, therefore high frequency stimulation in presence of Mg^{2+} ions is sufficient to induce this form of synaptic plasticity.

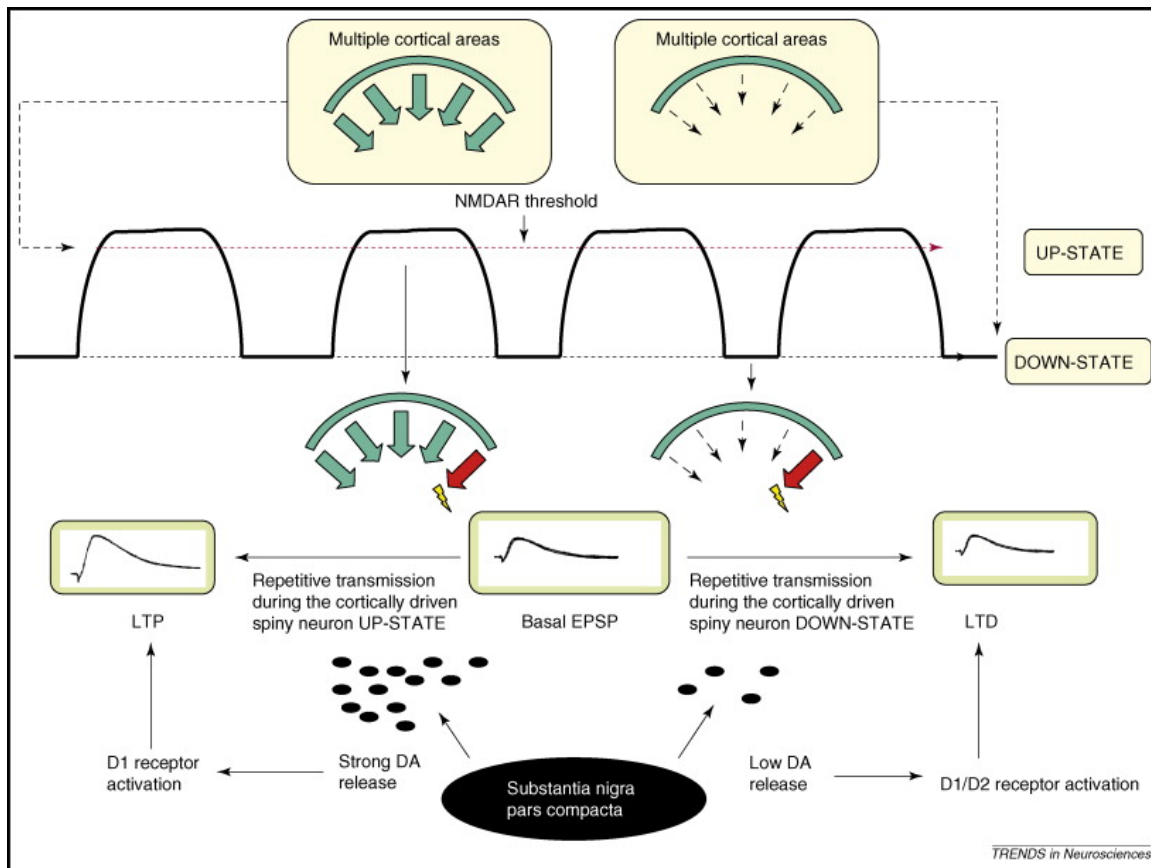


Fig. 11 Illustration of striatal LTP and LTD induction. The membrane potential of MSNs oscillates between depolarized 'up' and hyperpolarized 'down' state, upon glutamatergic cortical input. LTP induction requires a repetitive neuronal transmission during the 'up' state, in order to overcome the threshold needed to activate NMDA receptors, and strong dopamine release from the SNc. In contrast, LTD induction requires repetitive neuronal transmission that occurs at the 'down' state and lower dopamine release from the SNc. Figure was taken from (Calabresi et al., 2007).

In PD, the severe neurodegeneration of dopaminergic neurons leads to a deficit of dopamine in the striatum attended by alterations in striatal synaptic transmission and plasticity. Several studies indicate that the deficiency of striatal dopamine causes an overactivity of glutamatergic transmission that can be measured as increased excitatory spontaneous activity in MSNs (Calabresi et al., 1993, Tang et al., 2001, Gubellini et al., 2002), reflecting a reduced pre-synaptic D2 receptor activation, which in healthy conditions controls glutamate release (Cepeda et al., 2001). At the postsynaptic level, dopamine deficiency leads to decreased activation of D2 receptors and therefore to increased Ca^{2+} influx by voltage-gated ion channels that are usually inhibited by the D2 receptor (Desmond and Levy, 1990). The increased amounts of Ca^{2+} are possibly involved in the degenerative process of synaptic spines that can be observed in animal models of PD as well as in PD patients (Ingham et al., 1989, Nitsch and Riesenberg, 1995, Arbuthnott et al., 2000, Day et al., 2006). There is experimental evidence

that the morphological alterations of spines result in an impairment of either LTP (Centonze et al., 1999) or LTD (Calabresi et al., 1993).

As mentioned earlier, L-DOPA treatment of PD motor symptom results in more than 50% of all cases in severe side-effects known as levodopa induced dyskinesia. Studies using 6-hydroxydopamine lesioned (6-OHDA) rodent models of PD, showed that chronic administration of L-DOPA improves motor performance and admits the recovery of synaptic plasticity in MSNs of dyskinetic and non-dyskinetic animals (Picconi et al., 2003, Picconi et al., 2004). However, in dyskinetic animals an impossibility to restore the level of synaptic transmission prevenient to LTP may reflect an abnormality of synaptic plasticity (Picconi et al., 2003). In contrast, in non-dyskinetic 6-OHDA animals L-DOPA is able to restore the physiological synaptic plasticity. On a biochemical level the analysis of 6-OHDA animals revealed that the loss of synaptic plasticity in dyskinetic animals is attributed to changes within D1 receptor signaling pathways leading to abnormalities of the cGMP/phosphodiesterase/cAMP/DARPP-32 signaling cascade (Picconi et al., 2003, Giorgi et al., 2008), the extracellular signal-regulated kinases 1 and 2 (ERK1/2)(Gerfen et al., 2002, Pavon et al., 2006, Westin et al., 2007), as well as the retrograde endocannabinoid Cb1 neurotransmission including the mGluR5 pathway (Huot et al., 2013, Pinna et al., 2014).

1.4.1.1 Molecular Basis of Levodopa Induced Dyskinesia

Today's mainstream pathophysiological concept about the source of levodopa induced dyskinesia (LID) says that LID results both from pre- and postsynaptic abnormalities in dopamine signaling as well as from changes in synaptic plasticity (reviewed in (Brotchie and Jenner, 2011, Fisone and Bezard, 2011, Murer and Moratalla, 2011, Ghiglieri et al., 2012, Cenci, 2014). On a presynaptic level, studies in rodent models of PD as well as in dyskinetic patients revealed an association of abnormal involuntary movements that are characteristic for LID with a dysregulation of dopamine release and clearance (reviewed in (Cenci and Lundblad, 2006). On a postsynaptic level, LID is accompanied by maladaptations within the direct pathway of D1 receptor positive striatal MSNs (Aubert et al., 2005, Cenci, 2007, Darmopil et al., 2009). The signaling cascade that is acting as a master switch for striatal synaptic plasticity is the extracellular signal-regulated kinases 1 and 2 (ERK1/2) cascade (reviewed in (Cenci et al., 2009) , that is shown in a simplified cartoon in figure 12.

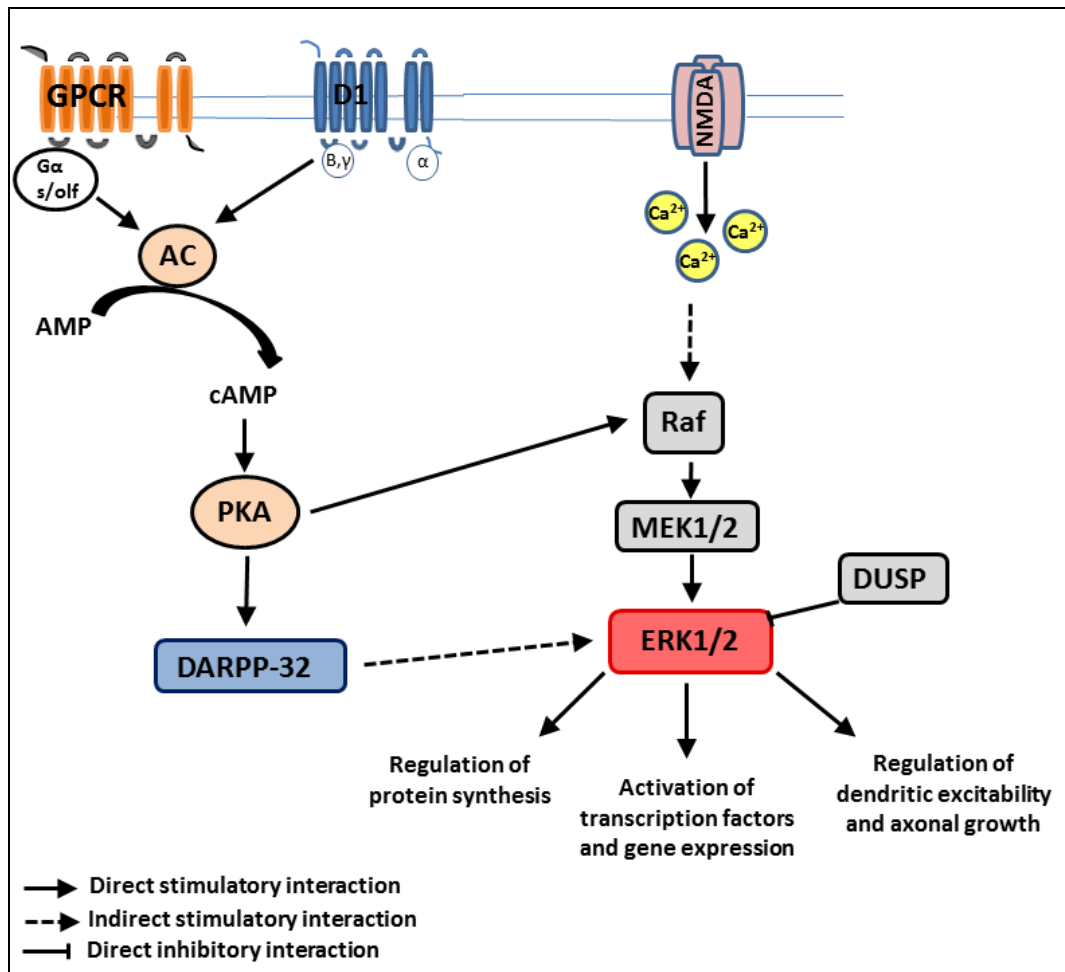


Fig. 12 Simplified cartoon of signaling pathways involved in synaptic plasticity. The extracellular signal-regulated kinases 1 and 2 (ERK1/2) signaling cascade: ERK1/2 is activated through phosphorylation by mitogen-activated protein kinase kinases (MEK1/2) and dephosphorylated by members of the dual-specific phosphatases family (DUSP). The cGMP/phosphodiesterase/cAMP/DARPP-32 signaling cascade: DARPP-32 is phosphorylated by protein kinase A (PKA) and via indirect stimulatory interaction influences ERK1/2 activity. Abbreviations: GPCR = G-protein coupled receptor; D1 = dopamine receptor D1; NMDA = ionotropic glutamate receptor.

ERK1/2 is activated through dual phosphorylation at the residues threonine-183 and tyrosine-185 by mitogen-activated protein kinase kinases (MEK) downstream of D1 receptors (Gerfen et al., 2002, Bezard et al., 2005, Pavon et al., 2006, Santini et al., 2007, Westin et al., 2007, Fasano et al., 2010) and is dephosphorylated by members of the dual-specific phosphatase family (DUSP) (Sun et al., 1993, Caunt and Keyse, 2013). Increased striatal phosphorylated ERK1/2 is correlated with abnormal involuntary movements in 6-OHDA-lesioned animals. Increased activity of the ERK1/2 signaling cascade is a possible response to exogenous L-DOPA stimulation of supersensitive D1 receptors in late stages of PD. The crucial role of supersensitive D1 receptors for LID has been demonstrated in rodent and monkey models of PD (Aubert et al., 2005, Santini et al., 2007, Westin et al., 2007, Darmopil et al., 2009, Lindgren

et al., 2009). In 6-OHDA mice and rats treatments that reduced ERK1/2 phosphorylation could reduce the severity of abnormal involuntary movements (Santini et al., 2007, Schuster et al., 2008, Lindgren et al., 2009). Thereupon, activated ERK1/2 induces the phosphorylation of mitogen- and stress-activated protein-kinase 1 (MSK-1) (Deak et al., 1998, Dunn et al., 2005) which then phosphorylates histone H3 (Soloaga et al., 2003, Santini et al., 2009) and mediates the activation of transcription factors and gene expression. Experimental studies in 6-OHDA animals could show that the expression pattern of several genes is correlated with LID, the most important among those is an upregulation of the immediate early genes *Fos*, *Homer1a* and *Nur77* (Sgambato-Faure et al., 2005). Studies analyzing the expression pattern of genes associated with LID stated that these gene expression changes point to elevated metabolic demands and energy consumption as well as alterations in synaptic plasticity (El Atifi-Borel et al., 2009).

1.5 Mouse Models of Parkinson's Disease

PD is clinically and genetically heterogeneous and is usually diagnosed when motor symptoms occur and about 50% of dopaminergic neurons are lost (Bernheimer et al., 1973, Fearnley and Lees, 1991). The main goal of PD research is to identify markers of early pre-symptomatic PD stages and develop specific therapeutic targets to prevent PD pathology and the development of motor impairments. In order to make this future dreams come true, one needs to understand the pathobiological underpinnings of the disease. Since PD is a very heterogeneous disorder, there is not one single model that displays the complete phenomenology as is occurs in humans, but the use of several different models mimicking a specific part of PD pathology provides a valuable tool in PD research. Genome-wide association studies and linkage analysis identified several genes and their encoded proteins that are associated with PD, and genetically engineered animal models offer a great platform to study the function of these genes and therefore explore the pathobiology of PD.

1.5.1 Genetically Engineered Mouse Models of PD

Genetically engineered mouse models of PD provide the possibility to model early stages and progression of PD. They also offer the benefit of studying the effect of mutations within the entire organism and most important in case of PD within the intact circuitry of the brain. To

date there are many rodent models of PD available, three of them will be introduced in more detail since they provide a key aspect of this study.

1.5.1.1 The A53T-SNCA Overexpressing Mouse Model

The A53T-SNCA overexpressing mouse line (PrPmtA) expresses human alpha-synuclein cDNA, including the missense mutation A53T, under control of the murine specific PrP promoter and was originally generated and characterized by Suzana Gispert and colleagues (Gispert et al., 2003). The PrPmtA mouse line shows a 1.5 fold nigrostriatal and corticostriatal overexpression of A53T-SNCA in absence of midbrain neuronal cell loss or aggregate formation (Gispert et al., 2003), which is in contrast to other SNCA overexpressing mouse models that show aggregate formation and cell loss (Masliah et al., 2000, Richfield et al., 2002, Tofaris et al., 2006). This mouse line is further characterized by an age-progressive pathology that becomes apparent between 6 and 18 months of age, showing on a behavioral level reduced spontaneous vertical motor activity (Gispert et al., 2003). On a molecular level PrPmtA mice show an impaired vesicle release (Platt et al., 2012, Tozzi et al., 2012) resulting in increased dopamine levels as well as in decreased dopamine-regulated expression profiles in the striatum (Kurz et al., 2010). Electrophysiological investigations revealed impaired long-term depression of glutamatergic neurotransmission in corticostriatal slices that can be rescued by phosphodiesterase antagonism (Kurz et al., 2010, Tozzi et al., 2012). Taken together, the A53T-SNCA overexpressing mouse line PrPmtA provides a useful tool to study presymptomatic stages of PD as well as possible postsynaptic maladaptions.

1.5.1.2 The *Pink1*KO Mouse Model

The *Pink1*KO mouse model was originally generated by Suzana Gispert and colleagues and characterized for the first time in Gispert et al., 2009 (Gispert et al., 2009). This mouse line shows a 97% knock-down of the *Pink1* transcript and a loss-of function mutation in the remaining mRNA, resulting in a model with similar quality to other *Pink1* knock-out mouse lines (Kitada et al., 2007). On a behavioral level, the *Pink1*KO mouse from Gispert demonstrates a progressive reduction of bodyweight as well as reduced spontaneous movements in open field analysis (Gispert et al., 2009). The reduced bodyweight became significant already at the age of 1 year with an average weight reduction of 19%, possibly reflecting impaired bioenergetics and mitochondrial dysfunction. Measurement of other behavioral parameters such as anxiety, strength and coordination remained unaffected. On a molecular level,

*Pink1*KO mice show a significant reduction of striatal dopamine content at the age of 9 and 22-24 month (Gispert et al., 2009). Furthermore, analysis of mitochondrial ATP levels and the mitochondrial proton gradient demonstrated a progressive mitochondrial dysfunction starting already at the age of 6 months (Gispert et al., 2009). Morphological analysis revealed no signs of neurodegeneration or aggregate formation in *Pink1*KO mice. At perinatal age mitochondria of *Pink1*KO mice showed normal morphology, but after stress they demonstrated altered fragmentation and enhanced perinuclear aggregation, illustrating the role of PINK1 in stress response (Gispert et al., 2009). The reduced locomotor activity is possibly due to impaired dopaminergic neurotransmission that was demonstrated in a different model of PINK1-deficiency (Kitada et al., 2007).

1.5.1.3 The A53T-SNCA + *Pink1*KO Mouse Model

Mice harboring both, the A53T-SNCA overexpression as well as the *Pink1*KO were originally generated by Suzana Gispert through crossbreeding of both single mutant mouse lines (PrPmtA and *Pink1*KO) and characterized for the first time in Gispert and Brehm et al., 2014 (Gispert et al., 2014a). The A53T-SNCA + *Pink1*KO double-mutant mouse line shows a potentiated phenotype becoming apparent in a novel biphasic pattern of mortality rates, reduced spontaneous motor activity already at the age of 3 months and a progressive paralysis in aged mice (Gispert et al., 2014a). Molecular analysis of this novel double-mutant mouse model of polygenic PD revealed an activation of cellular protein degradation efforts as well as dysfunctional pathways of mitochondrial dynamics, synaptic adaptation, microtubular trafficking, DNA-damage repair and cell adhesion (Gispert et al., 2014a). The detailed histological characterization of this novel mouse model is part of this study and therefore depicted within the result part of this thesis.

1.5.2 The 6-OHDA Lesioned Mouse Model

Unilateral, stereotactic injection of the neurotoxin 6-hydroxydopamine (6-OHDA) induces degeneration of monoamine neurons (Sachs and Jonsson, 1975). The chemical structure of 6-OHDA is similar to dopamine allowing its uptake into catecholaminergic neurons by dopamine transporters, where it is retrogradely transported, promoting neurodegeneration through a combination of mechanism including mitochondrial respiratory dysfunction, oxidative stress and cell death (Glinka et al., 1997, Kunikowska and Jenner, 2001, Mazzio et al., 2004). When injected unilaterally, 6-OHDA treated rodents will develop characteristic contra-

lateral turning behavior after L-DOPA or apomorphine treatment, possibly due to activation of supersensitive striatal postsynaptic dopamine receptors, ipsilateral to denervation (Ungerstedt, 1971, Deumens et al., 2002). Besides the turning behavior 6-OHDA lesioned rodents also develop abnormal involuntary movements that are highly correlated with striatal dopamine denervation as well as with the dose of L-DOPA administered (Lindgren et al., 2007, Paille et al., 2007, Nadjar et al., 2009). Abnormal involuntary movements are scored due to a rating scale that comprises three main sections each representing a topographical area of the body. The first section focuses on limb dyskinesia that is characterized by repetitive and rhythmic movements of the forelimb that is contralateral to the lesion side; the second section focuses on axial dyskinesia that is characterized by lateral flexion and axial rotation of the neck and the upper trunk towards the side of the contralateral side; and the third section focuses on orolingual dyskinesia that is characterized by chewing movements, tongue protrusions and jaw tremor (Cenci et al., 2002, Winkler et al., 2002). This scoring system for LID was originally developed in 6-OHDA rats and was only recently applied to mice (Lundblad et al., 2004). Generating 6-OHDA lesioned mice is difficult due to high mortality rates, but in 2011 Francardo et al. developed a detailed nursing protocol to ensure a successful recovery and good general health conditions after the lesion procedure (Francardo et al., 2011). The 6-OHDA mouse model shows easy to evaluate AIMs with low inter-individual variability and biochemical variations (Sedelis et al., 2000), and the possibility to mimic different stages of PD by using different doses and different administration sites, providing a useful tool to model late stages of PD and LID.

1.6 Aim of the Thesis

The most important medical need in PD research is to contribute to the development of therapeutics that can intervene in the progression of neurodegeneration. The first step in reaching this goal is to identify markers of early presymptomatic PD stages allowing an early diagnostic and therefore therapeutic intervention before neuronal cell loss occurs. In order to identify these early biomarkers as well as to develop specific pharmacological therapies we need to understand the pathobiological molecular events leading to this dramatic disease. Intense research within the last years highlighted alpha-synuclein to play a key role in the pathology of PD. Besides, there is experimental evidence that alterations in synaptic plasticity contribute not only to PD pathology but also to the development of LID. In this respect, the aim of this work was:

- to study the molecular underpinnings of synaptic plasticity with focus on alpha-synuclein gain-of-function effects as well as effects of PINK1 deficiency, using three different mouse models of PD. This is of particular interest since LTD deficiency was previously observed in the transgenic mouse model PrPmtA, therefore providing an excellent tool to study the molecular underpinnings of alpha-synuclein gain-of-function induced synaptic plasticity changes, a possible key event in early PD pathology. Findings within this approach can contribute to the early detection of PD pathogenesis and can help to assess progression versus therapeutic benefits.
- to study if presymptomatic stages of PD involve altered postsynaptic sensitivity, therefore the impact of alpha-synuclein gain-of-function on the behavioral and molecular response to apomorphine treatment was tested. This analysis is of particular interest since it included the investigation, whether the transgenic mouse model PrPmtA is useful to model postsynaptic signaling abnormalities at the basis of levodopa induced dyskinesia. This study represents the first approach in the field of LID research, using a genetically modified mouse model to investigate the behavioral and molecular response to apomorphine.
- to characterize a novel polygenic model of PD in order to study the role of PINK1 onto alpha-synuclein gain-of-function induced neurotoxicity. This is of particular interest since interactions of dominant and recessive causes of PD and their coincidence within shared pathways could be fundamental and currently conflicting evidence exists.

2. MATERIAL AND METHODS

2.1 MATERIAL

2.1.1 General Laboratory Equipment

Instrument/Material	Manufacturer/ Supplier	REF/Cat. No.
1000 µl XL, Graduated Filter Tip, sterile 200 µl, Graduated Filter Tip, sterile 20 µl, Bevelled, Filter Tip, sterile 10 µl, Graduated Filter Tip, sterile	STARLAB GmbH	S1122-1830 S1120-8810 S1120-1810 S1120-3810
1000 µl, Blue, Graduated Tip 200 µl, Yellow Tip 10 µl, Graduated Tip	STARLAB GmbH	S1111-2721 S1111-0706 S1111-3700
Centrifuge 5415D	Eppendorf AG	
Centrifuge 5415R	Eppendorf AG	
Confocal laser-scanning microscope, Nikon eclipse90i	Nikon®	
Freezer -20	Liebherr Premium	
Freezer -80, Forma 900 Series	Thermo Scientific	
Fume hood	wesemann® Laborein- richtungen	
Ice maschine (AF 80)	Scotsman®Ice Systems	AF80 AS-E 230/50/1
Microtube 1.5 ml	SARSTEDT AG & Co.	72.690.550
Microtube 2 ml	SARSTEDT AG & Co.	72.655
MS2 Minishaker	IKA® Labortechnik	
Nikon 80i digital microscope	Nikon®	
Parafilm® "M"	Pechiney plastic pur- chasing	01853-AB
Peha-Soft® nitrile gloves	Hartmann	942 190
Pipetboy acu	Integra Bioscience Brand GmbH & Co KG	

Pipettes "PIPETMAN® (0.2 µl - 1000 µl) P2 P10 P20 P200 P1000	Gilson	F144801 F144802 F123600 F123601 F123602
Polaroid Direct Screen Instant Camera EP H-7"	Polaroid	
Serological pipet sterile 5 ml 10 ml 25 ml	Costar®	CLS4487 CLS4488 CLS4489
Thermomixer 5436	Eppendorf AG	
Thermometer comfort 1.5 ml	Eppendorf AG	
Thermomixer compact	Eppendorf AG	
Q-Gard1 Milli-Q® Millipore-System	Millipore GmbH	QGARDOOR1
Vasco®Nitril white gloves	B. Braun	9208410
Zeiss Axiocam MRc	Carl Zeiss AG	
Zeiss Axioplan Mikroskop	Carl Zeiss AG	

2.1.2 Behavioral Analysis and Perfusion

2.1.2.1 Instruments

Instrument	Manufacturer
Analytical balance Typ A120S	Satorius Analytic
Forceps 7 INOX.	A. Dumont & Fils
Forceps with surgical hook	Carl Roth GmbH
Laboratory glassware	DURAN Group GmbH

Magnetic stirrer (“IKAMAG® RCT basic”)	IKA® Labortechnik
Magnetic stirring bars	neoLab® Migge GmbH
Microspoon spatula 140 mm, 5 mm	Carl Roth GmbH
Milli-Q Synthesis Ultrapure Water System	Millipore GmbH
Precision Balance 474-32	Kern & Sohn GmbH
Peristaltic pump, Minipuls 3	Abimed Gilson
pH 210 Microporcessor pH Meter	Hanna Insturments
Surgical scissor small	Carl Roth GmbH
Surgical scissor medium; h.m.P.-LINS HB7458	Carl Roth GmbH
Surgical scissor tall; ESC1604	Carl Roth GmbH
Transparent Cages (Type II Cages)	Techniplast
Video Camera	Panasonic HC-V707M

2.1.2.2 Expendable Materials

Material	Manufacturer/Supplier	REF/Cat. No.
Feather disposable scalpel No. 11	Pfm medical AG	02.001.300.11
Needle No. 20 27G ³ / ₄	BD Microlance™	302200
Safety-Multifly-Set	SARSTEDT AG & Co.	85.1638.235
Snap Cap Vial 10 ml	VWR International	548-0625
Syringe 1 ml	BD Plastipak™	300013
Weighing paper	neoLab® Migge GmbH	1-7217
Quantitative filter paper	VWR International	516-0820

2.1.2.3 Chemicals

Chemical	Manufacturer/Supplier	REF/Cat. No.
Natriumdihydrogenphosphat Monohydrat ($\text{NaH}_2\text{PO}_4 \times \text{H}_2\text{O}$)	AppliChem GmbH	131965
Paraformaldehyde	Sigma Aldrich	158127
Sodium azide (NaN_3)	Sigma Aldrich	71289
Sodium fluoride	Sigma Aldrich	S7920
Sodium Hydroxide Pellets (NaOH)	Sigma Aldrich	306576
Sodium phosphate dibasic dihydrate ($\text{Na}_2\text{HPO}_4 \times 2\text{H}_2\text{O}$)	Sigma Aldrich	71662
Sucrose	Sigma Aldrich	84100

2.1.2.4 Buffers and Solutions

Buffer/Solution	Composition
Phosphate Buffer	2.88% $\text{Na}_2\text{HPO}_4 \times 2\text{H}_2\text{O}$, 5.2% $\text{NaH}_2\text{PO}_4 \times \text{H}_2\text{O}$, bidistilled water
4% Paraformaldehyde (PFA)	4% Paraformaldehyde, 2 pellets NaOH , Phosphate buffer
Storing Solution	10% Sucrose, 0.05% NaN_3 , Phosphate buffer

2.1.2.5 Pharmaceuticals

Pharmaceutical	Manufacturer/Supplier	Cat. No.
Apomorphine	Sigma Aldrich	A4393
Heparin-Natrium-25000-ratiopharm®	Ratiopharm	
Nacoren	Merial	

2.1.3 RNA Purification and qPCR

2.1.3.1 Laboratory Instruments

Instruments	Manufacturer
BioPhotometer	Eppendorf AG
Liquid Nitrogen Tank	Isotherm
Megafuge 1.0 R	Thermo Schientific
Pellet pestle motor	Kontes
StepOnePlus Real-Time PCR System	Applied Bioscience

2.1.3.2 Expendable Materials

Material	Manufacturer/Supplier	Cat. No.
96W Multiply® Fast PCR-Plate	SARSTEDT AG & Co.	72.1981.202
Adhesive qPCR Seal	SARSTEDT AG & Co.	95.1999
RNase Zap Wipes	Ambion	Am9786; Am9788
UV-cuvette micro, PLASTIBRAND®	Brand GmbH & Co KG	759200

2.1.3.3 Chemicals

Chemical	Manufacturer/Supplier	REF/Cat. No.
2-Propanol ((CH ₃) ₂ CHOH)	Sigma Aldrich	33539
Chloroform (CHCl ₃)	Merck Millipore	1024451000
Distilled water DNase/RNase Free (H ₂ O)	Gibco®	10977-035
dNTP Set, molecular biology grade	Thermo Scientific	R0181
Ethanol (EtOH)	Sigma Aldrich	32205
FastStart Universal Probe Master (ROX)	Roche	04914058001

Oligo(dT) ₂₀ Primer	Invitrogen™	18418-020
Random Primers	Invitrogen™	48190-011
TRI®Reagent	Sigma Aldrich	T9424

2.1.3.4 Kits

Kit	Manufacturer/Supplier	REF/Cat. No.
DNase I Amplification Grade	Invitrogen™	18068-015
RNeasy®Lipid Tissue Mini Kit	Quiagen	74804
SuperScript III reverse transcriptase	Invitrogen™	18080-044

2.1.3.5 TaqMan Gene Expression Assays (Applied Biosystems)

Gene Symbol	Name	Assay ID
Arc	Activity regulated cytoskeletal-associated protein	Mm00479619_g1
Bad	BCL2-associated agonist of cell death	Mm00432042_m1
cFos	FBJ osteosarcoma oncogene	Mm00487425_m1
Dusp1	Dual specificity phosphatase 1	Mm00457274_g1
Dusp4	Dual specificity phosphatase 4	Mm01301009_m1
Dusp6	Dual specificity phosphatase 6	Mm00650255_g1
Dusp14	Dual specificity phosphatase 14	Mm01302405_m1
Egr1	Early growth response 1	Mm00656724_m1
Egr2	Early growth response 2	Mm00456650_m1
Fos B	FBJ murine osteosarcoma viral oncogene homolog	Mm00500401_m1

Foxo3	Forkhead box O3	Mm01185722_m1
Gria1	Glutamate receptor, ionotropic, AMPA1 (alpha 1)	Mm00433753_m1
Gria2	Glutamate receptor, ionotropic, AMPA2 (alpha 2)	Mm00442822_m1
Gria3	Glutamate receptor, ionotropic, AMPA3 (alpha 3)	Mm00497506_m1
Gria4	Glutamate receptor, ionotropic, AMPA4 (alpha 4)	Mm00444754_m1
Grin1	Glutamate receptor, ionotropic, NMDA1 (zeta 1)	Mm00433800_m1
Grin2a	Glutamate receptor, ionotropic, NMDA2A (epsilon 1)	Mm00433802_m1
Grin2b	Glutamate receptor, ionotropic, NMDA2B (epsilon 2)	Mm00433820_m1
Grin2c	Glutamate receptor, ionotropic, NMDA2C (epsilon 3)	Mm00439180_m1
Grin2d	Glutamate receptor, ionotropic, NMDA2D (epsilon 4)	Mm00433822_m1
Grin3a	Glutamate receptor ionotropic, NMDA3A	Mm01341722_m1
Grin3b	Glutamate receptor, ionotropic, NMDA3B	Mm00504568_m1
Grm1	Glutamate receptor, metabotropic 1	Mm00810219_m1
Grm2	Glutamate receptor, metabotropic 2	Mm01235831_m1
Grm3	Glutamate receptor, metabotropic 3	Mm00725298_m1
Grm4	Glutamate receptor, metabotropic 4	Mm01306128_m1
Grm5	Glutamate receptor, metabotropic 5	Mm00690332_m1

Grm6	Glutamate receptor, metabotropic 6	Mm00841148_m1
Grm7	Glutamate receptor, metabotropic 7	Mm01189424_m1
Grm8	Glutamate receptor, metabotropic 8	Mm00433840_m1
Homer1	Homer homolog 1 (Drosophila)	Mm00516275_m1
IP3R (SCA15)	Inositol 1,4,5-trisphosphate receptor 1	Mm00439907_m1
JunB	Jun B proto-oncogene	Mm01251660_s1
NOR1 (Nr4A3)	Nuclear receptor subfamily 4, group A, member 3	Mm00450074_m1
Nur77 (Nr4A1)	Nuclear receptor subfamily 4, group A, member 1	Mm00439358_m1
Nurr1 (Nr4A2)	Nuclear receptor subfamily 4, group A, member 2	Mm00443060_m1
Pcbd1	Pterin 4 alpha carbinolamine dehydratase/dimerization cofactor of hepatocyte nuclear factor	Mm00481144_m1
Psd95 (Dlg4)	Discs, large homolog 4 (Drosophila)	Mm00492193_m1
RGS2	Regulator of G-protein signaling 2	Mm00501385_m1
SNCA	Alpha-synuclein	Hs00240906_m1
Sqstm1	Sequestosome 1	Mm01070495_m1
Tac1	Tachykinin 1	Mm00436880_m1
Tbp	TATA box binding protein	Mm00446973_m1

2.1.4 Western Blot

2.1.4.1 Instruments

Instrument	Manufacturer
Blotting chamber	Bio-Rad
Gel-electrophoresis chamber Biometra	Whatman
Hamilton Syringe	Hamilton
Multifunction Microplate Reader	Tecan Group, GENios
Odyssey LI-COR Infrared Imaging System	LI-COR Biosciences
Pellet pestle motor	Kontes
Power supply	Consort
Roll mixer BTR10-12V	Ingenieurbüro CAT, M. Zipperer GmbH
Rotating Mixer Typ RM5	Karl Hecht KG
Shaker	Heidolph Instruments
Ultrasonic homogenizers Typ UW 2070	Bandelin electronic

2.1.4.2 Material

Material	Manufacturer/Supplier	Cat. No.
15 ml Cellstar®Tubes, sterile	greiner bio-one	188 271
50 ml Cellstar®Tubes, sterile	greiner bio-one	227 261
50 ml Cellstar®Tubes, brown, sterile	greiner bio-one	227 280
Combitips advanced® 5ml	Eppendorf AG	0030 089.456
Lid for Microtest Plate 96-well	SARSTEDT AG & Co.	82.1584.500
Microtest Plate 96-well	SARSTEDT AG & Co.	82.1581.500
Multipette®plus	Eppendorf AG	4981 000.019
Whatman™ Chromatography paper 3 mm Chr	Whatman™ GmbH	3030917

Whatman™ Protran BA 83 Nitrocellulose Transfermembrane	Whatman™ GmbH	10402452
--	---------------	----------

2.1.4.3 Reagents

Reagent	Manufacturer/Supplier	Cat. No.
Acrylamid/Bis 29:1 Premixed Powder Electrophoresis purity reagent	Bio-Rad	161-0124
Ammonium peroxodisulfate (APS)	MERCK	1.012.010.100
β-Mercaptoethanol	AppliChem GmbH	A1108.100
BSA Albumin from bovine serum	Sigma Aldrich	A7906
Bromophenol Blue	Sigma Aldrich	B6131
Ethanol absolute (C ₂ H ₆ O)	Sigma Aldrich	32205
Glycerol	Sigma Aldrich	G5516
Glycine p.A.	AppliChem GmbH	A1377.5000
Hydrochloric acid 37% (HCl)	AppliChem GmbH	A2427.0500
Kaliumchloride (KCl)	Applichem GmbH	A2939
Methanol (CH ₄ O)	Sigma Aldrich	32213
milk powder (Sucofin)	Tsi GmbH & Co KG	
Precision Plus Protein standard All Blue	Bio-Rad	161-0373
Phosphatase Inhibitor Cocktail I	Sigma Aldrich	P2850
Phosphatase Inhibitor Cocktail II	Sigma Aldrich	P5726
Protease inhibitor cocktail tablets complete Mini, EDTA-free	Roche Diagnostics GmbH	11 836 170 001
Protein determination BCA kit	VWR International	UP75860A
SDS Pellets	Carl Roth GmbH & Co KG	CN30.2
Sodium chloride (NaCl)	Sigma Aldrich	31434
Sodium hydroxide (NaOH)	Sigma Aldrich	306576

TEMED p.a. for electrophoresis	Carl Roth GmbH & Co KG	2367.3
Tris ultrapure	AppliChem GmbH	A1086.1000
Triton®X-100	AppliChem GmbH	A1388.0500
TRI®Reagent	Sigma Aldrich	T9424
Tween 20 Bio Chemica	AppliChem GmbH	A1389.0500

2.1.4.4 Buffers and Solutions

Buffer/Solution	Composition
2x Loading-/sample-buffer	250 mM Tris/HCL pH 6.9, 20% Glycerol, 4% SDS, 10% β -Mercaptoethanol, 0.005% Bromophenol blue, 5% dist. Water
10x Phosphate buffered saline (PBS)	137 mM NaCl, 2.7 mM KCl, 4.3 mM $\text{Na}_2\text{HPO}_4 \times 2\text{H}_2\text{O}$, 1.4 mM KH_2PO_4 , pH 7.4
PBS-Tween (PBS-T)	PBS, 0.1% Tween
10x Running-Buffer	25 mM Tris pH 8, 192 mM Glycin, 0.1% SDS, add 1000 ml H_2O
SDS Protein Lysis Buffer	1M Tris/HCl pH 6.8, 20% Glycerol, 4% SDS, dest. H_2O Before use: 10 $\mu\text{l}/\text{ml}$ Protease Inhibitor, 1 $\mu\text{l}/\text{ml}$ Phosphatase Inhibitor Cocktail 1, 1 $\mu\text{l}/\text{ml}$ Phosphatase Inhibitor Cocktail 2
10x Tris-buffered saline (TBS)	50 mM Tris, 150 mM NaCl, pH 7.5, adjusted with HCl; add bidistilled H_2O to end volume
TBS-Tween (TBS-T)	TBS, 0.1% Tween
1x Transfer-Buffer	25 mM Tris, 192 mM glycine, 10% methanol

2.1.4.5 Primary Antibodies

Antibody	Dilution	IgG	Size [kDa]	Cat. No.	Company / Distributor
P44/42 MAPK (ERK1/2)	1:1000	rb	42, 44	9102	Cell Signaling Technology®
anti-beta-actin	1:10000	ms	42	A5441	Sigma-Aldrich
Anti-DUSP6 antibody	1:500	rb	42	ab76310	abcam®
Phospho-p44/42 MAPK (ERK1/2)(Thr201/Tyr20)	1:1000	rb	42, 44	9101	Cell Signaling Technology®

2.1.4.6 Secondary Antibodies

Antibody	Dilution	Cat. No.	Company / Distributor
IRDye 680 conjugated goat anti-rabbit IgG	1:15000	926-32221	LI-COR Biosciences
IRDye 800 conjugated goat anti-mouse IgG	1:15000	926-32210	LI-COR Biosciences

2.1.5 Immunohistochemistry

2.1.5.1 Instruments

Instrument	Manufacturer
Brushes	Faber-Castell
Confocal laser-scanning microscope, Nikon eclipse90i	Nikon®
Electrothermal watherbath	Associated Electrical Industries LTD
Freezing microtome (Lund) HM 430	MICROM
Heating plate Typ HP100 (220 V; 300 W)	Guwina Berlin
Heidelberger Pinzette	Ingenieurbüro s-w.-s.- druckdrey

Microtome	JUNG AG
Microwave R-234	Sharp
Nikon 80i digital microscope	Nikon®
Vibrating blade microtome (VT1000 S)	Leica
Zeiss Axiocam MRc	Carl Zeiss AG
Zeiss Axioplan Mikroskop	Carl Zeiss AG

2.1.5.2 Material

Material	Manufacturer/Supplier	Cat. No.
Dako Cytomation Fluorescent Mounting medium	Dako Deutschland GmbH	52023
Dako Pen	Dako Deutschland GmbH	S2002
Feather® Microtome blades S-35	Pfm medical AG	02.075.00.000
Paraplast X-TRA tissue embedding medium	VWR International	15159-486
Pasteur pipette 145 mm cap. approx. 2 ml	BRAND GMBH + CO KG	747715
Microscope Slides SU-PERFROST® PLUS	Thermo Scientific	J1800AMNZ
Microscope Cover glasses, Ø24 mm	Gerhard Menzel GmbH	CB00240RA1
Snap Cap Vial 10 ml	VWR International	548-0625
Stainless Steel Blades	Campden Instruments Limited	752/1/SS
VectaMount™ permanent mounting medium	Vector Laboratories	H-5000

2.1.5.3 Chemicals

Reagent	Manufacturer/Supplier	Cat. No.
BSA Albumin from bovine serum	Sigma Aldrich	A7906
Citric acid	Appllichem GmbH	A2344
DPX Mountant for histology	Sigma Aldrich	06522
Ethanol absolute (C ₂ H ₆ O)	Sigma Aldrich	32205
Hydrogen peroxide (H ₂ O ₂) ROTI-PURAN®	Carl Roth	8070.1
Kaliumchlorid (KCl)	Appllichem GmbH	A2939
Methanol (CH ₄ O)	Sigma Aldrich	32213
Normal Goat Serum	Vector Laboratories	S-1000
Sodium Citrate	Sigma Aldrich	234265
Peroxidase Substrate Kit DAB	Vector Laboratories	SK-4100
Triton®X-100	AppliChem GmbH	A1388.0500
Vectastain® ABC-kit	Vector Laboratories	PK-4001
Vectastain® Horse Normal Serum	Vector Laboratories	PK-4001
Vector NovaRED® Substrate Kit	Vector Laboratories	SK-4800

2.1.5.4 Buffers and Solutions

Buffer/Solution	Composition
Citrate Buffer Solution A	29.4 g sodium citrate, 1l distilled water
Citrate Buffer Solution B	21 g citric acid, 1l distilled water
Citrate Buffer pH 6	1,8 ml Solution A, 82 ml Solution B
Phosphate buffered saline (PBS)	137 mM NaCl, 2.7 mM KCl, 4.3 mM Na ₂ HPO ₄ x 2H ₂ O, 1.4 mM KH ₂ PO ₄ , pH 7.4
Storing Solution 10%	10% Sucrose, 0.05% NaN ₃ , Phosphate buffer
Storing Solution 25%	25% Sucrose, Phosphate buffer

Tris buffered saline (TBS) 10x	50 mM Tris, 150 mM NaCl, pH 7.5, adjusted with HCl; add bidistilled H ₂ O to end volume
Tris buffer	12.1 g Tris, 18 g NaCl, 88 ml 1 M HCl, add 2000 ml H ₂ O, pH 7.5
TRIS pH 9	6.1 g Tris, 8.8 g NaCl, add 1000 ml H ₂ O, pH 9, adjusted with HCl

2.1.5.5 Primary Antibodies

Antibody	Dilution	IgG	Reactivity	Cat. No.	Company / Distributor
4B12	1:500	ms	Hs	MA1-90346	Pierce Antibodies
42/ α -Synuclein (syn-1)	1:500	ms	Hs, ms	610787	BD Transduction Laboratories™
FosB (102)	1:15000	rb	Hs, ms, rat	sc-48X	Santa Cruz Biotechnology, Inc.
P62/SQSTM1 Antibody	1:200	rb	Hs, ms	NBP1-49956	Novus Biologicals®
Phospho Histone H3 (ser10)	1:500	rb	Hs, ms	06-570	Merck Millipore
Phospho-p44/42 MAPK (ERK1/2)(Thr202/Tyr204)	1:300	rb	Hs, ms, rat	9101	Cell Signaling Technology®
Phospho-Ser129-alpha synuclein	1:500	rb	Hs, ms	Ab51252	Abcam
Tyrosine hydroxylase	1:1000	rb	Ms, rat	P40101-150	Pel-freez Biologicals
Tyrosine hydroxylase	1:1000	ms	Hs, ms, rat	MAB-318	Merck Millipore
Ubiquitin	1:1000	rb		Z045801-2	Dako Deutschland GmbH

2.1.5.6 Secondary Antibodies

Antibody	Dilution	Cat. No.	Company / Distributor
Biotinylated Goat Anti-Rabbit IgG Antibody	1:1000; 1:400	BA-1000	Vector Laboratories
Biotinylated Horse Anti-Mouse IgG Antibody	1:500	BA-2000	Vector Laboratories
Cy [™] 2 AffiniPure Donkey Anti-Mouse IgG (H+L)	1:1000	715-225-150	Jackson ImmunoResearch
Cy [™] 2 AffiniPure Donkey Anti-Rabbit IgG (H+L)	1:1000	711-225-152	Jackson ImmunoResearch
Cy [™] 3 AffiniPure Donkey Anti-Mouse IgG (H+L)	1:1000	715-165-150	Jackson ImmunoResearch
Cy [™] 3 AffiniPure Donkey Anti-Rabbit IgG (H+L)	1:1000	711-165-152	Jackson ImmunoResearch

2.1.6 Online Databases

Program	Reference	Application
Allen Brain Atlas	http://www.brain-map.org/	Anatomy mouse brain
Ensembl Genome Browser	http://www.ensembl.org/	Genome database
GeneCards V3	http://www.genecards.org/	Gene information
Leo	http://www.leo.org/	Dictionary
Pubmed, NCBI	http://www.ncbi.nlm.nih.gov/sites/entrez?db=pubmed	Literature Search
NCBI / BLAST	http://blast.ncbi.nlm.nih.gov/Blast.cgi	Multiple alignment tool database

NCBI / Entrez Gene	http://www.ncbi.nlm.nih.gov/gene/	Gene database
--------------------	---	---------------

2.1.7 Software

Software	Supplier	Application
Adobe Acrobat X pro	Adobe	PDF handling
Adobe Photoshop CS2	Adobe	Illustration
Excel 2010	Microsoft	Calculations
EndNote X4	Thomson Reuters	Citation management
GraphPad Prism 5	GraphPad Software Inc	Statistics
ImageJ 1.40g	National Institute of Health	Histological analysis
NIS-Elements Imaging Software 4.20.00	Nikon	Microscopy
Odyssey Software 2.1.2	LI-COR Biosciences	Western Blot analysis
Power Point 2010	Microsoft	Presentation
StepOnePlus Software v2.1	Applied Biosystems	qPCR analysis
Word 2010	Microsoft	Text processing
XFluor4	Tecan	Protein amount calculation
Zeiss Axiovision, Special Edition 64, Release 4.9.1	Zeiss	Microscopy

2.2 METHODS

2.2.1 Animals

2.2.1.1 Animal Housing and Welfare

Data presented in this study are based on male and female animals of the species *Mus musculus*. Experiments were performed in three different mouse strains and their corresponding wild-type controls. All three mouse lines were described previously, among those are mice overexpressing human alpha-synuclein under the murine neuron specific PrP promoter including the missense mutation A53T (PrPmtA) with FVB/N background (Gispert et al., 2003), mice with *Pink1*^{-/-} (*Pink1KO*) in 129/SvEv background (Gispert et al., 2009) and mice harboring both mutations (A53T-SNCA + *Pink1KO*) in a 50:50 (FVB/N:129/SvEv) background on average (Gispert et al., 2014b). All animals were housed in individually ventilated cages under 12 h light/dark cycles with food and water *ad libitum*, at the FELASA-certified Central Animal Facility (ZFE) of the Frankfurt Goethe University Medical School. All three mouse strains were housed in the same room in Type II L cages (365 x 207 x 140 mm, floor area 530 cm²; IVC-based) and experiments were performed in accordance with the European Communities Council Directive of 24 November 1986 (86/609/EEC) and the National Institute of Health Guide for the Care and Use of Laboratory Animals.

2.2.1.2 Generation and Breeding of A53T-SNCA Overexpressing Mice

Mice overexpressing human A53T alpha-synuclein cDNA under the control of the murine specific PrP promoter were originally generated by Suzana Gispert and colleagues as described in Gispert et al., 2003 (Gispert et al., 2003). The cDNA representing the entire human alpha-synuclein gene including the missense mutation A53T was cloned into a pSL301 vector (Invitrogen). The construct was driven by a ~3.5 kb fragment of the murine neuron specific prion protein promoter (PrP; Genbank #U52821) located at position 1 to 3479, followed by a polyadenylation signal sequences that originates from the 3' untranslated region of the bovine growth hormone (BGH) gene. Finally, pronuclei of fertilized FVB/N mouse ovary were microinjected with the transgene construct and transferred into oviducts of pseudopregnant foster mothers. Offspring resulting from microinjected ovary have a 10-20% chance to carry the transgene. In order to identify transgenic founder animals and estimate the transgenes' copy number, Southern Blot was performed. The founder line PrPmtA was chosen for further analysis due to its strong overexpression within nigrostriatal projection neurons. The PrPmtA mouse line was compared to its background strain FVB/N as wild-type control (WT). In order

to obtain homozygous transgenic and WT cohorts, heterozygous littermates were mated. Homozygosity was maintained by breeding of homozygous mice.

2.2.1.3 Generation and Breeding of *Pink1*KO Mice

In order to generate *Pink1*KO mice in 129/SvEv background, a mouse genomic bacterial artificial chromosome library was screened using a *Pink1* cDNA probe. A targeting vector with 4.2 kb *NheI*/*NheI* fragment containing exon II, III, IV and V, with exon IV harboring the mutation g/a in position 8343 at position NT_039267, plus a 3.2 kb fragment of *NheI*/*BstZ17I* was constructed. The mutation in exon IV was previously inserted with the QuickChange site directed mutagenesis kit (Stratagene). The resulting vector containing DNA homologous to the target gene as well as inserted DNA for positive selection is used to transfect embryonic stem cells with a pure 129/SvEv background. Homologous recombination allows the targeting vector to recombine with the target gene. Correctly targeted cell clones were identified by Southern Blot and used for blastocyst injection. Heterozygous F1 mice with 129/SvEv background were mated and homozygous mutant and wild-type animals were maintained through breeding of homozygotes.

2.2.1.4 Generation and Breeding of A53T-SNCA + *Pink1*KO Mice

In 2.2.1.1 and 2.2.1.2 the generation and breeding of A53T-SNCA as well as of *Pink1*KO single mutants was described. Double mutant mice harboring both the A53T-SNCA overexpression and the *Pink1*KO were generated by crossing the two single mutant lines. Homozygosity for both genotypes was established by inbreeding. Since the PrPmtA line is in FVB/N background and *Pink1*KO in 129/SvEv background, the double mutant would contain 129/SvEv and FVB/N in 50:50 distribution on average. Therefore, as wild-type control F1 hybrids from crossbreeding of 129/SvEv and FVB/N wild-type were used.

2.2.2 Genotyping

2.2.2.1 DNA Extraction from Tail

In order to genotype A53T-SNCA transgenic, *Pink1*KO or double mutant (A53T-SNCA + *Pink1*KO) mice, DNA from tail tips that were taken with sterile scissors, approximately 2 mm of the distal tail, was isolated. Tail tips were incubated in 500 μ l Proteinase K buffer [1M Tris pH8, 5M NaCl, 0.5M EDTA pH8, 10% SDS, H₂O] containing 250 μ g/ml Proteinase-K, at 55°C and 800 rpm overnight to digest protein contamination. Thereafter, 250 μ l 6M NaCl were

added and samples were mixed vigorously. Then samples were incubated on ice for 10 min followed by a 10 min centrifugation at 2300 g. The DNA-containing aqueous supernatant (approximately 500 µl) was taken, 1 ml 100% ethanol was added and samples were mixed to precipitate DNA. Afterwards, samples were centrifuged at 14000 g for 10 min and emerged supernatant was discarded. In order to remove residual salt from the DNA containing pellet, 500 µl of 70% ethanol were added and samples were vortexed. Then, samples were centrifuged for 5 min at 6000 g and the resulting supernatant was carefully discarded. The pellet was air dried and dissolved in 100 µl TE-buffer. DNA samples were stored at 4 °C until further use.

2.2.2.2 Polymerase Chain Reaction (PCR)

Polymerase chain reaction (PCR) is a biochemical technique that was developed in 1983 by Kary B. Mullis and is used to amplify a specific DNA sequence. The defined DNA region is amplified by DNA-polymerase using two oligonucleotides that bind to the DNA region flanking the sequence of interest and therefore defining their start- and stop-point. In this study PCR was used for genotyping. Therefore, a standard PCR protocol with 3 min of initialization at 94 °C followed by 35 cycles of the actual PCR reaction containing 30 seconds denaturation at 94 °C, 30 seconds of annealing at 63 °C and 50 seconds of elongation at 72 °C was applied. The PCR conditions are defined as following: the perfect annealing temperature can be calculated by multiplying the number of adenine and thymine present within the primer sequence with two and add this with the number of cytosine and guanine multiplied with four. The arising number accounts for the perfect annealing temperature. In case the two primer will give rise to two different annealing temperatures, the lower temperature is chosen. The perfect time of elongation is chosen as one second per kb. The chain reaction is ended with a final elongation step for 7 min at 72 °C. Thereafter, samples are stored at 4 °C until further use.

2.2.2.3 Genotyping of A53T-SNCA overexpressing mice

In order to differentiate between heterozygous and homozygous A53T-SNCA overexpressing mice, quantitative qPCR was performed using the following specially designed primers: TaqMan SynF (5' ACAGTGGAGGGAGCAGGGA 3'), TaqMan SynR (5' TCCTTCTTCATTCTTGCCCAACT 3') and the probe (FAM-ATTGCAGCAGCCACTGGCTTTGTCA). qPCR was performed as described in 2.2.6 with the exception of using 4 ng DNA/well. GAPDH serves as reference using the following primers: GapdhF (5' TGTGTCCGTCGTGGATCTGA 3'), GapdhR (5' CCTGCTTCACCACCTTCTTGA 3') and the probe (FAM-CCGCCTGGAGAAACCTGCCAAGTATG 3').

The DNA target is quantified by this approach allowing to separate heterozygous from homozygous A53T-SNCA overexpressing mice.

2.2.2.4 Genotyping of *Pink1*KO mice

PCR amplifications are used for *Pink1*KO genotyping. The following PRC conditions were used: 3' 94 °C, 35x (30" 94 °C, 30" 63 °C, 50" 72 °C) 7' 72 °C). The PCR is demonstrating the point mutation by using the primers exon 4 mouse F (5' GGAGAAGTCACCCCTGTTGG 3') and exon 4 mouse R (5' CTCTCATTCTGCGTGCTTTGTTTC 3'). The PCR generated an amplicon of 464 bp that is digested during 3 hours at 37 °C into 288 bp/176 bp in wild-type, 176 bp/154 bp/134 bp in homozygous and 288 bp/176 bp/154 bp/134 bp in heterozygous *Pink1*KO mice, using the restriction enzyme *Ava*II (New England Biolabs). Alleles are separated in 2% agarose gels and visualized by ethidium bromide staining.

2.2.2.5 Genotyping of A53T-SNCA + *Pink1*KO mice

Genotyping of double mutant mice harboring both the A53T-SNCA transgene and the *Pink1* deletion can be performed using multiple approaches. As described in 2.2.2.3 qPCR is performed to verify the presence of A53T-SNCA and to separate heterozygous from homozygous. In order to analyze the *Pink1*KO, PCR amplification was described in 2.2.2.4. To genotype double mutant mice, both the A53T-SNCA transgene as well as the *Pink1*KO need to be confirmed by applying multiple PCR reactions as well as the qPCR analysis to prove homozygosity for A53T-SNCA.

2.2.2.6 Agarose Gel Electrophoresis

The agarose gel electrophoresis is a biomolecular method used to separate nucleic acid strands (RNA or DNA) according to their size and charge. The resulting bands were subsequently identified by comparison to well-known fragments. For genotyping, the PCR-derived DNA fragments were loaded on a 1% agarose gel containing 0.001% ethidium bromide for visualization. Electrophoresis was performed for about 15 min at 100 V. Thereafter, the separated DNA fragments were visualized using an UV-light and an analog camera.

2.2.3 Apomorphine Treatment

In order to study post-synaptic sensitivity to dopamine receptor stimulation in the A53T-SNCA overexpressing mouse, the dopamine agonist apomorphine was administered. Therefore, 0.5 mg/ml apomorphine and 0.2 mg/ml ascorbic acid were dissolved in 0.9% sterile sa-

line. A single dose of 0.5 mg/kg or 5 mg/kg apomorphine or of the respective volume of vehicle (0.2 mg/ml ascorbic acid in saline) was administered subcutaneously.

2.2.4 Stereotyped Movement Scoring

After apomorphine administration, indicators of post-synaptic sensitivity to dopamine receptor stimulation were analyzed by applying a newly generated scoring system focusing on involuntary movements with stereotypic and dystonic features. The experimental design in which behavioral observations were obtained is shown in Fig.13.

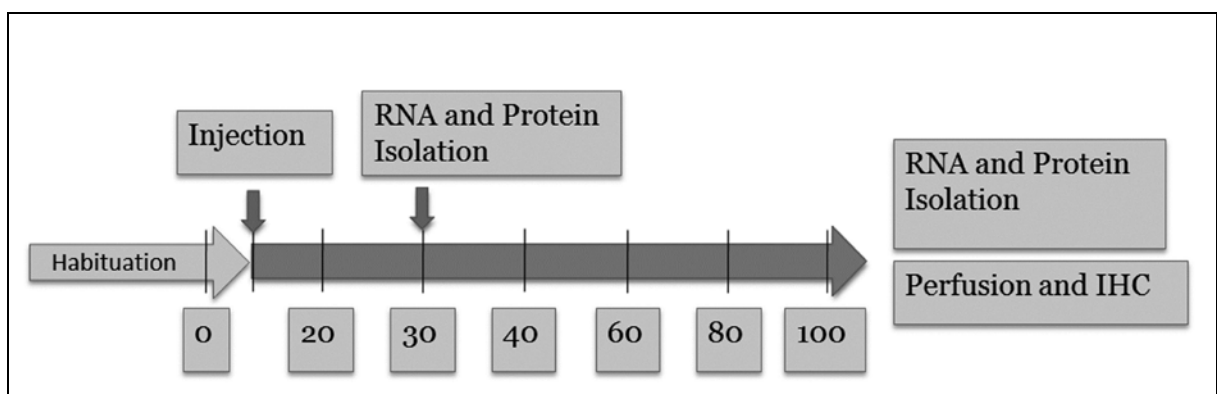


Fig. 13 Experimental Design. A53T-SNCA overexpressing mice aged 18 months, were individually placed into transparent cages and allowed to habituate for 30 min. Each mouse was videotaped prior to any treatment (0 min) as well as at 20 min, 40 min, 60 min, 80 min, and 100 min after s.c. injection of 5 mg/kg apomorphine or saline only (vehicle) in the respective volume. For RNA and protein analyses, mice were sacrificed by cervical dislocation either 30 min or 100 min after apomorphine treatment, and striatal tissue was dissected. For IHC, mice were perfused transcardially, 100 min after apomorphine treatment with 4% paraformaldehyde.

18 month old A53T-SNCA overexpressing mice were placed individually into transparent cages and habituated for 30 min. Each mouse was recorded using a video camera (Panasonic HC-V707M) for one minute, starting immediately before the injection of apomorphine (time 0) and after 20, 40, 60, 80 and 100 min. Involuntary movements with stereotypic or dystonic features namely, (i) stereotypic licking; (ii) head bobbing; (iii) forelimb tapping, (iv) persistent hyperextension of the body and the neck, were rated using criteria analogous to those applied in rodent dyskinesia rating scales (Cenci et al., 1998, Lee et al., 2000, Lundblad et al., 2002). In detail, at each monitoring period, a behavioral feature was scored from 0 to 4 based on the proportion of time in which the behavior was observed. 0 represents behavior not present; 1 behavior present during less than 50% of the observation interval; 2 behavior present during 50% of the observation interval; 3 behavior present during more than 50% of the

observation interval and 4 behavior present during 100% of the observation interval. Behavioral features like number of turns or rearings were counted manually.

2.2.4.1 Statistic of Behavioral Analysis

Behavioral data were compared between time points and genotypes using repeated measures analysis of variance (ANOVA), and post hoc Bonferroni test. Statistical analyses were performed using Prism 5 software (GraphPad, La Jolla, CA, USA). Data were presented as group means \pm SEM. Significant differences were highlighted in the Figures using asterisks ($T \leq 0.1$, * $P \leq 0.05$; ** $P \leq 0.01$; *** $P \leq 0.001$; **** $P \leq 0.0001$).

2.2.5 Dissection of Mouse Brain

Mice were euthanized by cervical dislocation, decapitated and brain structures were dissected according to the mouse brain atlas (Paxinos and Franklin, 2001). The dissected brain structures were striatum, midbrain, brainstem, cerebellum, frontal cortex, cortex and hippocampus. Tissue was immediately frozen in liquid nitrogen, and stored at $-80\text{ }^{\circ}\text{C}$ for further molecular analysis.

2.2.6 Quantitative Reverse Transcriptase Real-Time PCR (qPCR)

2.2.6.1 RNA Isolation

Tissue of specific mouse brain areas was dissected from the previously described mouse lines (PrPmtA, *Pink1*KO, A53T-SNCA + *Pink1*KO) at three different ages (3 months, 6 months, 18 months). Apart from striatal tissue, total RNA isolation was performed using TRI@Reagent according to manufacturer instructions. In brief, tissue was homogenized in 1 ml TRI@Reagent using a pellet pestle motor and incubated for 5 min at room temperature (RT). Afterwards, 0.2 ml chloroform was added, samples were inverted for 15 seconds followed by 2-3 min incubation at RT. Thereafter, samples were centrifuged for 15 min at 12000 rcf and $4\text{ }^{\circ}\text{C}$ and the aqueous supernatant was collected. A volume of 0.5 ml 2-propanol was added to the aqueous, RNA containing supernatant, samples were mixed and incubated for 10 min at RT. Subsequently, samples were centrifuged for 10 min at 12000 rcf with $4\text{ }^{\circ}\text{C}$ and the supernatant was discarded. The RNA containing pellet was washed and resuspended by adding 75% ethanol and vortexing, to remove salts, then centrifugation for 5 min at 7500 rcf and $4\text{ }^{\circ}\text{C}$

was applied. The complete supernatant was removed and the pellet was air-dried for 4-5 min at RT. Thereafter, RNA was eluted in 100 μ l RNase-free water using a heat block at 55 $^{\circ}$ C for 10 min.

In order to isolate total RNA from striatal tissue, the RNeasy@Lipid Tissue Mini Kit was used according to manufacturer's instructions. In brief, samples were homogenized in 1 ml Qiazol lysis reagent using a pellet pestle motor and incubated for 5 min at RT. Thereafter, 0.2 ml chloroform was added, samples were inverted and centrifuged for 15 min at 12000 rcf and 4 $^{\circ}$ C, leading to a separation into three layers. RNA was precipitated from the aqueous layer by adding the same volume of 70% ethanol and the use of RNeasy mini spin columns. Several washing steps with provided washing-buffers resulted in a high purity of isolated RNA bound to the RNeasy mini spin column. In order to elute the RNA, 50 μ l RNase-free water was added followed by centrifugation for 1 min at 8000 rcf and RT. Isolated RNA was stored at -80 $^{\circ}$ C until further molecular analysis.

2.2.6.2 Determination of RNA Concentration

The gene expression analysis using qPCR requires the application of a defined amount of RNA. To determine the concentration of previously isolated RNA, spectrophotometric quantification was applied using a spectrophotometer. The spectrophotometer was adjusted to a standard sample containing 80 μ l RNase-free water. RNA samples were diluted by adding 78 μ l RNase-free water to 2 μ l RNA sample. The diluted samples were transferred to plastic cuvettes and RNA-specific absorbance was measured at a wavelength of $\lambda = 260$ nm using the spectrophotometer. Samples were measured in duplicates and mean value was calculated for evaluation of the final RNA concentration.

2.2.6.3 DNase I Treatment and cDNA-Synthesis

Standard RNA isolation protocols do not guarantee RNA samples to be free of contaminating DNA. Since DNA contamination can lead to false-positive results, the removal of all DNA is a very important procedure. Therefore, all RNA samples were treated with desoxyribonuclease I (DNase I) prior to cDNA synthesis. DNase I treatment was performed due to manufacturer's instructions. In brief, samples were incubated with DNase I Amplification Grade for 15 min at RT. Digestion reaction was stopped by adding EDTA and incubating for 10 min at 65 $^{\circ}$ C. Thereafter, cDNA synthesis of one microgram DNase I treated RNA was performed due to manufacturer's instructions using the SuperScript III reverse transcriptase utilizing oligo(dt)20 and random primers.

2.2.6.4 Quantitative Real-Time PCR using TaqMan® Assays

Transcriptional changes were analyzed using the optimized and commercially available TaqMan® assay system. To quantify expression changes between PrPmtA, *Pink1*KO, A53T-SNCA + *Pink1*KO and their respective wild-type controls, cDNA samples were analyzed in a total reaction volume of 20 µl utilizing 1 µl of TaqMan gene expression assay (20x), 10 µl of 2x FastStart Universal Probe Master Mix and 5 µl of the respective cDNA. qPCR was carried out in a 96 well plate and total cDNA levels were quantified relative to the constitutively expressed housekeeping gene TATA box binding protein (Tbp) in a StepOnePlus Real-time PCR system. The following PCR conditions were applied: 50 °C-2', 95 °C-10' followed by 40 cycles of 95 °C-15" and 60 °C-60". Relative expression changes were calculated using the $2^{-\Delta\Delta CT}$ -method by Livak and Schmittgen (Livak and Schmittgen, 2001) as well as Microsoft Excel 2010 software.

2.2.6.5 Statistics

Statistical analysis of data obtained with qPCR was performed with respect to the experimental design. qPCR data that compare the gene expression of a mutant and their wildtype control mice were analyzed using an unpaired t-test and Prism 5 software. qPCR data that compare drug induced expression changes among PrPmtA and WT mice were analyzed using one-way ANOVA followed by Tukey's multiple comparison test, again using the Prism 5 software. Data were presented as group means \pm SEM. Significant differences were highlighted in the Figures using asterisks (T \leq 0.1, * P \leq 0.05; ** P \leq 0.01; *** P \leq 0.001; **** P \leq 0.0001).

2.2.7 Western Blot

2.2.7.1 Protein Isolation

Striatal tissue from one hemisphere of apomorphine and vehicle treated PrPmtA as well as WT mice was dissected as described in 2.2.5 and immediately frozen in liquid nitrogen. Striatal tissue for protein analysis was taken from -80 °C and homogenized with the use of a pellet pestle motor in 100 µl SDS-Buffer containing protease and phosphatase inhibitors. Thereafter, samples were sonicated and incubated for 15 min at RT on a shaker followed by centrifugation at full speed for 15 min. The supernatant was collected.

2.2.7.2 Determination of Protein Concentration

Protein level changes between apomorphine and vehicle treated PrPmtA and WT mice were analyzed using Western Blotting. In order to quantify protein levels of interest, the total amount of isolated protein needed to be determined. Protein determination was performed using the protein determination BCA kit according to manufacturer's instructions. In brief, protein determination was performed in a 96 well plate. To calculate the total amount of protein, each samples was analyzed relative to a BSA standard curve starting from 0 μg up to 14 μg BSA per well. Samples were measured in duplicates in parallel to the described BSA standard curve. 2 μl of protein sample were diluted with 150 μl 0.9% NaCl, followed by the administration 150 μl of BCA reagents (mixture of solution A+B+C 25:24:1), thereafter samples were incubated for 30 min at 37 °C. Absorbance was measured at 560 nm in a spectrafluorometer using xFluor4 software and protein concentration was calculated in $\mu\text{g}/\mu\text{l}$ by converting the linear equation of the BSA standard curve and subtracting of lysis buffer absorbance using Microsoft Excel 2010.

2.2.7.3 SDS-Polyacrylamide-Gelelectrophoresis (SDS-PAGE)

Sodium dodecyl sulfate polyacrylamide gel electrophoresis (SDS-PAGE) is a widely used method to separate proteins according to their size using their electrophoretic properties (Laemmli, 1970). The concentration of polyacrylamide gels is hereby crucial for the size of analyzed proteins. Here, proteins of 20 – 45 kDa were analyzed; therefore a gel concentration of 12% was sufficient. In order to prepare a 12% polyacrylamide gel, 6 ml of acrylamide/ bisacrylamide (29:1) (AA/BA), 3.75 ml Tris/HCl pH 8.9, 5.05 ml H₂O, 150 μl SDS (10%), 50 μl APS and 10 μl TEMED were mixed and transferred to sealed glass plates. The running gel was left for 1 h at room temperature, covered with 2-propanol for polymerization. Thereafter, 2-propanol was discarded and the stacking gel containing 650 μl AA/BA, 1.25 ml Tris pH 6.9, 3.05 ml H₂O, 50 μl SDS (10%) 25 μl APS and 5 μl TEMED was mixed and transferred onto the running gel. A comb was added to form sample slots. Then the stacking gel polymerized for 15 min at RT. Here, 20 ng of striatal protein were separated on the 12% polyacrylamide gels, therefore samples were adjusted to the same concentration and mixed with 2x loading-buffer. Thereafter, samples were transferred to the gel with the use of a Hamilton syringe and the gel was placed into an electrophoresis chamber containing 1x running buffer. Gel electrophoresis was carried out for ~2 h at 120 V. To determine the size of analyzed proteins, a protein standard containing different protein bands of defined size was applied to each experiment.

2.2.7.4 Western Blotting

After protein separation via SDS-polyacrylamide gel-electrophoresis, proteins were transferred onto a nitrocellulose membrane. Therefore, the polyacrylamide gel containing the separated proteins was placed onto a nitrocellulose membrane and covered with foams and filters as depicted in figure 14. Protein transfer was carried out in a transfer chamber filled with 1x transfer-buffer at 50 V for 90 min.

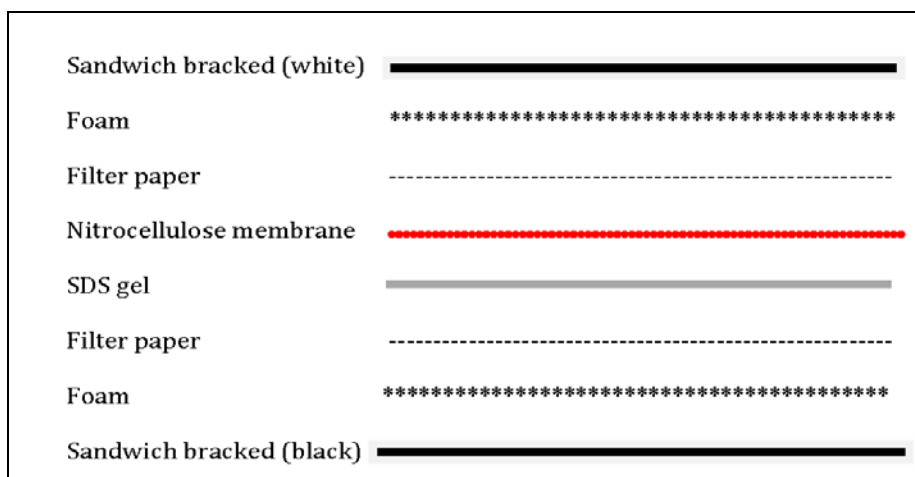


Fig. 14 Scheme of Western Blot organization.

2.2.7.5 Immunodetection

After transferring proteins to a nitrocellulose membrane, unspecific bindings need to be prevented. Therefore, the nitrocellulose membrane was blocked for 1 h at RT with blocking-buffer containing 5% BSA in TBS-T. The membrane was then incubated with the respective first antibody provided in TBS-T with 5% BSA at 4 °C over night. The next day, membranes were washed three times for 10 min each with TBS-T before incubating with the secondary antibody (in TBS-T).

2.2.7.6 Densitometric Analysis of Target Proteins

For visualization and densitometric analysis the Odyssey Infrared Imaging System (LI-COR) was employed, and quantification was performed with the appropriate Odyssey software as well as Excel 2010 calculation software.

2.2.7.7 Statistics

Data from immunoblots were compared using an unpaired *t*-test and Prism 5 software. Data were presented as group means \pm SEM. Significant differences were highlighted in the Figures using asterisks ($T \leq 0.1$, * $P \leq 0.05$; ** $P \leq 0.01$; *** $P \leq 0.001$; **** $P \leq 0.0001$).

2.2.8 Immunohistochemistry

2.2.8.1 Perfusion and Dissection of Mouse Brain and Spinal Cord

Mice used in immunohistochemistry studies were transcardially perfused using 4% paraformaldehyde pH 7.4 (PFA). Therefore, animals were deeply anaesthetized by injecting an over-dose of sodium pentobarbital intraperitoneal. The fixative solution (4% PFA) was delivered by a peristaltic pump at the speed of 20 ml/min during 5-7 min. A transcardial heparin injection was delivered right before PFA perfusion to ensure good perfusion quality. Afterwards, brains and spinal cords were rapidly extracted and post fixed in 4% PFA for 12 h at 4 °C. Thereafter, brains were cryoprotected in ice-cold phosphate-buffered sucrose (25% sucrose in 0.1 M phosphate buffer for the apomorphine experiments and 10% sucrose in 0.1 M phosphate buffer with 0.05% NaN_3 for the double-mutant project) for 48 h at 4 °C.

2.2.8.2 Immunohistochemistry – Free-Floating

Apomorphine project

After fixation and cryoprotection, brains were cut on a freezing microtome into coronal sections of 30 μm thickness and stored at -20 °C in a non-freezing solution (30% ethylene glycol and 30% glycerol in 0.1 M phosphate buffer). In case of immunohistochemistry for tyrosine hydroxylase (TH), alpha-synuclein and phospho-Ser129 SNCA, free-floating sections were rinsed three times in phosphate-buffered saline (PBS) for 10 min each. In case of immunohistochemistry for pERK1/2 as well as pHistoneH3, free-floating sections were rinsed three times in Tris-buffered saline containing 0.1 M NaF (TBS-NaF) and sections used for FosB immunohistochemistry were washed three times for 10 min in PBS-T. Thereafter, sections were pretreated with 3% H_2O_2 and 10% methanol in the respective washing solution for 15-20 min at 4 °C to reduce endogenous peroxidase activity. Then free-floating sections were washed again three times 10 min in the previously described washing buffer. For permeabilization, sections were incubated for 15 min in the respective washing buffer containing 0.1% Triton, followed by a new washing step three times 10 min. Thereafter, sections were blocked with

the proper serum from the host of the secondary antibody for 1 h either at RT (TH, SNCA, FosB) or at 4 °C (pERK1/2, pHistoneH3, pSer129-SNCA) to prevent nonspecific binding. Then sections were incubated with the following primary antibodies: rabbit anti-TH (1:1000, Pel-Freez), anti-mouse SNCA plus anti-human SNCA monoclonal antibody clone 42 (1:500, BD Transduction Laboratories), rabbit anti-pSer129-SNCA (1:500, Abcam), rabbit anti-phospho-p44/42 MAPK (Erk1/2)(Thr202/Tyr204) antibody (1:300, Cell Signaling), rabbit anti-phospho Histone H3 (ser10) antibody (1:500, Millipore) and rabbit anti-FosB (1:15000, Santa Cruz). Primary antibodies were incubated in 1% proper serum from the host of the secondary antibody and 0.5% Triton in PBS over night at 4 °C. Thereafter, sections were washed with the respective washing buffer (PBS, PBST, TBS+NaF) and incubated with the appropriate biotinylated secondary antibody for 2 hours at 4 °C in case of pSer129-SNCA, phospho Histone H3 and phospho-p44/42 MAPK (Erk1/2) and at RT for SNCA, TH and FosB. Tissue-bound antibodies were visualized using an avidin–biotin–peroxidase complex (Vectastain ABC-kit, 1 hour incubation) with 3'3'-diaminobenzidine (DAB, Sigma Aldrich) as the chromogen for anti-TH-IHC and a Peroxidase Vector NovaRED Substrate Kit for the other antibodies. Sections were dehydrated in ascending ethanol concentrations followed by xylene, and coverslipped using DPX mounting glue (Sigma Aldrich).

A53T-SNCA + Pink1KO project

After fixation and cryoprotection brains were cut into 30 µm and spinal cord into 40 µm coronal sections on a vibrating blade microtome (Leica VT1000 S). Free floating sections were rinsed three times for 10 min in phosphate-buffered saline (PBS) in case of pSer129-SNCA immunohistochemistry at 4 °C, for p62 at RT. Then sections were incubated for 1 h with blocking solution [10% normal goat serum, 0.5% TritonX-100, PBS] to prevent unspecific staining. Thereafter, sections were incubated with the respective first antibody, either rabbit anti-pSer129-SNCA (1:500, Abcam) or rabbit anti p62/SQSTM1 (1:200, Novus Biologicals) in carrier solution [1% normal goat serum, 0.5% TritonX-100, PBS] for 48 hours at 4 °C (pSer129-SNCA) or RT (p62). Then, sections were washed in PBS and incubated with the appropriate biotinylated secondary antibody for 2 h at room temperature (1:500, Vectastain anti-rabbit). Tissue-bound antibodies were visualized by incubating for 90 min with avidin–biotin–peroxidase complex (Vectastain ABC-kit) and Peroxidase substrate Vector NovaRED Substrate Kit. Sections were dehydrated in ascending ethanol concentrations followed by xylene; they were coverslipped using VectaMount permanent mounting medium.

2.2.8.3 Immunohistochemistry – Paraffin Embedded

Immunohistochemistry for ubiquitin within the A53T-SNCA + *Pink1KO* project was performed in paraffin embedded sections. Therefore, perfusion-fixed brains and spinal cords of A53T-SNCA + *Pink1KO*, PrPmtA and *Pink1KO* mice as well as of the respective control mice were dehydrated in ascending ethanol concentrations followed by xylene and molted paraffin. Brains were incubated for 24 h in each solution; spinal cord was incubated for 2 h in each solution. Thereafter, tissue was embedded in paraffin and stored at RT until sectioning. Coronal sections with 5 μ m thickness were cut using a microtome and floated in a 50 °C water bath containing distilled water. Sections were then mounted onto glass slides and deparaffinated in xylene and rehydrated in descending series of ethanol concentrations. Antigen retrieval was performed by boiling the sections in 0.01 M citrate buffer at pH 6 for five times, 3 min each in a microwave. Endogenous peroxidase activity was reduced by incubating sections in PBS containing 3% H₂O₂ and 20% ethanol for 5 min at RT. Subsequently, sections were blocked with TRIS containing 5% BSA, 20% normal goat serum and 0.5% TritonX-100 for 1 h at RT to prevent unspecific staining. Thereafter, sections were incubated with the specific primary rabbit anti Ubiquitin antibody (1:1000, DAKO) delivered in 1% normal goat serum, 0.5% TritonX-100 and PBS at 4 °C over night. The next day, sections were washed three times for 10 min each in TRIS followed by 90 min of incubation with the biotinylated secondary antibody (1:500, Vectastain anti-rabbit) at RT. Tissue-bound antibodies were visualized as described for free floating sections by incubating for 90 min with avidin–biotin–peroxidase complex (Vectastain ABC-kit) and a Peroxidase substrate Vector NovaRED Substrate Kit. Sections were dehydrated in ascending ethanol concentrations followed by xylene, and cover-slipped using VectaMount permanent mounting medium.

2.2.8.4 Immunohistochemistry – Double Immunofluorescence Paraffin Embedded

Double immunofluorescence was performed to characterize pSer129-SNCA, p62 and ubiquitin positive cells in midbrain sections of A53T-SNCA + *Pink1KO* mice. The first analyzed focused on the question if these cells are dopaminergic cells of the substantia nigra and therefore TH positive. In order to answer this question, a double immunofluorescence immunohistochemistry with TH plus SNCA, TH plus pSer129-SNCA, TH plus p62 and TH plus ubiquitin was performed. Therefore, 5 μ m thick paraffin sections were deparaffinated in xylene and rehydrated in descending series of ethanol as described in 2.2.8.3. Double immunofluorescence immunohistochemistry of alpha-synuclein an antibody recognizing the human isoform of SNCA specifically was applied. Antigen retrieval was performed by incubating the slices in

TRIS pH 9 for 15 min at 90 °C. In case of pSer129-SNCA plus TH staining, no antigen retrieval was necessary, but endogenous peroxidase staining was reduced by 30 min incubation in TRIS containing 20% methanol and 3% H₂O₂ at RT. Antigen retrieval for the double immunofluorescence of p62 and TH was done by incubating the slices in TRIS pH 9 for 15 min at 90 °C and for double immunofluorescence of ubiquitin and TH, slices were boiled five times in 0.01 M citrate buffer pH 6 for 3 min each in a microwave. Endogenous peroxidase was reduced for all stainings except the pSer129-SNCA with TH, by incubating sections in PBS containing 3% H₂O₂ and 20% ethanol for 5 min at RT. In order to block non-specific epitopes, slices were incubated with TRIS containing 5% BSA, 20% normal goat serum and 0.5% TritonX-100 for 1 h at RT. Subsequently, slices were incubated with the primary antibodies delivered in 1% normal goat serum, 0.5% TritonX-100 and PBS. The following primary antibody combinations were used: rabbit anti-pSer129-SNCA (1:500, Abcam) with mouse anti TH (1:1000, Pel-freez); rabbit anti-p62/SQSTM1 (1:200, Novus Biologicals) with mouse anti TH (1:1000, Pel-freez); rabbit anti-ubiquitin (1:1000, DAKO) with mouse anti TH (1:1000, Pel-freez) and mouse anti-alpha-synuclein (4B12) (1:500, Pierce Antibodies) with rabbit anti TH (1:1000, Millipore). All primary antibodies were incubated for 24 h at 4 °C. The next day, slices were rinsed in TRIS-buffer and incubated for 6 h with the appropriate secondary antibodies at room temperature. Secondary antibodies were anti-rabbit or anti-mouse Cy2- or Cy3-conjugated IgG (1:1000; Jackson ImmunoResearch). Slices were coverslipped using fluorescence mounting medium.

2.2.8.5 Immunohistochemistry – Double Immunofluorescence Free-Floating

In order to specify the cell type of pSer129-SNCA, p62 and ubiquitin positive but TH negative cells, double immunofluorescence immunohistochemistry for pSer129-SNCA and GFAP as a marker for glial cells, pSer129-SNCA and NeuN a neuron marker, pSer129-SNCA and GAD65 as marker for GABAergic neurons, pSer129-SNCA and VGLUT2 as marker for glutamatergic neurons and pSer129-SNCA and parvalbumin as marker for interneurons were applied. 30 µm thick, free floating midbrain sections of paralyzed A53T-SNCA + *Pink1*KO mice were rinsed in PBS. Thereafter, sections were blocked for 1 h in blocking solution [10% normal goat serum, 0.5% TritonX-100, PBS] to prevent unspecific staining. Subsequently, slices were incubated with the respective primary antibodies delivered in 1% normal goat serum, 0.5% TritonX-100 and PBS for 48 h at 4 °C. The following primary antibody combinations were used: rabbit anti pSer129-SNCA (1:500, Abcam) and mouse anti GFAP (1:500, Cell Signaling); rabbit anti pSer129-SNCA (1:500, Abcam) and mouse anti NeuN (1:1000, Chemicon); rabbit anti pSer129-SNCA (1:500, Abcam) and mouse anti GAD65 (1:500, Sigma); rabbit anti

pSer129-SNCA (1:500, Abcam) and mouse anti VGLUT2 (1:500, Millipore); rabbit anti pSer129-SNCA (1:500, Abcam) and mouse anti parvalbumin (1:500, Chemicon). Thereafter, sections were washed three times for 10 min in PBS before they were incubated for 6 h at room temperature with the appropriate secondary antibodies. Secondary antibodies were anti-rabbit Cy2-conjugated IgG (1:1000, Jackson ImmunoResearch) and anti-mouse Cy3-conjugated IgG (1:1000, Jackson ImmunoResearch). Slices were coverslipped using fluorescence mounting medium (DAKO).

2.2.8.6 Microscopy

Images for immunohistochemistry within the apomorphine project were acquired using a Nikon 80i microscope with an x-y motorized stage controlled by IrfanView software. Microscopy was performed in the laboratory of Prof Angela Cenci in Lund / Sweden and the help of Francesco Bez. Low magnification pictures were taken with a 4x or 10x objective and high magnification pictures using an oil immersion 100x objective. Images were taken with a built-in digital Olympus DP72 camera.

Immunohistochemistry pictures of the A53T-SNCA + *Pink1*KO project were acquired using a Zeiss Axioplan Microscope. Images were taken with the use of Zeiss Axiovision, Special Edition 64, Release 4.9.1 software and a Zeiss AxioCam MRc camera. Microscopy within this project was done in the laboratory of PD Dr. Udo Rüb with the help of Dr. Kay Seidel at the Dr. Senckenbergisches Chronomedizinisches Institut, J. W. Goethe University, Frankfurt/Main, Germany.

Images for double immunofluorescence were acquired using a confocal laser-scanning microscope (Nikon eclipse90i) and a 60x objective and NIS-Elements Imaging Software 4.20.00. Microscopy for double immunofluorescence was done in the laboratory of Prof Jochen Roeper with the help of Beatrice Kern at the Institute of Neurophysiology, Neuroscience Center, Goethe University Frankfurt.

2.2.8.7 Quantitative Densiometric Analysis of Target Proteins

Quantitative analysis of pERK1/2, pHistoneH3 and FosB

In order to perform quantitative densiometric analysis of pERK1/2, pHistoneH3 and FosB, in apomorphine and vehicle treated PrPmtA and WT mice, different brain regions were analyzed using the freeware ImageJ 1.46r software. Analyzed brain regions were cortex, nucleus accumbens, substantia nigra and two levels of striatum. Thresholds were adjusted for each

brain structure as well as for each staining. After threshold adjustment, analysis of particles was performed counting positive cells within the image.

Tyrosine hydroxylase optical density

The optical density of tyrosine hydroxylase immunostaining was analyzed in PrPmtA and WT mice in the striatum and substantia nigra using the freeware ImageJ 1.46r software. Optical density was analyzed in four different rostrocaudal levels of the striatum taken from bregma +0.74 mm to +0.14 mm as well as four levels of the substantia nigra taken from bregma -1.94 mm to -3.8 mm. For each analysis, optical density of white matter areas was subtracted from values obtained in the region of interest.

2.2.8.8 Statistics

Quantitative data from densitometric analysis of pERK1/2, pHistoneH3 and FosB as well as TH optical density analysis were compared using unpaired *t*-test and Prism 5 software. Data were presented as group means \pm SEM. Significant differences were highlighted in the Figures using asterisks ($T \leq 0.1$, * $P \leq 0.05$; ** $P \leq 0.01$; *** $P \leq 0.001$; **** $P \leq 0.0001$).

3. RESULTS

3.1 **PROJECT I: ALPHA-SYNUCLEIN GAIN-OF-FUNCTION EFFECTS ON CANDIDATE GENES POSSIBLY INVOLVED IN SYNAPTIC PLASTICITY**

The work of the former PhD student Dr A. Kurz focused on the analysis of alpha-synuclein dependent effects that possibly underlie PD. In this work markers of alpha-synuclein function and pathology were studied in a hypothesis free manner using microarray transcriptome analyses of different brain regions obtained from A53T-SNCA overexpressing mice at different ages. Besides the hypothesis free microarray analysis that revealed molecular alterations within the PrPmtA mouse line, A. Kurz also showed subtle changes in dopamine neurotransmission as well as in synaptic plasticity using an electrophysiological approach (Kurz et al., 2010, Platt et al., 2012).

In order to further analyze the molecular mechanism leading to the previously characterized long-term depression (LTD) deficiencies as well as to clarify the role of alpha-synuclein gain-of-function in this process, candidate genes involved in the generation of LTD were validated in the striatum and midbrain of A53T-SNCA overexpressing mice using qPCR. Since most PD patients do not suffer from monogenic forms of PD but rather from polygenic interactions, a mouse model combining the PD-specific stressor of A53T-SNCA overexpression with the absence of the PD-specific stress response factor PINK1 was generated. Therefore, the well characterized PrPmtA mouse line with inbred FVB/N background was crossed to double homozygosity with the well characterized *Pink1*KO mouse line in 129/SvEv background. Wild-type control mice were derived from F1-hybrids of FVB/N and 129/SvEv, aged in parallel to the double-mutant mice. In respect to this valuable new mouse model, the candidate gene analysis was extended to a hypothesis driven candidate gene analysis in midbrain and striatum of PrPmtA, *Pink1*KO as well as A53T-SNCA + *Pink1*KO mice.

3.1.1 **Pre- and Post-Synaptic Expression Changes of Glutamate Receptor Subunits in 6-Month-Old Mice**

The first set of candidate genes possibly involved in the observed LTD deficiencies are subunits of metabotropic and ionotropic glutamate receptors. Glutamate receptors show a pre- and postsynaptic localization and are essential for glutamatergic neurotransmission that is

known to play a role in memory, learning and motor control. There are two groups of glutamate receptors, the ionotropic and the metabotropic glutamate receptors. Ionotropic glutamate receptors are ligand-gated ion channels mediating glutamatergic neurotransmission. Ionotropic glutamate receptors appear in different classes that share a similar structure but differ in their agonist sensitivity. Both classes of ionotropic glutamate receptors, AMPA and NMDA receptors were found to play a role in synaptic plasticity and are hence highly interesting in respect of the A53T-SNCA overexpressing mouse model that already showed changes in neurotransmission and synaptic plasticity using independent techniques. Therefore, this hypothesis driven analysis focused on the pre- and postsynaptic expression of AMPA receptor (Gria1-Gria4) and NMDA receptor (Grin1, Grin2a-d, Grin3a-b) subunits in 6 month-old PrPmtA mice as well as in *Pink1KO* and A53T-SNCA + *Pink1KO* mice using qPCR. Metabotropic glutamate receptors are G-protein-coupled receptors that based on sequence similarity and signal transduction mechanisms, which can be classified into three subgroups. The group I comprises Grm1 and Grm5 and is preferentially coupled to the IP₃/Ca²⁺/PKC pathway promoting the hydrolysis of phosphoinositides. Group II, comprising Grm 2 and Grm3, as well as group III, comprising Grm4, Grm6, Grm7 and Grm8, are negatively coupled to adenylate cyclase leading to an inhibition of cAMP formation. Metabotropic receptors play a modulatory role in glutamatergic neurotransmission, they are widely expressed in the basal ganglia and there is evidence for metabotropic receptors to be effective therapeutic targets in PD. In this respect the pre- and postsynaptic expression of metabotropic glutamate receptor subunits was analyzed in 6-month-old PrPmtA, *Pink1KO* and A53T-SNCA + *Pink1KO* mice. In table 2 an overview of the glutamate receptor subunit analysis in all three mouse lines at 6-month of age is shown. The left rows illustrate results obtained in PrPmtA striatum and midbrain, thereafter results obtained in double-mutant mice striatum and midbrain are depicted and the last two rows show results obtained in *Pink1KO* striatum and midbrain tissue. Every single subunit was analyzed in the striatum and midbrain tissue of all three mouse lines.

Tab. 2 Overview of results obtained in glutamate receptor subunit analysis of the striatum and midbrain of 6-month-old PrPmtA, A53T-SNCA + *Pink1*KO and *Pink1*KO mice using qPCR. Red illustrates significant upregulation, yellow a trend towards upregulation, light green a trend towards downregulation and dark green significant downregulation. White boxes show unregulated transcripts. Asterisks indicate the degree of significance.

	PrPmtA str	PrPmtA mb	Pink1KO + A53T-SNCA str	Pink1KO + A53T-SNCA mb	Pink1KO str	Pink1KO mb
<i>Gria1</i>			*			
<i>Gria2</i>	**		*			
<i>Gria3</i>		*				
<i>Gria4</i>		*				
<i>Grin1</i>		*				
<i>Grin2a</i>		*				
<i>Grin2b</i>						
<i>Grin2c</i>				*		
<i>Grin2d</i>		**			*	
<i>Grin3a</i>	**					
<i>Grin3b</i>	*		*			
<i>Grm1</i>	*		*			
<i>Grm2</i>						*
<i>Grm3</i>	*	**				
<i>Grm4</i>						
<i>Grm5</i>		**				
<i>Grm6</i>						
<i>Grm7</i>						
<i>Grm8</i>						

Legend	
	downregulated (Trend)
	downregulated (significant)
	upregulated (Trend)
	upregulated (significant)

3.1.1.1 PrPmtA Mice Show an Increased Glutamate Receptor Subunit Expression

The analysis of ionotropic glutamate receptor subunits revealed an increased upregulation of the AMPA receptor subunit *Gria2* (Fig. 15A) as well as increased upregulations of the NMDA receptor subunits *Grin3a* and *Grin3b* (Fig. 15B), in striatal tissue of 6-month-old A53T-SNCA overexpressing mice. The analysis of metabotropic glutamate receptor subunits again illustrated significant higher transcript levels in the striatum of transgenic compared to wild-type mice (Fig. 15C) for *Grm1* a group I and *Grm3* a group II metabotropic glutamate receptor.

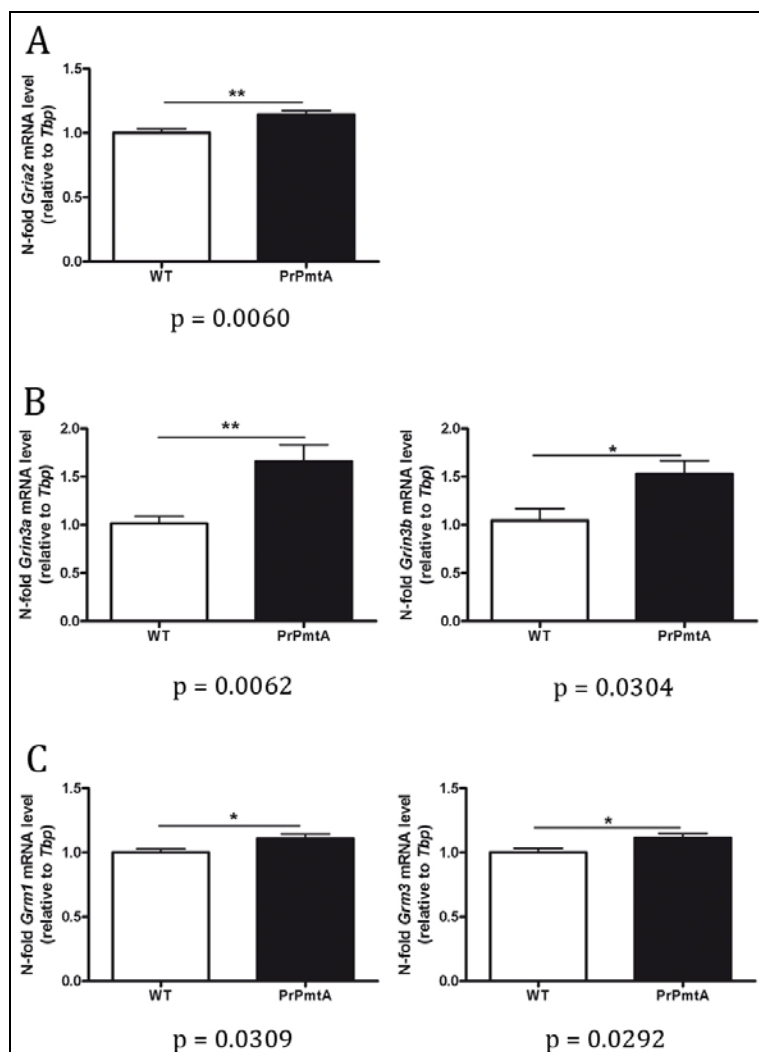


Fig. 15 Striatal glutamate receptor subunit analysis in PrPmtA mice. Quantitative analysis of qPCR data from striatum of 6-month-old wild-type and PrPmtA mice showed significant higher transcript level for the ionotropic glutamate receptor subunits *Gria2* (A), *Grin3a* and *Grin3b* (B) as well as for the metabotropic glutamate receptor subunits *Grm1* and *Grm3* (C). The amount of candidate gene transcripts was normalized relative to the housekeeping gene *Tbp*. Data are presented as mean \pm SEM; n=6 WT and 6 PrPmtA.

The analysis of ionotropic glutamate receptor subunits in midbrain depicted significant higher transcript levels for the AMPA receptor subunits *Gria2*, *Gria3* and *Gria4* (Fig. 16A) as well as significant higher transcript levels for the NMDA receptor subunits *Grin1*, *Grin2a* and *Grin2d* (Fig. 16B) in 6-month-old PrPmtA compared to wild-type mice. The analysis of metabotropic glutamate receptor subunits revealed significant higher group I (*Grm1* and *Grm5*), group II (*Grm3*) and group III (*Grm4*) transcript levels in midbrain of PrPmtA compared to WT (Fig. 16C). In this analysis the alpha-synuclein gain-of-function was found to increase the transcript levels of ionotropic and metabotropic glutamate receptor subunits both in striatal and midbrain tissue.

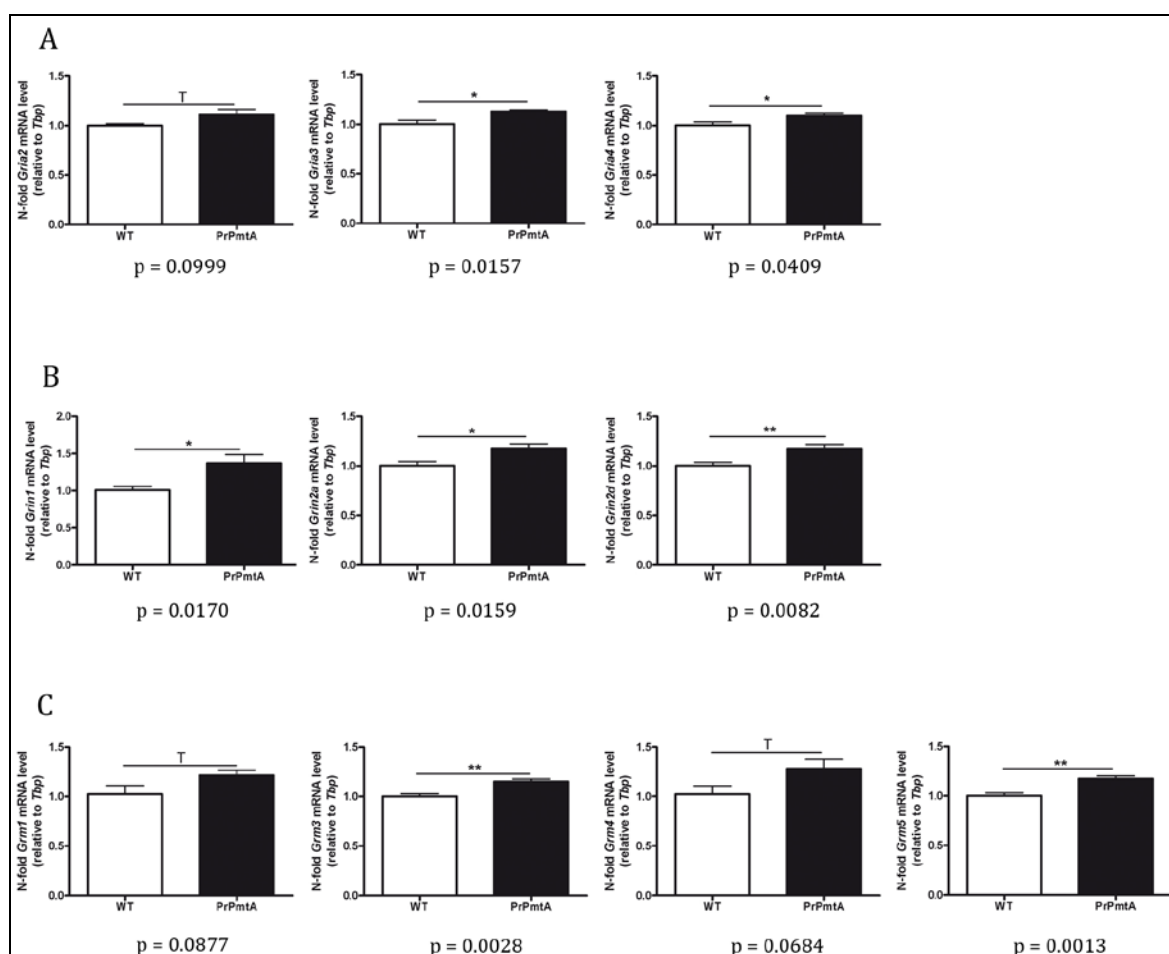


Fig. 16 Midbrain glutamate receptor analysis in PrPmtA mice. Quantitative analysis of qPCR data from mid-brain of 6-month-old wild-type and PrPmtA mice showed significant higher transcript level for the ionotropic glutamate receptor subunits *Gria2*, *Gria3* and *Gria4* (A), *Grin1*, *Grin2a* and *Grin2b* (B) as well as for the metabotropic glutamate receptor subunits *Grm1*, *Grm3*, *Grm4* and *Grm5* (C). The amount of candidate gene transcripts was normalized relative to the housekeeping gene *Tbp*. Data are presented as mean \pm SEM; n=6 WT and 6 PrPmtA.

3.1.1.2 Additional *Pink1* Ablation (A53T-SNCA + *Pink1*KO Mice) Leads to Reduced Expression Levels

The analysis of ionotropic glutamate receptor subunits in A53T-SNCA overexpressing mice with additional *Pink1* ablation showed significantly reduced striatal transcript levels of *Gria1*, *Gria2* and *Grin3b* in 6 month-old double-mutants compared to the respective wild-type controls (Fig. 17A-B). The striatal transcript level analysis of metabotropic glutamate receptor subunits depicted *Grm1*, a group I member to be significantly and *Grm8*, a group III member to show a trend towards reduction (Fig. 17C).

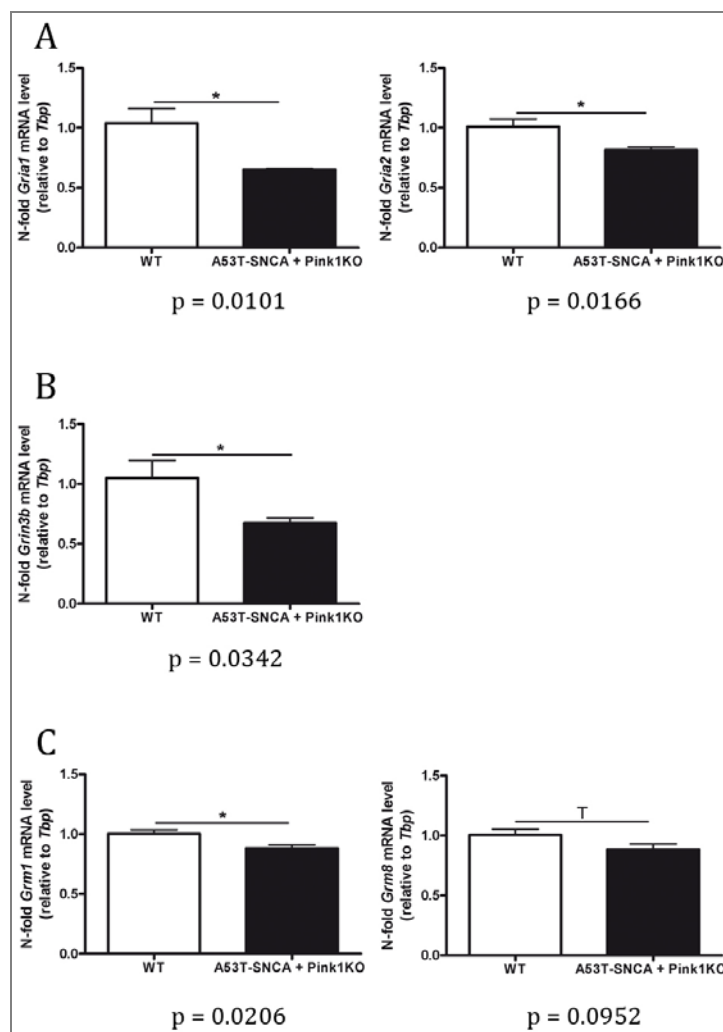


Fig. 17 Striatal glutamate receptor analysis in A53T-SNCA + *Pink1*KO mice. Quantitative analysis of qPCR data from striatum of 6-month-old A53T-SNCA + *Pink1*KO and wild-type mice showed significant lower transcript level for the ionotropic glutamate receptor subunits *Gria1*, *Gria2* (A) and *Grin3b* (B) as well as for the metabotropic glutamate receptor subunit *Grm1*. A trend towards reduction was found for the group III metabotropic glutamate receptor subunit *Grm8* (C). The amount of candidate gene transcripts was normalized relative to the housekeeping gene *Tbp*. Data are presented as mean \pm SEM; n=6 WT and 6 A53T-SNCA + *Pink1*KO.

The analysis of ionotropic and metabotropic glutamate receptor subunits in midbrain of double-mutant mice revealed a significant lower transcript level for *Grin2c* in 6-month-old double-mutant compared to wild-type mice and a trend towards reduction for *Grin3a* transcript level (Fig. 18). In this analysis the impaired stress response through *Pink1* ablation in combination with the PD specific stressor A53T-SNCA overexpression resulted in reduced transcript level of ionotropic and metabotropic glutamate receptor subunits both on a pre- and postsynaptic level (Fig. 17 - Fig. 18).

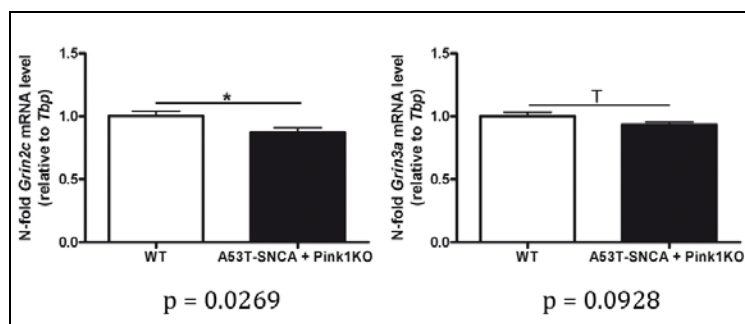


Fig. 18 Midbrain glutamate receptor analysis in A53T-SNCA + *Pink1*KO mice. Quantitative analysis of qPCR data from midbrain of 6-month-old A53T-SNCA + *Pink1*KO and wild-type mice showed a significant lower transcript level for the ionotropic glutamate receptor subunit *Grin2c* and a trend towards reduction for *Grin3a*. The amount of candidate gene transcripts was normalized relative to the housekeeping gene *Tbp*. Data are presented as mean \pm SEM; n=6 WT and 6 A53T-SNCA + *Pink1*KO.

3.1.1.3 Exclusive *Pink1* Ablation has Only Minor Effects on Glutamate Receptor Subunit Expression

In order to study the effect of *Pink1* ablation itself onto transcript level of glutamate receptor subunits, the analysis was conducted in *Pink1*KO mice and their respective wild-type control mice at the age of 6 months. The analysis revealed a significant reduction in striatal tissue of the ionotropic glutamate receptor subunit transcript level *Grin2d* (Fig. 19B), whereas for *Gria1* a trend towards induction was observed (Fig. 19A). The transcript level analysis of metabotropic glutamate receptor subunits in the striatum of *Pink1*KO mice depicted a trend towards reduction for *Grm8* (Fig. 19C).

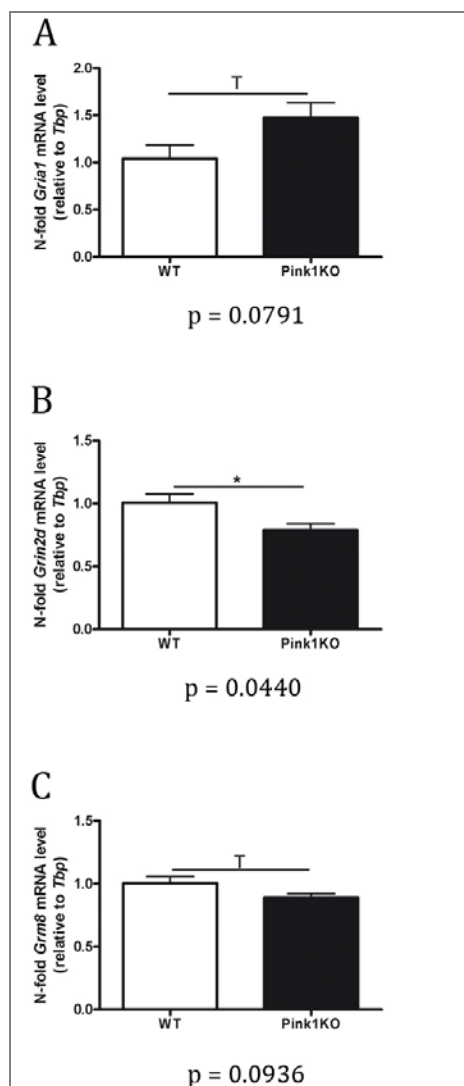


Fig. 19 Striatal glutamate receptor analysis in *Pink1*KO mice. Quantitative analysis of qPCR data from striatum of 6-month-old *Pink1*KO and wild-type mice showed a significant lower transcript level for the ionotropic glutamate receptor subunit *Grin2d* (B) and a trend towards induction for *Gria1* (A). A trend towards reduction was also found for the group III metabotropic glutamate receptor subunit *Grm8* (C). The amount of candidate gene transcripts was normalized relative to the housekeeping gene *Tbp*. Data are presented as mean \pm SEM; n=5 WT and 5 *Pink1*KO.

The presynaptic transcript level analysis of ionotropic and metabotropic glutamate receptor subunits obtained a significantly reduced *Grm2* transcript level in midbrain of 6-month-old *Pink1*KO compared to wild-type mice (Fig. 20). The comparative analysis of all three mouse lines illustrated that *Pink1* ablation exclusively has only a minor impact on the pre- and postsynaptic expression of glutamate receptor subunits, whereas alpha-synuclein gain-of-function showed substantial stronger transcriptional effects (Tab. 2).

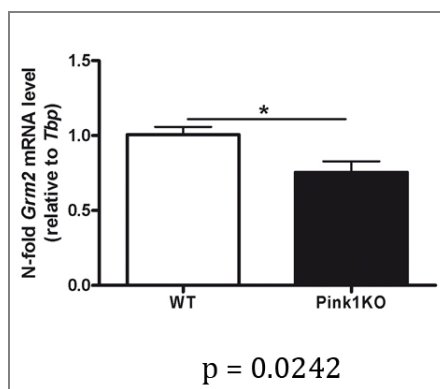


Fig. 20 Midbrain glutamate receptor analysis in *Pink1KO* mice. Quantitative analysis of qPCR data from mid-brain of 6-month-old *Pink1KO* and wild-type mice showed a significant lower transcript level for the metabotropic glutamate receptor subunit *Grm2*. The amount of candidate gene transcripts was normalized relative to the housekeeping gene *Tbp*. Data are presented as mean \pm SEM; n=5 WT and 5 *Pink1KO*.

3.1.2 Pre- and Post-Synaptic Expression Changes of Scaffolding Proteins in 6-Month-Old Mice

The next candidate genes possibly involved in the documented LTD deficiency were the scaffolding proteins Homer1 and PSD95. LTD is known to involve the generation of cAMP/cGMP, the phosphorylation of relevant proteins, calcium influx as well as the initiation of immediate early genes in an immediate response, as well as changes of glutamate receptor trafficking in a chronic response. Homer1 assembles group I metabotropic glutamate receptors and couples them to inositol trisphosphate receptors or ion-channels and therefore modulates synaptogenesis. It is also well understood that excessive synaptic activity induces the expression of the dominant negative isoform Homer1a that is acting as endogenous negative modulator of mGluR/IP3 receptor signaling and therefore prevents excessive glutamate-induced neuronal activity. Psd95 assembles ionotropic NMDA receptors and shaker type potassium channels. Psd95 is essential for NMDA receptor signaling associated forms of synaptic plasticity. Both scaffolding proteins are potentially involved in processes of impaired neurotransmission and LTD deficiency that was observed in A53T-SNCA overexpressing mice and were therefore studied in the PrPmtA mouse line. The analysis of Homer1 and Psd95 in double-mutant and *Pink1KO* mice can provide further information about common downstream pathways. An overview of results obtained in the pre- and postsynaptic analysis of 6-month-old mice is shown in table 3, where green represents downregulated and red upregulated transcript levels.

Tab. 3 Overview of results obtained in the analysis of the scaffolding proteins *Homer1* and *Psd95* in the striatum and midbrain of 6-month-old PrPmtA, A53T-SNCA + *Pink1*KO and *Pink1*KO mice using qPCR. Red illustrates significant upregulation and green significant downregulation. White boxes show unregulated transcripts. Asterisks indicate the degree of significance.

	PrPmtA str.	PrPmtA mb	Pink1KO + A53T-SNCA str	Pink1KO + A53T-SNCA mb	Pink1KO str.	Pink1KO mb
<i>Homer1</i>	***	**	***	***	*	
<i>Psd95</i>		**				

Legend	
	downregulated (significant)
	upregulated (significant)

3.1.2.1 PrPmtA Mice Show an Reduced *Homer1* and Increased *Psd95* Expression

The analysis of *Homer1* and *Psd95* transcript level in striatal and midbrain tissue of 6-month-old A53T-SNCA overexpressing mice revealed significantly reduced pre- and postsynaptic level of *Homer1* as well as increased postsynaptic *Psd95* transcript level in PrPmtA compared to wild-type mice (Fig. 21).

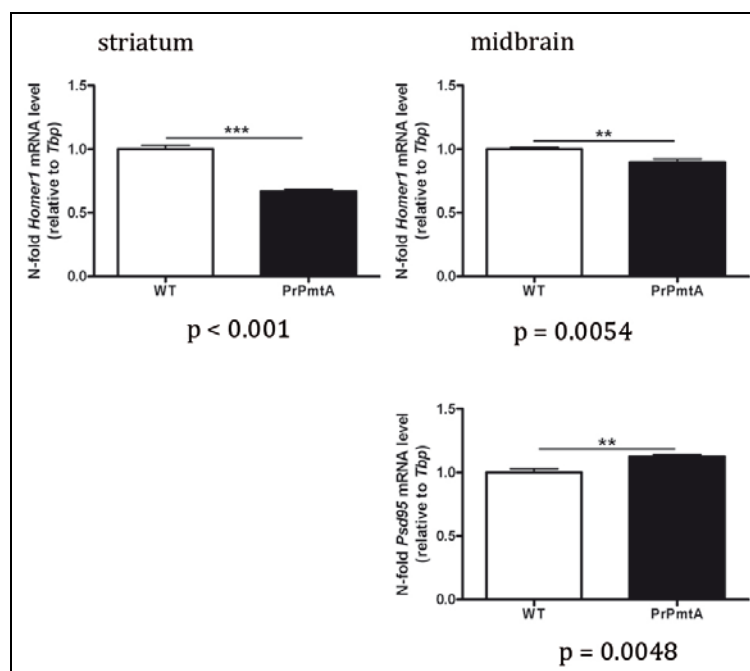


Fig. 21 Striatal scaffolding protein analysis in PrPmtA mice. Quantitative analysis of qPCR data from striatum and midbrain of 6-month-old PrPmtA and wild-type mice showed a significant lower *Homer1* transcript level in striatum and midbrain as well as significantly higher *Psd95* transcript level in midbrain. The amount of candidate gene transcripts was normalized relative to the housekeeping gene *Tbp*. Data are presented as mean \pm SEM; n=6 WT and 6 PrPmtA.

3.1.2.2 Additional *Pink1* Ablation (A53T-SNCA + *Pink1*KO Mice) Maintains Reduced *Homer1* Expression but not *Psd95*

The transcript level analysis of the scaffolding proteins *Homer1* and *Psd95* in A53T-SNCA overexpressing mice with additional *Pink1* ablation demonstrated significantly reduced pre- and postsynaptic *Homer1* transcript levels (Fig. 22), whereas *Psd95* level were unchanged. The additional *Pink1* ablation maintained or even supported the alpha-synuclein gain-of-function dependent effects on *Homer1* expression but altered the one responsible for *Psd95*.

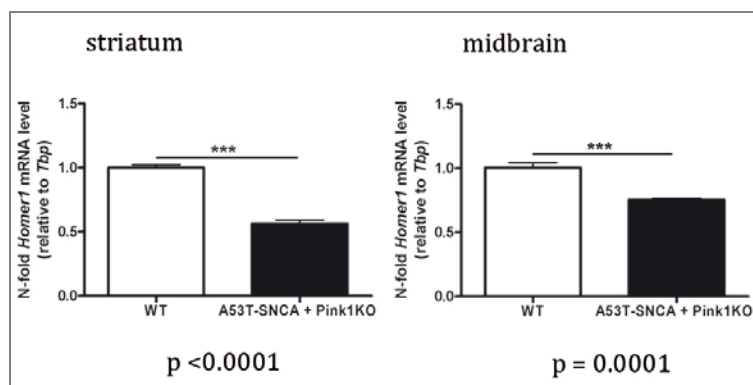


Fig. 22 Striatal and midbrain analysis of scaffolding proteins in A53T-SNCA + *Pink1*KO mice. Quantitative analysis of qPCR data from striatum and midbrain of 6-month-old A53T-SNCA + *Pink1*KO and wild-type mice showed a significant lower *Homer1* transcript level in striatum and midbrain. The amount of candidate gene transcripts was normalized relative to the housekeeping gene *Tbp*. Data are presented as mean \pm SEM; n=6 WT and 6 A53T-SNCA + *Pink1*KO.

3.1.2.3 Exclusive *Pink1* Ablation Affects *Homer1* Expression only in the Striatum

In order to depict effects that are exclusive to *Pink1* ablation, *Homer1* and *Psd95* transcript level were analyzed in striatal and midbrain tissue of 6-month-old *Pink1*KO mice. The analysis exhibited reduced postsynaptic *Homer1* transcript level but no presynaptic alterations (Fig. 23). Regarding *Psd95*, neither pre- nor postsynaptic alterations were detectable, suggesting alpha-synuclein gain-of-function having the dominant effect on *Homer1* and *Psd95* expression. Accordingly, *Pink1* ablation without a cellular stressor has only minor effects on transcript regulation and hence synaptic plasticity.

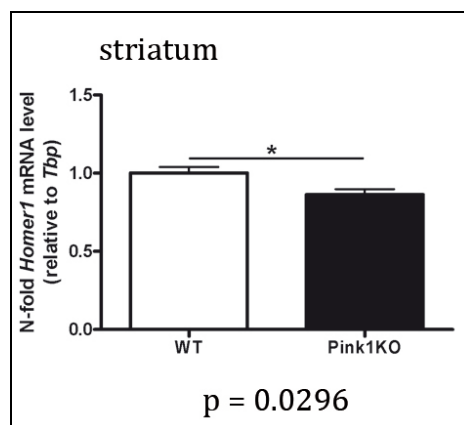


Fig. 23 Striatal analysis of scaffolding proteins in *Pink1KO* mice. Quantitative analysis of qPCR data from striatum of 6-month-old *Pink1KO* and wild-type mice showed a significant lower *Homer1* transcript level. The amount of candidate gene transcripts was normalized relative to the housekeeping gene *Tbp*. Data are presented as mean \pm SEM; n=5 WT and 5 *Pink1KO*.

3.1.3 Pre- and Post-Synaptic Expression Changes of Immediate-Early-Genes and Transcription Factors in 6-Month-Old Mice

As previously mentioned, one of the earliest effects of LTD involves the initiation of immediate-early-gene (IEG) transcripts. Therefore, the next transcript analysis focused on immediate-early-genes that are known to mediate neuronal excitability. The analysis focused on *Arc* since *Arc* is a stabilizer of synaptic plasticity that regulates the endocytosis of AMPA receptors. *cFos* was studied due to its important role in signal transduction as well as the high inducibility in striatal medium spiny neurons by D1 receptor stimulation (Graybiel et al., 1990, Young et al., 1991). Just as *cFos*, *JunB* and *FosB* are transcription factors that are activated in response to stimuli such as growth factors. The transcription factor *Creb1* is the cAMP-responsive element binding protein 1, a sequence that is present in many cellular promoters. *Creb1* is involved in the neuroprotective response to pathophysiological effectors (for review see(Sakamoto et al., 2011)) and was found to be necessary in the formation of late phase LTD in Purkinje cells derived from mice (Ahn et al., 1999). *Egr1* and *Egr2* are transcriptional regulator that specifically activate the transcription of their target genes. They are induced by a variety of extracellular stimuli such as synaptic activity and long-term potentiation. *Foxo3* is a transcriptional activator initiating apoptosis in absence of survival factors or in consequence to oxidative stress. *Nr4a1*, *Nr4a2* and *Nr4a3* are members of the nuclear hormone receptor superfamily also known as *Nur77*, *Nurr1* and *NOR1* playing an important role in the adaption and homeostatic regulation of the dopaminergic system (Maxwell and Muscat, 2006). In order to further understand the molecular effect of alpha-synuclein gain-of-function on LTD, IEGs were investigated in all three mouse lines (PrPmtA, *Pink1KO* and A53T-SNCA +

Pink1KO) at the age of 6 month. An overview of results obtained in this analysis is shown in table 4, where green represents significantly downregulated transcript level, light green a trend towards downregulation, yellow a trend towards upregulation and red significantly upregulated transcript level. Asterisks indicate the degree of significance.

Tab. 4 Overview of results obtained in the analysis of immediate early genes and transcription factors in the striatum and midbrain of 6-month-old PrPmtA, A53T-SNCA + *Pink1KO* and *Pink1KO* mice using qPCR. Red illustrates significant upregulation, yellow a trend towards upregulation, light green a trend towards downregulation and dark green significant downregulation. White boxes show unregulated transcripts. Asterisks indicate the degree of significance.

	PrPmtA str	PrPmtA mb	Pink1KO + A53T-SNCA str	Pink1KO + A53T-SNCA mb	Pink1KO str	Pink1KO mb
<i>Arc</i>	**					
<i>cFos</i>	*	**		*		
<i>Creb1</i>				**		
<i>FosB</i>	*		*	***		
<i>Egr1</i>	***	*				
<i>Egr2</i>	**			*		**
<i>Foxo3</i>						
<i>JunB</i>			***	***		
<i>Nur77</i>	**		*	***		
<i>Nurr1</i>				*		
<i>NOR1</i>	***	**	*	***		

Legend	
	downregulated (Trend)
	downregulated (significant)
	upregulated (Trend)
	upregulated (significant)

3.1.3.1 PrPmtA Mice Show a Reduced Expression of Immediate-Early-Genes and Transcription Factors

The postsynaptic analysis of immediate-early-genes and transcription factors in 6-month-old A53T-SNCA overexpressing mice revealed a significant reduction for most of the analyzed transcript levels. Significantly reduced transcript level were observed for *Arc* (Fig. 24A), *cFos* (Fig. 24B), *FosB* (Fig. 24C), *Egr1* (Fig. 24D), *Egr2* (Fig. 24E), *NOR1* (Fig. 24G) and *Nur77* (Fig. 24H). The transcript level of *Foxo3* was found to show a trend towards upregulation (Fig. 24F). The analysis of *Creb1*, *JunB* and *Nurr1* observed no alterations in striatal tissue of 6-month-old PrPmtA mice compared to wild-type.

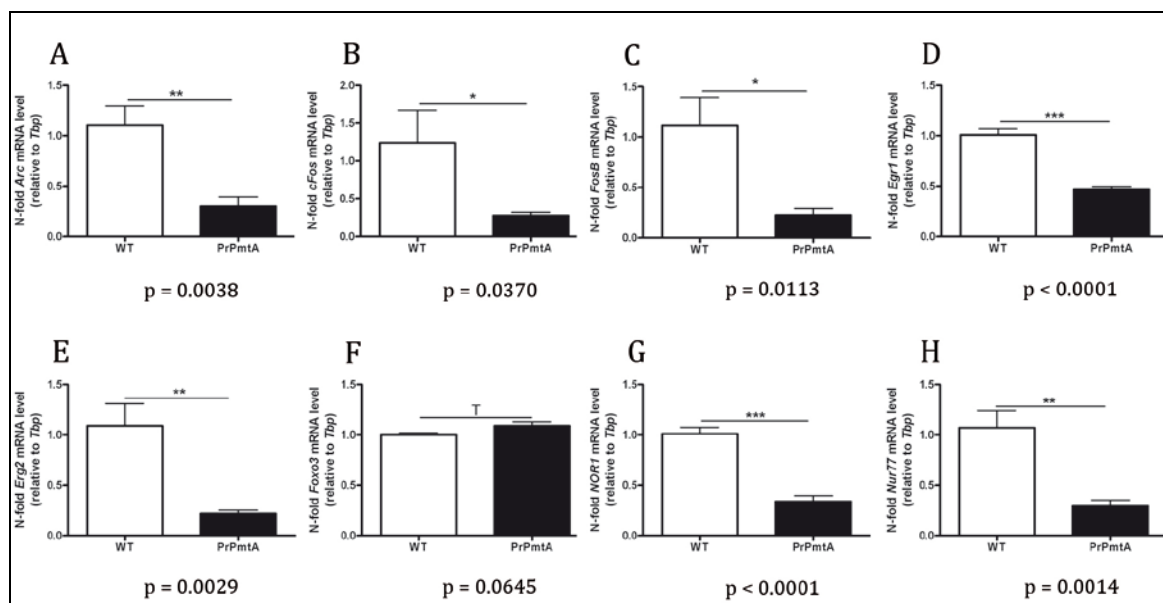


Fig. 24 Striatal analysis of immediate early genes and transcription factors in PrPmtA mice. Quantitative analysis of qPCR data from striatum of 6-month-old wild-type and PrPmtA mice showed significant lower transcript level for the IEGs and transcription factors *Arc* (A), *cFos* (B), *FosB* (C), *Egr1* (D), *Egr2* (E), *NOR1* (G) and *Nur77* (H). Transcript level of the transcriptional activator *Foxo3* was found to show a trend towards increased level (F). The amount of candidate gene transcripts was normalized relative to the housekeeping gene *Tbp*. Data are presented as mean \pm SEM; n=6 WT and 6 PrPmtA.

The presynaptic analysis of immediate-early-genes and transcription factors in 6-month-old PrPmtA and wild-type mice revealed again significant lower transcript level for *cFos* (Fig. 25A), *Egr1* (Fig. 25B), *NOR1* (Fig. 25C) and *Nur77* (Fig. 25D). The transcript level analysis of immediate-early-genes and transcription factors in A53T-SNCA overexpressing mice showed a consistent downregulation in striatal and midbrain tissue at the age of 6 months, representing a molecular readout of the electrophysiologically characterized LTD deficiency.

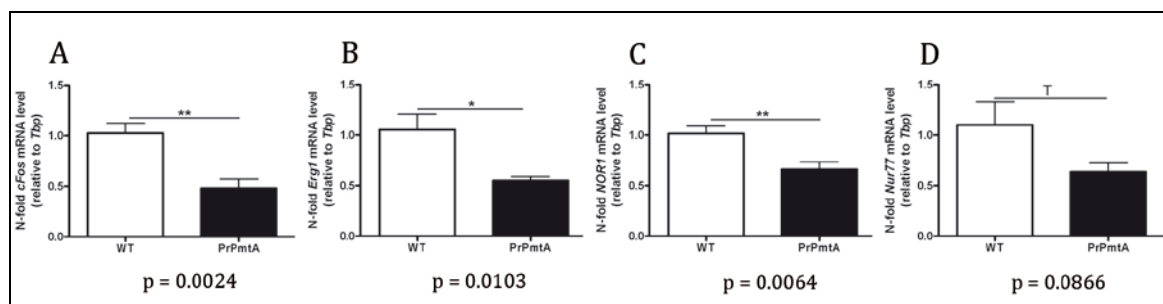


Fig. 25 Midbrain analysis of immediate early genes and transcription factors in PrPmtA mice. Quantitative analysis of qPCR data from midbrain of 6-month-old wild-type and PrPmtA mice showed significant lower transcript level for the IEG and transcription factors *cFos* (A), *Egr1* (B), *NOR1* (C) and *Nur77* (D). The amount of candidate gene transcripts was normalized relative to the housekeeping gene *Tbp*. Data are presented as mean \pm SEM; n=6 WT and 6 PrPmtA.

3.1.3.2 Additional *Pink1* Ablation (A53T-SNCA + *Pink1*KO Mice) Maintains a Reduced Expression of Immediate-Early-Genes and Transcription Factors

The analysis of immediate-early-genes and transcription factors was thereafter performed in striatal and midbrain tissue of 6-month-old double-mutant mice, where the PD specific stressor A53T-SNCA overexpression is combined with the loss of PINK1-dependent stress response. The postsynaptic analysis revealed significantly reduced transcript level for *FosB* (Fig. 26A), *JunB* (Fig. 26B), *NOR1* (Fig. 26C) and *Nur77* (Fig. 26D).

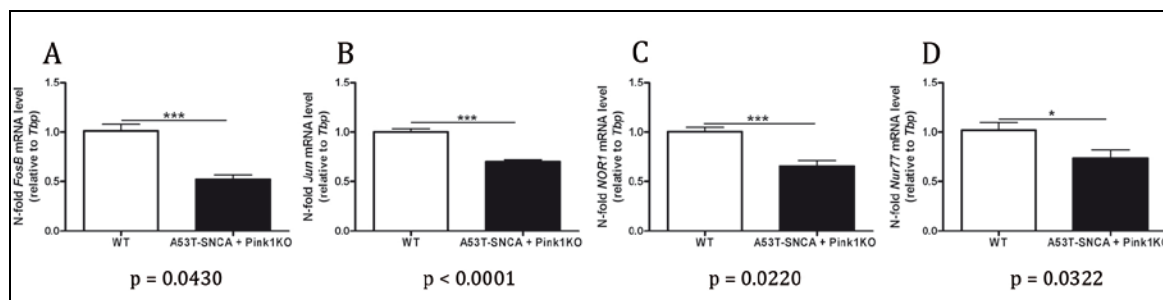


Fig. 26 Striatal analysis of immediate early genes and transcription factors in A53T-SNCA + *Pink1*KO mice. Quantitative analysis of qPCR data from striatum of 6-month-old A53T-SNCA + *Pink1*KO and wild-type mice showed significant lower transcript levels for the IEGs and transcription factors *cFos* (A), *JunB* (B), *NOR1* (C) and *Nur77* (D). The amount of candidate gene transcripts was normalized relative to the housekeeping gene *Thp*. Data are presented as mean \pm SEM; n=6 WT and 6 A53T-SNCA + *Pink1*KO.

The presynaptic analysis of immediate-early-genes and transcription factors depicted again a significant reduction for most of the analyzed transcript levels (Fig. 27). *cFos* (Fig. 27A), *Creb1* (Fig. 27B), *FosB* (Fig. 27C), *Egr2* (Fig. 27D), *JunB* (Fig. 27E), *NOR1* (Fig. 27F), *Nurr1* (Fig. 27G) and *Nur77* (Fig. 27H) were found significantly downregulated in midbrain tissue of 6-month-old double-mutant mice compared to wild-type. The consistent downregulation of immediate-early-genes and transcription factors in striatal and midbrain tissue of PrPmtA and double-mutant mice illustrates the strong influence of alpha-synuclein gain-of-function onto synaptic plasticity that is, at the observed age, shifted from a mainly postsynaptic to a predominantly presynaptic effect through additional *Pink1* ablation.

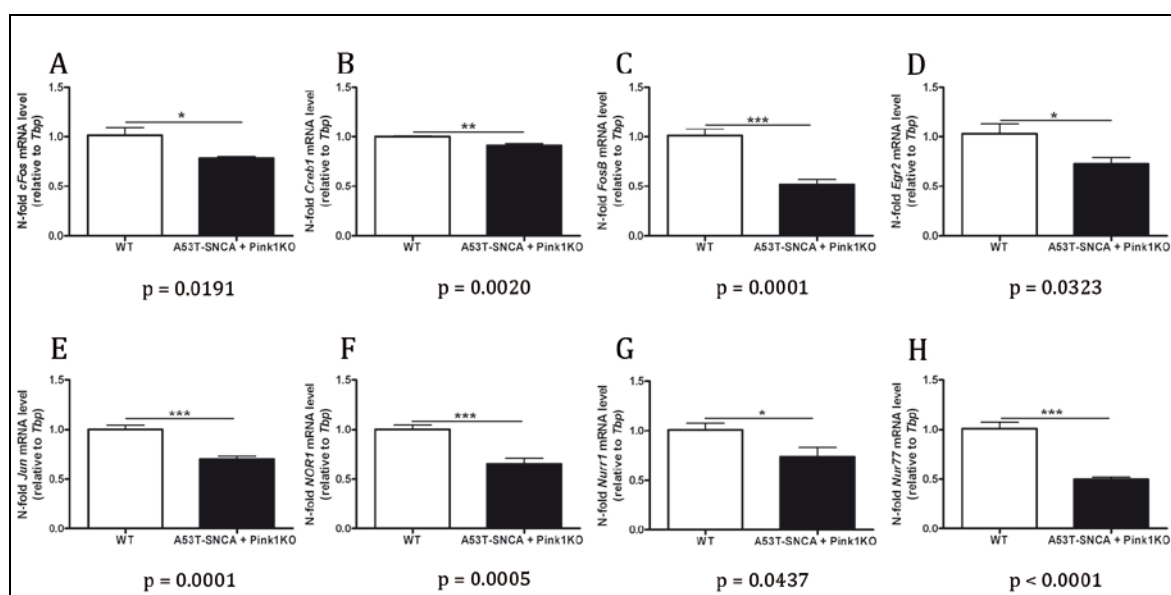


Fig. 27 Midbrain analysis of immediate early genes and transcription factors in A53T-SNCA + *Pink1*KO mice. Quantitative analysis of qPCR data from midbrain of 6-month-old A53T-SNCA + *Pink1*KO and wild-type mice showed significant lower transcript levels for the IEGs and transcription factors *cFos* (A), *Creb1* (B), *FosB* (C), *Egr2* (D), *JunB* (E), *NOR1* (F), *Nurr1* (G) and *Nur77* (H). The amount of candidate gene transcripts was normalized relative to the housekeeping gene *Tbp*. Data are presented as mean \pm SEM; n=6 WT and 6 A53T-SNCA + *Pink1*KO.

3.1.3.3 Exclusive *Pink1* Ablation has only Minor Effects on the Expression of Immediate-Early-Genes and Transcription Factors

In order to depict the effect of *Pink1* ablation onto the transcript level of immediate-early-genes and transcription factors, the same analysis was performed in striatal and midbrain tissue of 6-month-old *Pink1*KO mice compared to the respective wild-type controls. This analysis showed no significant alterations in striatal transcript levels, but depicted a trend towards upregulation for *cFos* (Fig. 28A) and a trend towards downregulation for *Nurr1* (Fig. 28B).

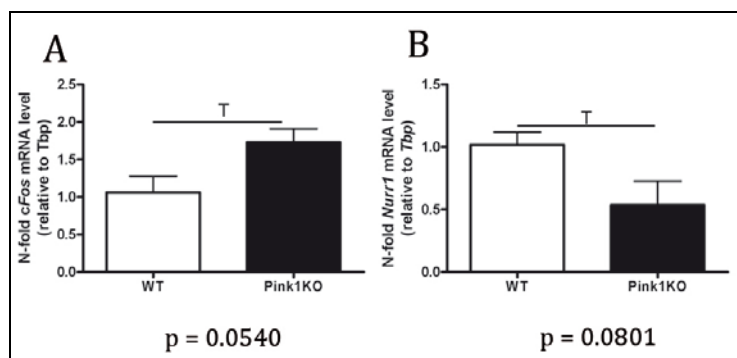


Fig. 28 Striatal analysis of immediate early genes and transcription factors in *Pink1KO* mice. Quantitative analysis of qPCR data from striatum of 6-month-old *Pink1KO* and wild-type mice showed a trend towards increased transcript level for the IEGs and transcription factors *cFos* (A) as well as a trend towards reduced transcript level for *Nurr1* (B). The amount of candidate gene transcripts was normalized relative to the housekeeping gene *Tbp*. Data are presented as mean \pm SEM; n=5 WT and 5 *Pink1KO*.

The presynaptic analysis of 6-month-old *Pink1KO* mice compared to wild-type controls, observed significantly reduced transcript levels for the transcriptional regulator *Egr2* (Fig. 29A) and a trend towards reduction for the nuclear hormone receptor *NOR1* (Fig. 29B). In contrast with the expression changes obtained in the analysis of PrPmtA or double-mutant mice, *Pink1* ablation has only minor effects on the expression of immediate-early-genes and transcription factors. Therefore, the huge expression alterations observed in PrPmtA and double-mutant mice are clearly effects of alpha-synuclein gain-of-function.

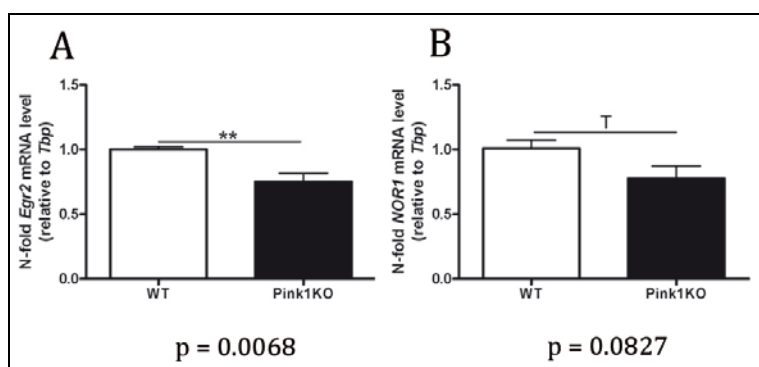


Fig. 29 Midbrain analysis of immediate early genes and transcription factors in *Pink1KO* mice. Quantitative analysis of qPCR data from midbrain of 6-month-old *Pink1KO* and wild-type mice showed significant reduced transcript level for the IEGs and transcription factors *Egr2* (A) as well as a trend towards reduced transcript level for *NOR1* (B). The amount of candidate gene transcripts was normalized relative to the housekeeping gene *Tbp*. Data are presented as mean \pm SEM; n=5 WT and 5 *Pink1KO*.

3.1.4 Pre- and Post-Synaptic Expression Changes of Additional Candidate Genes in 6-Month Old Mice

In a last approach of analyzing transcript levels that possibly reflect the observed LTD deficiency as well as the impaired neurotransmission, additional hypothesis driven candidates were chosen and analyzed mainly in the A53T-SNCA overexpressing mouse line but also in the double-mutant and *Pink1*KO line. The first candidate of interest is *Bad*, Bcl2-associated agonist of cell death. *Bad* indirectly promotes apoptosis by sequestering the anti-apoptotic BCL-2 proteins (Yang et al., 1995). Apoptosis was already described in 1991 to play a role in PD (Dipasquale et al., 1991) and furthermore A53T-SNCA overexpressing mice have been shown to express markers of apoptosis in neocortex, brainstem and spinal cord (Martin et al., 2006). The next candidate *IP3R*, inositol 1,4,5-trisphosphate receptor, was chosen due to its ability to associate with Homer1 (Tu et al., 1998). In this context *IP3R* could interact with other association partners of Homer1 such as metabotropic glutamate receptors and affect neural functions. *IP3* receptor function has also been widely studied in the cerebellum, where a loss of *IP3R* leads to abnormal dendritic morphology (Hisatsune et al., 2006). In this context a mediator of G-protein coupled signaling, *RGS2*, was studied. *RGS2* is a member of the RGS family that regulated G-protein signaling and therefore the intercellular communication. *RGS2* is a substrate specific inhibitor of Gq α that is involved in inositol lipid signaling (Heximer et al., 1997) and was therefore studied in this approach. *Pcbd1* is a dehydratase that is involved in the biosynthesis of tetrahydrobiopterin (BH4) (Thony et al., 2000). In the nervous system BH4 has been found to enhance dopamine release (Koshimura et al., 1990) and decreased levels are associated with PD (Curtius et al., 1984). In this respect, *Pcbd1* was studied in all three mouse lines. *Sqstm1* also known as p62 is involved in the degradation of proteins through the proteasome or lysosome (Vadlamudi et al., 1996) and Braak showed p62 positive nerve cells in the hypothalamus and brainstem of PD patients (Braak et al., 2011), highlighting its importance in PD research. The last candidate of interest is tachykinin 1 (*Tac1*), a gene encoding the neuropeptides substance P and neurokinin A that are implicated in the modulation of glutamate-driven neurotransmission and excitotoxicity (Vargas et al., 2005). Table 5 shows an overview of results obtained in the transcript level analysis of the previously mentioned candidate genes in 6-month-old mice. The analysis focused on striatal and midbrain tissue of PrPmtA, A53T-SNCA + *Pink1*KO and *Pink1*KO mice. The left rows show results obtained in PrPmtA striatum and midbrain, thereafter results obtained in double-mutant mice striatum and midbrain are depicted and the last two rows illustrate results obtained in *Pink1*KO striatum and midbrain tissue.

Tab. 5 Overview of results obtained in the pre- and postsynaptic analysis of additional candidate genes in 6-month-old PrPmtA, A53T-SNCA + *Pink1*KO and *Pink1*KO mice using qPCR. Red illustrates significant upregulation, yellow a trend towards upregulation, light green a trend towards downregulation and dark green significant downregulation. White boxes show unregulated transcripts and grey boxes indicate untested genes. Asterisks indicate the degree of significance.

	PrPmtA str	PrPmtA mb	Pink1KO + A53T-SNCA str	Pink1KO + A53T-SNCA mb	Pink1KO str	Pink1KO mb
<i>Bad</i>	**					
<i>IP3R</i>	**	**				
<i>Pcbd1</i>	**					
<i>RGS2</i>	***					
<i>Sqstm1</i>		*		*		
<i>Tac1</i>		**				

Legend	
	downregulated (Trend)
	downregulated (significant)
	upregulated (Trend)
	upregulated (significant)
	not tested

3.1.4.1 PrPmtA Mice Show an Increased Expression of *Pcbd1*, *Bad*, *Tac1*, *Sqstm1*, *IP3R* and *RGS2*

The analysis of hypothesis driven additional candidate genes in A53T-SNCA overexpressing mice revealed significantly increased transcript levels for *Bad* (Fig. 30A), *IP3R* (Fig.30B) and *Pcbd1* (Fig. 30C) in striatal tissue of 6-month-old PrPmtA compared to wild-type mice, whereas the striatal transcript level analysis of *Tac1* obtained a trend towards induction (Fig. 30E). In contrast, transcript levels of *RGS2* were found significantly reduced in PrPmtA compared to wild-type mice (Fig. 30D).

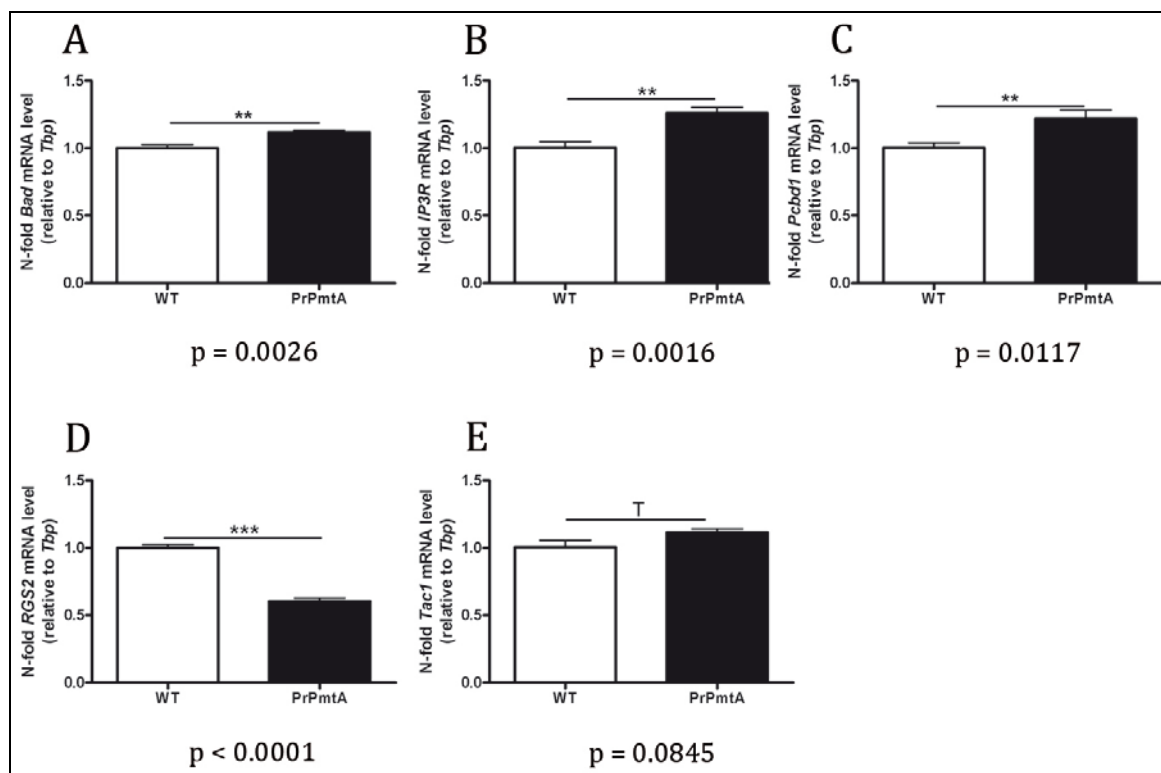


Fig. 30 Striatal analysis of additional candidates in PrPmtA mice. Quantitative analysis of qPCR data from striatum of 6-month-old wild-type and PrPmtA mice showed significantly higher transcript level for *Bad* (A), *IP3R* (B) and *Pcbd1* (C). Transcript levels of *Tac1* (E) showed a trend towards induction and of *RGS2* (D) were found significantly reduced. The amount of candidate gene transcripts was normalized relative to the housekeeping gene *Tbp*. Data are presented as mean \pm SEM; n=6 WT and 6 PrPmtA.

The presynaptic transcript level analysis of additional candidate genes observed again significantly reduced expression levels for *IP3R* (Fig. 31A) and *Tac1* (Fig. 31C) whereas reduced *Sqstm1* transcript level was exclusively found in midbrain of A53T-SNCA overexpressing mice (Fig. 31B). In summary the hypothesis driven transcript level analysis of additional candidate genes possibly involved in molecular mechanism of synaptic plasticity and neurotransmission substantiates the hypothesis of impaired neurotransmission and LTD deficiencies to occur as an early effect of alpha-synuclein gain-of-function that is effectively compensated in early ages and becomes prominent in old age.

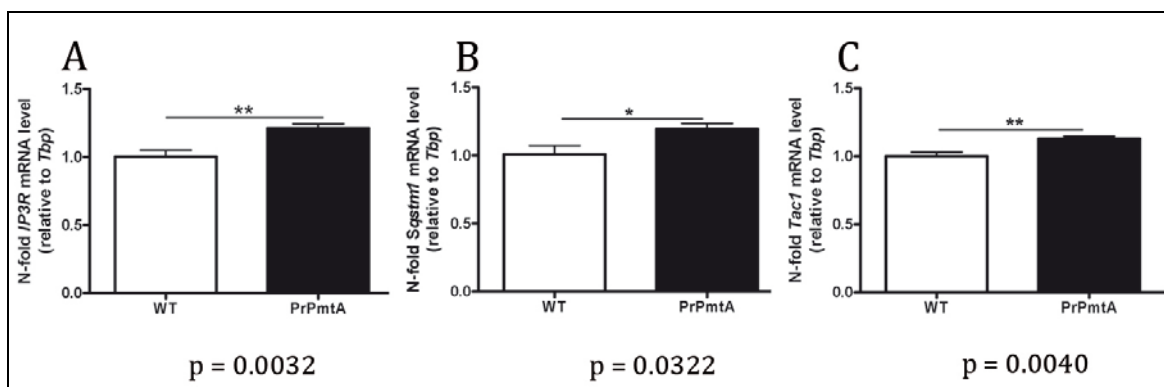


Fig. 31 Midbrain analysis of additional candidates in PrPmtA mice. Quantitative analysis of qPCR data from midbrain of 6-month-old wild-type and PrPmtA mice showed significantly higher transcript level for *IP3R* (A), *Sqstm1* (B) and *Tac1* (C). The amount of candidate gene transcripts was normalized relative to the housekeeping gene *Tbp*. Data are presented as mean \pm SEM; n=6 WT and 6 PrPmtA.

3.1.4.2 Additional *Pink1* Ablation (A53T-SNCA + *Pink1*KO Mice) Leads to Reduced Expression Level for *Sqstm1*

The pre- and postsynaptic transcript level analysis of additional candidate genes in double-mutant mice revealed a trend towards downregulation for *Tac1* in striatal tissue (Fig. 32A) as well as significantly reduced *Sqstm1* transcript level in midbrain (Fig. 32B). In comparison to PrPmtA mice, double-mutant mice showed only minor transcript level alteration.

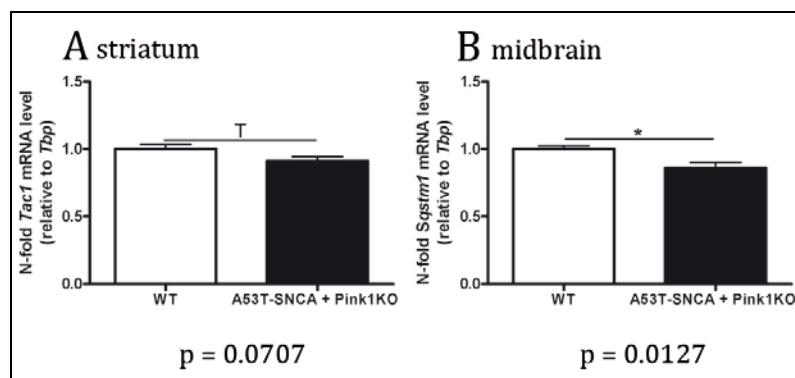


Fig. 32 Striatal and midbrain analysis of additional candidates in A53T-SNCA + *Pink1*KO mice. Quantitative analysis of qPCR data from striatum and midbrain of 6-month-old A53T-SNCA + *Pink1*KO and wild-type mice showed a significant lower *Sqstm1* transcript level in midbrain (B) and a trend towards reduced *Tac1* transcript level in striatal tissue (A). The amount of candidate gene transcripts was normalized relative to the housekeeping gene *Tbp*. Data are presented as mean \pm SEM; n=6 WT and 6 A53T-SNCA + *Pink1*KO.

3.1.4.3 Exclusive *Pink1* Ablation has no Effect on the Expression of *Pcbd1*, *Bad*, *Tac1* and *Sqstm1*

The pre- and postsynaptic transcript level analysis of *Bad*, *Pcbd1*, *Sqstm1* and *Tac1* revealed no expression alteration in *Pink1*KO mice compared to wild-type controls (Tab. 5). Therefore, exclusive *Pink1* ablation has no effects on the gene expression of analyzed candidates. Hence the observed expression alterations in PrPmtA and double-mutant mice result from alpha-synuclein gain-of-function rather than *Pink1* ablation or the background of the mouse strain.

3.1.5 Analysis of 3-Month-Old PrPmtA Mice to Depict the Earliest Effects of Alpha-Synuclein Gain-of-Function

Most transcript level alterations were observed in PrPmtA mice, the mouse line that was previously proven to show impaired neurotransmitter release and LTD deficiency. For this reason the upcoming analysis, to depict the earliest effects of alpha-synuclein gain-of-function, was done exclusively in PrPmtA mice and their respective controls. In order to depict the earliest effects of alpha-synuclein gain-of-function all candidates that were found significantly regulated in striatal or midbrain tissue of 6-month-old mice were analyzed in striatal and midbrain tissue of 3-month-old PrPmtA and wild-type mice using qPCR.

3.1.5.1 The Regulation of Glutamate Receptor Subunits Appears with Age Progression and is not Present in Young Mice

Among the first results of the hypothesis driven transcript level analysis in A53T-SNCA overexpressing mice to depict molecular alterations possibly reflecting alpha-synuclein gain-of-function dependent effects on neurotransmission and LTD, were expression changes in subunits of glutamate receptors (Tab. 2). In order to analyze if glutamate receptor alterations are among the earliest detectable effects of alpha-synuclein overexpression, transcript level of glutamate receptor subunits that were shown to be significantly regulated in 6-month-old PrPmtA compared to wild-type mice, were studied in 3-month-old striatal and midbrain tissue. In this early age no significant expression changes were observed (Tab. 6), demonstrating that the regulation of glutamate receptor subunits appears with age progression and is therefore not present in young mice.

Tab. 6 Overview of pre- and postsynaptic results obtained in the glutamate receptor subunit analysis of 3-month-old PrPmtA mice using qPCR.

	PrPmtA str	PrPmtA mb
Gria2	ns	ns
Gria3	ns	ns
Gria4	ns	ns
Grin1	ns	ns
Grin2a	ns	ns
Grin2d	ns	ns
Grin3a	ns	ns
Grin3b	ns	ns
Grm1	ns	ns
Grm3	ns	ns
Grm4	ns	ns
Grm5	ns	ns

3.1.5.2 Among the Earliest Effects of Alpha-Synuclein Gain-of-Function are Expression Alterations for *Homer1*, *cFos*, *NOR1*, *Nurr1* and *Nur77*

Continuing the approach to detect the earliest effects of alpha-synuclein gain-of-function the scaffolding proteins *Homer1* and *Psd95* (Tab. 3), immediate-early-genes and transcription factors that were significantly regulated in 6-month-old mice (Tab. 4) as well as the hypothesis driven additional candidate genes (Tab. 5) were studied in striatal and midbrain tissue of 3-month-old PrPmtA compared to wild-type mice. Among the earliest postsynaptic effects of alpha-synuclein gain-of-function was a significantly reduced *Homer1* (Fig. 33B) transcript level as well as an increased expression of the nuclear hormone receptor superfamily members *NOR1* (Fig. 33C) and *Nur77* (Fig. 33D). *cFos* (Fig. 33A) and *RGS2* (Fig. 33E) transcript level were found to show a trend towards induction in 3-month-old PrPmtA compared to wild-type mice. Comparing the transcript level of 6-month-old with those obtained in 3-month-old PrPmtA (compared to wild-type mice), only *Homer1* is consistently downregulated whereas *cFos*, *NOR1*, *Nur77* and *RGS2* change from early upregulated to later downregulated with age progression.

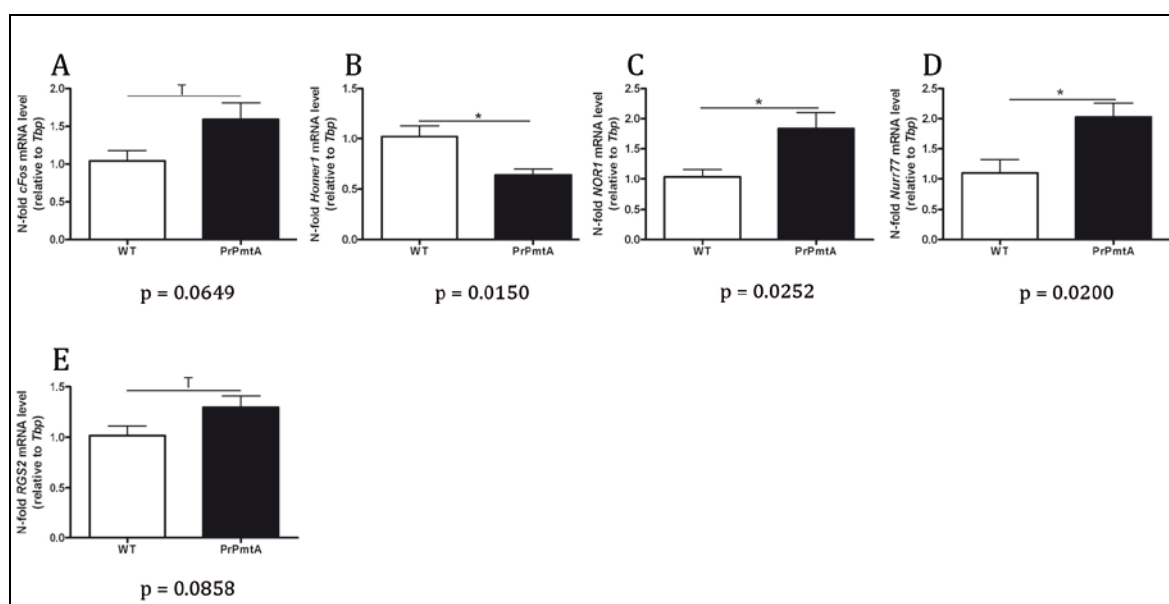


Fig. 33 Striatal analysis of the earliest effects in PrPmtA mice. Quantitative analysis of qPCR data from striatum of 3-month-old wild-type and PrPmtA mice showed a significantly lower transcript levels for *Homer1* (B). *NOR1* (C) and *Nur77* (D) levels were found significantly increased, whereas *cFos* (A) and *RGS2* (E) showed a trend towards induction. The amount of candidate gene transcripts was normalized relative to the housekeeping gene *Tbp*. Data are presented as mean \pm SEM; n=5 WT and 5 PrPmtA.

The presynaptic analysis revealed again *Homer1* to be one of the earliest effects of alpha-synuclein gain-of-function being significantly reduced in midbrain of 3-month-old PrPmtA compared to wild-type mice (Fig. 34B). The transcript level analysis of midbrain tissue depicted *cFos* as well as all three members of the nuclear hormone receptor superfamily *NOR1* (Fig. 34C), *Nurr1* (Fig. 34D) and *Nur77* (Fig. 34E) to be significantly increased again displaying the expression change occurring with age progression from early upregulated to later downregulated.

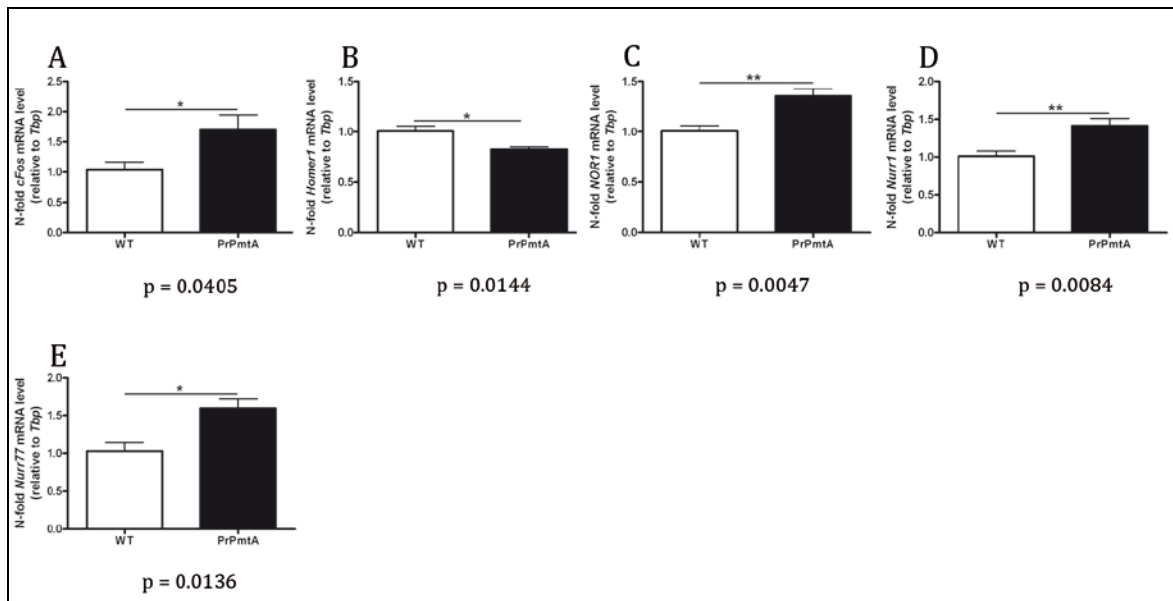


Fig. 34 Striatal analysis of the earliest effects in PrPmtA mice. Quantitative analysis of qPCR data from mid-brain of 3-month-old wild-type and PrPmtA mice showed a significantly lower transcript levels for *Homer1* (B). *cFos* (A), *NOR1* (C), *Nurr1* (D) and *Nur77* (E) levels were found significantly increased. The amount of candidate gene transcripts was normalized relative to the housekeeping gene *Tbp*. Data are presented as mean \pm SEM; n=5 WT and 5 PrPmtA.

3.2 PROJECT II: THE IMPACT OF ALPHA-SYNUCLEIN GAIN-OF-FUNCTION ON THE BEHAVIORAL AND MOLECULAR RESPONSE TO APOMORPHINE TREATMENT

After several years, most PD patients treated with L-DOPA develop severe side effects known as L-DOPA induced dyskinesia (LID). The underlying pathophysiological concept says, that LID results both from pre- and postsynaptic abnormalities in dopamine signaling as well as changes in synaptic plasticity (reviewed in (Brotchie and Jenner, 2011, Fisone and Bezard, 2011, Murer and Moratalla, 2011, Ghiglieri et al., 2012, Cenci, 2014)). In order to understand the correlation between abnormal involuntary movements and striatal postsynaptic supersensitivity, neurotoxin-induced lesion models were studied. These studies revealed the induction of immediate early genes like *cFos* and ERK1/2 phosphorylation to be the earliest molecular readouts of postsynaptic supersensitivity. Neurotoxin-induced lesion models mimic a static model of late stage PD and hence are constricted in studying the alpha-synuclein driven PD progression.

Previous studies of the A53T-SNCA overexpressing mouse model mimicking presymptomatic stages of PD, showed altered neurotransmission to be an early effect of alpha-synuclein gain-of-function. In order to study if presymptomatic stages of PD already involve an altered postsynaptic sensitivity, a dopaminergic challenge was applied to PrPmtA mice by injecting apomorphine. For the first time, the behavioral and molecular response in respect of altered striatal postsynaptic sensitivity to the dopaminergic challenge in a genetic model of alpha-synucleinopathy was analyzed.

3.2.1 PrPmtA Mice Show Increased Involuntary Movements with Stereotypic and Dystonic Features after Apomorphine Treatment

The behavioral analysis of A53T-SNCA overexpressing mice aged to 18 months and their corresponding control animals (FVB/N) revealed, that a single subcutaneous injection of 5 mg/kg apomorphine or the respective volume of vehicle, significantly induced the frequency and severity of involuntary movements with stereotypic and dystonic features in PrPmtA compared to WT mice. In figure 35, representative pictures of quantified behavioral observations after apomorphine treatment are illustrated both for PrPmtA and WT mice.

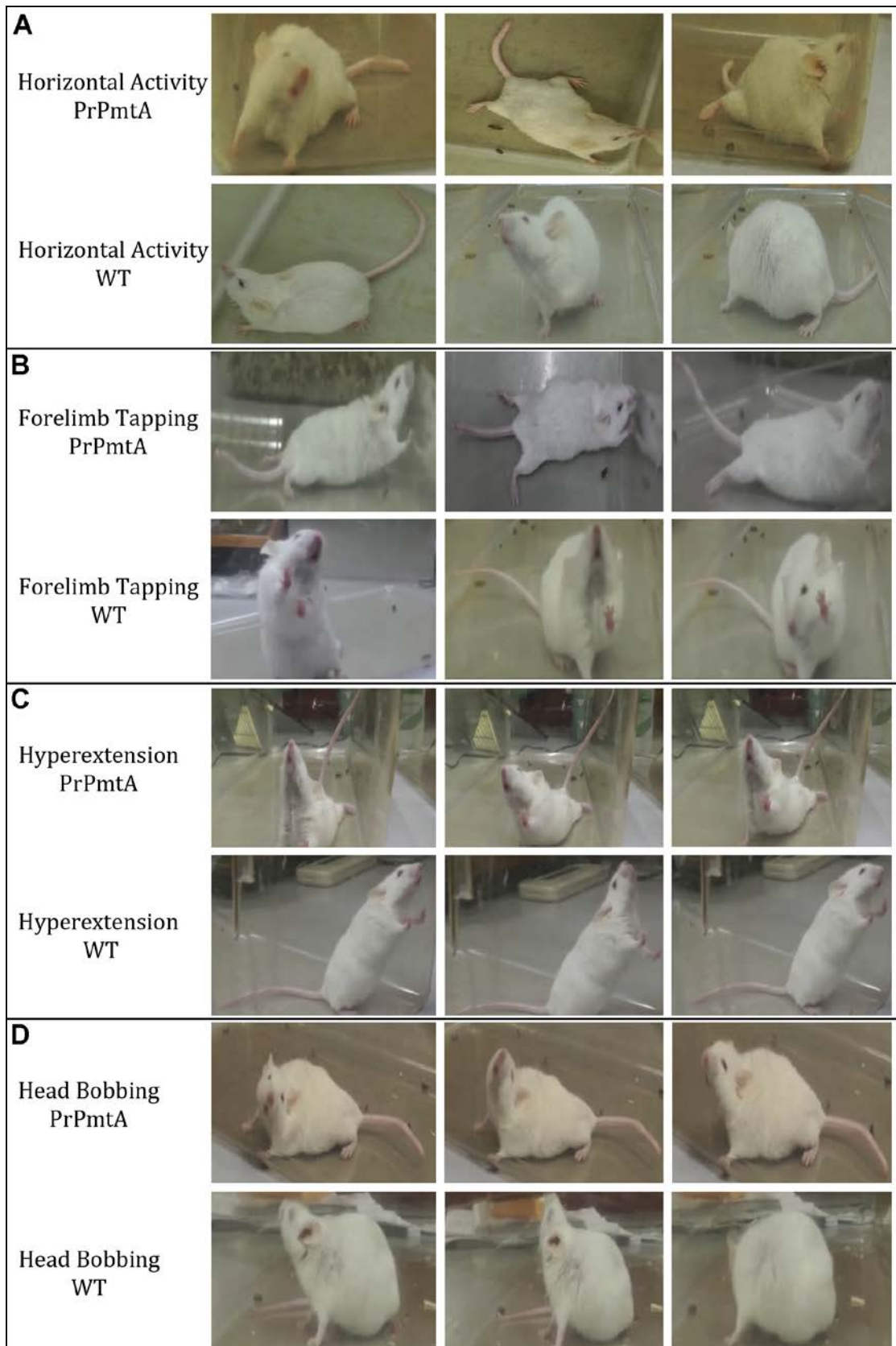


Fig. 35 Representative pictures of PrPmtA and WT mice after treatment with 5 mg/kg apomorphine. Panel **A** shows pictures representing horizontal activity of PrPmtA and WT mice, **B** pictures representing forelimb tapping, **C** hyperextension of the body and neck and **D** pictures representing head bobbing in PrPmtA and WT mice.

The quantitative analysis focused on involuntary movements with stereotypic or dystonic features namely, stereotypic licking; head bobbing; forelimb tapping and persistent hyperextension of the body and the neck as well as on the analysis of locomotor impairments by scoring horizontal movements (Fig. 36).

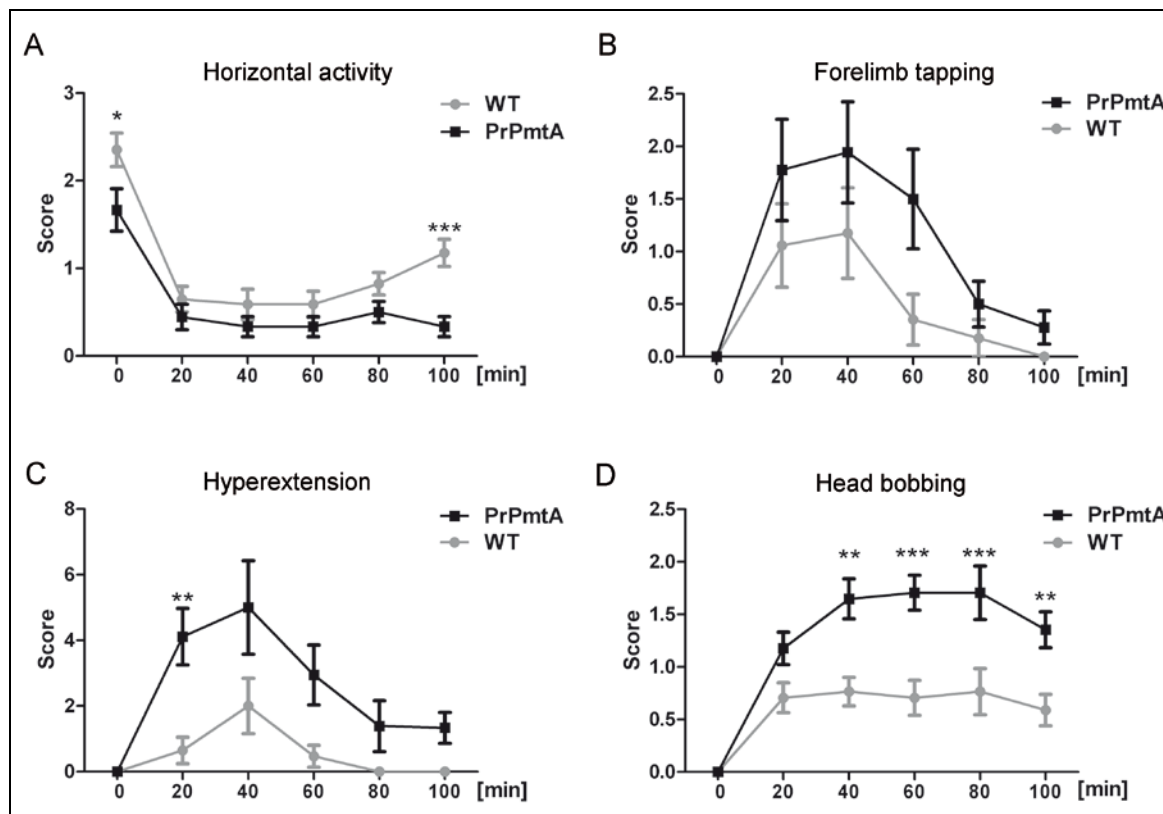


Fig. 36 Quantitative analysis of stereotypic behavior within 100 min sessions following apomorphine treatment. Time point 0 shows untreated mice. **A** shows the quantitative analysis of horizontal activity, **B** the forelimb tapping scores, **C** score of head hyperextension and **D** the quantification of head bobbing. Repeated measures ANOVA: a time $F(5, 165)=31.05$, $P<0.0001$; interaction $F(5, 165)=1.57$, $P=0.1700$; group $F(1, 33)=20.04$, $P<0.0001$; b time $F(5, 165)=11.12$, $P<0.0001$; interaction $F(5, 165)=1.068$, $P=0.3801$; group $F(1, 33)=4.259$, $P=0.0470$; c time $F(5, 165)=8.543$, $P<0.0001$; interaction $F(5, 165)=2.074$, $P=0.0711$; group $F(1, 33)=13.48$, $P=0.0008$; d time $F(5, 160)=22.19$, $P<0.0001$; interaction $F(5, 160)=3.616$, $P=0.004$; group $F(1, 32)=23.34$, $P<0.0001$ ($n=17$ WT vs. 18 PrPmtA; $T\leq 0.1$, $*P\leq 0.05$; $**P\leq 0.01$; $***P\leq 0.001$)

Since stereotypic involuntary movements (SIM) affect the animals' locomotor abilities, horizontal activity was measured (Fig. 36A). PrPmtA mice showed reduced spontaneous horizontal activity prior to apomorphine treatment (time point 0) illustrating the well-established phenotype of alpha-synuclein overexpression (Gispert et al., 2003). After apomorphine treatment both mouse lines showed strongly impaired horizontal locomotor abilities but WT mice showed a gradual recovery that differed significantly from PrPmtA mice. Therefore, 100 min after apomorphine treatment WT mice showed significantly higher scores of horizontal

activity compared to PrPmtA mice (Fig. 36A). Prior to apomorphine treatment no SIMs were observed (time point 0 in Fig. 36B-D) in PrPmtA or WT mice, indicating that SIMs are clearly apomorphine induced. Forelimb tapping, licking and head bobbing were analyzed and quantified as SIM with stereotypic features (Fig. 36B, D). Forelimb tapping scores were persistently higher in PrPmtA than in WT mice but failed to reach statistical significance during the observation period (Fig. 36B). Axial hyperextension, a dystonic feature of SIMs, was very infrequent in WT but prominent in PrPmtA mice (Fig. 36C), with PrPmtA mice showing significantly higher scores 20 min after apomorphine treatment. Head bobbing as stereotypic feature of SIMs, was scored higher in PrPmtA mice at every observed time point with 40, 60, 80 and 100 min after treatment being significantly different to WT mice (Fig. 36D). The quantitative analysis of stereotypic licking, rearing and rotation events revealed no differences for PrPmtA and WT mice, and is therefore not shown.

3.2.2 Immunohistochemical Analysis of PrPmtA mice Reveals Alpha-Synuclein Overexpression without Dopaminergic Cell Loss

Previous studies of the A53T-SNCA overexpressing mouse model used IHC, immunogold electron microscopy as well as immunofluorescence to study the transgenic expression pattern in this mouse model (Gispert et al., 2003). These previous studies were performed in mice of 1 to 16 months of age. In the present approach 18-month-old female mice were used and therefore an additional characterization of SNCA protein distribution at this advanced age was performed. The antibody used for immunohistochemistry detects both, the human and murine alpha-synuclein binding to its central domain resulting in a pale background staining in sections of wild-type mice (Fig. 37A, C, E). Figure 37 shows representative pictures of cortex, striatum and substantia nigra in wild-type and transgenic mice, with higher magnification pictures present for each brain region (i-ii). Transgenic mice, as expected, displayed an enhanced SNCA immunoreactivity in synapses, showing a fine granular pattern in cortical and striatal sections (Fig. 37B, D). In the substantia nigra of transgenic mice the immunohistological analysis showed a coarser-grained emergence of SNCA along neurites (Fig. 37F). In order to study morphological circumstances, immunohistochemistry using an antibody against tyrosine hydroxylase (TH) was used (Fig. 37G-J).

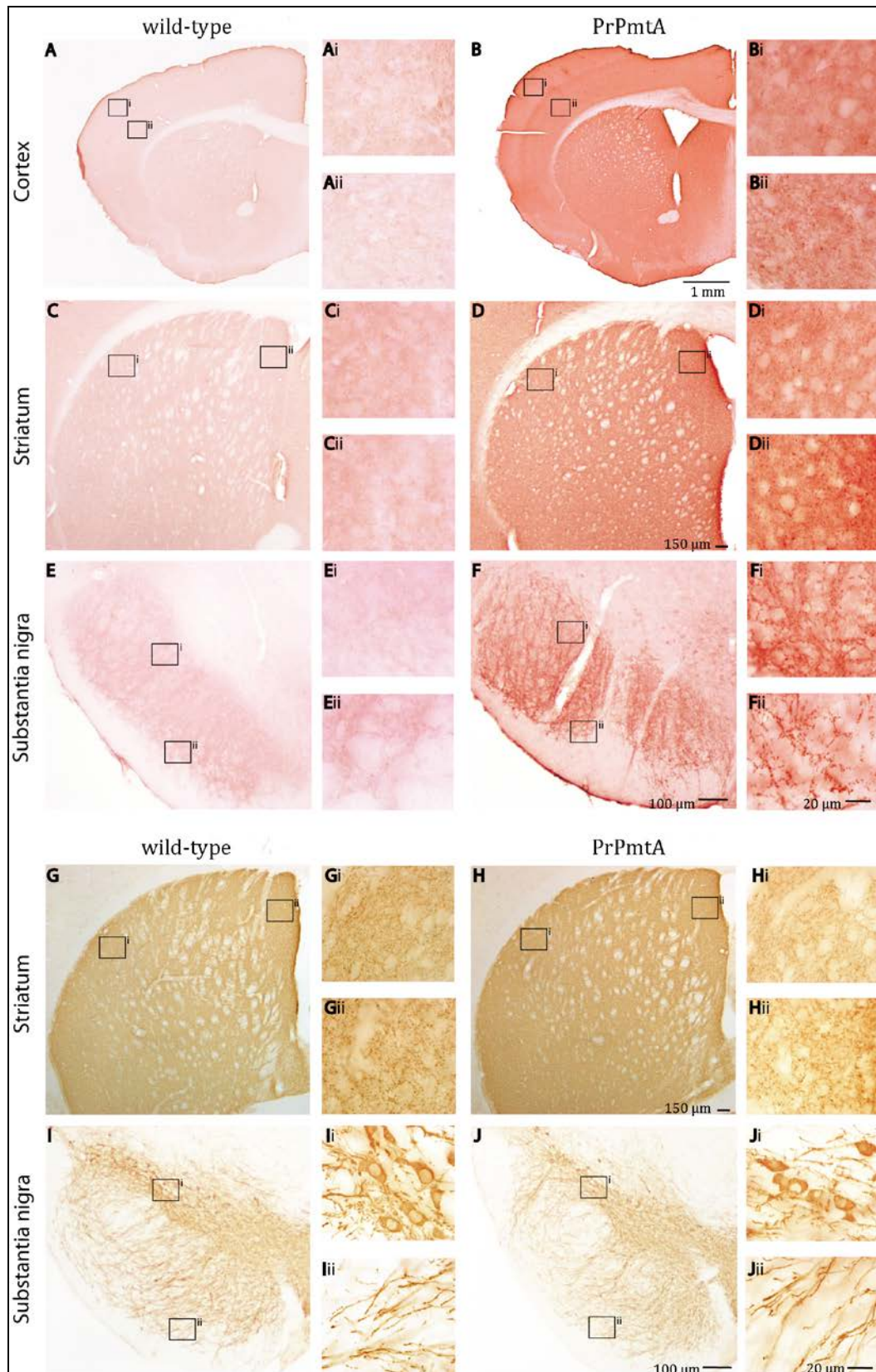


Fig. 37 Bright-field immunohistochemistry pictures of 18-month-old female PrPmtA and wild-type mice. A-F shows SNCA immunoreactivity in the cortex (A, B), striatum (C, D) and substantia nigra (E, F). G-J shows TH immunoreactivity in the striatum (G, H) and substantia nigra (I, J). For each brain region representative high-resolution pictures (i-ii) were taken. Photo credit goes to Francesco Bez.

PrPmtA and wild-type mice displayed the same pattern of TH immunoreactivity, indicating normal morphology within the striatum and substantia nigra. To further prove this statement, optical density analysis of striatal and nigral sections was performed. The optical density analysis in PrPmtA and wild-type mice depicted no differences; hence there is no anatomical evidence of a dopaminergic cell loss in 18-month-old female transgenic PrPmtA mice (Fig. 38).

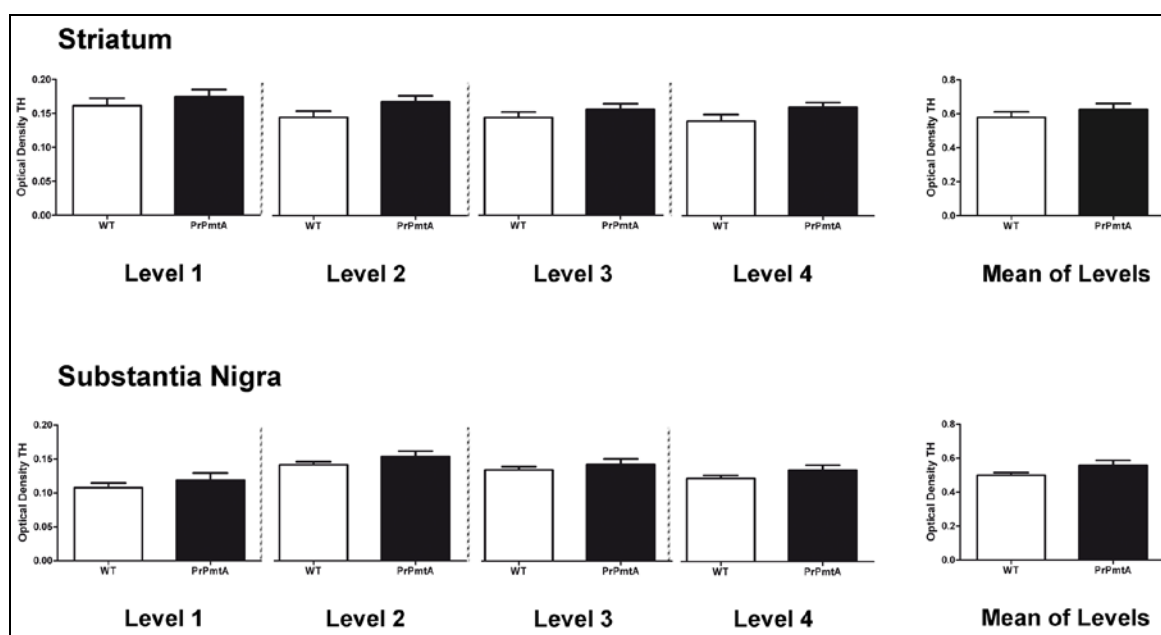


Fig. 38 Analysis of tyrosine hydroxylase optical density in the striatum and substantia nigra of 18-month-old female PrPmtA compared to wild-type mice. Quantitative analysis was performed in four levels of the striatum and four levels of the substantia nigra. Striatal levels were taken from rostral to caudal, bregma +0.74 mm to +0.14 mm. Substantia nigra levels were taken from bregma -1.94 mm to -3.8 mm.

3.2.3 Alpha-Synuclein Dependent Alterations of Striatal Erk1/2 Phosphorylation in Response to Apomorphine – Analysis via Quantitative Immunoblots

In order to explore the underlying molecular mechanism of the observed behavioral abnormalities, the phosphorylation of ERK1/2 was analyzed in striatal tissue dissected either 30 min or 100 min after apomorphine respectively vehicle treatment.

3.2.3.1 Analysis of Striatal Tissue 30 min after Apomorphine Treatment Reveals no Genotype Dependent Differences

The analysis of early changes in phosphorylation levels of ERK1/2 was done using striatal tissue of 18-month-old female PrPmtA and wild-type mice, dissected 30 min after subcutaneous injection of 5 mg/kg apomorphine or the respective volume of vehicle. Phospho-ERK2 was significantly induced in wild-type (Fig. 39A) and PrPmtA mice (Fig. 39B), whereas a trend towards induction was observed for phospho-ERK1 levels both in wild-type and PrPmtA mice (Fig. 39).

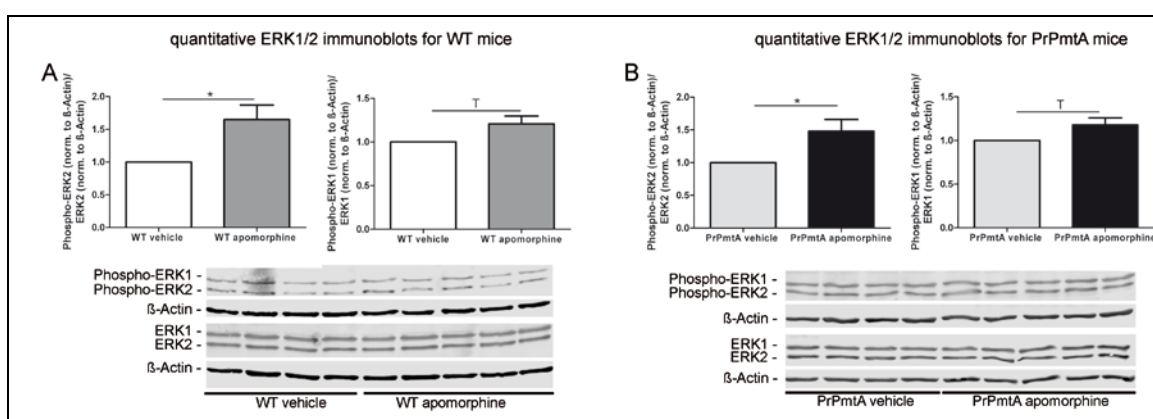


Fig. 39 Apomorphine dependent phosphorylation of ERK1/2 30 min after treatment. Quantitative immunoblots and bar graphs of phospho-ERK1/2 levels in the striatum of 18-month-old female wild-type (A) and PrPmtA (B) mice showed increased phospho-ERK1/2 levels in the striatum. Striatal tissue was dissected 30 min after apomorphine or vehicle treatment.

In order to statistically prove the depicted similar induction pattern for wild-type and PrPmtA mice an additional quantitative immunoblot for either vehicle treated (Fig. 40A) or apomorphine treated (Fig. 40B) WT and PrPmtA mice was done. The quantitative analysis of genotype dependent alterations showed no differences and therefore does not reflect the behavioral differences observed between wild-type and transgenic mice at that time point. The analysis of phospho-ERK1/2 levels independent of apomorphine treatment (Fig. 40A) did not differ between PrPmtA and WT animals; however the analysis of phospho-ERK1/2 levels after apomorphine treatment could detect a trend towards reduction for phospho-ERK1 level in PrPmtA mice compared to WT (Fig. 40B).

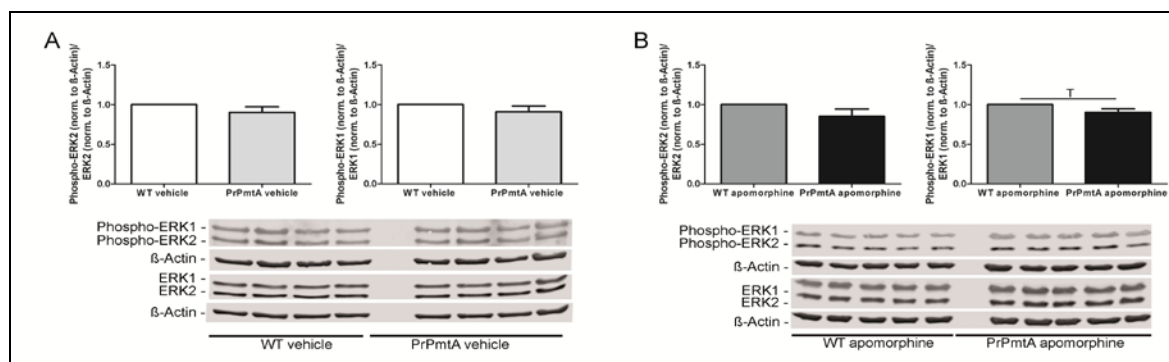


Fig. 40 Genotype dependent differences in apomorphine induced ERK1/2 phosphorylation 30 min after treatment. Quantitative immunoblots and bar graphs of phospho-ERK1/2 levels analyzed in striatal tissue of 18-month-old female wild-type and PrPmtA mice, dissected 30 min after apomorphine or vehicle treatment revealed no significant genotype dependent differences. The analysis of phospho-ERK1 showed a trend towards reduction for WT animals compared to PrPmtA after apomorphine treatment (**B**). Phospho-ERK1/2 levels of wild-type vehicle treated did not differ from transgenic vehicle treated mice (**A**).

3.2.3.2 Analysis of Striatal Tissue 100 min after Apomorphine Treatment Revealed Reduced pERK1/2 Level in PrPmtA Mice

In order to discover molecular alterations that could explain the observed behavioral differences between transgenic and wild-type mice after apomorphine treatment, a later time point of analysis was chosen. Therefore, 18-month-old female mice were sacrificed 100 min after apomorphine or vehicle treatment and striatal tissue was processed for phospho-ERK1/2 analysis. At this late time point the analysis of phospho-ERK1/2 levels in wild-type animals showed only a trend towards apomorphine dependent induction for phospho-ERK2 and no alterations for phospho-ERK1 (Fig. 41A). The same analysis in transgenic animals depicted a complete different response pattern (Fig. 41B). Apomorphine treatment in PrPmtA mice caused significantly reduced phospho-ERK1/2 levels, revealing increased striatal sensitivity of dopamine agonist-dependent dephosphorylation pathways.

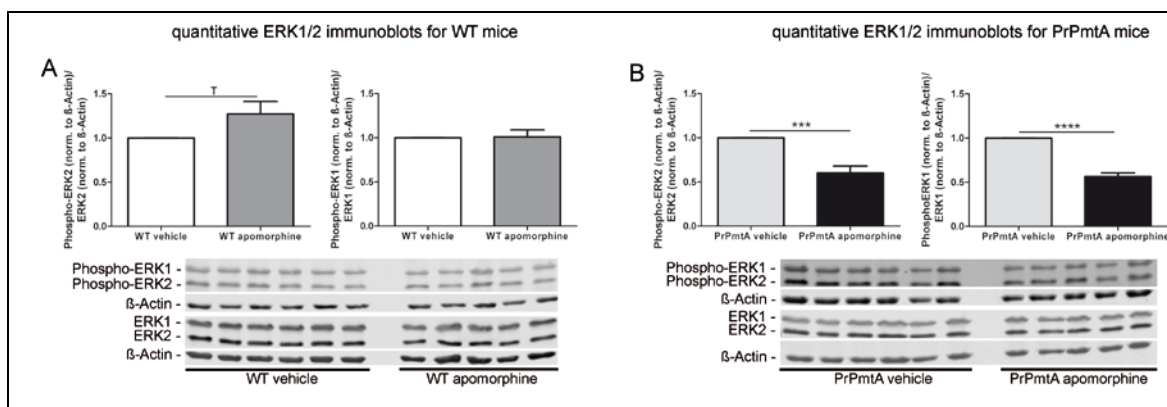


Fig. 41 Apomorphine dependent phosphorylation of ERK1/2 100 min after treatment. Quantitative immunoblots and bar graphs of phospho-ERK1/2 levels in the striatum of 18-month-old female wild-type (A) and PrPmtA (B) mice showed unchanged phospho-ERK1/2 levels in wild-type mice (A) where only a trend was detectable for phospho-ERK2, but significantly decreased phospho-ERK1/2 levels in transgenic animals (B). Striatal tissue was dissected 100 min after apomorphine or vehicle treatment.

In order to prove the illustrated phosphorylation pattern and analyze the genotype dependent differences in more detail, additional quantitative immunoblots for phospho-ERK1/2 in either vehicle treated (Fig. 42A) or apomorphine treated (Fig. 42B) wild-type compared to transgenic mice was done. The quantitative analysis depicted genotype dependent differences in vehicle treated animals that were dissected 100 min after treatment, showing significantly increased phospho-ERK1/2 levels in PrPmtA compared to WT (Fig. 42A). The same analysis was performed in apomorphine treated wild-type and transgenic animals and showed significantly increased phospho-ERK1 levels in transgenic animals (Fig. 42B).

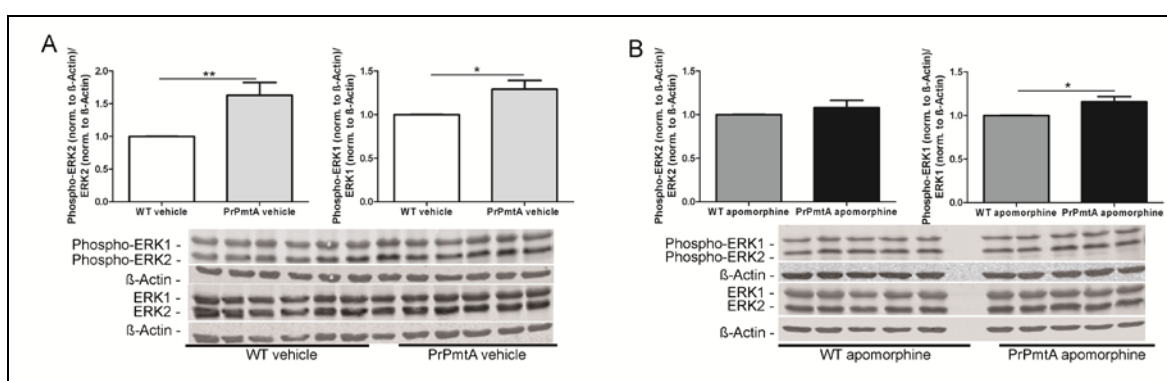


Fig. 42 Genotype dependent differences in apomorphine induced ERK1/2 phosphorylation 100 min after treatment. Quantitative immunoblots and bar graphs of phospho-ERK1/2 levels, analyzed in striatal tissue of 18-month-old female wild-type and PrPmtA mice, dissected 100 min after apomorphine or vehicle treatment revealed genotype dependent differences. The analysis independent of apomorphine treatment showed increased phospho-ERK1/2 levels in PrPmtA compared to WT mice (A). The analysis of a genotype dependent effect of apomorphine revealed a significant increased phospho-ERK1 level in transgenic compared to wild-type mice (B).

3.2.4 Alpha-Synuclein Dependent Alterations of Striatal Histone H3 Phosphorylation in Response to Apomorphine - Analysis via IHC

The analysis of striatal ERK1/2 phosphorylation revealed promising insights, pointing to molecular alterations within striatal postsynaptic sensitivity mechanism to be changed in transgenic mice, leading to the observed apomorphine-triggered behavioral response. In 6-hydroxydopamine-lesioned mice, not only the phosphorylation of ERK1/2 was found increased in striatal medium spiny neurons after L-DOPA treatment but also the phosphorylation of histone H3 (Santini et al., 2009). Given that increased phosphorylation of histone H3 leads to chromatin decondensation as well as regulation of nucleosomal responses (Cheung et al., 2000, Soloaga et al., 2003), the enhanced phosphorylation found in L-DOPA treated 6-hydroxydopamine-lesioned animals could underlie gene expression alterations that were observed in this model (Andersson et al., 1999). In this approach, the phosphorylation of histone H3 was therefore analyzed using an immunohistochemical approach. Figure 43 depicts representative bright-field microscopy pictures of female, 18-month-old wild-type and PrPm-tA mice either vehicle or apomorphine treated. The pictures clearly show an increased, apomorphine dependent histone H3 phosphorylation pattern for both wild-type and transgenic mice. In order to quantitatively analyze if the phosphorylation pattern of histone H3 differs between genotypes and therefore represents alpha-synuclein dependent alterations in striatal postsynaptic sensitivity, quantitative densitometric analysis of the striatum was performed.

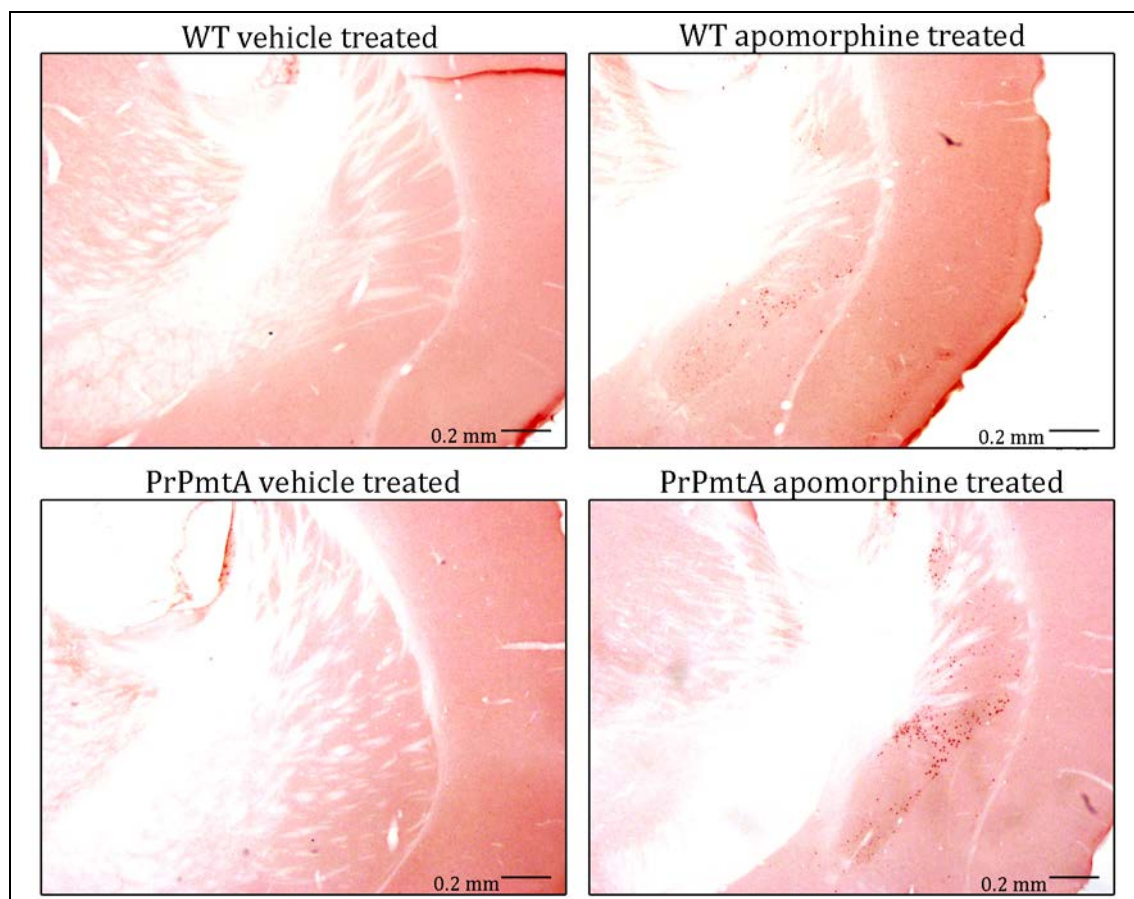


Fig. 43 Representative bright-field microscopy pictures of phospho-histone H3 immunohistochemistry in the striatum of female 18-month-old PrPmtA and WT mice after vehicle or apomorphine treatment.

The densitometric analysis revealed a significant induction of phospho-histone H3 after apomorphine treatment in both wild-type and transgenic mice (Fig. 44A, B). The quantitative analysis of histone H3 phosphorylation in PrPmtA compared to WT mice after apomorphine treatment showed a significant higher phosphorylation of histone H3 in transgenic compared to wild-type mice (Fig. 44C). This analysis focused on the very caudal part of the striatum since most immunoreactivity was found in this region.

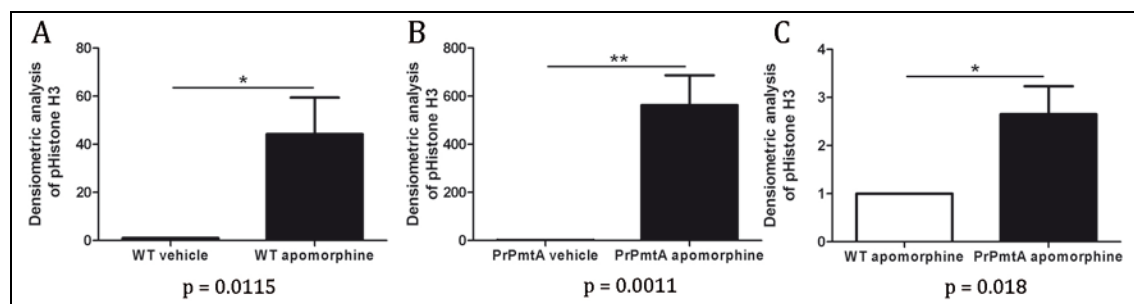


Fig. 44 Quantitative densitometric analysis of phospho-Histone H3 in striatal sections of 18-month-old female PrPmtA and wild-type mice after apomorphine treatment. A shows the analysis of wild-type vehicle treated compared to wild-type apomorphine treated mice, **B** the analysis of PrPmtA vehicle versus apomorphine treated and **C** the analysis of wild-type apomorphine treated compared to PrPmtA apomorphine treated mice.

3.2.5 Alpha-Synuclein Gain-of-Function Affects the Expression of ERK Pathway Elements in Response to Apomorphine Treatment

The early activation of ERK1/2 by phosphorylation was the first evidence of a molecular alteration in the transgenic mouse model underlying the described behavioral response to apomorphine treatment (Fig. 39 - Fig. 42). Additionally, the phosphorylation of Histone H3 was also significantly increased in the striatum of PrPmtA compared to WT mice (Fig. 44). In order to further characterize the molecular mechanisms involved in this behavioral response to apomorphine, striatal tissue was analyzed by qPCR focusing on candidate genes that can illustrate striatal postsynaptic supersensitivity. Dual-specific (Thr/Tyr) phosphatases (*Dusp*) and ERK1/2 activation are induced by similar stimuli (Owens and Keyse, 2007), additionally a recent transcriptome profile in 6-hydroxydopamine-lesioned mice showed striatal induction of dual-specific (Thr/Tyr) phosphatases after repeated L-DOPA treatment (Heiman et al., 2014) putting dual-specific (Thr/Tyr) phosphatases into the focus of interest. The immediate early gene *cFos* was studied in this approach since it is inducible in striatal medium spiny neurons by D1 receptor stimulation (Graybiel et al., 1990, Young et al., 1991) and is described to be apomorphine-dependently induced (Cenci et al., 1992). The transcription factor *Nur77*, also called *Nr4A1*, is also an immediate early gene responding to a variety of growth stimuli (Williams and Lau, 1993). Within this approach *Nur77* attracted attention since it is progressively increased in 6-hydroxydopamine-lesioned rats after repeated L-DOPA administration (No et al., 2010). Using qPCR of striatal tissue dissected either 30 min or 100 min after apomorphine treatment, *Dusp1*, *Dusp6*, *cFos* and *Nur77* were analyzed in an apomorphine and genotype dependent manner.

3.2.5.1 Analysis of Striatal Tissue 30 min after Apomorphine Treatment Reveals Genotype Dependent Differences for *cFos*

In order to depict the early molecular effects of apomorphine treatment, striatal tissue from mice dissected 30 min after treatment with either 5 mg/kg apomorphine or the respective volume of vehicle were analyzed. The expression analysis showed *Dusp1*, *Dusp6* and *cFos* mRNA to be significantly induced in both genotypes (WT and PrPmtA) in response to apomorphine administration (Fig. 45A-C). The analysis of *Nur77* expression revealed a very moderate apomorphine dependent induction for both wild-type and PrPmtA mice that failed to reach statistical significance (Fig. 45D). In order to depict genotype dependent differences that could illustrate striatal postsynaptic sensitivity, apomorphine treated WT and PrPmtA were compared. At this early time point *cFos* already exhibited a significantly stronger induction in PrPmtA compared to WT mice after apomorphine treatment (Fig. 45C), providing the next molecular correlate of enhanced postsynaptic sensitivity, a possible underlying mechanism of the behavioral readout. The comparative analysis of vehicle treated WT and PrPmtA mice revealed no differences (Fig. 45A-D), indicating that the baseline expression levels of all four candidates were similar in WT and PrPmtA mice.

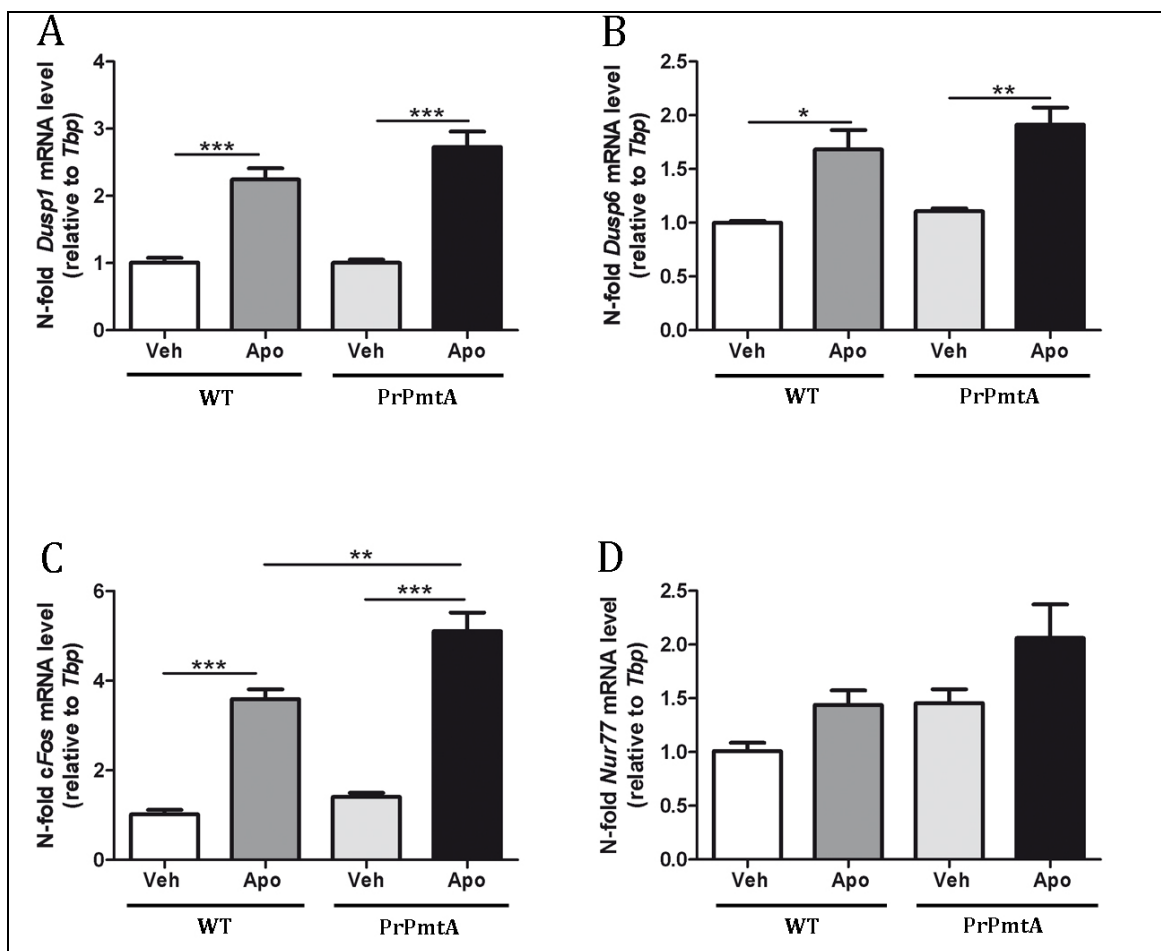


Fig. 45 Statistical analysis of qPCR data from striatum of wild-type and PrPmtA mice, 30 min after vehicle or apomorphine treatment. This analysis showed a significant apomorphine dependent induction of *dual-specific phosphatases 1* (A) and 6 (B), as well as for *cFos* (C) in both WT and PrPmtA mice. The analysis of *Nur77* showed no significant apomorphine dependent induction (D). PrPmtA mice exhibited a significantly stronger apomorphine dependent *cFos* induction compared to WT mice (C). The amount of candidate gene transcripts was normalized relative to the housekeeping gene *Tbp*. Data are presented as mean \pm SEM; n=4 WT vehicle, 5 WT apomorphine, 4 PrPmtA vehicle and 5 PrPmtA apomorphine.

3.2.5.2 Analysis of Striatal Tissue 100 min after Apomorphine Treatment Reveals Increased *cFos*, *Dusp1*, *Dusp6* and *Nur77* Levels

In order to depict subsequent molecular effects that occurred in the striatum of 18-month-old PrPmtA mice through dopaminergic challenge, striatal tissue dissected 100 min after treatment was analyzed. The analysis revealed a stronger apomorphine dependent induction of *Dusp1*, *Dusp6*, *cFos* and *Nur77* in PrPmtA, whereas in WT mice only *Dusp1* and *cFos* were found to be apomorphine dependently induced (Fig. 46A-D). Striatal postsynaptic sensitivity can quantitatively be depicted by comparing apomorphine treated transgenic to wild-type mice. This analysis revealed significantly stronger inductions of all four candidate genes (*Dusp1* 1.4-fold, *Dusp6* 1.3-fold, *cFos* 1.4 fold and *Nur77* 1.7 fold) in striatum of PrPmtA when

compared to wild-type mice (Fig. 46), providing further evidence for increased striatal postsynaptic sensitivity in A53T-SNCA overexpressing mice. The comparison of vehicle treated wild-type and PrPmtA mice showed no differences again indicating that the baseline expression levels of all four candidates are similar in WT and PrPmtA mice.

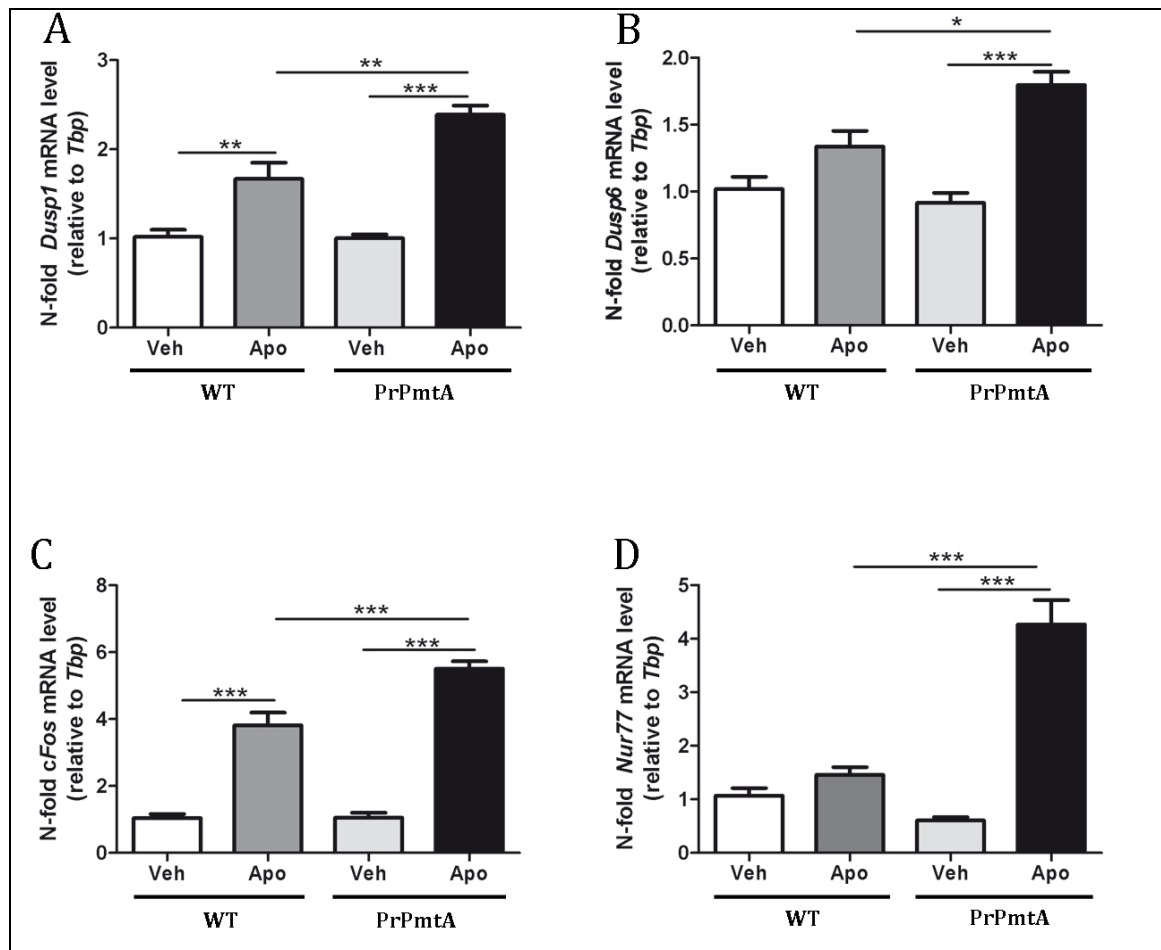


Fig. 46 Statistical analysis of qPCR data from striatum of wild-type and PrPmtA mice 100 min after vehicle or apomorphine treatment. The analysis showed a significant stronger apomorphine dependent induction of *Dusp1* (A), *Dusp6* (B), *cFos* (C) and *Nur77* (D) mRNA levels in PrPmtA compared to WT. In WT mice only *Dusp1* (A) and *cFos* (C) were found to be induced apomorphine dependent, whereas all four candidates show an apomorphine dependent induction for PrPmtA mice (A-D). The amount of candidate gene transcripts was normalized relative to the housekeeping gene *Tbp*. Data are presented as mean \pm SEM; n=6 WT vehicle, 5 WT apomorphine, 6 PrPmtA vehicle and 5 PrPmtA apomorphine.

3.2.5.3 Analysis of Additional Dusp Family Members Reveals Increased Apomorphine Dependent mRNA levels but no Genotype Dependent Differences

The analysis of *Dusp1*, *Dusp6*, *cFos* and *Nur77* in 30 and 100 min after apomorphine treatment illustrated expression changes that are apomorphine induced but also clearly trace back to the A53T-SNCA overexpression. *Dusp1* and *Dusp6* are members of the dual-specific phos-

phatase gene family, so consequently other dual-specific phosphatase family members were analyzed in striatal tissue of PrPmtA and wild-type mice that were dissected 100 min after either vehicle or apomorphine treatment. The time-point 100 min after treatment was chosen, because genotype dependent differences were only detectable at that late time-point (Fig. 46). The analysis of *Dusp4* (Fig. 47A) and *Dusp14* (Fig. 47B) levels revealed an apomorphine dependent induction for both transcripts in transgenic mice, but only for *Dusp4* in wild-type animals. However, genotype dependent differences, so an effect of alpha-synuclein gain-of-function on the expression profile of *Dusp4* and *Dusp14* as observed for *Dusp1* and *Dusp6* was not detectable.

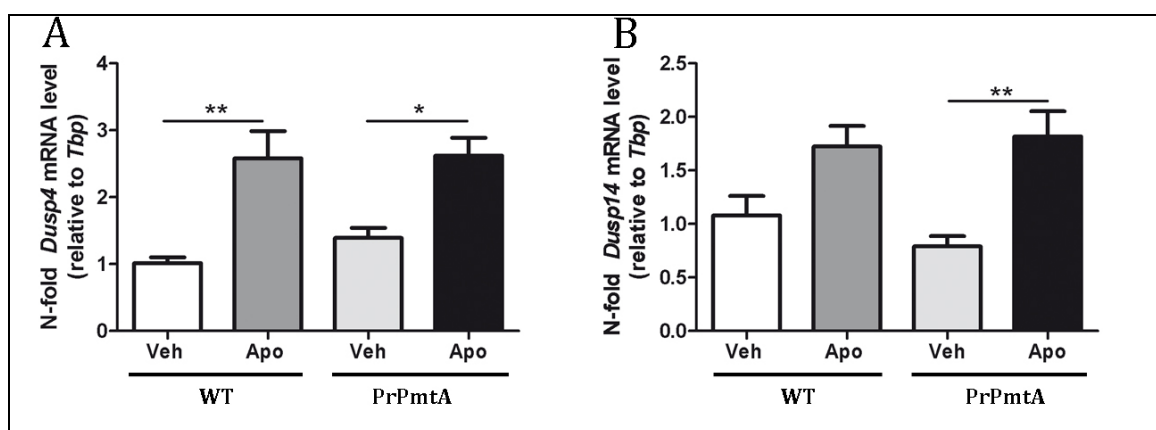


Fig. 47 Statistical analysis of qPCR data from striatum of wild-type and PrPmtA mice 100 min after vehicle or apomorphine treatment. The analysis revealed a significant apomorphine dependent induction of *Dusp4* (A) and *Dusp14* (B) levels in PrPmtA mice, whereas in wild-type mice only *Dusp4* showed a significant apomorphine dependent induction. The amount of candidate gene transcripts was normalized relative to the housekeeping gene *Tbp*. Data are presented as mean \pm SEM; n=6 WT vehicle, 5 WT apomorphine, 6 PrPmtA vehicle and 5 PrPmtA apomorphine.

3.2.5.4 Apomorphine and Genotype Dependent Increases of *cFos*, *Dusp1*, *Dusp6* and *Nur77* Level are Predominantly but not Exclusively Found in Striatal Tissue

The analysis of striatal tissue dissected 100 min after apomorphine or the respective vehicle treatment, revealed significant changes for *Dusp1*, *Dusp6*, *cFos* and *Nur77*. The analysis of other dual-specific phosphatase family members emphasized the specificity of *Dusp1* and *Dusp6* as targets of an apomorphine-triggered reaction that underlies striatal postsynaptic sensitivity. In order to study if the apomorphine dependent increase of candidate genes correlated with postsynaptic sensitivity is exclusive to the striatum, midbrain tissue dissected 100 min after treatment was analyzed. The analysis in midbrain tissue focused on *Dusp1*, *Dusp6*, *cFos* and *Nur77* since these candidates showed apomorphine and genotype dependent differences in striatal tissue (Fig. 46). The analysis exhibited an apomorphine dependent in-

crease for *Dusp1*, *Dusp6*, *cFos* and *Nur77* in transgenic animals as well as an significant increase for *Dusp1*, *cFos* and *Nur77* in wild-type mice (Fig. 47). The only genotype dependent difference was detected for *cFos* (Fig. 47C), highlighting the molecular underpinnings of increased *Dusp1*, *Dusp6* and *Nur77* expression in PrPmtA after apomorphine treatment to be striatum specific and therefore postsynaptic.

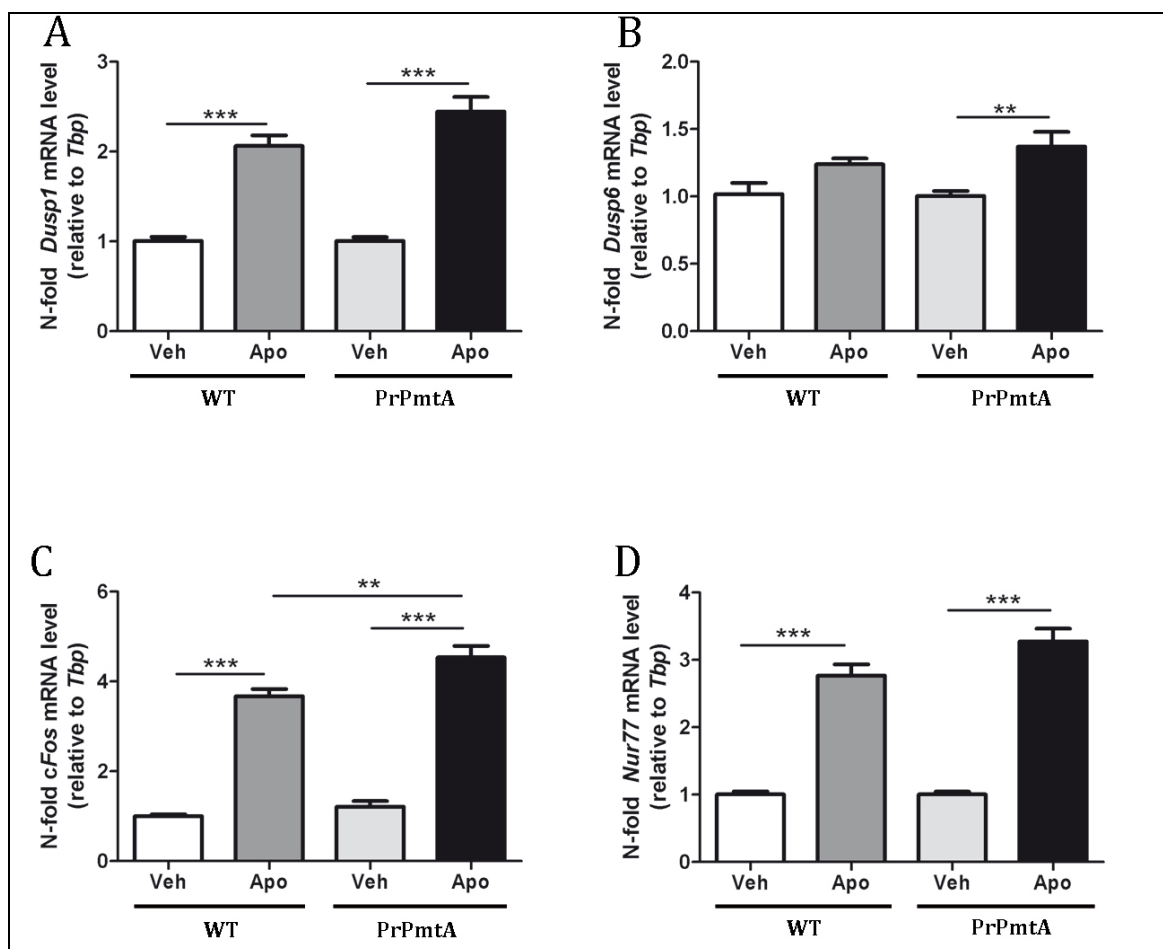


Fig. 48 Statistical analysis of qPCR data from midbrain of wild-type and PrPmtA mice 100 min after vehicle or apomorphine treatment. This analysis showed a significant stronger apomorphine dependent induction of *cFos* (C) in PrPmtA compared to WT. In PrPmtA *Dusp1* (A), *Dusp6* (B), *cFos* (C) and *Nur77* (D) levels were found to be apomorphine dependent induced. In WT mice only *Dusp1* (A), *cFos* (C) and *Nur77* (D) were found to be apomorphine dependently induced. The amount of candidate gene transcripts was normalized relative to the house-keeping gene *Tbp*. Data are presented as mean \pm SEM; n=6 WT vehicle, 5 WT apomorphine, 6 PrPmtA vehicle and 5 PrPmtA apomorphine

3.2.6 Alpha-Synuclein Gain-of-Function Effects on DUSP6 Abundance in Response to Apomorphine Treatment – Analysis on Protein Level

The analysis of mRNA expression changes in transgenic compared to wild-type mice after apomorphine treatment revealed the family of dual-specific phosphatases to have an important role. Precisely, *Dusp1* and *Dusp6* were found to be apomorphine dependent increased in PrPmtA compared to WT mice. *Dusp6* is activated by an ERK-dependent phosphorylation and therefore plays a major role as negative feedback regulator controlling mitogenic-signaling (Caunt and Keyse, 2013). It is also known, that DUSP6 induction occurs in parallel with the induction of ERK1/2 kinases in neuronal cells. Taken the current literature knowledge as well as the *Dusp6* mRNA findings and phospho-ERK1/2 results, DUSP6 was considered to be analyzed on protein level as well. DUSP6 protein levels were analyzed in the same striatal tissue dissected 100 min after treatment that was used to analyze ERK1/2 phosphorylation. The analysis revealed a significant apomorphine dependent induction of DUSP6 levels in wild-type mice (Fig. 49A) but not in transgenic animals (Fig. 49B). In order to depict genotype dependent differences vehicle treated and apomorphine treated wild-type and PrPmtA mice were compared (Fig. 49C-D). The analysis of vehicle treated mice obtained a significant higher DUSP6 level in PrPmtA compared to wild-type mice (Fig. 49C), indicating higher baseline DUSP6 level possibly due to the transgene. The analysis of apomorphine treated wild-type and PrPmtA mice showed significantly lower DUSP6 levels in PrPmtA compared to wild-type mice (Fig. 49D), most likely arising from the strong apomorphine dependent induction that was observed in WT (Fig. 49A) but not in PrPmtA (Fig. 49B).

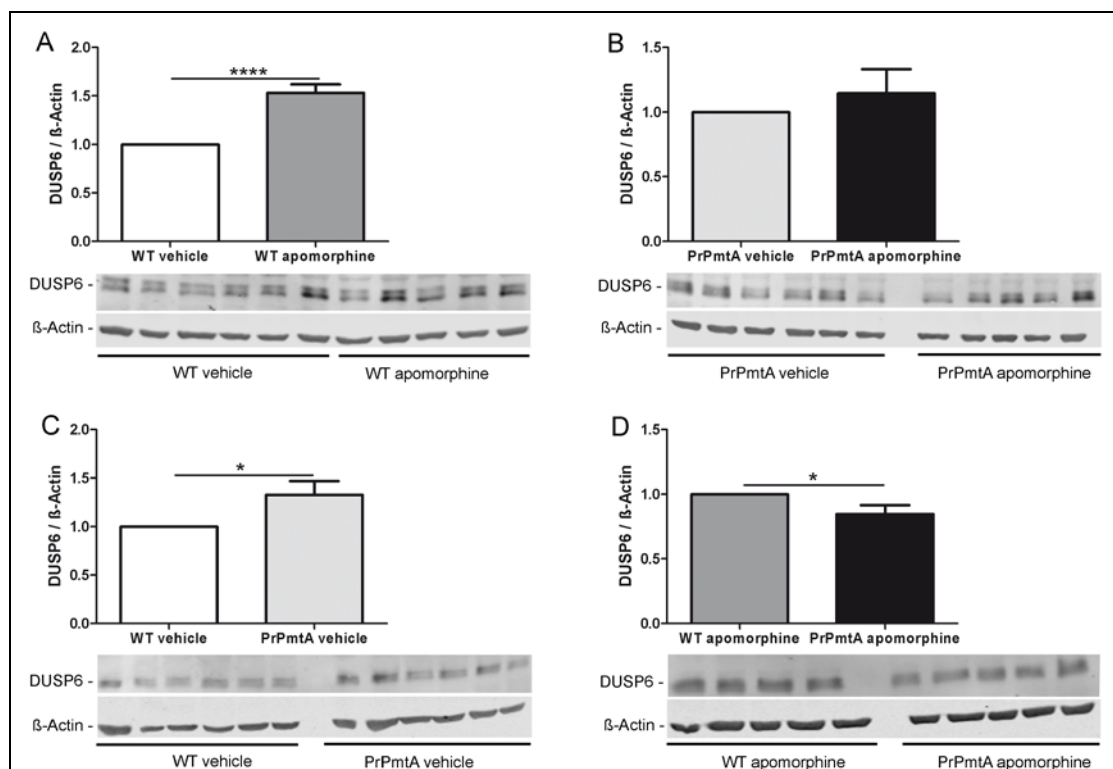


Fig. 49 Quantitative immunoblots and bar graphs of DUSP6. DUSP6 level were analyzed in striatal tissue of 18-month-old female wild-type and PrPmtA mice, dissected 100 min after apomorphine or vehicle treatment. The analysis revealed genotype dependent differences. In WT mice DUSP6 was apomorphine dependently induced (A) whereas no apomorphine dependent alteration was found in PrPmtA (B). The analysis independent of apomorphine treatment showed increased DUSP6 levels in PrPmtA compared to WT mice (C), and the analysis of a genotype dependent effect to apomorphine revealed a significant lower DUSP6 level in transgenic compared to wild-type mice (D).

3.3 PROJECT III: POTENTIATION OF ALPHA-SYNUCLEIN GAIN-OF-FUNCTION EFFECTS IN DOUBLE-MUTANT MICE WITH PINK1 AB- LATION

In 3.2 alpha-synuclein gain-of-function effects were studied in a monogenic model of PD, but most PD patients actually suffer from polygenic interactions with environmental stressors. In order to study polygenic PD as well as to clarify the role of PINK1 onto alpha-synuclein dependent neurotoxicity, a mouse model harboring both, the A53T-SNCA overexpression as well as *Pink1*KO was generated. Therefore, the well characterized PrPmtA mouse line with inbred FVB/N background was crossed to double homozygosity with the well characterized *Pink1*KO mouse line in 129/SvEv background. Wild-type control mice were derived from F1-hybrids of FVB/N and 129/SvEv, aged in parallel to the double-mutant mice.

The A53T-SNCA + *Pink1*KO mouse line was aged and behavioral analysis as well as a lifespan documentation were carried out (Gispert et al., 2014a). Besides a potentiated phenotype with significantly reduced spontaneous locomotor activity at the age of 3 months, double mutant mice showed a progressive hind limb paralysis (Fig. 50) in a relatively big cohort of mice aged beyond 1 year. Initially the paralysis was observed unilateral with progression to full bilateral paralysis within days. This phenotypic abnormality has never been observed in both single mutant mouse lines. Hence, to investigate the molecular and anatomical changes leading to the observed paralysis in double-mutant mice, intense immunohistological analysis of spinal cord and midbrain was performed.



Fig. 50 Representative pictures of hind limb paralysis in A53T-SNCA + *Pink1*KO mice. The picture to the left shows a unilateral paralysis, the one in the middle the beginning of a bilateral paralysis and the one to the right a complete bilateral hind limb paralysis.

3.3.1 The Spinal Cord of A53T-SNCA + *Pink1*KO Mice Shows pSer129-SNCA, p62/SQSTM1 and Ubiquitin Positive Cells

Autopsy-based studies of PD patients showed alpha-synuclein positive inclusions in the spinal cord, predominantly in axons but also in Lewy neurites and Lewy bodies (Del Tredici and Braak, 2012). Hence, a self-evident step in characterizing a mouse model that shows progressive paralysis, was to immunohistologically analyze the spinal cord of these animals. Therefore, the lumbar spinal cord of paralyzed double-mutant mice as well of age matched wild-type controls and single mutant mice (PrPmtA, *Pink1*KO) was stained with pSer129-SNCA an PD pathology associated marker, with p62/SQSTM1 a general aggregation marker and ubiquitin, an universal marker for degradation. The immunoreactivity for pSer129-SNCA was very prominent within the gray matter of the anterior horn of the lumbar spinal cord in double-mutant mice (Fig. 51 J, M). The observed histological pattern comprises morphological signs of neurodegeneration, such as corkscrew morphology of neurites and a pSer129-SNCA distribution in granules or fibers within the cytoplasm of positive cells. In wild-type and *Pink1*KO mice no pSer129-SNCA staining was observed in anatomically identical regions of spinal cord (Fig. 51A, D). In PrPmtA mice, a light nuclear immunoreactivity for pSer129-SNCA was observed within the lumbar spinal cord, but no aggregates or signs of neurodegeneration were found (Fig. 51G). In A53T-SNCA + *Pink1*KO mice a similar histological staining pattern was observed for p62/SQSTM1, with the anterior horn of the lumbar spinal cord showing p62/SQSTM1 positive aggregates with granular distribution, but with less sensitivity compared to the pSer129-SNCA staining (Fig. 51K, N). The analysis of p62/SQSTM1 in wild-type mice and in both single mutant mouse lines revealed no immunoreactivity within the same anatomical region (Fig. 51B, E, H). Ubiquitin immunoreactivity was found in a similar staining pattern such as p62/SQSTM1 in double-mutant mice (Fig. 51L, O) again showing a granular cytoplasmic localization. In wild-type mice as well as in both single mutants ubiquitin immunoreactivity was found, but no aggregation or signs of neurodegeneration were observed in these mouse lines (Fig. 51C, F, I).

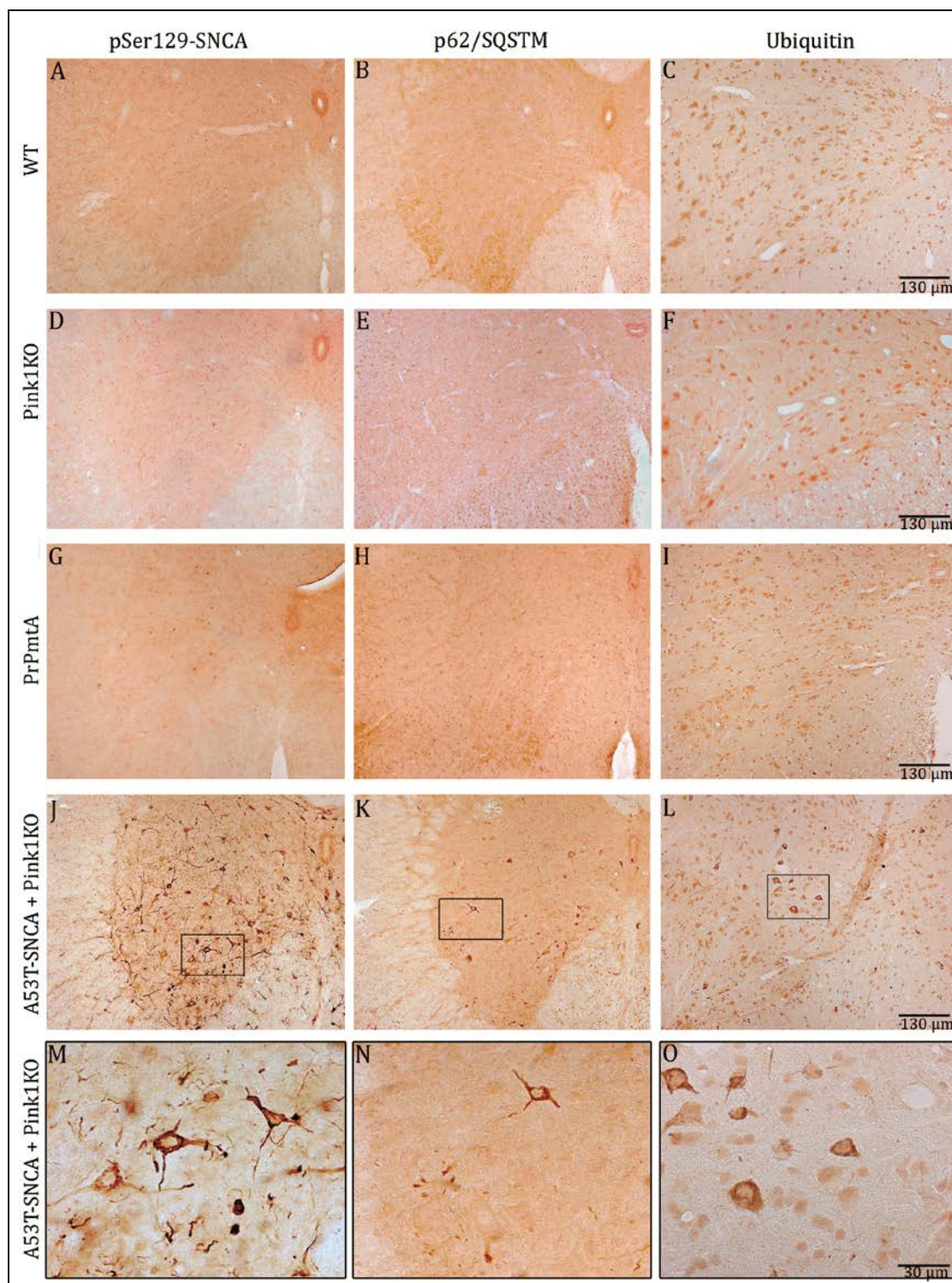


Fig. 51 Bright-field microscopy pictures from immunohistochemistry in spinal cord of WT, *Pink1KO*, *PrPmtA* and double-mutant mice aged until 15-17 months. The representative pictures shown focused on the ventral horn of the lumbar spinal cord. Immunohistochemistry was performed in each mouse line for pSer129-SNCA (A, D, G, J, M), p62/SQSTM1 (B, E, H, K, N) and ubiquitin (C, F, I, L, O). Protein aggregation, positive for pSer129-SNCA, p62/SQSTM1 and ubiquitin was detected in spinal cord of double mutant mice but not for WT controls or single mutant (*PrPmtA*, *Pink1KO*) mice (J-O). M-O show higher magnification pictures, highlighting the pathology of these mice by showing the corkscrew-appearance of some neurites. Pictures were taken with the help of Dr. Kay Seidel.

3.3.2 The Midbrain of A53T-SNCA + *Pink1*KO Mice Shows pSer129-SNCA, p62/SQSTM1 and Ubiquitin Positive Cells

The classical motor symptoms of Parkinson's disease are thought to be caused by a progressive loss of dopaminergic neurons in the substantia nigra, a brain region located in the mesencephalon (midbrain) (Damier et al., 1999, Thomas and Beal, 2007). Lewy body pathology in autopsy-based studies showed alpha-synuclein inclusions within the substantia nigra of PD patients. The analysis of spinal cord in double-mutant mice revealed huge accumulation of protein aggregates that were positive for pSer129-SNCA, p62/SQSTM1 and ubiquitin. Consequently, midbrain sections of paralyzed double-mutant mice were analyzed in respect to pSer129-SNCA, p62/SQSTM1 and ubiquitin immunoreactivity. The immunohistological analysis depicted again protein aggregates with a cytoplasmatic granular or fibrillar pattern within midbrain sections of paralyzed double-mutant mice (Fig. 52).

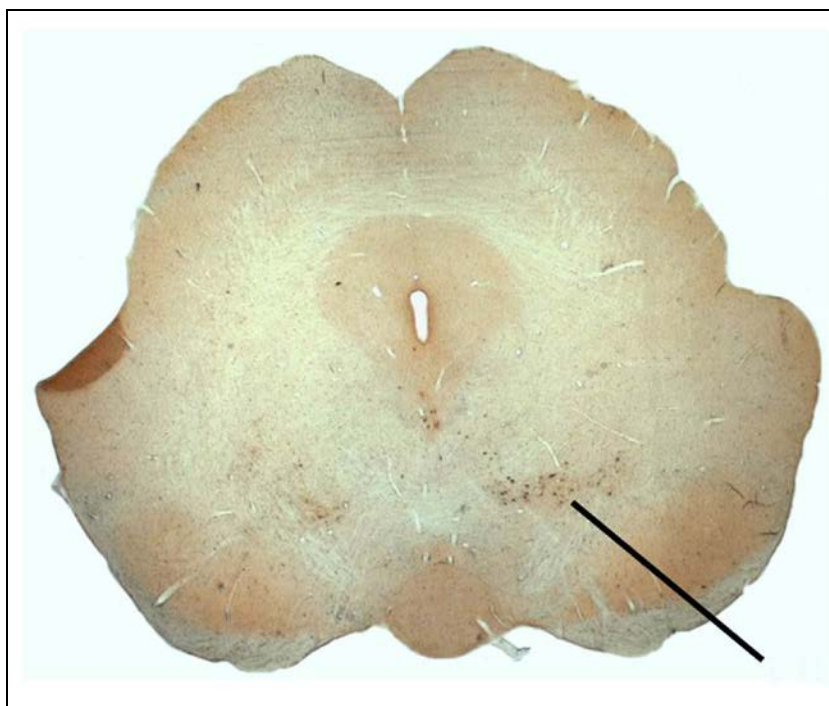


Fig. 52 Representative bright-field microscopy picture of pSer129-SNCA immunoreactivity in midbrain of a paralyzed A53T-SNCA + *Pink1*KO double-mutant mouse. The arrow highlights pSer129-SNCA positive protein aggregates. The picture was taken with the help of Dr. Kay Seidel.

As illustrated in figure 52 pSer129-SNCA positive protein aggregates were found bilaterally but with a stronger pattern in one hemisphere. Anatomically, the distribution of aggregates

found in this analysis reaches from the ventral tegmental area (VTA) to the subthalamic nucleus and substantia nigra as well as to the zona incerta (Fig. 52).

In order to investigate whether these protein aggregates are specific to paralyzed double-mutant mice, immunohistochemistry of pSer129-SNCA, p62/SQSTM1 and ubiquitin was performed in parallel in paralyzed and non-paralyzed double-mutant, wild-type and single-mutant mice (Fig. 53, Fig. 54). The analysis of paralyzed double-mutant mice revealed protein aggregates positive for pSer129-SNCA (Fig. 53J, M), p62/SQSTM1 (Fig. 53K, N) and ubiquitin (Fig. 53L, O), with the strongest immunoreactivity for pSer129-SNCA. As already described for spinal cord, PrPmtA mice showed light nuclear pSer129-SNCA immunoreactivity but again no protein aggregation or signs of neurodegeneration (Fig. 53G). In wild-type and *Pink1*KO mice no specific immunoreactivity of pSer129-SNCA, p62/SQSTM1 or ubiquitin was detected (Fig. 53A-F). In high-magnification pictures (Fig. 53M-O) the granular and thread-like composition of cells positive for pSer129-SNCA (Fig. 53M), p62/SQSTM1 (Fig. 53N) and ubiquitin (Fig. 53O) becomes visible. These pictures illustrate immunopositive neurites with corkscrew-structures, a sign of neurodegeneration (Fig. 53M).

In order to specify if the observed pathology is exclusive for the spinal cord and midbrain of paralyzed double-mutant mice, other brain areas of paralyzed mice as well as non-paralyzed age matched A53T-SNCA + *Pink1*KO mice were analyzed with respect to pSer129-SNCA immunoreactivity (Fig. 54). The lumbar level of spinal cord showed strong pathology in paralyzed double-mutants (Fig. 51), whereas thoracic and cervical levels showed only mild pSer129-SNCA immunoreactivity (Fig. 54A). The strong lumbar spinal cord pathology, however, seems exclusive to paralyzed double-mutant mice, since the analysis in non-paralyzed age matched double-mutants revealed only little pSer129-SNCA immunoreactivity mainly within the cytoplasm and only little in neurites (Fig. 54D). The same result was obtained in the analysis of the midbrain region of non-paralyzed double-mutant mice. Here the VTA showed only marginal immunoreactivity for pSer129-SNCA (Fig. 54E), whereas paralytic mice showed a strong pathology (Fig. 53J). Beside spinal cord and midbrain, paralyzed A53T-SNCA + *Pink1*KO mice displayed very modest pSer129-SNCA immunoreactivity in other brain regions. In the motor cortex very little immunoreactivity was found (Fig. 54B) but the striatum appeared aggregation free showing no immunoreactivity for pSer129-SNCA (Fig. 54C).

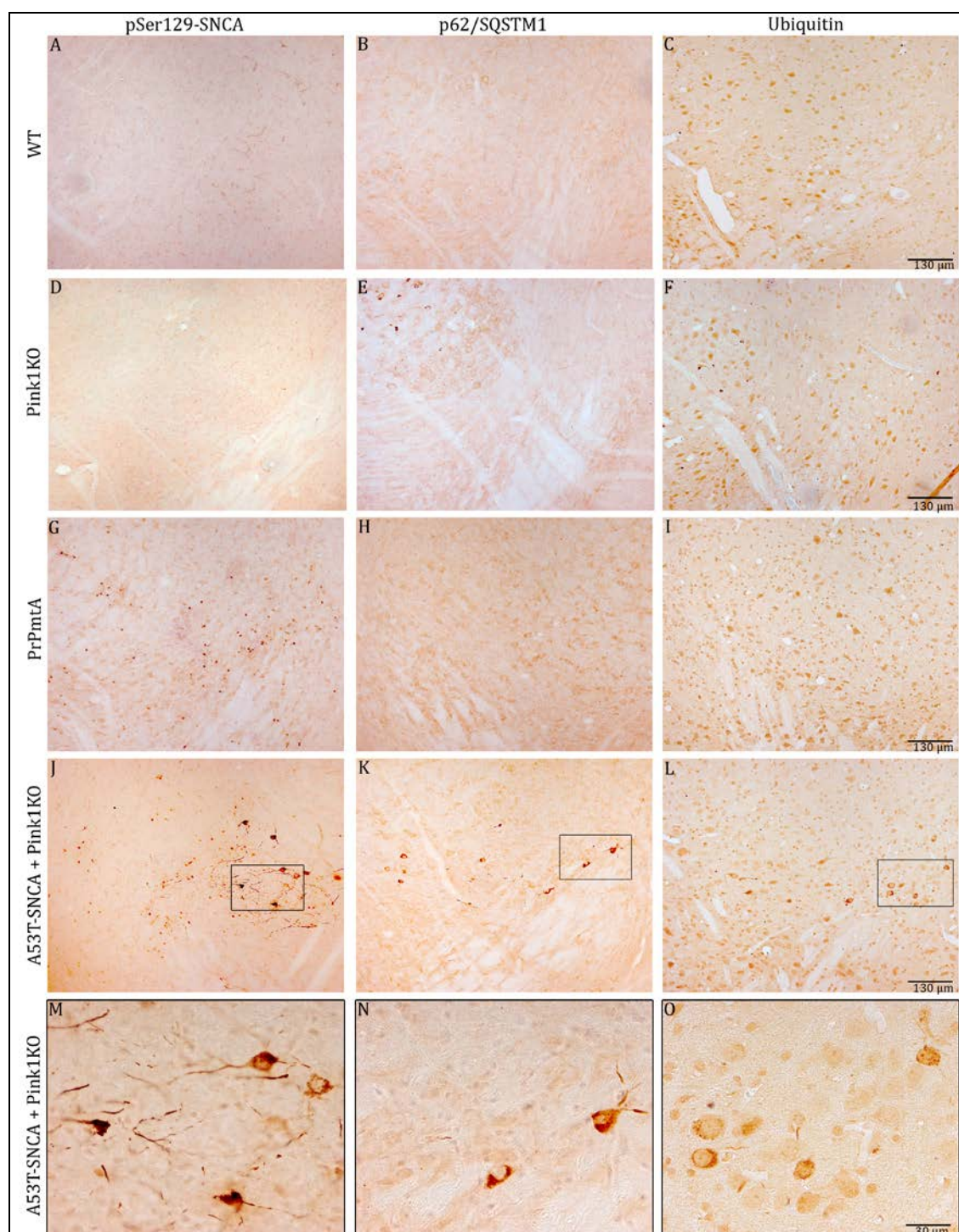


Fig. 53 Bright-field microscopy pictures from immunohistochemistry in midbrain of WT, *Pink1KO*, PrPmtA and double-mutant mice. Representative pictures show immunohistochemistry in midbrain of double mutant A53T-SNCA + *Pink1KO* (J-O), single mutant (PrPmtA (G-I) and *Pink1KO* (D-F)) as well as wild-type control mice (A-C) at the age of 15-17 months. Representative pictures were taken in the same midbrain region between VTA and SNC. Immunohistochemistry was performed in each mouse line for pSer129-SNCA (A, D, G, J, M), p62/SQSTM1 (B, E, H, K, N) and ubiquitin (C, F, I, L, O). Protein aggregation, positive for pSer129-SNCA, p62/SQSTM1 and ubiquitin was detected in midbrain neurons of double-mutant mice but not for WT controls or single-mutant mice (J-O). M-O show higher magnification pictures of J-L. Pictures were taken with the help of Dr. Kay Seidel.

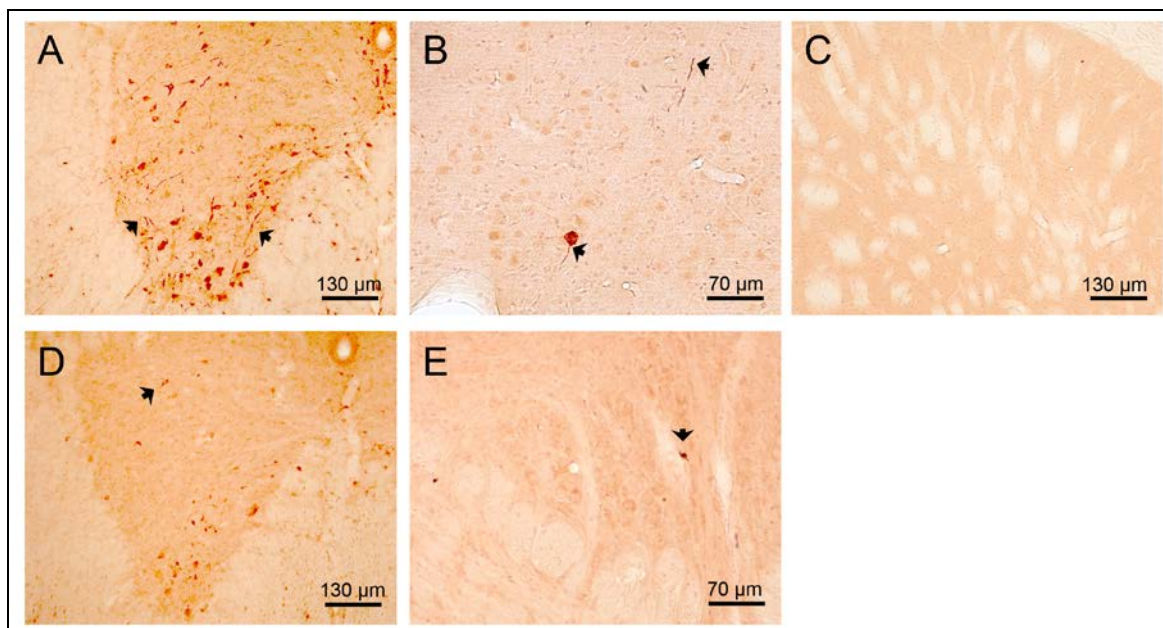


Fig. 54 Representative bright-field microscopy pictures of pSer129-SNCA immunoreactivity in the thoracic and cervical spinal cord (A), the motor cortex (B) and the striatum of paralyzed double-mutant mice. The thoracic and cervical level of spinal cord showed milder pathology than lumbar levels, whereas in motor cortex very little pathology was observed and the striatum appeared free of aggregates and pathology. The lumbar spinal cord (D) and the VTA (E) of non-paralyzed double-mutant mice revealed only scant pathology in comparison to paralyzed mice. Pictures were taken with the help of Dr. Kay Seidel.

3.3.3 pSer129-SNCA, p62/SQSTM1 and Ubiquitin Positive Cells of A53T-SNCA + *Pink1*KO Midbrain Slices are not TH Positive

The immunohistological analysis of paralyzed A53T-SNCA + *Pink1*KO mice revealed pSer129-SNCA, p62/SQSTM1 and ubiquitin positive aggregates in spinal cord and midbrain. In order to specify the observed midbrain pathology, double-immunofluorescence histochemistry was performed in midbrain sections of paralyzed double-mutant mice. Since Parkinson's disease is characterized by a loss of dopaminergic neurons of the substantia nigra, and the previously observed midbrain pathology was located closely to the substantia nigra (Fig. 52), a double-immunofluorescence with tyrosine hydroxylase (TH), a marker of dopaminergic neurons was performed. First, double-immunofluorescence with alpha-synuclein (4B12) and TH was performed to confirm the overexpression of human alpha-synuclein in the double-mutant model. Thereafter, each of the previously reported antibodies that were found to show immunopositive midbrain pathology was analyzed in parallel with TH using double-immunofluorescence (Fig. 55).

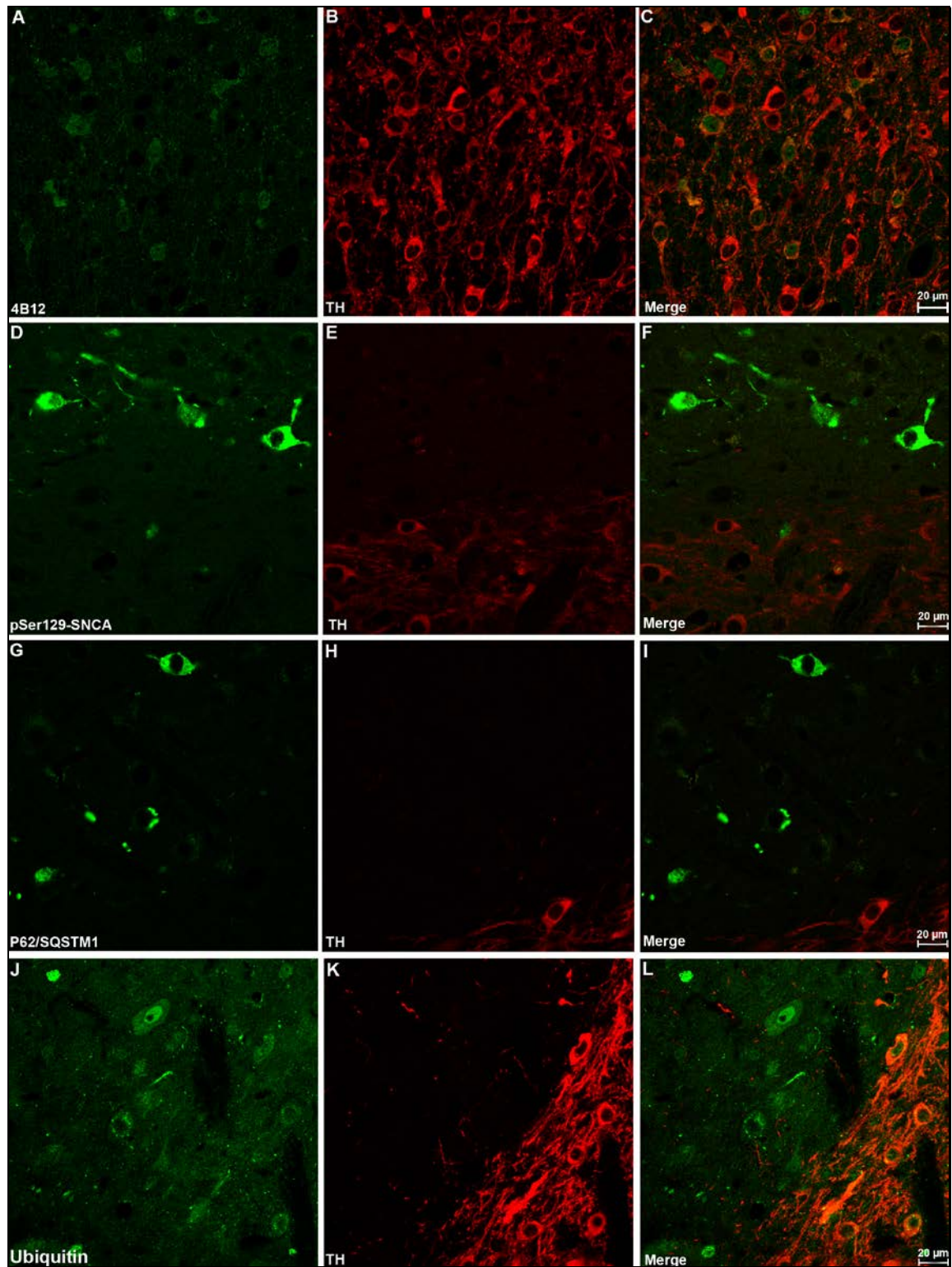


Fig. 55 Representative pictures showing double-immunofluorescence histology in paralyzed A53T-SNCA + *Pink1*KO mice. The first panel shows alpha-synuclein (4B12) (A) and TH (B) staining as well as the colocalization (C). Alpha-synuclein distribution appeared mainly nuclear, whereas TH was found cytoplasmatic. The second panel shows pSer129-SNCA (D) and TH (E) immunoreactivity, where no colocalization was found (F). The third row shows p62/SQSTM1 (G) and TH (H) immunoreactivity, where again no colocalization was detected (I). In the last panel ubiquitin (J) was analyzed in parallel to TH (K), showing no colocalization in midbrain cells of paralyzed double-mutant mice (L). Pictures were taken with the help of Beatrice Kern.

The double-immunofluorescence of alpha-synuclein and TH confirmed the overexpression of human alpha-synuclein showing a mainly nuclear pattern among dopaminergic neurons of the substantia nigra (Fig. 55A), whereas TH immunoreactivity (Fig. 55B) was found cytoplasmatic. The analysis of pSer129-SNCA in parallel to TH (Fig. 55D-F) depicted pSer129-SNCA positive cells (Fig. 55D) located dorsal to the substantia nigra that occurred TH positive (Fig. 55E). The same localization pattern was observed for p62/SQSTM1 (Fig. 55G-I) and ubiquitin (Fig. 55J-L), where again, positive cells were observed in a band dorsal to the substantia nigra that showed TH immunoreactivity (Fig. 55H, K). Therefore, no colocalization for pSer129-SNCA, p62/SQSTM1 and ubiquitin with TH was detected (Fig. 55 F, I, L).

3.3.4 pSer129-SNCA, p62/SQSTM1 and Ubiquitin Positive Cells of A53T-SNCA + *Pink1*KO Midbrain Slices are Positive for Interneuron Specific Markers

The double-immunofluorescence for pSer129-SNCA, p62/SQSTM1 and ubiquitin with TH revealed that midbrain aggregate formation did not occur in dopaminergic neurons of the substantia nigra but in a band of non-dopaminergic cells located dorsal to the substantia nigra. In order to further characterize these cells, double-immunofluorescence using pSer129-SNCA as marker of the affected cells and GFAP as marker of astroglial cells (Fig. 56A-C) or NeuN as neuronal marker (Fig. 56D-F) was performed. The analysis revealed, that the affected cells are not GFAP positive (Fig. 56C) and therefore not astroglial cells. The double-immunofluorescence of pSer129-SNCA and NeuN depicted a colocalization for several cells (Fig. 56F), highlighting the aggregate containing cells to be of neuronal origin. In order to further specify the affected neuronal celltype, double-immunofluorescence for pSer129-SNCA and parvalbumin as interneuron specific marker (Fig. 56G-I), GAD65 as marker for GABAergic neurons (Fig. 56J-L) and VGLUT2 as marker for glutamatergic neurons (Fig. 56M-O) was executed. The analysis revealed a very light colocalization for pSer129-SNCA and parvalbumin (Fig. 56I) indicating the affected cells to be interneurons. The double-immunofluorescence of pSer129-SNCA and GAD65 as well as of pSer129-SNCA and VGLUT2 revealed no colocalization (Fig. 56L, O) therefore affected neurons are probably not GABA- or glutamatergic.

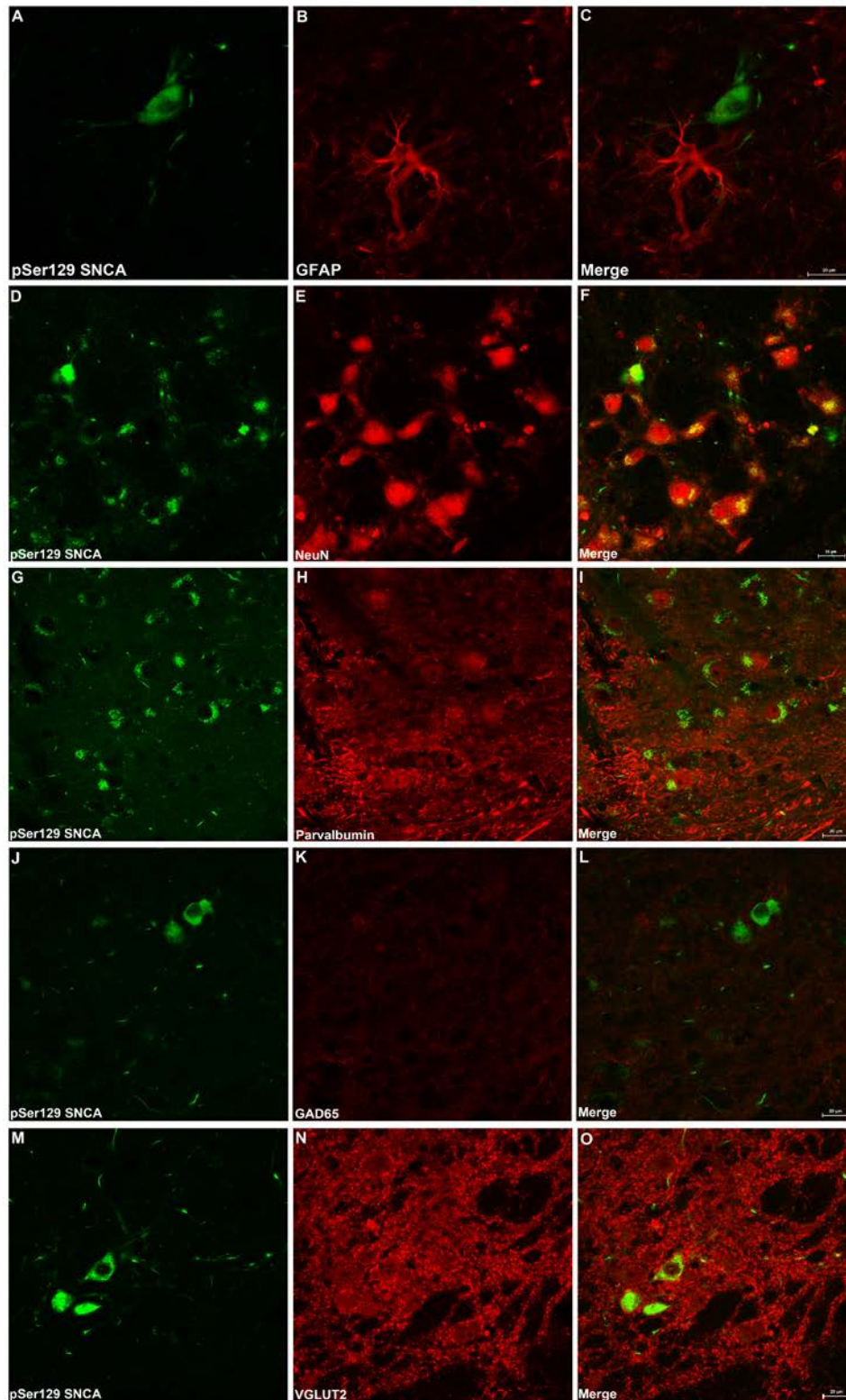


Fig. 56 Representative pictures showing double-immunofluorescence histology in paralyzed A53T-SNCA + *Pink1*KO mice. The first panel shows pSer129-SNCA (A) and GFAP (B), a marker of astroglia. The analysis depicted no colocalization (C). The second panel shows immunoreactivity for pSer129-SNCA (D) and the neuronal marker NeuN (E), where colocalization was found for several cells (F). Row 3-5 depict the further characterization using parvalbumin as an interneuron marker (H), GAD65 as a marker of GABAergic neurons (K) and VGLUT2 as a marker of glutamatergic neurons (N). The double-immunofluorescence revealed a light colocalization for parvalbumin (I) and no colocalization for GAD65 (L) and VGLUT2 (O). Pictures were taken with the help of Beatrice Kern.

4. DISCUSSION

4.1 **PROJECT I: ALPHA-SYNUCLEIN GAIN-OF-FUNCTION EFFECTS ON CANDIDATE GENES POSSIBLY INVOLVED IN SYNAPTIC PLASTICITY**

By the time Parkinson's disease (PD) is manifested through severe motor symptoms, about 80% of dopaminergic neurons are irreversibly degenerated (Bernheimer et al., 1973). In order to intervene in this progressive neurodegeneration, it is essential to understand the molecular mechanism that occurs in early stages PD, prior to the onset of neurodegeneration and cell death. In this respect, the previous work of Dr A. Kurz focused on the analysis of alpha-synuclein dependent physiological as well as pathophysiological mechanisms that underlie PD. The main intention in this work was to identify biomarker of alpha-synuclein function and pathology in a hypothesis free manner. A. Kurz organized a microarray analysis of different brain regions obtained from A53T-SNCA overexpressing mice at different ages, to analyze on one hand alpha-synuclein dependent expression alterations and on the other hand age dependent alterations to unravel biomarker of progression. After the hypothesis free approach A. Kurz also focused on a subset of expression alterations obtained from the microarray and analyzed them in a hypothesis driven manner using independent techniques. Besides these molecular alterations, A. Kurz also showed subtle changes in dopamine neurotransmission as well as synaptic plasticity (Kurz et al., 2010, Platt et al., 2012).

In order to decode the molecular underpinnings of early stages PD, as well as to clarify the role of alpha-synuclein for synaptic plasticity, this work focused on the molecular analysis of the previously described LTD deficiency in A53T-SNCA overexpressing mice (PrPmtA). In respect to PD being a polygenic disease rather than a monogenic, the analysis was extended to two additional mouse models of PD, namely the previously described *Pink1KO* mouse model as well as the novel double-mutant model harboring both the A53T-SNCA overexpression and the *Pink1KO*. This work is particularly interesting, since alterations in synaptic plasticity seem to be a key event in the pathobiology of PD. Post mortem studies of PD patients demonstrated a reduced length and number of dendritic spines in MSNs of the putamen (McNeill et al., 1988). Additionally, post-mortem studies of PD patients and studies using animal models of PD could demonstrate that the loss of dendritic spines in MSNs results from striatal dopamine depletion (Ingham et al., 1989, Stephens et al., 2005, Zaja-Milatovic et al., 2005, Day et al., 2006). Furthermore, the study of Day et al. in 2006 showed a 50% reduction of dendritic spines in D2 receptor containing MSNs, whereas D1 receptor containing MSNs remained un-

changed (Day et al., 2006), suggesting that a reduction of dendritic spines and therefore alterations in synaptic plasticity within the indirect-pathway presents one of the key features in the pathophysiology of PD.

4.1.1 Alpha-Synuclein Gain-of-Function Increases the Expression of Candidate Genes Involved in Synaptic Signaling Efforts and Decreases the Expression of Candidate Genes Downstream of Synaptic Signaling Cascades in A53T-SNCA Mice

With regards to the current opinion in the field of PD research, highlighting synaptic plasticity alterations within the indirect pathway to present a main pathological hallmark, the previously identified LTD deficiency (Kurz et al., 2010) and the impaired vesicle release (Platt et al., 2012) in our A53T-SNCA overexpressing mouse model provides an excellent tool to study the molecular mechanisms leading to this key event as well as the contribution of alpha-synuclein. Considering the hypothesis free microarray data as well as intense study of the literature, the first set of candidate genes analyzed were subunits of glutamate receptors. Glutamate receptors are essential for glutamatergic neurotransmission playing a role for memory, learning and motor control. The human brain comprises two classes of glutamate receptors, ionotropic glutamate receptors and metabotropic glutamate receptors (Kandel E. R., 1995). The group of ionotropic glutamate receptors is further divided due to their agonist sensitivity into N-methyl-D-aspartate-receptors (NMDA) and α -amino-3-hydroxy-5-methyl-4-isoazolpropionacid receptors (AMPA). Most AMPA receptors show permeability for K^+ and Na^+ and no permeability for Ca^{2+} , however depending on the subunit composition and the RNA editing they also permit Ca^{2+} influx, whereas NMDA receptors are permeable for K^+ , Na^+ and for Ca^{2+} . The Ca^{2+} influx activates second messenger cascades leading to long-term synaptic changes in excitability (Kandel E. R., 1995). AMPA receptors are the main source of the excitatory postsynaptic potential (EPSP) in MSNs and are composed of four subunits that are highly homologous forming a tetrameric, cation-permeable glutamate receptor that is expressed throughout the brain (Beneyto and Meador-Woodruff, 2004, Collingridge et al., 2004). The four AMPA receptor subunits, *Gria1-Gria4* are encoded by four genes and alternative splicing and RNA editing contributes to additional variants (Lambolez et al., 1996). In the adult brain 99% of AMPA receptors are not Ca^{2+} permeable (Greger et al., 2003) but the 1% receptors lacking *Gria2* subunits do show Ca^{2+} permeability (Swanson et al., 1997). AMPA receptors are mainly localized in the postsynaptic membrane but they show a high dynamic

with lateral mobility along the cell surface between synaptic and extrasynaptic site and they also undergo trafficking (Nishimune et al., 1998, Matsuzaki et al., 2001). Therefore, changes in AMPA receptor number and localization at the synapse are key aspects to modulate the efficacy of synaptic transmission. The insertion of AMPA receptors into the postsynaptic plasma membrane occurs via SNARE protein mediated exocytosis (Luscher et al., 1999), whereas the removal is controlled by dynamin-dependent endocytosis (Carroll et al., 1999). Alpha-synuclein was shown to promote SNARE complex assembly (Burre et al., 2010), therefore possibly influencing the AMPA receptor insertion into the postsynaptic plasma membrane. In this respect the expression of AMPA receptor subunits was studied in the previously described A53T-SNCA overexpressing mouse line at the age of 6 months in striatal and mid-brain tissue. The analysis revealed increased mRNA level for *Gria2* in striatal tissue of A53T-SNCA overexpressing mice and increased mRNA level for *Gria3* and *Gria4* in midbrain tissue of A53T-SNCA overexpressing mice. The increased *Gria2* level possibly represents an effort to reduce the postsynaptic Ca^{2+} influx, since *Gria2* lacking AMPA receptors are Ca^{2+} permeable (Swanson et al., 1997). The increased *Gria3* and *Gria4* level in midbrain possibly represents an compensatory effort to increase glutamatergic neurotransmission signals that are impaired in A53T-SNCA overexpressing mice (Platt et al., 2012), however simply increasing the number of AMPA receptor subunit does not guarantee a higher number of functional AMPA receptors nor a sufficient insertion into the plasma membrane that could be impaired by alpha-synuclein dependent effects on SNARE mediated exocytosis, nor is a higher expression completely sufficient to potentiate synapses as seen in studies of Schnell et al. (Schnell et al., 2002). This awareness implies that additional steps are necessary to potentiate synapses through AMPA receptor regulation. These additional steps include the stabilization of AMPA receptors at the synapse, which is conducted by the scaffolding protein PSD-95 (postsynaptic density protein 95). The study of Bats et al. showed that overexpression of PSD-95 promotes the accumulation of AMPA receptors (Bats et al., 2007) and the analysis of *Psd-95* mRNA expression in the A53T-SNCA overexpressing mouse revealed an increased expression in mid-brain tissue (see Results 3.1.2.1), supporting the hypothesis of a compensatory upregulation of candidate genes involved in promoting synaptic plasticity. However, on a postsynaptic level in striatal tissue no expression alterations were detected, indicating that PSD-95 is not a key regulator of the observed LTD deficiency in PrPmtA mice. PSD-95 not only accumulates AMPA receptors it also links NMDA receptors, controlling their interaction with each other as well as their interaction with intracellular proteins and signaling enzymes. An increased interaction of PSD-95 with the NMDA receptor subunit *Grin2b* for example was shown to increase NMDA receptor stability at extrasynaptic sites in a mouse model of Huntington's dis-

ease (Fan et al., 2009, Fan et al., 2012). In PD dopamine deficiency causes the decreased activation of D2 receptors resulting in increased Ca^{2+} influx by voltage-gated ion channels (Desmond and Levy, 1990). Several studies proposed that increased Ca^{2+} influx impacts the degenerative process of synaptic spines observed in animal models of PD and in PD patients (Ingham et al., 1989, Nitsch and Riesenberger, 1995, Arbuthnott et al., 2000) and Tymianski et al. showed that this Ca^{2+} mediated excitotoxicity occurs primarily through NMDA receptors than through other voltage-gated ion channels (Tymianski et al., 1993). In line with this are the results of Weihmuller et al., showing an 20-40% elevation of NMDA receptors in PD patients compared to controls (Weihmuller et al., 1992). Even if glutamate acts via several receptors, NMDA receptors play the biggest role in mediating neuronal toxicity which is due to their high Ca^{2+} permeability as well as their slow deactivation (Choi et al., 1987, DiFiglia et al., 1997). This NMDA dependent excitotoxicity is in contrast to studies demonstrating that cell survival of several neurons is dependent on synaptic NMDA activity (Ikonomidou and Turski, 2002, Hardingham, 2006, Hetman and Kharebava, 2006). Taken together NMDA on one hand can promote cell survival but on the other hand can trigger neuronal death, therefore both too much and too little response to NMDA activity is harmful for neurons (Lipton and Kater, 1989, Lipton and Nakanishi, 1999, Hardingham and Bading, 2003). It is well understood that NMDA receptors mediate synaptic plasticity and synaptic transmission (Bliss and Collingridge, 1993, Aamodt and Constantine-Paton, 1999), however besides this synaptic NMDA receptors that are well characterized there are also extrasynaptic NMDA receptors (Petrulia et al., 2010) that can represent up to three-quarters of all NMDA receptors (Tovar and Westbrook, 1999). The physiological function of these extrasynaptic NMDA receptors is not fully understood, however there is evidence that they contribute to LTD (Rusakov and Kullmann, 1998, Massey et al., 2004, Zhao and Constantine-Paton, 2007). NMDA receptors are composed of four subunits that are organized around a central ion channel. The four subunits are encoded by seven genes, with one gene encoding eight GluN1 subunit splice variants, four genes encoding GluN2 subunits (Grin2a-Grin2d) and two genes encoding GluN3 subunits (Grin3a-Grin3b) (for review see (Glasgow et al., 2015)). A functional NMDA receptor comprises a combination of two GluN1 subunits and two GluN2 or GluN3 subunits, leading to a great diversity which is accompanied by NMDA subtype-dependent properties (reviewed in (Glasgow et al., 2015)) such as different deactivation kinetics (Monyer et al., 1992, Monyer et al., 1994, Vicini et al., 1998), different agonist potency (Kutsuwada et al., 1992, Priestley et al., 1995, Varney et al., 1996, Erreger et al., 2007, Traynelis et al., 2010), different Ca^{2+} permeability (Burnashev et al., 1995, Schneggenburger, 1996), different voltage dependence of channel gating (Clarke and Johnson, 2006, 2008, Clarke et al., 2013), different sensitivity to block by

external Mg^{2+} (Monyer et al., 1994, Kuner and Schoepfer, 1996) and a different sensitivity to endogenous inhibitors (Traynelis et al., 1995, Williams, 1996, Chen et al., 1997, Paoletti et al., 1997, Traynelis et al., 1998). In this respect the expression of NMDA receptor subunits was studied in the previously described A53T-SNCA overexpression mouse line at the age of 6 months in striatal and midbrain tissue. With respect to the finding, that NMDA receptor can promote cell survival or cell death, either increased or decreased mRNA expression of NMDA receptor subunits was expected, but due to the finding of increased NMDA receptors in PD patients (Weihmuller et al., 1992) increased levels seemed more plausible. Indeed in the A53T-SNCA overexpressing mouse line an increased expression of the NMDA receptor subunits *Grin3a* and *Grin3b* was observed in striatal tissue and increased levels of *Grin1*, *Grin2a* and *Grin2b* mRNA level in midbrain tissue (see Results 3.1.1.1). The previously demonstrated LTD deficiency in this mouse line is therefore accompanied by an increased pre- and postsynaptic NMDA receptor subunit expression. The increased expression of NMDA receptor subunits is possibly a compensatory effort to boost the reduced neurotransmission signaling due to the impaired vesicle release that was demonstrated in electrophysiological studies (Platt et al., 2012). The clear separation into pre- and postsynaptic expression alterations is difficult, since dissection methods used do not allow a clear separation. Therefore, this analysis cannot provide detailed information about the localization of the analyzed NMDA receptor subunits nor of the exact localization of the analyzed AMPA or metabotropic glutamate receptors.

Besides ionotropic glutamate receptors, metabotropic glutamate receptors are involved in the generation of LTP and LTD. Metabotropic glutamate receptors belong to the family of G-protein-coupled receptors that modulate relatively slow synaptic transmission via second messengers (Nakanishi et al., 1998). There are at least eight subtypes of metabotropic glutamate receptors and based on their sequence similarity and signal transduction mechanism, they are classified into three groups. Group one comprises Grm1 and Grm5, group two Grm2 and Grm3 and group three Grm4, Grm6, Grm7 and Grm8 (for review see (Gubellini et al., 2004)). The different groups of metabotropic glutamate receptors are coupled to different second messengers, group one receptors are coupled to the $IP_3/Ca^{2+}/PKC$ pathway leading to increased intracellular Ca^{2+} release when activated, whereas group two and three receptors are negatively coupled to adenylate cyclase leading to a presynaptic inhibition of neurotransmitter release when activated (for review see (Gubellini et al., 2004)). As already described for ionotropic glutamate receptors, metabotropic glutamate receptors are localized at the pre- and postsynapse but are also found perisynaptically (Ottersen and Landsend, 1997). However, within the striatum group one metabotropic glutamate receptors are found at the postsynaptic level and group two and three are found presynaptically on excitatory corti-

costriatal terminals (Calabresi et al., 1993, Testa et al., 1994, Testa et al., 1995, Kerner et al., 1997, Tallaksen-Greene et al., 1998, Testa et al., 1998, Marino and Conn, 2002, Pisani et al., 2002). Hence, one of the key functions of metabotropic glutamate receptors is the direct modulation of neurotransmitter release. With respect to PD, there have been studies showing an interaction of metabotropic glutamate receptors with dopamine in the striatum, suggesting an increased dopamine release due to activation of group two metabotropic glutamate receptors (Cartmell et al., 2000). In order to boost the impaired neurotransmission that was previously observed in the PrPmtA model using an electrophysiological approach as well as in line with the findings regarding AMPA and NMDA receptor subunits, the expression analysis of metabotropic glutamate receptor subunits in striatal and midbrain tissue of 6-month-old A53T-SNCA overexpressing mice was expected to show increased mRNA level for several subunits. In line with this hypothesis the qPCR analysis depicted *Grm1* and *Grm3* to be increased in striatal tissue and *Grm3* and *Grm5* in midbrain tissue (see Results 3.1.1.1). The study of Gubellini et al. in 2001 showed, that the induction of LTD requires the selective activation of group one metabotropic glutamate receptors especially of *Grm1* (Gubellini et al., 2001, Sung et al., 2001) and in line with this finding, Conquet et al. showed that *Grm1* lacking mice have a reduced amplitude of LTD (Conquet et al., 1994), therefore the increased striatal *Grm1* as well as the *Grm5* midbrain levels in PrPmtA mice possibly represent a compensatory effort to counteract the LTD deficiency. *Grm3* that was found increased in striatal and midbrain tissue, is a group two metabotropic glutamate receptor subunit that does not seem to be involved in the induction of corticostriatal LTD (Sung et al., 2001), but studies in mice lacking group two and three metabotropic glutamate receptors can induce a different form of LTD that is due to presynaptic inhibition of glutamate release but is independent of long-term postsynaptic modifications (Kahn et al., 2001). So taken together, there is a pre- and postsynaptic effort to increase metabotropic glutamate receptors that are involved in the generation of LTD in PrPmtA mice at 6 months of age. As mentioned previously increasing the expression of receptor subunits is not sufficient to modulate synaptic plasticity, therefore additional steps such as modulating the expression of scaffolding proteins are necessary. As previously described the scaffolding protein PSD-95 assembles AMPA and NMDA receptors at the postsynaptic density. In respect to metabotropic glutamate receptors the scaffolding protein Homer1 is the most relevant (Brakeman et al., 1997). The Homer protein family includes three isoforms in mammals, Homer1, Homer2 and Homer3, and all of them have different isoforms due to alternative splicing. Homer proteins are localized at the postsynaptic density and interact with several other postsynaptic density proteins (de Bartolomeis and Fiore, 2004, Shiraishi-Yamaguchi and Furuichi, 2007). The Homer proteins are classified into con-

stitutively expressed isoforms (Homer1b/c, Homer2 and Homer3) as well as into activity-dependent expressed isoforms (Homer1a). The constitutively expressed isoforms can bind other proteins of the postsynaptic density using their N-terminal domain, but they also show self-assembly using their C-terminal coiled-coil domain. The activity-dependent splice variant Homer1a however, lacks the C-terminal domain so it interacts with other proteins of the postsynaptic density but cannot self-assemble. Homer1a is therefore a short form that is induced like an immediate early gene after neuronal stimulation and acts in an endogenous dominant-negative fashion by disrupting the protein assembly of long Homer isoforms (Shiraishi-Yamaguchi and Furuichi, 2007), therefore disrupting the signaling complex of metabotropic glutamate receptors and IP3 receptors which prevents glutamate-induced neuronal activity (Tappe and Kuner, 2006). The analysis of *Homer1* transcript level in the A53T-SNCA overexpressing mouse line revealed significantly reduced *Homer1* mRNA level both in striatal and midbrain tissue of 6-month-old mice (see Results 3.1.2.1). The TaqMan assay applied for *Homer1* qPCR cannot distinguish between *Homer1a* and *Homer1b/c* isoforms, but due to the rapid induction of *Homer1a* as an immediate early gene, *Homer1a* possibly represents most of the quantified *Homer1* transcripts. In line with this assumption is that *Homer1a* is induced by glutamate (Sato et al., 2001) as well as by dopamine signaling (Henning et al., 2007, Yamada et al., 2007), both of which are altered in PrPmtA mice. The reduced *Homer1* level found in striatal and midbrain tissue of PrPmtA mice possibly reflect a reduction of *Homer1a* transcripts, which are responsible in regulating glutamate dependent Ca^{2+} influx through activation of IP3 receptors. Therefore, the reduced *Homer1* levels represent a cellular effort to increase glutamate dependent neuronal activity. In line with this hypothesis is that overexpression of *Homer1a* was found to reduce postsynaptic AMPA and NMDA currents in hippocampal neurons (Sala et al., 2003) and a disrupted interaction of Homer1 with metabotropic glutamate receptors, possibly through Homer1a, was shown to impair LTD in rat hippocampal slices (Ronesi and Huber, 2008). Since Homer1 assembles group one metabotropic glutamate receptors with intracellular IP3 receptors in order to control intracellular Ca^{2+} dynamics, the next candidate studied was the IP3 receptor (Tu et al., 1998). The IP3 receptor is ubiquitously expressed in the mammalian brain and predominantly localized at the endoplasmic reticulum membrane (Putney and Bird, 1993). IP3 receptors are ion-channels that release intracellular Ca^{2+} from the endoplasmic reticulum when activated through extracellular signals that act via group one metabotropic glutamate receptors and the scaffolding protein Homer1 as described previously in this discussion (Berridge, 1993). In accordance to the already identified effort in A53T-SNCA overexpressing mice, to increase synaptic signaling via increased transcripts of AMPA, NMDA and metabotropic glutamate receptor subunits as well

as decreased *Homer1*, the *IP3 receptor* transcript level analysis depicted increased *IP3 receptor* levels in striatal and midbrain tissue of 6-month-old PrPmtA mice (see Results 3.1.4.1). Therefore, in PrPmtA mice the electrophysiologically identified LTD deficiency is accompanied by increased ionotropic and metabotropic glutamate receptor transcript levels, especially by group one metabotropic glutamate receptor subunits that are required for LTD induction (Gubellini et al., 2001) as well as *IP3 receptor* transcript level that are coupled to group one metabotropic glutamate receptors via *Homer1*. Three additional candidate gene analysis support this hypothesis of an increased signaling effort, one is the analysis of *RGS2* transcript level, second is the analysis of *Pdbd1* and third the analysis of *Tac1* (see Results 3.1.4.1). RGS proteins act as GTPase activating proteins, therefore blocking G-protein function which limits the lifetime of the active GTP-G α complex (Berman et al., 1996, Hunt et al., 1996, Watson et al., 1996). RGS2 is a mediator of G-protein coupled signaling that specifically inhibits Gq α which is involved in inositol lipid signaling (Heximer et al., 1997). *RGS2* transcript was found reduced in striatal tissue of PrPmtA mice at 6 months of age, again reflecting an increased effort to enhance the mGluR/IP3R signaling. The *Pdbd1* gene encodes a member of the pterin-4-alpha-carbinolamine dehydratase family that is involved in the biosynthesis of tetrahydrobiopterin (BH4) (Thony et al., 2000). In respect to BH4 function which increases dopamine release within the nervous system (Koshimura et al., 1990) as well as the fact that decreased BH4 level were associated with PD (Curtius et al., 1984), *Pdbd1* represents an interesting candidate possibly involved in the enhanced signaling effort. The analysis of *Pdbd1* transcript level in striatal and midbrain tissue of 6-month-old PrPmtA mice revealed significantly upregulated *Pdbd1* level in striatal tissue but no changes in midbrain (see Results 3.1.4.1), again reflecting an increased effort of synaptic signaling in this mouse line of LTD deficiency. The third and last candidate gene that supports this hypothesis of increased signaling efforts within the nigrostriatal and corticostriatal pathway is tachykinin 1 (*Tac1*). The *Tac1* gene encodes the two neuropeptides substance P and neurokinin A, both involved in the regulation of glutamate-driven neurotransmission and excitotoxicity (Vargas et al., 2005). The transcript level analysis of *Tac1* in PrPmtA mice depicted increased *Tac1* levels in midbrain tissue and a trend towards induction for striatal tissue, again supporting the hypothesis of altered corticostriatal glutamate neurotransmission and cellular compensatory efforts.

The downstream consequences of glutamatergic and dopaminergic signaling are increased expression level of specific immediate early genes such as *cFos*, *FosB*, *JunB* and many others. In the A53T-SNCA overexpression mouse model of early PD pathology, a whole set of immediate early genes was analyzed in striatal and midbrain tissue of 6-month-old mice using qPCR. This analysis illustrated reduced striatal transcript levels for *Arc*, *cFos*, *FosB*, *Egr1*,

Egr2, *Nur77* and *Nor1* as well as reduced midbrain transcript level for *cFos*, *Egr1* and *Nor1*. Striatal reduction of the activity-regulated cytoskeleton-associated protein *Arc* is of particular interest, since *Arc* mRNA is known to rapidly localize to dendritic regions that received synaptic stimulation (Steward et al., 1998, Steward and Worley, 2002). *Arc* is also known to play a role for LTP and memory in the hippocampus (Guzowski et al., 2000, Ying et al., 2002) and its induction was proven to depend on NMDA receptors (Steward and Worley, 2001). So the reduced striatal mRNA level are the first evidence that the increased signaling effort that is visible through increased expression of receptors involved in generating synaptic plasticity is not sufficient to induce downstream effects such as the induction of immediate early genes. This first hint is in line with the finding of reduced striatal *cFos*, *FosB*, *Egr1*, *Egr2*, *Nur77* and *Nor1* levels. *cFos* is an immediate early gene that is known to be induced in striatal MSN due to dopamine receptor 1 stimulation (Graybiel et al., 1990, Young et al., 1991) and there is also evidence of *cFos* being modulated by glutamate transmission (Paul et al., 1992, Paul et al., 1995), highlighting its downstream position of dopaminergic and glutamatergic signaling. *FosB* is known to heterodimerize with JUN family proteins forming the transcription factor complex AP-1 that regulates the gene expression of several signaling pathways and was found to play a role in neurological and psychiatric disorders (Ohnishi et al., 2011, Yutsudo et al., 2013). *Egr1* and *Egr2* are as well regulator of transcription that are induced by extracellular stimuli such as synaptic activity and LTP and are involved in synaptic plasticity and memory formation (Bozon et al., 2002, Veyrac et al., 2014). Studies focusing on *Egr1* showed, that NMDA receptor antagonists can dramatically reduce the *Egr1* mRNA/protein expression (Worley et al., 1991), implying again, that the increased NMDA receptor subunit expression is not sufficient to actually increase glutamatergic signaling to the striatum. The last set of immediate early genes that was analyzed in striatal and midbrain tissue of A53T-SNCA overexpressing mice were members of the NR4A family of nuclear receptors, namely *Nurr1*, *Nur77* and *NOR1* (Maxwell and Muscat, 2006). The Nr4A members are induced by stimuli such as growth factors, glutamatergic neurotransmission, calcium influx as well as membrane depolarization and stress (Maxwell and Muscat, 2006). The molecular pathways that modulate the expression of *Nurr1*, *Nur77* and *Nor1* include the protein kinase A and cAMP responsive element-binding protein (CREB), calcium/calmodulin kinase (CaMK), NFκB and MAPK (Hawk and Abel, 2011). In respect to PD research, *Nurr1* is the nuclear receptor that is studied in greatest detail showing that overexpression of *Nurr1* can rescue alpha-synuclein induced neurotoxicity (Decressac et al., 2012) and that alpha-synuclein expression itself suppresses the expression of *Nurr1* (Lin et al., 2012). In PD patients mutations in *Nurr1* are associated with an increased risk and in post-mortem analysis of human tissue of PD cases *Nurr1* ex-

pression was found reduced, specifically in neurons with alpha-synuclein inclusions (Chu et al., 2006, Moran et al., 2007). NUR77 is known to have a direct action in apoptosis, where certain death stimuli such as glutamate excitotoxicity induce the translocation of NUR77 from the nucleus to the cytosol and mitochondria where it binds BCL2 and converts it from cell protector to cell killer (Li et al., 2000, Lin et al., 2004). BAD, the BCL2-associated agonist of cell death that indirectly promotes cell death was also studied in PrPmtA mice and showed significantly increased level in striatal tissue, so the same tissue where *Nur77* was found reduced. Since mRNA level do not reflect protein level, NUR77 protein could still be increased and promote the expression of *Bad*. In order to clearly state about interactions, protein analysis is needed. NOR1 is the member of the nuclear receptor family that is studied to the least extend. A recent study showed its localization in the nucleus and could demonstrate only a very rare translocation to the cytoplasm or mitochondria in neuronal cell death, implicating only a minor function for NOR1 compared to NUR77 (Boldingh Debernard et al., 2012). The analysis of *Nurr1*, *Nur77* and *Nor1* in striatal and midbrain tissue of 6-month-old A53T-SNCA overexpressing mice revealed reduced striatal *Nur77* and *Nor1* levels as well as reduced *Nor1* midbrain levels, whereas *Nur77* only showed a trend towards reduction. These findings are particularly interesting in the light of the study of Decressac et al., showing that reduced expression levels of NR4A family members increase the vulnerability of neurons to neurodegeneration (Decressac et al., 2012). In this respect the reduced expression of NR4A family members possibly reflect an alpha-synuclein dependent vulnerability of striatal MSN and dopaminergic midbrain neurons to cell death.

Summarizing this transcriptome analysis in general, 6-month-old A53T-SNCA overexpressing mice show increased expression of candidate genes involved in modulating neurotransmission and synaptic plasticity, but due to the finding of decreased immediate early genes predominantly in striatal tissue, this signaling efforts does not reach striatal MSNs, resulting in reduced synaptic plasticity seen on a molecular level as well as on an electrophysiological level by LTD deficiency. In order to depict the very earliest effects of alpha-synuclein overexpression, the candidate genes that were found significantly regulated in striatal or midbrain tissue of 6-month-old mice were analyzed in striatal and midbrain tissue of 3-month-old mice. This analysis illustrated, that alterations of glutamate receptor subunits occur with age progression but are not present in young mice (see Results 3.1.5.1). The analysis of immediate early genes, scaffolding proteins and additional candidates showed, that among the earliest effects of alpha-synuclein gain-of-function are expression alterations for *Homer1*, *cFos*, *Nor1*, *Nurr1* and *Nur77* (see Results 3.1.5.2). *Homer1* transcript level were found significantly reduced in striatal and midbrain tissue of 3-months-old mice such as in 6-month-old mice,

highlighting reduced *Homer1* level to illustrate one of the earliest marker of alpha-synuclein induced nigrostriatal and corticostriatal synaptic plasticity alterations. *cFos*, *Nur77* and *Nor1* were found reduced in 6-month-old mice but show increased expression level in striatal and midbrain tissue of 3-month-old mice. Additionally, the most important member of the NR4A family in respect of PD research, *Nurr1*, was also found increased in midbrain tissue of young mice. The increased expression of these genes possibly illustrate a high alpha-synuclein dependent cellular stress level, since *cFos* expression is very sensitive to stress and NR4A family members were found increased after intense Ca^{2+} influx (Boldingh Debernard et al., 2012). The increased *Nur77* expression at young age potentially accounts for the increased *Bad* expression at 6 months of age that promotes neurodegeneration after intense cellular stress, in our model possibly due to alpha-synuclein overexpression. At this early age neurotransmission alterations or LTD deficiency were not found, which is in line with the molecular finding that glutamate receptor expression is normal at this age. So taken together, among the earliest effects of alpha-synuclein gain-of-function are reduced *Homer1* transcript level as well as increased transcript levels of *cFos* and NR4A family members. This finding can contribute to the early detection of PD pathogenesis and can help to assess progression versus therapeutic benefits.

4.1.2 Alpha-Synuclein Gain-of-Function and Additional *Pink1* Ablation Decreases the Expression of Candidate Genes Involved in Synaptic Signaling Efforts and Decreases the Expression of Candidate Genes Downstream of Synaptic Signaling Cascades

For most cases Parkinson's disease is a polygenic rather than a monogenic disease, therefore the analysis of candidate genes possibly involved in synaptic plasticity was extended to an additional mouse model of PD harboring the A53T-SNCA overexpression and the *Pink1KO*, both of which are associated with familial cases of PD. This mouse model is expected to show increased pathology but electrophysiological studies regarding LTD were not conducted so far. However, on a behavioral level these double-mutant mice show a potentiated phenotype compared to each of the single mutants with reduced spontaneous activity becoming significant already at the age of 3 months and a progressive paralysis in aged mice (Gispert et al., 2014a). Due to the potentiated phenotype as well as the same murine specific PrP promoter driven alpha-synuclein overexpression but an additional *Pink1KO*, the candidate gene analysis of double-mutant mice was expected to show similar but possibly stronger expression al-

terations in striatal and midbrain tissue of 6-month-old mice. As described for the candidate gene analysis in PrPmtA mice, the first set of genes potentially involved in synaptic plasticity were glutamate receptor subunits. In double-mutant mice, the exact same subunits as described in great detail for PrPmtA in 4.1.1 were studied. The qPCR analysis of AMPA receptor subunits revealed reduced expression level for *Gria1* and *Gria2* in striatal tissue and no alteration in midbrain. As mentioned previously, *Gria2* subunit lacking AMPA receptors show Ca^{2+} permeability (Swanson et al., 1997), the reduced expression of *Gria2* mRNA in double-mutant mice possibly reflects an effort to increase Ca^{2+} permeability due to less *Gria2* containing AMPA receptors. However, this is not a strong hypothesis and alterations regarding AMPA receptor subunit expression are very low compared to alterations found in PrPmtA mice. In line with these limited expression changes in AMPA receptor expression is the finding of unaltered expression of the AMPA receptor and NMDA receptor scaffolding protein *Psd-95*, implicating AMPA receptor modulations to only play a minor role in double-mutant mice. The same is true for the analysis of NMDA receptor subunits where reduced striatal *Grin3b* and reduced midbrain *Grin2c* levels were found (see Results 3.1.1.2). As mentioned previously, too much as well as too little response to NMDA activity is harmful for neurons (Lipton and Kater, 1989, Lipton and Nakanishi, 1999, Hardingham and Bading, 2003), therefore reduced NMDA receptor subunit expression found in double-mutant mice possibly demonstrates pathological alterations of synaptic plasticity. The analysis of metabotropic glutamate receptor subunits revealed striatal *Grm1* level to be significantly reduced in 6-month-old double-mutant mice but no significant alterations were observed in midbrain tissue. *Grm1* is a group one metabotropic glutamate receptor that was found increased in PrPmtA striatal tissue of the same age, so reduced *Grm1* level illustrate alterations within the same pathway but with opposite directions. Taken together, the analysis of glutamate receptor subunits in double-mutant mice depicted only minor expression changes and those expression changes found were opposite to those of A53T-SNCA overexpressing single-mutant mice. This conflict may be explained by the different background of the two strains, with PrPmtA mice having a pure FVB/N background whereas double-mutant mice are homozygous for both genotypes and therefore show a mixed background of FVB/N and 129/SvEv with 50:50 distributions on average. The diversity in genetic background can influence the alpha-synuclein gain-of-function effects leading to different adaptations to compensate for this stressor. Besides the SNCA overexpression this mouse model lacks the protective function of PINK1 possibly leading to earlier problems of protein aggregation and therefore increased efforts of protein degradation rather than efforts to enhance a signaling deficiency. Additionally, no electrophysiological study of LTD was conducted in this mouse line so far, so there is the possibility that this line

does not show impaired LTD or neurotransmission deficiencies at this age, since dopamine level in HPLC analysis appeared normal (personal communication Suzana Gispert). Considering PD to be a polygenic disease with several mutations leading to the same pathological and phenotypical abnormalities, there is huge evidence that not one single pathway but different signaling pathways contribute to PD pathology and progression therefore different expression alterations in different mouse models of PD represent the rule rather than the exception.

The next set of candidate genes analyzed in 6-month-old striatal and midbrain tissue of double-mutant mice, were the scaffolding protein *Homer1* as well as the set of immediate early genes and additional candidates already described for PrPtmA mice in 4.1.1. This mRNA analysis depicted reduced *Homer1* level in striatum and midbrain of double-mutant mice as well as reduced midbrain levels for the immediate early genes *cFos*, *Creb1*, *FosB*, *Egr2*, *JunB*, *Nurr1*, *Nur77* and *Nor1* as well as reduced striatal level of *FosB*, *JunB*, *Nur77* and *Nor1*. The general pre- and postsynaptic reduction of immediate early genes implies an altered synaptic plasticity for this mouse line compared to wild-type controls. Interestingly, immediate early genes were found reduced in both the single-mutant and the double-mutant mice with alpha-synuclein overexpression, highlighting alpha-synuclein gain-of-function to represent a key event in the process of neurotransmission and synaptic plasticity. However, the alpha-synuclein gain-of-function seems to affect the signaling cascades in a different way. In PrPtmA mice through alteration of glutamate receptors leading to reduced expression level of immediate early genes predominantly in striatal tissue and in double-mutant mice via pathways that are not known yet, leading to reduced expression of immediate early genes predominantly in the midbrain. So taken together, among the strongest effects of alpha-synuclein gain-of-function are reduced *Homer1* transcript level as well as reduced transcript levels of immediate early genes especially of NR4A family members. In order to specify if those changes are clearly alpha-synuclein dependent, the same analysis was conducted in *Pink1*KO mice.

4.1.3 Exclusive *Pink1* Ablation has Only Minor Effects on the Expression of Candidate Genes Involved in Synaptic Plasticity

In order to specify the role of *Pink1*KO for synaptic plasticity as well as to clearly state which of the observed expression alterations in double-mutant mice relates to alpha-synuclein gain-of-function, the same set of candidate genes was analyzed in striatal and midbrain tissue of 6-month-old *Pink1*KO mice. The first set of genes analyzed were again subunits of ionotropic and metabotropic glutamate receptors. This analysis showed a significantly reduced striatal

expression for *Grin2d* as well as a reduced expression for *Grm2* in midbrain. Compared to the effects observed in PrPmtA single-mutants as well as in double-mutants these are only minor effects and therefore *Pink1*KO obviously is not a key regulator of synaptic plasticity. The analysis of scaffolding proteins, immediate early genes and additional candidates revealed reduced striatal expression of *Homer1* as well as reduced *Egr2* level in midbrain. Besides these, no significant expression alterations could be detected (see Results 3.1.1.3, 3.1.2.3, 3.1.3.3, 3.1.4.3). Taken together, *Pink1* ablation does not significantly influence synaptic plasticity. In line with this finding is, that these mice display a very mild phenotype, show no signs of neurodegeneration or protein aggregation, however they do show reduced spontaneous movements in open field, that is possibly due to impaired dopaminergic neurotransmission (Kitada et al., 2007, Gispert et al., 2009). In 2004 Valente et al. gave the first functional evidence of PINK1 having a protective role in neurons from stress-induced mitochondrial dysfunction (Valente et al., 2004), a potential explanation of the very mild pathology in the *Pink1*KO mouse line. The *Pink1*KO mice are housed in individually ventilated cages under controlled light/dark cycles, controlled temperature and controlled humidity with food and water available *ad libitum*. Under these controlled and actually unnatural conditions *Pink1*KO mice are not exposed to stressors, therefore the absence of a protein involved in stress response is rather inconspicuous. This absence of stressors leading to only minor molecular alterations within this mouse model of PD is in contrast to the double-mutant model where the need of PINK1 protective function becomes visible since SNCA overexpression presents sufficient cellular stress. However, taking together *Pink1*KO has only minor effect on the expression of candidate genes involved in the modulation of neurotransmission and synaptic plasticity and the huge effects on the expression of glutamate receptor subunit, scaffolding proteins, immediate early genes and additional candidate genes seen in PrPmtA and double-mutant mice, are clearly driven by alpha-synuclein gain-of function.

4.2 PROJECT II: THE IMPACT OF ALPHA-SYNUCLEIN GAIN-OF-FUNCTION ON THE BEHAVIORAL AND MOLECULAR RESPONSE TO APOMORPHINE TREATMENT

Among the major interference with progression of PD are severe side effects to L-DOPA treatment known as levodopa induced dyskinesia (LID). The current opinion is, that LID results both from pre- and postsynaptic abnormalities in dopamine signaling and changes in synaptic plasticity (Brotchie and Jenner, 2011, Fisone and Bezard, 2011, Murer and Moratalla, 2011, Ghiglieri et al., 2012, Cenci, 2014). As described in detail within the introduction of this thesis, studies in PD patients as well as in rodent models of PD could associate the behavioral aspect of LID with a dysregulation of dopamine release and clearance (Cenci and Lundblad, 2006) whereas on a molecular level LID is conducted by alterations within the direct pathway of D1 receptor positive striatal MSNs (Aubert et al., 2005, Cenci, 2007, Darmopil et al., 2009). Studies using 6-OHDA rodent models of PD identified markers of postsynaptic supersensitivity to be associated with LID, particularly the phosphorylation of ERK1/2 could be positively correlated to abnormal involuntary movements in L-DOPA treated animals (Pavon et al., 2006, Santini et al., 2007, Westin et al., 2007). However, these studies were performed in a model of PD that is induced by stereotactic unilateral injection of the neurotoxin 6-OHDA leading to an acute loss of dopaminergic terminals and neurons. This model represents a static model of late stage PD after completion of the neurodegenerative process, but this model lacks the ability to study presymptomatic stages and PD progression. In this respect the 6-OHDA model, in line with other neurotoxin induced models of PD, is not suitable to identify therapeutic targets that are specific to early stages PD. Furthermore, these neurotoxin-induced models of PD do not model crucial PD progression events that are alpha-synuclein driven (Angot and Brundin, 2009, Nakamura et al., 2011, Taschenberger et al., 2012). Considering the status quo of LID research it would be of great value to model LID in a model of early stages PD and study the molecular events leading to the severe abnormalities. In order to investigate whether a transgenic mouse model of synucleinopathy could be useful to model LID, we studied the response of our A53T-SNCA overexpressing mice to a dopamine agonist, documented their behavior and investigated established molecular markers of striatal postsynaptic supersensitivity as well as novel candidates of the same signaling cascade. The choice of using the A53T-SNCA overexpressing mouse model of PD within this novel approach was supported by previous data obtained in this mouse model of early stages PD. This model was proven to show impaired neurotransmission (Platt et al., 2012) as well as LTD deficiency in corticostriatal slices, which could be rescued by phosphodiesterase antagonists (Kurz et al., 2010). Furthermore, the molecular analysis of midbrain and striatal tissue dis-

cussed in 2.1.1 revealed an increased expression of glutamate receptor subunits as compensatory effort to enhance the signaling deficit as well as a reduced expression of immediate early genes implicating that this effort does not reach striatal MSNs and synaptic plasticity is impaired. A novel electrophysiological approach showed an increase in firing frequency in dopaminergic midbrain neurons and stated this selective enhancement as “stressful pace-making” (Subramaniam et al., 2014). Additionally, the PrPmtA model is a model of synucleinopathy that does not show neurodegeneration so it mimics early stages of PD as well as PD progression providing the chance to identify beneficial therapeutic targets. Summarizing these previous findings, the PrPmtA model provides a valuable model to study whether pre-symptomatic stages of PD may already involve altered postsynaptic sensitivity to dopamine receptor stimulation. To our knowledge there was only one additional approach focusing on the pre- and postsynaptic compartments in the pathophysiology of LID in a morphologically intact nigrostriatal projection. This approach used viral vector-mediated silencing of TH in order to induce striatal dopamine depletion (Ulusoy et al., 2010). This model highlights the presynaptic neurotransmission machinery as a key factor for the induction and maintenance of LID. This model showed, that unlike the 6-OHDA model, where LID is highly correlated with the lesion intensity, the postsynaptic dopamine receptor stimulation using apomorphine induces dyskinesia even in absence of neuronal degeneration (Ulusoy et al., 2010). So taken together, the evidence of an powerful mouse model of early stages PD as well as the information provided by Ulusoy showing that LID can be modeled in absence of neurodegeneration, highlights this novel approach of studying LID in a genetic model of synucleinopathy as a relevant next step to identify new molecular markers of postsynaptic sensitivity that could serve as beneficial therapeutic targets in the treatment of early stages PD.

4.2.1 Alpha-Synuclein Gain-of-Function Increases Involuntary Movements with Stereotypic and Dystonic Features after Apomorphine Treatment

Behavioral validation of abnormal involuntary movements (AIMs) was established for the first time in the 6-OHDA rat model of LID by the group of Angela M. Cenci (Cenci et al., 1998, Andersson et al., 1999). The group established a scoring system using three main sections, each representing one topographical area of the body as already described in detail within the introduction (see 1.5.2). In 2004 the first 6-OHDA mouse model of LID has been reported again by the group of Angela M. Cenci and authors reported similar AIMs as those observed in

the rat model (Lundblad et al., 2004). The group used the same rating scale described for 6-OHDA lesioned rats but also included the frequency, the duration and the intensity of topographical limb, axial and orolingual dyskinesia (Francardo et al., 2011, Heuer et al., 2012). However, up to now there is no general agreement in the field of LID research upon the use of one general rating scale, in contrast different groups use different rating scales and those are still highly dependent upon subjectivity that is based on the visual observation of one single person (Breger et al., 2013). In this respect characterizing the behavioral response to apomorphine in a novel model in the field of LID was quite challenging. In order to reach the most valuable and trustworthy result the rating scale used to score A53T-SNCA overexpressing mice after apomorphine treatment was developed in collaboration with the group of Angela M. Cenci (detailed description of the rating scale shown in Material and Methods 2.2.4). The approach focused on the analysis of horizontal activity as well as on involuntary movements with stereotypic or dystonic features. Among the stereotypic features that differed quantitatively between PrPmtA and WT mice after apomorphine treatment were forelimb tapping and head bobbing and (as dystonic feature) hyperextension was scored. The behavioral analysis of 18-months-old A53T-SNCA overexpressing mice after a single subcutaneous injection of 5 mg/kg apomorphine using the novel stereotypic rating scale that was adapted from the AIMS score performed in 6-OHDA mice, revealed an significant induction of involuntary movements with stereotypic and dystonic features when compared to WT mice (see Results 3.2.1). Also in comparison to WT mice, the transgenic mice displayed a delayed recovery of spontaneous locomotion after apomorphine treatment, which is possibly due to the intensity of involuntary movements still observed at this time point (see Results Fig.33). The significant difference at time point 0 in horizontal activity reflects the well-established phenotype of PrPmtA mice at old age with reduced spontaneous locomotor activity (Gispert et al., 2003). The analysis of forelimb tapping showed persistently higher scores in PrPmtA than in WT mice but the statistical analysis failed to reach significance, which can be explained by the high standard deviation. The high standard deviation in forelimb tapping is due to the fact, that not all of the scored mice showed forelimb tapping within the time videotaped, leading to highly different scores within each group. However, looking at the individual data one can state, that forelimb tapping tends to be increased in PrPmtA compared to WT mice after apomorphine treatment. Head bobbing, the second stereotypic movement that was quantified in this analysis, showed significant differences from time point 40 on with PrPmtA displaying a higher score compared to WT mice. Considering that this is the very first behavioral analysis of a transgenic mouse displaying AIMS closely to what was shown for 6-OHDA, head bobbing presented the most sensitive behavioral trait to accurately describe stereotypic move-

ments. Dystonic behavior was quantified by the analysis of axial hyperextension, showing a significant higher score only at time point 20. However, as described for forelimb tapping, the analysis of hyperextension failed to reach statistical significance at the other time points due to the high standard deviation. The high standard deviation, again, resulted from differences within each group (PrPmtA and WT), since not all animals showed axial hyperextension during the observation period. However, a close look at the data revealed that hyperextension tended to be increased over the complete observation period.

In order to prove that the corticostriatal and nigrostriatal overexpression of alpha-synuclein (Gispert et al., 2003) occurred in absence of neuronal cell loss, immunohistochemistry of alpha-synuclein and TH was performed in mice used for behavioral validation. The immunohistochemical analysis depicted a clear alpha-synuclein overexpression in PrPmtA compared to WT mice showing enhanced immunoreactivity in synapses with granular pattern in striatal and cortical sections as well as a coarser grained appearance of SNCA immunoreactivity along neurites of the substantia nigra (see Results 3.2.2). Morphological circumstances were studied using TH immunohistochemistry, followed by optical density analysis in the striatum and midbrain of PrPmtA mice compared to WT. The detailed analysis of different striatal and midbrain level by optical density revealed no anatomical evidence of a dopaminergic cell loss in 18-month-old PrPmtA mice, giving evidence that the observed behavioral response is independent of neuronal loss. Considering the previously reported impaired vesicle release (Platt et al., 2012), the impaired LTD (Kurz et al., 2010) as well as the expression alterations of candidates involved in synaptic plasticity, the increased behavioral sensitivity to apomorphine can be ascribed to the deficiency in dopaminergic signaling. Taken together, the transgenic expression of A53T-SNCA in the nigrostriatal and corticostriatal projections has an impact on the behavioral response to apomorphine, leading to increased involuntary movements with stereotypic and dystonic features even in the absence of neurodegeneration.

4.2.2 Alpha-Synuclein Gain-of-Function Changes the Temporal Dynamics of Striatal Signaling Responses to Apomorphine Treatment

Previous studies in 6-OHDA mouse models of LID identified a correlation between abnormal involuntary movements and indexes of striatal postsynaptic supersensitivity. One of the key molecules associated with LID are the extracellular signal-regulated kinases 1 and 2 (ERK1/2). ERK1/2 have been described as mediators of activity-dependent plasticity seen in studies of hippocampal LTP, where ERK2 activity through NMDA receptor activation presents

a potential component of the LTP induction pathway (English and Sweatt, 1996). Thereafter, an involvement in classical conditioning (Crow et al., 1998) and memory formation was shown (Brambilla et al., 1997, Atkins et al., 1998). As described previously, the ERK1/2 signaling cascade is also acting as a master switch for striatal synaptic plasticity and altered phosphorylation of ERK1/2 is correlated with abnormal involuntary movements in 6-OHDA rodent models of LID (Pavon et al., 2006, Santini et al., 2007, Westin et al., 2007). In 6-OHDA rodent models of LID, increased phosphorylation of ERK1/2 was shown after L-DOPA treatment as an early marker of aberrant neuroplasticity and post-synaptic D1 receptor supersensitivity (Westin et al., 2007). However, it is necessary to mention, that 6-OHDA mice with striatal lesion showed a significant increase of phospho-ERK1/2 only in severely denervated striatal regions and not in regions with more than 60% residual dopaminergic neurons (Francardo et al., 2011).

In order to study the molecular underpinnings of the behavioral response to apomorphine in this novel transgenic model of LID, candidates previously identified in the 6-OHDA mouse model such as the phosphorylation of ERK1/2 as well as novel candidates that are involved in regulating the ERK1/2 signaling cascade, were studied. The analysis of early changes in phosphorylation levels of ERK1/2 were performed in striatal tissue dissected 30 min after apomorphine challenge. This time point was chosen in accordance to studies in the 6-OHDA rodent model in which 20 minutes after acute L-DOPA administration ERK1/2 phosphorylation was detectable (Westin et al., 2007), as well as in accordance to a study showing that acute apomorphine administration increases ERK phosphorylation 30 minutes after injection in rats (Sanguedo et al., 2014). Our analysis revealed significantly induced phospho-ERK2 level in both groups after apomorphine treatment, whereas a trend towards induction was observed for phospho-ERK1, so apomorphine treatment clearly induces the striatal phosphorylation of ERK1/2 both in PrPmtA and WT mice. The finding of ERK2 being significantly altered and ERK1 only depicting a trend is particularly interesting in the light of the previously mentioned study showing ERK2 phosphorylation to be an important modulator of synaptic plasticity, whereas ERK1 did not seem to play a major role (English and Sweatt, 1996). However, in order to explain the observed behavioral differences after apomorphine treatment, the most important analysis is the direct comparison of PrPmtA and WT mice both after apomorphine and vehicle treatment. This comparison in phospho-ERK1/2 level revealed no significant phenotype dependent differences regarding the response to apomorphine or to vehicle, so at baseline levels, at the early time point of 30 minutes. In order to identify striatal effects of apomorphine treatment, an additional later time point was chosen that reflects the recovery phase, which was seen altered in PrPmtA compared to WT mice. The analysis of

phospho-ERK1/2 level 100 minutes after treatment revealed no significant apomorphine dependent alterations in WT mice, implicating that the activity of compensatory mechanism has already balanced the cellular stress, leading to a reduction of phospho-ERK1/2 in apomorphine treated WT mice back to normal level (vehicle level). In contrast, the analysis of PrPmtA mice sacrificed 100 min after treatment illustrated a reduced ERK1/2 phosphorylation in striatal tissue, implicating an increased sensitivity of dopamine agonist-dependent dephosphorylation pathways. However, in order to explain the behavioral differences between WT and PrPmtA mice after apomorphine treatment, the direct comparison of WT and PrPmtA mice is essential. This analysis revealed significant genotype dependent differences in vehicle treated mice, with PrPmtA mice showing increased phospho-ERK1/2 level compared to WT mice. This finding is in contrast to the observation at 30 minutes after apomorphine/vehicle treatment where no genotype dependent alterations for vehicle treated mice were found. The same analysis only 70 minutes later should not change these results, therefore we can only speculate about the underlying mechanism leading to this unexpected result. One potential explanation for the different baseline phospho-ERK1/2 levels is the fact, that PrPmtA and WT mice handle stress differently due to the increased alpha-synuclein expression. During the behavioral observation period it became clear, that WT mice relax much faster after being placed individually and tend to fall asleep earlier compared to PrPmtA mice. Sleeping animals were excluded from behavioral analysis but they were included in the molecular analysis. 30 minutes after apomorphine treatment neither WT nor PrPmtA mice were sleeping when sacrificed, so the general stress level was comparable. At 100 minutes after apomorphine treatment many of the studied mice were sleeping before sacrificing them for molecular analysis. We do not have statistical evidence for WT mice being more asleep than PrPmtA mice, but the personal feeling during the observation of all animals used for these tests is that WT mice tend to sleep at time point 100 but PrPmtA mice were still active. This behavioral difference could serve for the different phospho-ERK1/2 level after vehicle treatment. Importantly to mention, this difference in stress handling could also influence the result obtained for the genotype independent analysis of apomorphine treatment. The analysis of vehicle treated PrPmtA mice compared to apomorphine treated PrPmtA mice displayed a significant reduction in phospho-ERK1/2 level with a relatively high fold-change (PrPmtA vehicle treated compared to PrPmtA apomorphine treated = 1 -1.77 reduction of phospho-ERK1 and -1.66 reduction of phospho-ERK2 levels). The strong alteration in baseline phosphorylation level seen in the analysis of vehicle treated PrPmtA and WT mice, could serve as an explanation of the strong effect seen in PrPmtA mice, therefore the phospho-ERK1/2 analysis in PrPmtA vehicle compared to PrPmtA apomorphine potentially represents a false posi-

tive. However, the difference in stress accomplishment does not influence the molecular analysis of apomorphine treated mice, since they show a completely different behavior with both genotypes being active for the whole observation period. In this respect the analysis of a genotype dependent difference after apomorphine treatment represents a faithful analysis and revealed an increased phospho-ERK1 level in PrPmtA compared to WT mice but no alterations in phospho-ERK2 level, highlighting the ERK1/2 signaling cascade to be altered due to the A53T-SNCA overexpression.

Previous research showed, that the L-DOPA dependent activation of ERK1/2 mediates the sequential phosphorylation of the mitogen and stress-activated kinase-1 (MSK1) and histone H3, which is phosphorylated in response to MSK1 activity and that this activation occurs in dyskinetic but not in non-dyskinetic mice (Soloaga et al., 2003, Brami-Cherrier et al., 2005, Chwang et al., 2007, Santini et al., 2007). The group of Fisone could additionally demonstrate that the concomitant phosphorylation of ERK, MSK1 and histone H3 occurs at MSNs of the striatonigral pathway but not in striatopallidal MSNs (Santini et al., 2009). In this respect the phosphorylation of histone H3 was studied in PrPmtA and WT mice after apomorphine treatment. The analysis depicted an apomorphine dependent significant induction of phosphorylated histone H3 in the caudal part of the striatum in PrPmtA compared to WT mice, supporting the finding of increased ERK1 phosphorylation in striatal tissue of these mice. The phosphorylation of histone H3 is involved in the decondensation of chromatin and the regulation of nucleosomal response, therefore increased level in phosphorylated histone H3 modulate the expression of several genes most important of the immediate early gene FosB and prodynorpin (Andersson et al., 1999, Cheung et al., 2000, Soloaga et al., 2003). With regard to these findings of ERK1/2 and histone H3 phosphorylation pattern, that were validated using two independent methods namely Western Blot and immunohistochemistry, the analysis of underlying molecular alterations that are possibly associated with the observed behavioral response to apomorphine was extended to a third method and a third set of candidates previously described to be associated with LID, the analysis of immediate early genes in striatal tissue using qPCR. The analysis of candidate genes in striatal tissue revealed alterations for the immediate early genes *cFos* and *Nur77* that have been associated with LID in 6-OHDA rodent models as well as of two novel genes, namely *Dusp1* and *Dusp6* that are involved in the regulation of ERK1/2 but so far have not been associated with LID. The qPCR analysis focused on one hand on the apomorphine but genotype independent expression by comparing vehicle treated mice with apomorphine treated mice, and on the other hand on genotype dependent differences by comparing vehicle treated WT and PrPmtA as well as apomorphine treated WT and PrPmtA mice. The analysis was performed in a set of animals that was sacrificed 30

minutes after treatment as well as in an additional set sacrificed 100 minutes after treatment, representing the same experimental approach as described for the analysis of ERK1/2. The comparability of these two approaches is actually guaranteed by using one hemisphere of the mouse for phospho-ERK1/2 analysis and the other hemisphere for the qPCR analysis.

The first candidate found to show an apomorphine dependent induction was *cFos*. As described previously, *cFos* is an immediate early gene that was shown to be induced in striatal MSNs upon dopamine receptor 1 stimulation (Graybiel et al., 1990, Young et al., 1991, Herrera and Robertson, 1996). Additionally, studies in rats could confirm the predominant location of apomorphine-dependent *cFos* induction within striatal output neurons (Cenci et al., 1992). In light of the findings in project I showing an increased expression of glutamate receptor subunits in striatal tissue of 6 month PrPmtA mice, the findings of Paul et al. showing that glutamate transmission has a role in modulating the expression of *cFos* induced through dopamine agonists, are especially valuable (Paul et al., 1992, Paul et al., 1995). The analysis of striatal tissue dissected 30 minutes and the analysis of striatal tissue dissected 100 minutes after treatment revealed an apomorphine dependent *cFos* induction in both genotypes as well as increased genotype dependent *cFos* level in PrPmtA compared to WT mice (see Results 3.2.5.1 and 3.2.5.2), providing the first evidence of an postsynaptic supersensitivity to dopamine receptor stimulation in this novel model of LID.

The next candidate found to show apomorphine dependent alteration was *Nur77*. Within recent years there is emerging evidence of transcription factors of the Nr4A family to have an important role in dopamine-mediated effects. There is experimental evidence that the striatal expression of *Nur77* is strongly modified by dopamine transmission, so in response to drug treatment such as L-DOPA or apomorphine. In this respect the group of Levesque and Rouillard showed that 6-OHDA lesioned rats, after L-DOPA treatment, depict increased *Nur77* mRNA level in the intact side of the striatum but reduced *Nur77* mRNA level in the denervated side of the striatum (St-Hilaire et al., 2003), an imbalance that potentially contributes to behavioral sensitization. In accordance to this finding, the analysis of *Nur77* in striatal tissue of our mice which do not show neurodegeneration, revealed increased apomorphine dependent *Nur77* expression level. The expression analysis in our study showed a significant apomorphine dependent *Nur77* induction only in the group of mice that were sacrificed 100 minutes after apomorphine treatment (see Results 3.2.5.2) but not in animals sacrificed 30 minutes after treatment (see Results 3.2.5.1). Additionally, the analysis revealed an apomorphine dependent induction only in PrPmtA and not in WT mice, as well as an increased genotype dependent expression in PrPmtA compared to WT mice. Comparing this result to other

candidates such as *cFos*, the alterations of *Nur77* represent the only expression change that is exclusive to PrPmtA mice. Studies using *Nur77*^{-/-} mice observed impaired behavioral and molecular adaptations to denervation and L-DOPA treatment (St-Hilaire et al., 2006), suggesting a role for *Nur77* in the development of abnormal involuntary movements that are characteristic for LID.

In an effort to identify novel candidate genes that are altered in response to apomorphine treatment possibly reflecting the molecular basis of the observed behavioral response, the expression of genes that are involved in the regulation of ERK1/2 phosphorylation were studied. This analysis depicted two novel genes, namely *Dusp1* and *Dusp6* to be significantly induced in response to apomorphine at both time points, but genotype dependent differences were detected only in mice sacrificed 100 minutes after apomorphine treatment with PrPmtA showing significantly higher *Dusp1* and *Dusp6* level compared to WT mice (see Results 3.2.5.1 and 3.2.5.2). Additionally, the apomorphine dependent *Dusp6* induction in WT mice was only significant in mice sacrificed 30 minutes after treatment, the group sacrificed 100 minutes after treatment showed slightly enhanced *Dusp6* level, but no significant differences. This finding is in line with the results obtained for ERK1/2, showing phosphorylation to be back to normal levels in WT mice 100 minutes after treatment but not in PrPmtA mice. In an effort to specify if this apomorphine dependent induction is specific to *Dusp1* and *Dusp6* additional members of the Dusp gene family were studied. This analysis depicted two additional members, namely *Dusp4* and *Dusp14* to show an apomorphine dependent expression pattern for both genes in PrPmtA mice, but only for *Dusp4* in WT mice. However, genotype dependent differences could not be detected (see Results 3.2.5.3), emphasizing the specificity of the novel results obtained for *Dusp1* and *Dusp6*. *Dusp1* and *Dusp6* are members of the dual-specific phosphatase gene family that is known to be activated through induction of mRNA levels by several transcription factors such as CREB, NF- κ B and ETS-1 (Huang and Tan, 2012). *Dusp1* is an immediate response gene and its mRNA expression was previously found decreased in dopaminergic neurons of 6-OHDA lesioned rats, whereas *Dusp1* overexpression showed a protective effect against 6-OHDA (Collins et al., 2013). Thereafter, the study from Sun et al. showed that *Dusp1* basal expression level are relatively low but highly inducible in response to growth factors and stress (Sun et al., 1993). The DUSP1 protein also known as MKP-1, shows an exclusive nuclear localization and was shown to not only dephosphorylate ERK but also p38 and JNK (Wu et al., 2005). In contrast DUSP6, also known as MKP-3, shows a cytoplasmatic localization and its phosphatase activity is highly specific to ERK1/2. Studies could demonstrate, that DUSP6 through its activation by ERK-dependent phosphorylation, has a role as a negative feedback regulator, controlling mitogenic signaling (Caunt and Keyse,

2013). The novel finding of elevated *Dusp6* level in striatal tissue of PrPmtA mice after apomorphine treatment is especially interesting in the light of previous data obtained in our laboratory, that showed elevated *Dusp6* mRNA in primary skin fibroblasts of PD patients, providing evidence of a direct correlation of *Dusp6* and increased alpha-synuclein level (Hoepken et al., 2008). Consistent with our findings are two recent transcriptome profiling studies in 6-OHDA lesioned mice that showed a strong upregulation of *Dusp* transcripts within striatal projection neurons of the direct pathway after L-DOPA treatment, however this study neglected the validation of these findings using an independent method (Heiman et al., 2014, Visanji, 2014, Charbonnier-Beaupel et al., 2015). In this respect our study provides novel results that identified *Dusp1* and *Dusp6* as molecular markers of an altered striatal postsynaptic supersensitivity to dopaminergic challenge that potentially provided the underlying mechanism of the observed behavioral differences in response to apomorphine. Taken these novel *Dusp1* and *Dusp6* mRNA findings as well as the previously described phospho-ERK1/2 findings, DUSP6 was considered to be analyzed by Western Blot. This analysis performed in striatal tissue dissected 100 minutes after treatment revealed an significant apomorphine dependent induction in WT but not in PrPmtA mice and the analysis of genotype dependent differences illustrated and increased baseline level of DUSP6 in PrPmtA compared to WT mice as well as decreased DUSP6 level in PrPmtA mice compared to WT after apomorphine treatment (see Results 3.2.6). Hence, on protein level DUSP6 showed a stronger apomorphine dependent induction in WT than in PrPmtA mice, however the phosphorylation level of DUSP represents its activity and this analysis failed since no antibodies that specifically detect phosphorylated DUSP6 or antibodies specific for DUSP1 and phosphorylated DUSP1 were available.

In respect to the finding of *Dusp1* and *Dusp6* being novel and specific targets of an apomorphine-triggered reaction that underlies postsynaptic sensitivity, we aimed to determine if these results are exclusive to the striatum. Therefore, we analyzed the same candidates in midbrain tissue that was dissected 100 minutes after treatment. This analysis exhibited an apomorphine dependent increase for all four candidates in PrPmtA mice but only for *Dusp1*, *cFos* and *Nur77* in WT mice (see Results 3.2.5.4). However, genotype dependent differences were only detected for *cFos* showing increased expression level in PrPmtA compared to WT, highlighting the effects in *Dusp1*, *Dusp6* and *Nur77* expression observed in striatal tissue to be an alpha-synuclein dependent alteration that is striatum specific and therefore a possible readout of postsynaptic supersensitivity.

Taken together this analysis uncovered the impact of alpha-synuclein dependent effects on the behavioral and molecular response to apomorphine. The severe involuntary movements observed in A53T-SNCA overexpressing mice after apomorphine treatment are accompanied by increased striatal phospho-ERK1 and phospho-histon H3 level as well as by genotype dependent increased level of *cFos*, *Nur77*, *Dusp1* and *Dusp6* (shown in a simplified cartoon in Fig. 57). Those molecular alterations provide strong evidence of postsynaptic supersensitivity to dopamine receptor stimulation in this novel model of LID. Therefore, our data together with previous studies highlight a fundamental role of alpha-synuclein as a modifier of neurotransmission and synaptic plasticity. Thereafter, our data support the hypothesis that the PrPmtA mouse model is an authentic novel model of PD progression to study the presynaptic dysfunction of early stages PD as well as the postsynaptic pathobiology of alpha-synuclein overexpression at the basis of LID.

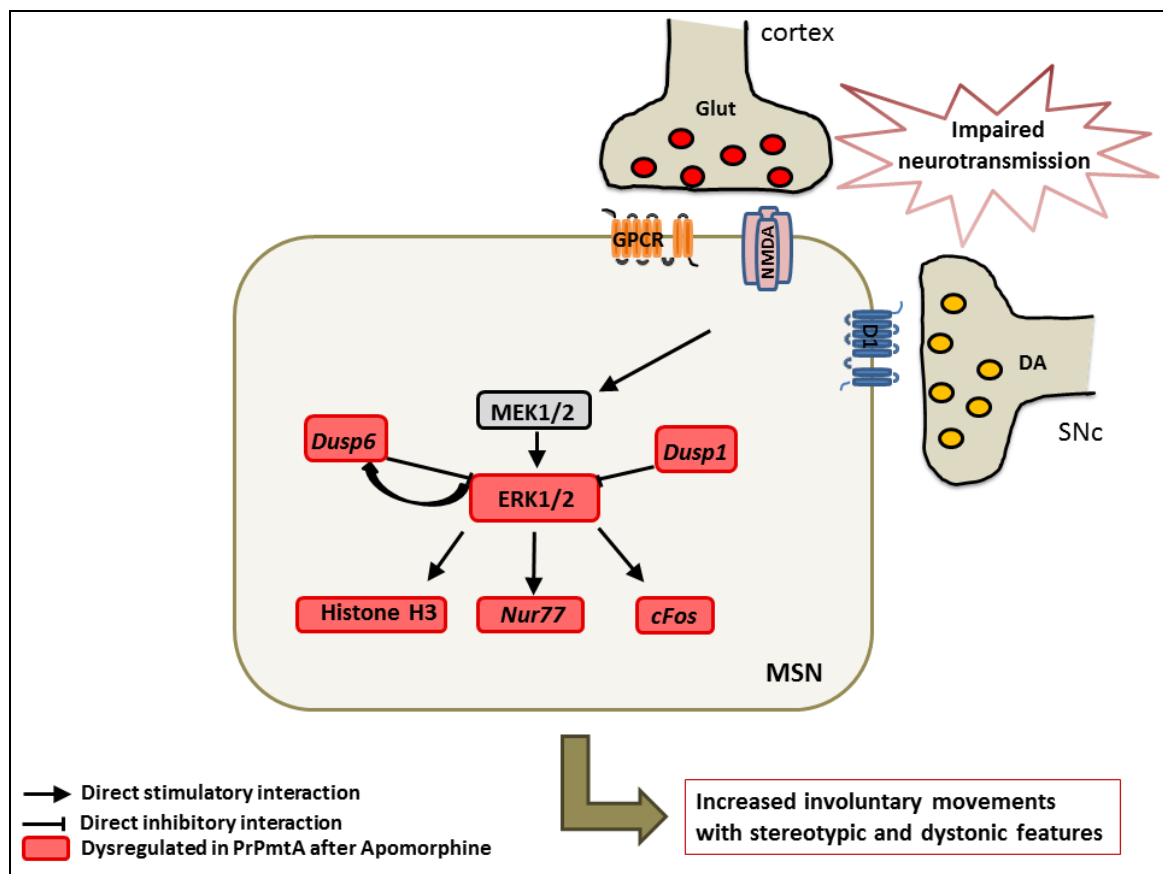


Fig. 57 Simplified cartoon of the main results obtained in project II. Highlighted are genotype dependent results obtained after apomorphine treatment. Abbreviations: DA: dopamine; Glut: glutamate MSN: medium spiny neuron; SNc: substantia nigra pars compacta

4.3 PROJECT III: POTENTIATION OF ALPHA-SYNUCLEIN GAIN-OF-FUNCTION EFFECTS IN DOUBLE MUTANT MICE WITH PINK1 AB- LATION

Intense research in the field of PD identified several genes that are associated with PD pathology (Corti et al., 2011), but only 5-10% of PD cases arise from mutations in one of the identified genes, whereas at least 85% occur in a sporadic manner (Thomas and Beal, 2007). However, there is evidence that in sporadic PD cases the same molecular alterations contribute to PD pathology. In this respect and in light of the fact that most PD cases actually suffer from polygenic interactions rather than from a monogenic disorder, studying the interaction of two PD relevant genes can provide valuable insights and provide a better understanding of both idiopathic and sporadic cases of PD, and therefore help to develop beneficial therapeutics. In order to study potential interactions of two PD associated mutations to possibly identify converging downstream pathways, a double-mutant mouse harboring both the A53T-SNCA overexpression as well as the *Pink1*KO was generated. Besides the transcript analysis that was shown in 3.1 this mouse is characterized by severe phenotypical abnormalities such as reduced spontaneous locomotor activity at the age of 3 month as well as a progressive hind limb paralysis. Comparing these phenotypical traits to both single-mutant mice that have been described earlier in this thesis, double-mutant mice display a significantly potentiated phenotype. In addition, the hind limb paralysis that starts unilateral and progresses to a full bilateral paralysis has never been observed in single-mutant mice. So in order to characterize this novel mouse model of PD, to identify the molecular and morphological changes leading to the observed phenotypical abnormalities as well as to study the role of PINK1 onto alpha-synuclein gain-of-function induced neurotoxicity, an intense immunohistological study in spinal cord and midbrain tissue was performed.

4.3.1 PINK1 Deficiency is a Relevant Modulator of Alpha-Synuclein Aggregation

The first self-evident step in characterizing a mouse model that shows a progressive hind limb paralysis was to immunohistologically analyze spinal cord sections of paralyzed mice. Therefore, spinal cord sections of paralyzed double-mutant mice as well as of age- and sex-matched controls were stained with well-established markers for PD pathology, namely pSer129-SNCA, p62/SQSTM1 and ubiquitin. The immunohistochemical analysis of pSer129-SNCA is quite established in the field of PD research and patients studies showed, that about

90% of insoluble alpha-synuclein found in PD brains is phosphorylated at serine 129 whereas in healthy subjects only 4% of total alpha-synuclein is phosphorylated (Fujiwara et al., 2002, Anderson et al., 2006), indicating extensive phosphorylation to be pathological. These patient studies are in line with studies in animal models of PD, where increased phosphorylation of alpha-synuclein at the residue Ser129 is associated with pathology. In a *Drosophila melanogaster* fly model of PD, Chen and Feany could show, that Ser129-phosphorylated alpha-synuclein enhances alpha-synuclein dependent toxicity, whereas blocking this phosphorylation enhances aggregate formation. Hence, in this fly model of PD, the Ser129-phosphorylation of alpha-synuclein is a crucial event in mediating neurotoxicity and aggregate formation (Chen and Feany, 2005). In line with these findings are results obtained in rodent models of PD where Ser129-phosphorylated alpha-synuclein was shown to accelerate A53T-SNCA-induced neurodegeneration (Sato et al., 2011). In post mortem brains of synucleinopathy, Hasegawa et al. showed that phosphorylated alpha-synuclein is ubiquitinated (Hasegawa et al., 2002) and they suggested that this may impact PD pathology. Prior to this coherence of ubiquitin and alpha-synuclein, ubiquitin has already been described to be present in Lewy bodies of PD patients, suggesting that abnormal aggregated or misfolded proteins are targeted for degradation (Kuzuhara et al., 1988, Arnold et al., 1998). Thereafter, the presence of ubiquitinated protein aggregates has also been described in rodent models of PD that focus on the autophagy aspect of PD (Ahmed et al., 2012). These autophagy based mouse models of PD showed protein aggregates that are not only ubiquitin positive but do also contain p62/SQSTM1 which functionally links the ubiquitination to the autophagy pathway (Bjorkoy et al., 2005, Pankiv et al., 2007). In addition p62/SQSTM1 was also found accumulated in various neurodegenerative diseases and among those with PD (Kuusisto et al., 2001).

In light of these former studies, the immunohistological analysis of our novel double-mutant mouse line focused on pSer129-SNCA, p62/SQSTM1 and ubiquitin. The histological analysis of spinal cord depicted a very prominent immunoreactivity for pSer129-SNCA within the gray matter of the anterior horn in paralyzed double-mutant mice, with distinct morphological signs of neurodegeneration, whereas no immunoreactivity was found in wild-type controls (see Results 3.3.1). In order to clearly assign if alterations in immunoreactivity are specific to double-mutant mice, immunohistological staining was also applied to age-matched single mutant mice as well as to non-paralytic double-mutant mice. This analysis revealed no immunoreactivity in the spinal cord of *Pink1*KO mice and a light nuclear immunoreactivity for pSer129-SNCA in PrPmtA single mutant mice, which can be attributed to the A53T-SNCA overexpression, but there were no visible signs of neurodegeneration or aggregation. The analysis of non-paralytic double-mutant mice disclosed that the strong spinal cord pathology

is exclusive to paralyzed double-mutant mice since non-paralytic mice displayed much milder pSer129-SNCA immunoreactivity mainly in the cytoplasm and only little in neurites where strong staining was found in paralyzed mice (see Results 3.3.2). A similar pattern of immunoreactivity was observed for ubiquitin and p62/SQSTM1, with the anterior horn of the lumbar spinal cord showing p62/SQSTM1 and ubiquitin positive aggregates but with lower intensity compared to pSer129-SNCA immunoreactivity (see Results 3.3.1). Again, the pathological immunoreactivity was exclusive to paralyzed double-mutant mice, and no immunoreactivity was found in WT or single-mutant mice. Ubiquitin immunoreactivity was found in WT and single-mutant mice but in a very mild form and in absence of neurodegeneration or aggregation signs.

In PD patients Lewy body pathology, as described within the introduction of this thesis, has been found in spinal cord, however the pathological hallmark of PD is the presence of Lewy bodies in the substantia nigra pars compacta. In this respect the immunohistological analysis was extended to midbrain sections. This analysis depicted again protein aggregates with cytoplasmic granular or fibrillar pattern, positive for pSer129-SNCA, p62/SQSTM1 and ubiquitin in midbrain sections of paralyzed double-mutant mice (see Results 3.3.2), showing a similar intensity pattern as found in spinal cord. So pSer129-SNCA showed the strongest immunoreactivity and p62/SQSTM1 and ubiquitin depicted a milder immunoreactivity but with a similar pattern as well as clear signs of pathology. The presence of protein aggregates was found bilaterally but with a stronger pattern in one hemisphere. This finding is especially interesting in light of the paralysis that starts as a unilateral paresis of the hind limb and progresses within a few days to a full bilateral paralysis, so the stronger immunoreactivity pattern for one hemisphere may reflect this phenomenon. The anatomical distribution of these aggregates reaches from the ventral tegmental area (VTA) via the subthalamic nucleus and the substantia nigra to the zona incerta. Analysis in single mutant-mice, wild-type mice as well as in non-paralytic double-mutant mice revealed no pathological immunoreactivity, clearly correlating the phenotypical abnormalities with the severe accumulation of protein aggregates. Additionally, the analysis of other brain regions such as the striatum and the motor cortex of paralyzed mice revealed only very little pathology, so the dominant pathology is anatomically located to the midbrain. However, in order to clearly state that the observed midbrain pathology occurs in the substantia nigra, a double-immunofluorescence histochemistry was performed, using the three well established markers of pathology in parallel to TH as a marker for dopaminergic neurons. The double-immunofluorescence depicted no colocalization for any of the three aggregation markers with TH (see Results 3.3.3) but showed the localization of aggregates dorsal to the substantia nigra. Therefore, in contrast to our expecta-

tion, the aggregation pathology did not occur in dopaminergic neurons of the substantia nigra but in other cells of the midbrain. In order to further specify if these cells are of neuronal or glia origin, double-immunofluorescence with GFAP as a marker of astroglial cells (Gomes et al., 1999) and NeuN as a neuronal marker (Wolf et al., 1996) was performed in midbrain slices of paralyzed double-mutant mice. This analysis showed a clear overlap of pSer129-SNCA with NeuN and no overlap with GFAP, assigning the aggregate-affected cells to be neuronal. In an effort to further characterize this neuronal cell population that showed aggregation pathology, double-immunofluorescence analysis with pSer129-SNCA and parvalbumin as a marker of interneurons (Celio and Heizmann, 1981), with GAD65 as a marker of GABAergic neurons (Hurd and Eldred, 1989) and with VGLUT2 as a marker for glutamatergic neurons (Morales and Root, 2014) was performed. This analysis revealed a very light colocalization for parvalbumin suggesting the affected neuronal cell population to be interneuron specific. However, due to the very light colocalization no guarantee can be offered about the pathological neuronal population to be interneuron specific.

Taken together, these findings show PINK1 as an essential modulator of alpha-synuclein aggregation. PINK1 was previously shown to be a relevant modulator of mitochondrial quality control and degradation (Corti et al., 2011, Youle and Narendra, 2011, Koyano et al., 2014) so the absence of PINK1 in cells that are stressed through alpha-synuclein gain-of-function obviously promotes the formation of alpha-synuclein fibrils. Studies in our laboratory as well as in other laboratories could show a role for PINK1 in the initiation and composition of the autophagy machinery (Michiorri et al., 2010, Klinkenberg et al., 2012, Parganlija et al., 2014) and only recently evidence emerged that PINK1 modulates the vesicular trafficking pathway responsible for the ability of mitochondria to selectively degrade oxidized and damaged proteins through the lysosomal pathway (McLelland et al., 2014). In respect to previous studies in single mutant *Pink1*KO mice that showed only mild signs of pathology, we conclude that alpha-synuclein gain-of-function mutations act as sufficient stressor to put in evidence the PINK1-dependent stress response and neuroprotective actions. The absence of this PINK1-dependent stress response potentially impairs an autophagic degradation of protein aggregates leading to the observed morphological characteristics not only within our novel model of PD leading to the resultant phenotypical abnormalities, but also within a recently published short-term model of alpha-synuclein induced neurodegeneration in *Pink1*KO mice, where alpha-synuclein overexpression is driven by stereotactic injections of adeno-associated viruses into the substantia nigra of *Pink1*KO mice (Oliveras-Salva et al., 2014). Additionally, Todd and colleagues showed a protective effect of PINK1 overexpression in dopaminergic neurons of a fly model of PD that additionally overexpresses alpha-synuclein

(Todd and Staveley, 2012), highlighting the value of PINK1-dependent neuroprotective responses. In summary, our findings highlight this novel mouse model of PD as valuable tool to further investigate molecular alterations and to identify the underlying mechanism as well as shared pathways contributing to PD pathology. We also highlighted a role of PINK1 as modulator for alpha-synuclein dependent neurotoxicity and emphasized the PINK1-dependent neuroprotective response as a potential target for novel beneficial therapeutics.

5. PERSPECTIVES

In Project I, the analysis of alpha-synuclein gain-of-function effects in different mouse models depicted alterations in synaptic plasticity that seem alpha-synuclein dependent and underlie the previously shown impaired neurotransmission and LTD deficiency in PrPmtA mice. In order to further characterize the alpha-synuclein dependent pre- and postsynaptic dysfunction glutamate receptors should be analyzed in more detail. The analysis using Western Blot appeared difficult due to the unavailability of appropriate antibodies; therefore autoradiography could preserve the method of choice not only providing quantitative data but also data about the anatomical distribution. The analysis of candidate genes in double-mutant mice revealed strong alterations within immediate early genes and transcription factors, supporting the hypothesis that those effects are alpha-synuclein driven. In order to specify the effect of *Pink1* deletion onto synaptic plasticity, LTD should be analyzed in corticostriatal slices of double-mutant mice as previously described for PrPmtA single-mutant mice.

The experimental approach described within project II uncovered the impact of alpha-synuclein dependent effects on the behavioral and molecular response to acute apomorphine treatment. Considering the strong behavioral and molecular alterations in this acute treatment approach, an additional approach studying the long-term treatment effects in this transgenic model of LID should be considered. Thereafter, the anatomical distribution of ERK1/2, DUSP1 and DUSP6 could provide further insights onto the postsynaptic pathobiology, so immunohistochemical analysis or autoradiography should be taken into account. Furthermore, in respect to the novel polygenic model of PD described within this thesis, an experimental approach using acute apomorphine challenge in double-mutant mice could provide additional information about the role of PINK1 as modulator of alpha-synuclein dependent neurotoxicity.

In Project III the immunohistochemical characterization of the novel double-mutant mouse model depicted an essential role for PINK1 as modulator of alpha-synuclein aggregation leading to immense morphological alterations in spinal cord and midbrain as well as phenotypical abnormalities. The analysis depicted a neuronal cell population that was shown to harbor pSer129-SNCA, p62/SQSTM1 and ubiquitin positive aggregates with cytoplasmic granular or fibrillar pattern in midbrain sections of paralyzed double-mutant mice. In order to further characterize these novel and undescribed neuronal cells, an electrophysiological study could be performed as well as further immunohistochemical analysis to clearly describe this interesting cell population.

6. SUMMARY

Introduction

Parkinson's disease (PD) is the second most frequent neurodegenerative disorder affecting 0.3% of the population in industrialized countries. PD is characterized by severe motor impairments such as rigidity, postural instability, bradykinesia/akinesia, flexed posture, freezing and low-frequency resting tremor as well as by non-motor symptoms such as depression, cognitive impairments, olfactory dysfunction, anxiety, REM-sleep disturbance and many others. The pathological process responsible for the severe motor deficits of this progressive neurodegenerative disease is the loss of dopaminergic neurons in the substantia nigra leading to reduced dopamine content within the striatum. Typical PD motor symptoms occur when about 70% of striatal dopamine content was lost. The striatum constitutes the largest and main input step of the basal ganglia, an important brain region for goal-directed behavior and habit formation. The majority of neuronal cells within the striatum are medium spiny neurons (MSNs), a neuronal population that is characterized by a huge number of spines. The basal ganglia circuitry comprises two major projection systems, the D1 receptor expressing MSNs of the direct and the D2 receptor expressing MSNs of the indirect pathway. These two pathways are activated concurrently and act in a coordinated way to support or suppress actions and there is evidence of an opposing effect of striatal dopamine release on these two pathways. In PD patients the reduced striatal dopamine content results on one hand in a reduction of locomotor activity and on the other hand in morphological alterations of MSNs.

For many years PD was considered a sporadic disorder and only with the development of genome-wide association studies the understanding of a genetic contribution evolved. Using these techniques several genes could be identified highlighting mitochondria or lysosomal dysfunction, protein aggregation and protein degradation as well as kinase signaling pathways to contribute to PD pathology. However, only 10% of PD cases are idiopathic while 90% occur sporadic. One key molecule associated with both idiopathic and sporadic PD cases is alpha-synuclein. Alpha-synuclein gain-of-function mutations have been shown to cause autosomal dominant variants of PD, whereas genetic variants at both ends of the gene act as risk factors in sporadic PD. Thereafter, alpha-synuclein is the main protein found in Lewy bodies, another pathological hallmark of PD pathology. Lewy bodies are found in the remaining dopaminergic cells of the substantia nigra giving evidence that protein aggregation might be a crucial factor for PD pathology. The complete physiological function of alpha-synuclein is still enigmatic; however there is evidence of SNCA being involved in SNARE-complex assembly, the trafficking of neurotransmitter vesicles and striatal dopamine release.

The currently known monogenic cases of PD are either autosomal dominant or autosomal recessive. Among the genes with a clear autosomal dominant inheritance was the previously described alpha-synuclein. Among mutations in genes showing an autosomal recessive inheritance the second most frequent is PTEN-induced kinase 1 (PINK1), where a loss-of function is associated with early onset PD. PINK1 was previously shown to play a protective role in stress induced mitochondrial dysfunction and the loss of PINK1 was proven to drive PD pathology due to impaired mitochondrial quality control leading to the accumulation of damaged mitochondria.

Today's standard treatment of PD motor symptoms is the dopamine replacement therapy using the dopamine precursor L-DOPA. Besides the immense beneficial effects of L-DOPA treatment on PD motor performance, more than 50% of PD patients treated with L-DOPA develop severe side effects known as levodopa induced dyskinesia (LID). The current pathophysiological concept about the source of LID is that it results from both pre- and postsynaptic abnormalities in dopamine signaling as well as from changes in synaptic plasticity. On a presynaptic level studies using rodent models of PD as well as patient studies could associate abnormal involuntary movements, a characteristic of LID, with dysregulated dopamine release and clearance. On a postsynaptic level, these studies showed that LID is accompanied by maladaptations within the direct pathway of D1 receptor positive striatal MSNs. The key signaling cascade involved in striatal synaptic plasticity, therefore acting as the master switch in LID is the extracellular signal-regulated kinase 1 and 2 cascade (ERK1/2).

Aim

The aim of this study was

1. To study alpha-synuclein gain-of-function as well as PINK1 deficiency effects on molecular pathways of synaptic plasticity, a possible key event in early PD pathology
2. To study the impact of alpha-synuclein gain-of-function on the behavioral and molecular response to apomorphine treatment and specify if the transgenic PrPmtA mouse model is valuable to model postsynaptic signaling abnormalities at the basis of LID
3. To characterize a novel double-mutant mouse model of PD and study the role of PINK1 deficiency onto alpha-synuclein induced neurotoxicity

Results and Discussion

Alpha-synuclein gain-of-function effects on candidate genes possibly involved in synaptic plasticity

The work of a previous PhD student focused on alpha-synuclein function and pathology in a hypothesis free manner using microarray-transcriptome profiling. This work was conducted in the A53T-SNCA overexpressing mouse line (PrPmtA) and revealed molecular alterations, subtle changes in dopamine neurotransmission as well as in synaptic plasticity with LTD being impaired. In order to clarify the role of alpha-synuclein gain-of function in the process of LTD as well as to further characterize alpha-synuclein dependent effects in striatal and mid-brain tissue, candidate genes involved in synaptic plasticity were studied in 6-month-old PrPmtA mice. In accordance to most PD patients suffering from a polygenic rather than a monogenic form of PD, the analysis was extended to two additional mouse models of PD, namely the *Pink1*KO and the A53T-SNCA + *Pink1*KO double-mutant mouse line. The analysis of PrPmtA single-mutant mice depicted increased mRNA level of glutamate receptor subunits and candidates genes involved in synaptic signaling as well as decreased expression level of immediate early genes and transcription factors in striatal and midbrain tissue at the age of 6 month compared to WT mice. In an effort to depict the earliest effects of alpha-synuclein gain-of-function, the qPCR analysis was extended to 3-month-old mice. This analysis showed, that among the earliest effects of alpha-synuclein gain-of-function are expression alterations for *Homer1*, *cFos*, *Nor1*, *Nurr1* and *Nur77*. These early findings can contribute to the early detection of PD pathogenesis and can help to assess progression versus therapeutic benefits. In double-mutant mice harboring both the A53T-SNCA overexpression as well as the *Pink1*KO, the analysis of the same candidate genes depicted only little effects on the expression of glutamate receptor subunits but those found regulated were significantly reduced in striatal or midbrain tissue of 6-month-old mice. The analysis of IEGs and transcription factors depicted reduced expression level in double-mutant mice compared to the respective wild-type control both in striatal and midbrain tissue. The qPCR analysis of striatal and midbrain tissue of 6-month-old *Pink1*KO mice showed only minor effects on glutamate receptor subunits, IEGs and transcription factors, highlighting the previously described expression alterations in PrPmtA and double-mutant mice to clearly depend on the alpha-synuclein gain-of-function.

The impact of alpha-synuclein gain-of-function on the behavioral and molecular response to apomorphine treatment

Previous studies within the PrPmtA mouse model that mimics presymptomatic stages of PD showed altered neurotransmission and LTD deficiency to be an early effect of alpha-synuclein gain-of-function. In order to study if presymptomatic stages of PD already involve altered postsynaptic sensitivity, that provides the basis of LID, a dopamine challenge was applied to 18-month-old PrPmtA mice. This experimental approach revealed increased involuntary movements with stereotypic and dystonic features in PrPmtA compared to WT mice after acute apomorphine administration. Thereafter, immunohistological analysis confirmed the behavioral alterations to be independent of neuronal dopaminergic cell loss. Further molecular characterization revealed an increased apomorphine dependent phosphorylation of ERK1/2 but no genotype dependent differences in mice sacrificed 30 min after apomorphine treatment. However, the same analysis in striatal tissue of mice sacrificed 100 min after apomorphine treatment revealed increased phospho-ERK1 level in PrPmtA compared to WT mice. In an effort to study downstream effects of this first hint of striatal postsynaptic sensitivity in a transgenic model of LID, phospho-histone H3 was analyzed using IHC. This analysis depicted increased phospho-histone H3 level in a very caudal region of the striatum in PrPmtA compared to WT mice after apomorphine treatment. Thereafter, alpha-synuclein gain-of-function effects on candidate genes that regulate the ERK1/2 pathway, in response to apomorphine treatment were studied at both previously mentioned time points. This analysis revealed increased apomorphine dependent expression level for *Dusp1*, *Dusp6* and *cFos* in both PrPmtA and WT mice but the only genotype dependent effect was observed for *cFos* showing increased expression level in PrPmtA compared to WT mice 30 min after apomorphine treatment. The analysis of striatal tissue dissected 100 min after treatment revealed again apomorphine dependent expression level, but most interestingly a genotype dependent increased expression of *Dusp1*, *Dusp6*, *cFos* and *Nur77* in PrPmtA compared to WT mice, giving a strong evidence of postsynaptic supersensitivity to dopamine receptor stimulation. Additional experiments highlighted the genotype dependent increased expression of *Dusp1*, *Dusp6* and *Nur77* to be striatum specific as well as specific to the dual-specific phosphatase family members 1 and 6.

This experimental approach uncovered the impact of alpha-synuclein dependent effects on the behavioral and molecular response to apomorphine. Thereafter, our data highlight the fundamental role of alpha-synuclein as modifier of neurotransmission and synaptic plasticity, supporting the PrPmtA mouse model to be an authentic novel model to study the presynaptic

dysfunction of early stages PD as well as the postsynaptic pathobiology of alpha-synuclein overexpression at the basis of LID.

Potential of alpha-synuclein gain-of-function effects in double-mutant mice with Pink1 ablation

Since most PD patients suffer from polygenic interactions rather than from a monogenic form of PD, as well as to clarify the role of PINK1 on alpha-synuclein dependent neurotoxicity, a mouse harboring both the A53T-SNCA overexpression as well as the *Pink1*KO was generated. This novel mouse line showed a potentiated phenotype with reduced spontaneous locomotor activity at the age of 3 month as well as a progressive hind limb paralysis in a relatively big cohort of double-mutant mice aged beyond 1 year. In respect to this strong phenotype, immunohistological characterisation of spinal cord and midbrain was performed. The histological analysis revealed aggregates in the gray matter of the anterior horn of the lumbar spinal cord as well as in a neuronal cell population dorsal of the substantia nigra that were positive for pSer129-SNCA, p62/SQSTM1 and ubiquitin in paralyzed double-mutant mice. The observed histological pattern that comprises morphological signs of neurodegeneration was shown to be specific to paralyzed double-mutant mice, whereas non-paralytic mice or single-mutant mice did not show aggregation or signs of neurodegeneration. In an effort to further characterize the cell population positive for pSer129-SNCA, p62/SQSTM1 and ubiquitin that was found dorsal to the substantia nigra, double-immunofluorescence was performed. This analysis proved the cell population to be of neuronal origin and most likely to be parvalbumin positive and therefore represents interneurons.

The histological data in line with the severe phenotypical abnormalities highlight this novel double-mutant model as a valuable tool to investigate molecular alterations and to identify underlying mechanisms and shared pathways that contribute to PD pathology. Additionally, this approach highlighted the role of PINK1 dependent neuroprotective response as potential target for novel beneficial therapeutics.

7. ZUSAMMENFASSUNG

Einleitung

Die Parkinson Erkrankung ist die zweithäufigste neurodegenerative Erkrankung nach der Alzheimer Erkrankung und betrifft etwa 0,3% der Bevölkerung in industrialisierten Ländern. Die Parkinson Erkrankung ist durch schwere Beeinträchtigungen des Bewegungsablaufes charakterisiert zu welchen Rigor, Bradykinese, Akinese, Tremor und posturale Instabilität zählen. Neben diesen charakteristischen Symptomen einer Parkinson Erkrankung geht diese auch mit Symptomen einher, welche unabhängig von Bewegungsstörungen auftreten, wie zum Beispiel Depression, kognitive Beeinträchtigungen, olfaktorische Dysfunktion, Angstzustände, REM-Schlafstörungen und viele andere. Der pathologische Prozess welcher für diese progressiven neurodegenerativen Erkrankung charakteristisch ist und zu den beschriebenen Bewegungsstörungen führt, ist der Verlust dopaminerger Neurone innerhalb der Substantia nigra, welches eine Reduktion des Dopamine Gehaltes im Striatum zur Folge hat. Die für die Parkinson Erkrankung typischen Bewegungsstörungen treten auf, wenn etwa 70% des ursprünglichen Dopamingehaltes im Striatum verloren sind. Das Striatum stellt die Haupteingangsstation der Basalganglien dar, einer wichtigen Hirnregion für gewohnheitsformendes und zielgerichtetes Verhalten. Bei dem Großteil der im Striatum befindlichen Neuronen handelt es sich um mittelgroß bedornte Projektionsneurone, die sogenannten MSNs. Der Basalganglien Schaltkreis besteht aus zwei Hauptschaltkreisen, dem direkten Signalweg welcher durch die Expression von D1 Rezeptoren gekennzeichnet ist sowie dem indirekten Signalwege, welcher durch D2 Rezeptoren exprimierende MSNs gekennzeichnet ist. Beide Signalwege sind simultan aktiv und agieren in einer aufeinander abgestimmten Weise um Aktivität entweder zu unterstützen oder zu unterdrücken. In an Parkinson erkrankten Patienten führt der reduzierte striatale Dopamin Spiegel auf der einen Seite zu einer Reduktion der Beweglichkeit und zum anderen zu morphologischen Veränderungen der MSNs.

Die Parkinson Erkrankung wurde über viele Jahre als eine rein sporadische Erkrankung angesehen. Erst mit der Entwicklung von neuen Techniken wie der genomweiten-Assoziationsstudie entwickelte sich ein Verständnis für genetische Komponenten einer Erkrankung. Mittels dieser Techniken konnten bereits mehrere Parkinson relevante Gene identifiziert werden, welche eine Beteiligung von mitochondrialer und lysosomaler Dysfunktion, Protein Aggregation und Degradation sowie von Kinase-Signalkaskaden an der Pathologie von Parkinson aufzeigen. Dennoch können nur 10% aller Parkinson Erkrankungen auf eines der beschriebenen Gene zurückgeführt werden und 90% der Erkrankungen treten sporadisch auf. Ein Schlüsselmolekül, welches zum einen mit idiopathischen aber auch mit spora-

dischen Erkrankungen assoziiert ist, ist alpha-Synuklein (SNCA). Mutationen welche einen Funktionsgewinn von alpha-Synuklein zur Folge haben konnten mit autosomal dominanten Varianten der Parkinson Erkrankung assoziiert werden und genetische Veränderungen an beiden Enden des *SNCA*-Gens agieren als Risikofaktor für sporadische Formen der Erkrankung. Des Weiteren wird alpha-Synuklein als Hauptbestandteil der Lewy Körperchen gefunden, einem weiteren pathologischen Kennzeichen der parkinsonschen Erkrankung. Lewy Körperchen lassen sich in den verbleibenden dopaminergen Neurone der Substantia nigra nachweisen und weisen daher darauf hin, dass Protein Aggregation möglicherweise eine kritische Rolle für die Pathologie von Parkinson spielt. Die komplette physiologische Funktion von alpha-Synuklein ist immer noch unverstanden, dennoch gibt es Anhaltspunkte für eine Funktion bei der Anordnung des SNARE-Komplexes, dem Transport von mit neurotransmitter angereicherten Vesikeln sowie der striatalen Dopamin Ausschüttung.

Die derzeit bekannten monogenen Fälle einer Parkinson Erkrankung werden entweder autosomal dominant oder autosomal rezessiv vererbt. Unter den Genen mit klarer autosomal dominanter Vererbung ist das zuvor beschriebene alpha-Synuklein zu finden. Unter den Genen mit rezessiver Vererbung findet sich die PTEN-induzierte Kinase 1 (PINK1), dessen Funktionsverlust mit einem frühen Erkrankungsausbruch von Parkinson in Verbindung gebracht wird. Studien konnten zeigen, dass PINK1 eine schützende Funktion bei stressinduzierter mitochondrialer Dysfunktion hat, und dass ein Funktionsverlust zu einer verminderten mitochondrialen Qualitätskontrolle sowie der Akkumulation von beschädigten Mitochondrien führt.

Die derzeitige Standardbehandlung der mit einer Parkinson Erkrankung einhergehenden Bewegungsstörungen stellt die Dopamin Ersatztherapie mittels L-DOPA, einer metabolischen Vorstufe von Dopamin, dar. Neben dem enorm positiven Effekt auf die Bewegungsstörungen der Parkinson Patienten, geht die Behandlung mit L-DOPA jedoch auch mit ernststen Nebenwirkungen einher, welche als Levodopa induzierte Dyskinesien (LID) beschrieben werden. Das aktuelle pathobiologische Konzept über die Hintergründe von LID besagt, dass diese auf prä- und postsynaptische Veränderungen der Dopamin Ausschüttung und Signalweiterleitung sowie auf Veränderungen der synaptischen Plastizität zurückzuführen ist. Auf der präsynaptischen Ebene konnten Studien in Nagetiermodellen und Patienten zeigen, dass abnormale unwillkürliche Bewegungen, welche ein charakteristisches Merkmal von LID darstellen, mit einer Fehlregulierung der Dopaminausschüttung sowie der Klärung einhergehen. Auf der postsynaptischen Ebene konnten diese Studien zeigen, dass LID mit Fehlanpassungen innerhalb des D1 Rezeptor positiven direkten Signalweges in striatalen MSNs einhergeht. Die für

striatale synaptische Plastizität entscheidende und damit auch für LID grundlegende Signalkaskade ist die extrazelluläre signalregulierte Kinase 1 und 2 Signalkaskade (ERK1/2).

Ziel der Arbeit

Das Ziel dieser Arbeit war

1. Die Analyse von Effekten des alpha-Synuklein Funktionsgewinns sowie des PINK1 Funktionsverlustes auf molekulare Signalwege der synaptischen Plastizität
2. Die Analyse der Auswirkung eines alpha-Synuklein Funktionsgewinns auf das Verhalten und auf molekulare Parameter nach Apomorphin Behandlung, sowie die Untersuchung ob das transgene Mausmodell PrPmtA ein nützliches Modell darstellt um postsynaptische Veränderungen der Signalweiterleitung, welchen LID zugrunde liegt, zu studieren.
3. Charakterisierung eines neuen Doppelmutanten-Mausmodells für die Parkinson Erkrankung und Analyse des Effekts von PINK1 auf die alpha-Synuklein induzierte Neurotoxizität.

Ergebnisse und Diskussion

Effekte des alpha-Synuklein Funktionsgewinns auf die Expression von Kandidatengen, welche eine Rolle für synaptische Plastizität spielen

Die Arbeit eines ehemaligen Doktoranden hatte die Funktion und Pathologie von alpha-Synuklein in einer hypothesenfreien Analyse mittels Microarray-Transkriptomprofilen zur Aufgabe. Diese Arbeit wurde in A53T-SNCA überexprimierenden Mäusen durchgeführt und zeigte molekulare Veränderungen, Veränderungen der Dopaminfreisetzung und verminderte synaptische Plastizität. Die hier beschriebene Studie wurde durchgeführt um die Rolle des alpha-Synuklein Funktionsgewinns für den LTD Prozess zu beschreiben und um weitere alpha-Synuklein abhängige Effekte im Striatum und Mittelhirn genauer zu charakterisieren. Zu diesem Zweck wurden Kandidatengene, welche eine Rolle für synaptische Plastizität spielen, in 6 Monate alten PrPmtA Mäusen untersucht. Da der Großteil der Parkinson Erkrankungen nicht auf ein Gen zurückzuführen ist sondern vielmehr polygene Interaktionen eine Rolle spielen, wurde die Analyse auf zwei weitere Mausmodelle für Parkinson erweitert. Bei diesen beiden Modellen handelt es sich zum einen um das bereits beschriebene *Pink1*KO Modell und zum anderen um das neue A53T-SNCA + *Pink1*KO Doppelmutanten-Mausmodell. Die Analyse der PrPmtA Einzelmutante ergab erhöhte mRNA Spiegel von Untereinheiten der Glutamatrezeptoren sowie von Kandidatengen welche eine Rolle bei der synaptischen Signalweiterlei-

tung spielen. Die mRNA Spiegel von unmittelbaren, früh aktivierten Genen den sogenannten „immediate early genes“ sowie von Transkriptionsfaktoren, wurden in Striatum- und Mittelhirn-Gewebe von 6 Monate alten PrPmtA Mäusen reduziert vorgefunden. In dem Bestreben die frühesten Effekte eines alpha-Synuklein Funktionsgewinns zu studieren, wurde die qPCR Analyse auf 3 Monate alte PrPmtA Mäuse ausgeweitet. Diese Analyse ergab, dass Expressionsveränderungen für *Homer1*, *cFos*, *Nor1*, *Nurr1* und *Nur77* zu den frühesten Effekten eines alpha-Synuklein Funktionsgewinns zählen, eine wichtige Erkenntnis die zur Früherkennung einer Parkinson Erkrankung beitragen kann und damit einen therapeutischen Vorteil liefert. In Doppelmutanten-Mäusen welche zum einen den alpha-Synuklein Funktionsgewinn und zum anderen einen PINK1 Funktionsverlust aufzeigen, zeigte die Expressionsanalyse nur wenige Veränderungen für Untereinheiten der Glutamatrezeptoren, die gefundenen Veränderungen zeigten jedoch reduzierte mRNA Spiegel in Striatum- und Mittelhirn-Gewebe 6 Monate alter Tiere auf. Die Analyse der unmittelbaren, früh aktivierten Gene sowie der Transkriptionsfaktoren ergab reduzierte Expressionsspiegel in Doppelmutanten-Mäusen im Vergleich zu Wildtyp-Kontrollen in beiden untersuchten Geweben. Die qPCR Analyse der *Pink1*KO Einzelmutante ergab nur minimale Veränderungen in 6 Monate altem Striatum und Mittelhirn-Gewebe, was den Schluss zulässt, dass die zuvor beschriebenen Expressionsveränderungen in PrPmtA und Doppelmutanten-Mäusen eindeutig auf den alpha-Synuklein Funktionsgewinn zurückzuführen sind.

Der Einfluss eines alpha-Synuklein Funktionsgewinns auf das Verhalten und auf molekulare Parameter nach Apomorphin Behandlung

Frühere Studien welche die PrPmtA Einzelmutante zur Grundlage hatten und damit ein präsymptomatisches Parkinsonmodell, zeigten eine veränderte Neurotransmission sowie Defizite in der Generierung von LTD als eine der frühen Effekte des alpha-Synuklein Funktionsgewinns. Um zu untersuchen ob ein präsymptomatisches Stadium der Parkinson Erkrankung bereits mit Veränderungen der postsynaptischen Sensibilität, der Grundlage für LID einhergeht, wurden 18 Monate alte Tiere einem Dopamin-Stress ausgesetzt. Dieser Versuchsansatz zeigte ein erhöhtes Niveau an unwillkürlichen Bewegungsmustern mit stereotypen und dystonischen Eigenschaften in PrPmtA Mäusen im Vergleich zu Wildtypen. In einem weiteren Versuch wurde mittels immunhistologischer Analysen bestätigt, dass diese Veränderungen im Verhaltensmuster unabhängig von einem neuronalen Zellverlust auftreten. Des Weiteren wurde eine molekulare Charakterisierung durchgeführt, welche eine erhöhten Apomorphin abhängige Phosphorylierung von ERK1/2 in PrPmtA und Wildtyp Mäusen aufzeigte, Genotyp abhängige Veränderungen konnten jedoch 30 Minuten nach Apomorphine Behandlung nicht

nachgewiesen werden. Die gleiche Analyse in Mäusen welche 100 Minuten nach Apomorphin Behandlung präpariert wurden, zeigte eine erhöhte Phosphorylierung von ERK1 in PrPmtA Mäusen. In einem Bestreben die nachgeschalteten Effekte dieses ersten Anzeichens für postsynaptische Sensibilität zu analysieren, wurde die Phosphorylierung von Histon H3 mittels IHC untersucht. Diese Analyse zeigte erhöhte Phospho-Histon H3 Spiegel in PrPmtA Mäusen im Vergleich zu Kontrolltieren in einem relativ caudalen Bereich des Striatums auf. Anschließend wurden Effekte des alpha-Synuklein Funktionsgewinns auf Kandidatengene welche an der Regulation der ERK1/2 Signalkaskade beteiligt sind, in Bezug auf ihre apomorphinabhängige Expression untersucht. Die Analyse von striatalem Hirngewebe, welches 30 Minuten nach Apomorphin Injektion entnommen wurde, ergab eine apomorphinabhängige erhöhte Expression von *Dusp1*, *Dusp6* und *cFos* in PrPmtA und Kontrolltieren, ein genotypabhängiger Expressionunterschied konnte nur für *cFos* aufgezeigt werden. Die Analyse von striatalem Gewebe, welches 100 Minuten nach Apomorphingabe präpariert wurde, ergab wieder eine apomorphinabhängige Expressionsinduktion für PrPmtA und Kontrolltiere, wirklich interessant war jedoch, dass diese genotypabhängig zu beobachten war. Die mRNA Spiegel von *Dusp1*, *Dusp6*, *cFos* und *Nur77* wurden erhöht in PrPmtA Tieren im Vergleich zu Wildtyp Kontrolltieren nachgewiesen, was ein starkes Indiz für postsynaptische Sensibilität nach Dopaminrezeptor Stimulation darstellt. Zusätzliche Experimente ergaben, dass der genotypabhängige erhöhte Expressionsspiegel von *Dusp1*, *Dusp6* und *Nur77* zum einen spezifisch für das Striatum und zum anderen spezifisch für die Mitglieder *Dusp1* und *Dusp6* der Genfamilie sind. Der hier beschriebene experimentelle Ansatz hat dazu beigetragen den Einfluss eines alpha-Synuklein Funktionsgewinns auf das Verhalten sowie auf molekulare Parameter nach Apomorphingabe aufzudecken. Des Weiteren unterstreichen unsere Daten die fundamentale Rolle von alpha-Synuklein auf die Neurotransmission sowie die synaptische Plastizität. Unsere Daten zeigen damit, dass unsere transgene PrPmtA Maus ein zuverlässiges Modell für die Analyse von präsynaptischer Dysfunktion in Frühstadien der Parkinson Erkrankung sowie der alpha-Synuklein abhängigen postsynaptischen Pathologie als Ursache von LID, darstellt.

Die Potenzierung der alpha-Synuklein Funktionsgewinn abhängigen Effekte in Doppelmutanten-Mäusen mit Pink1 Ablation

Da die meisten an Parkinson erkrankten Patienten nicht an einer monogenen Form der Erkrankung leiden sondern vielmehr unter polygenen Interaktionen verschiedener Einflüsse, wurde ein Mausmodell welches sowohl A53T-SNCA überexprimiert als auch einen PINK1 Funktionsverlust aufweist, generiert. Dieses Modell dient damit auch der genaueren Analyse von PINK1 abhängigen Effekten auf die alpha-Synuklein abhängige Neurotoxizität. Dieses

neue Mausmodell zeichnet sich durch einen verstärkten Phänotyp aus, welcher sich durch eine stark reduzierte Spontanmotorik im Alter von 3 Monaten sowie einer progressiven Lähmung der Hinterläufe zeigt. Auf Grund der starken phänotypischen Beobachtungen in diesem neuen Mausmodell wurde eine immunhistologische Charakterisierung mittels Schnitten des Gehirns und Rückenmarks durchgeführt. Die histologische Analyse zeigte pSer129-SNCA, p62/SQSTM1 und Ubiquitin positive Aggregate innerhalb der grauen Substanz des anterioren Horns im lumbalen Bereich des Rückenmarks sowie innerhalb einer neuronalen Zellpopulation, welche dorsal der Substantia nigra angeordnet ist. Das histologische Erscheinungsbild, welches morphologische Veränderungen und Anzeichen für Neurodegeneration aufwies, wurde spezifisch in gelähmten Doppelmutanten-Mäusen gefunden und nicht in Einzelmutanten oder Doppelmutanten-Tieren ohne Lähmung. Um die zuvor beschriebene Aggregate aufweisende Zellpopulation, welche dorsal der Substantia nigra beschrieben wurde, weiter zu charakterisieren wurden Doppelimmunfluoreszenz-Färbungen durchgeführt. Die Doppelimmunfluoreszenzanalyse konnte aufzeigen, dass es sich bei der gezeigten Zellgruppe sicher um Neurone handelt und am ehesten um Parvalbumin positive Interneurone.

Die histologischen Befunde und die phänotypischen Besonderheiten dieser Doppelmutanten-Mauslinie heben dieses neue Modell als wertvolles Instrument für die Identifizierung von pathologischen Mechanismen und Signalkaskaden welche beiden Parkinson relevanten Genen gemeinsam sind, hervor. Des Weiteren hebt dieser experimentelle Ansatz die PINK1-abhängigen, neuroprotektiven Mechanismen als möglichen Angriffspunkt für neue effektive Medikamente hervor.

8. REFERENCES

- Aamodt SM, Constantine-Paton M (1999) The role of neural activity in synaptic development and its implications for adult brain function. *Adv Neurol* 79:133-144.
- Aarsland D, Larsen JP, Lim NG, Janvin C, Karlsen K, Tandberg E, Cummings JL (1999) Range of neuropsychiatric disturbances in patients with Parkinson's disease. *J Neurol Neurosurg Psychiatry* 67:492-496.
- Abeliovich A, Schmitz Y, Farinas I, Choi-Lundberg D, Ho WH, Castillo PE, Shinsky N, Verdugo JM, Armanini M, Ryan A, Hynes M, Phillips H, Sulzer D, Rosenthal A (2000) Mice lacking alpha-synuclein display functional deficits in the nigrostriatal dopamine system. *Neuron* 25:239-252.
- Abou-Sleiman PM, Healy DG, Wood NW (2004) Causes of Parkinson's disease: genetics of DJ-1. *Cell Tissue Res* 318:185-188.
- Ahlskog JE (2005) Challenging conventional wisdom: the etiologic role of dopamine oxidative stress in Parkinson's disease. *Mov Disord* 20:271-282.
- Ahlskog JE, Muentner MD (2001) Frequency of levodopa-related dyskinesias and motor fluctuations as estimated from the cumulative literature. *Mov Disord* 16:448-458.
- Ahmad M, Attoub S, Singh MN, Martin FL, El-Agnaf OM (2007) Gamma-synuclein and the progression of cancer. *FASEB J* 21:3419-3430.
- Ahmed I, Liang Y, Schools S, Dawson VL, Dawson TM, Savitt JM (2012) Development and characterization of a new Parkinson's disease model resulting from impaired autophagy. *J Neurosci* 32:16503-16509.
- Ahn S, Ginty DD, Linden DJ (1999) A late phase of cerebellar long-term depression requires activation of CaMKIV and CREB. *Neuron* 23:559-568.
- Albin RL, Young AB, Penney JB (1989) The functional anatomy of basal ganglia disorders. *Trends Neurosci* 12:366-375.
- Alimova-Kost MV, Ninkina NN, Imreh S, Gnuchev NV, Adu J, Davies AM, Buchman VL (1999) Genomic structure and chromosomal localization of the mouse *persyn* gene. *Genomics* 56:224-227.
- Allen W (1937) Inheritance of the shaking palsy. *Arch Int Med* 60:424-436.
- Anderson JP, Walker DE, Goldstein JM, de Laat R, Banducci K, Caccavello RJ, Barbour R, Huang J, Kling K, Lee M, Diep L, Keim PS, Shen X, Chataway T, Schlossmacher MG, Seubert P, Schenk D, Sinha S, Gai WP, Chilcote TJ (2006) Phosphorylation of Ser-129 is the dominant pathological modification of alpha-synuclein in familial and sporadic Lewy body disease. *J Biol Chem* 281:29739-29752.
- Andersson M, Hilbertson A, Cenci MA (1999) Striatal fosB expression is causally linked with L-DOPA-induced abnormal involuntary movements and the associated upregulation of striatal prodynorphin mRNA in a rat model of Parkinson's disease. *Neurobiol Dis* 6:461-474.
- Angot E, Brundin P (2009) Dissecting the potential molecular mechanisms underlying alpha-synuclein cell-to-cell transfer in Parkinson's disease. *Parkinsonism Relat Disord* 15 Suppl 3:S143-147.
- Apaydin H, Ahlskog JE, Parisi JE, Boeve BF, Dickson DW (2002) Parkinson disease neuropathology: later-developing dementia and loss of the levodopa response. *Arch Neurol* 59:102-112.
- Appel-Cresswell S, Vilarino-Guell C, Encarnacion M, Sherman H, Yu I, Shah B, Weir D, Thompson C, Szu-Tu C, Trinh J, Aasly JO, Rajput A, Rajput AH, Jon Stoessl A, Farrer MJ (2013) Alpha-synuclein p.H50Q, a novel pathogenic mutation for Parkinson's disease. *Mov Disord* 28:811-813.

- Arai R, Karasawa N, Geffard M, Nagatsu I (1995) L-DOPA is converted to dopamine in serotonergic fibers of the striatum of the rat: a double-labeling immunofluorescence study. *Neurosci Lett* 195:195-198.
- Arai R, Karasawa N, Geffard M, Nagatsu T, Nagatsu I (1994) Immunohistochemical evidence that central serotonin neurons produce dopamine from exogenous L-DOPA in the rat, with reference to the involvement of aromatic L-amino acid decarboxylase. *Brain Res* 667:295-299.
- Arai R, Karasawa N, Nagatsu I (1996) Aromatic L-amino acid decarboxylase is present in serotonergic fibers of the striatum of the rat. A double-labeling immunofluorescence study. *Brain Res* 706:177-179.
- Arbuthnott GW, Ingham CA, Wickens JR (2000) Dopamine and synaptic plasticity in the neostriatum. *J Anat* 196 (Pt 4):587-596.
- Arnold J, Dawson S, Fergusson J, Lowe J, Landon M, Mayer RJ (1998) Ubiquitin and its role in neurodegeneration. *Prog Brain Res* 117:23-34.
- Atkins CM, Selcher JC, Petraitis JJ, Trzaskos JM, Sweatt JD (1998) The MAPK cascade is required for mammalian associative learning. *Nat Neurosci* 1:602-609.
- Aubert I, Guigoni C, Hakansson K, Li Q, Dovero S, Barthe N, Bioulac BH, Gross CE, Fisone G, Bloch B, Bezard E (2005) Increased D1 dopamine receptor signaling in levodopa-induced dyskinesia. *Ann Neurol* 57:17-26.
- Bagetta V, Ghiglieri V, Sgobio C, Calabresi P, Picconi B (2010) Synaptic dysfunction in Parkinson's disease. *Biochem Soc Trans* 38:493-497.
- Barbour R, Kling K, Anderson JP, Banducci K, Cole T, Diep L, Fox M, Goldstein JM, Soriano F, Seubert P, Chilcote TJ (2008) Red blood cells are the major source of alpha-synuclein in blood. *Neurodegener Dis* 5:55-59.
- Bartels T, Choi JG, Selkoe DJ (2011) alpha-Synuclein occurs physiologically as a helically folded tetramer that resists aggregation. *Nature* 477:107-110.
- Bats C, Groc L, Choquet D (2007) The interaction between Stargazin and PSD-95 regulates AMPA receptor surface trafficking. *Neuron* 53:719-734.
- Beal MF (1995) Aging, energy, and oxidative stress in neurodegenerative diseases. *Ann Neurol* 38:357-366.
- Beilina A, Van Der Brug M, Ahmad R, Kesavapany S, Miller DW, Petsko GA, Cookson MR (2005) Mutations in PTEN-induced putative kinase 1 associated with recessive parkinsonism have differential effects on protein stability. *Proc Natl Acad Sci U S A* 102:5703-5708.
- Beneyto M, Meador-Woodruff JH (2004) Expression of transcripts encoding AMPA receptor subunits and associated postsynaptic proteins in the macaque brain. *J Comp Neurol* 468:530-554.
- Berman DM, Wilkie TM, Gilman AG (1996) GAIP and RGS4 are GTPase-activating proteins for the Gi subfamily of G protein alpha subunits. *Cell* 86:445-452.
- Bernheimer H, Birkmayer W, Hornykiewicz O, Jellinger K, Seitelberger F (1973) Brain dopamine and the syndromes of Parkinson and Huntington. Clinical, morphological and neurochemical correlations. *J Neurol Sci* 20:415-455.
- Berridge MJ (1993) Inositol trisphosphate and calcium signalling. *Nature* 361:315-325.
- Bertler A, Falck B, Owman C, Rosengrenn E (1966) The localization of monoaminergic blood-brain barrier mechanisms. *Pharmacol Rev* 18:369-385.
- Bertoncini CW, Fernandez CO, Griesinger C, Jovin TM, Zweckstetter M (2005) Familial mutants of alpha-synuclein with increased neurotoxicity have a destabilized conformation. *J Biol Chem* 280:30649-30652.
- Beyer K (2006) Alpha-synuclein structure, posttranslational modification and alternative splicing as aggregation enhancers. *Acta Neuropathol* 112:237-251.

- Beyer K, Domingo-Sabat M, Santos C, Tolosa E, Ferrer I, Ariza A (2010) The decrease of beta-synuclein in cortical brain areas defines a molecular subgroup of dementia with Lewy bodies. *Brain* 133:3724-3733.
- Bezard E, Gross CE, Qin L, Gurevich VV, Benovic JL, Gurevich EV (2005) L-DOPA reverses the MPTP-induced elevation of the arrestin2 and GRK6 expression and enhanced ERK activation in monkey brain. *Neurobiol Dis* 18:323-335.
- Bjorkoy G, Lamark T, Brech A, Outzen H, Perander M, Overvatn A, Stenmark H, Johansen T (2005) p62/SQSTM1 forms protein aggregates degraded by autophagy and has a protective effect on huntingtin-induced cell death. *J Cell Biol* 171:603-614.
- Bliss TV, Collingridge GL (1993) A synaptic model of memory: long-term potentiation in the hippocampus. *Nature* 361:31-39.
- Bohus B, Koolhaas JM, Luiten PG, Korte SM, Roozendaal B, Wiersma A (1996) The neurobiology of the central nucleus of the amygdala in relation to neuroendocrine and autonomic outflow. *Prog Brain Res* 107:447-460.
- Boka G, Anglade P, Wallach D, Javoy-Agid F, Agid Y, Hirsch EC (1994) Immunocytochemical analysis of tumor necrosis factor and its receptors in Parkinson's disease. *Neurosci Lett* 172:151-154.
- Boldingh Debernard KA, Mathisen GH, Paulsen RE (2012) Differences in NGFI-B, Nurr1, and NOR-1 expression and nucleocytoplasmic translocation in glutamate-treated neurons. *Neurochem Int* 61:79-88.
- Bonifati V, Rizzu P, van Baren MJ, Schaap O, Breedveld GJ, Krieger E, Dekker MC, Squitieri F, Ibanez P, Joosse M, van Dongen JW, Vanacore N, van Swieten JC, Brice A, Meco G, van Duijn CM, Oostra BA, Heutink P (2003) Mutations in the DJ-1 gene associated with autosomal recessive early-onset parkinsonism. *Science* 299:256-259.
- Bozon B, Davis S, Laroche S (2002) Regulated transcription of the immediate-early gene Zif268: mechanisms and gene dosage-dependent function in synaptic plasticity and memory formation. *Hippocampus* 12:570-577.
- Braak H (1980) *Architectonics of the Human Telencephalic Cortex*: Springer Berlin Heidelberg.
- Braak H, Bohl JR, Muller CM, Rub U, de Vos RA, Del Tredici K (2006) Stanley Fahn Lecture 2005: The staging procedure for the inclusion body pathology associated with sporadic Parkinson's disease reconsidered. *Mov Disord* 21:2042-2051.
- Braak H, Braak E (1986) Nuclear configuration and neuronal types of the nucleus niger in the brain of the human adult. *Hum Neurobiol* 5:71-82.
- Braak H, Braak E, Yilmazer D, de Vos RA, Jansen EN, Bohl J, Jellinger K (1994) Amygdala pathology in Parkinson's disease. *Acta Neuropathol* 88:493-500.
- Braak H, Del Tredici K (2004) Poor and protracted myelination as a contributory factor to neurodegenerative disorders. *Neurobiol Aging* 25:19-23.
- Braak H, Del Tredici K, Rub U, de Vos RA, Jansen Steur EN, Braak E (2003) Staging of brain pathology related to sporadic Parkinson's disease. *Neurobiol Aging* 24:197-211.
- Braak H, Ghebremedhin E, Rub U, Bratzke H, Del Tredici K (2004) Stages in the development of Parkinson's disease-related pathology. *Cell Tissue Res* 318:121-134.
- Braak H, Rub U, Jansen Steur EN, Del Tredici K, de Vos RA (2005) Cognitive status correlates with neuropathologic stage in Parkinson disease. *Neurology* 64:1404-1410.
- Braak H, Rub U, Sandmann-Keil D, Gai WP, de Vos RA, Jansen Steur EN, Arai K, Braak E (2000) Parkinson's disease: affection of brain stem nuclei controlling premotor and motor neurons of the somatomotor system. *Acta Neuropathol* 99:489-495.
- Braak H, Thal DR, Del Tredici K (2011) Nerve cells immunoreactive for p62 in select hypothalamic and brainstem nuclei of controls and Parkinson's disease cases. *J Neural Transm* 118:809-819.

- Brakeman PR, Lanahan AA, O'Brien R, Roche K, Barnes CA, Huganir RL, Worley PF (1997) Homer: a protein that selectively binds metabotropic glutamate receptors. *Nature* 386:284-288.
- Brambilla R, Gnesutta N, Minichiello L, White G, Roylance AJ, Herron CE, Ramsey M, Wolfer DP, Cestari V, Rossi-Arnaud C, Grant SG, Chapman PF, Lipp HP, Sturani E, Klein R (1997) A role for the Ras signalling pathway in synaptic transmission and long-term memory. *Nature* 390:281-286.
- Brami-Cherrier K, Valjent E, Herve D, Darragh J, Corvol JC, Pages C, Arthur SJ, Girault JA, Caboche J (2005) Parsing molecular and behavioral effects of cocaine in mitogen- and stress-activated protein kinase-1-deficient mice. *J Neurosci* 25:11444-11454.
- Breger LS, Dunnett SB, Lane EL (2013) Comparison of rating scales used to evaluate L-DOPA-induced dyskinesia in the 6-OHDA lesioned rat. *Neurobiol Dis* 50:142-150.
- Brenz Verca MS, Bahi A, Boyer F, Wagner GC, Dreyer JL (2003) Distribution of alpha- and gamma-synucleins in the adult rat brain and their modification by high-dose cocaine treatment. *Eur J Neurosci* 18:1923-1938.
- Brotchie J, Jenner P (2011) New approaches to therapy. *Int Rev Neurobiol* 98:123-150.
- Buchman VL, Adu J, Pinon LG, Ninkina NN, Davies AM (1998) Persyn, a member of the synuclein family, influences neurofilament network integrity. *Nat Neurosci* 1:101-103.
- Burnashev N, Zhou Z, Neher E, Sakmann B (1995) Fractional calcium currents through recombinant GluR channels of the NMDA, AMPA and kainate receptor subtypes. *J Physiol* 485 (Pt 2):403-418.
- Burre J, Sharma M, Tsetsenis T, Buchman V, Etherton MR, Sudhof TC (2010) Alpha-synuclein promotes SNARE-complex assembly in vivo and in vitro. *Science* 329:1663-1667.
- Burre J, Vivona S, Diao J, Sharma M, Brunger AT, Sudhof TC (2013) Properties of native brain alpha-synuclein. *Nature* 498:E4-6; discussion E6-7.
- Cabin DE, Shimazu K, Murphy D, Cole NB, Gottschalk W, McIlwain KL, Orrison B, Chen A, Ellis CE, Paylor R, Lu B, Nussbaum RL (2002) Synaptic vesicle depletion correlates with attenuated synaptic responses to prolonged repetitive stimulation in mice lacking alpha-synuclein. *J Neurosci* 22:8797-8807.
- Calabresi P, Centonze D, Bernardi G (2000) Electrophysiology of dopamine in normal and denervated striatal neurons. *Trends Neurosci* 23:S57-63.
- Calabresi P, Maj R, Mercuri NB, Bernardi G (1992a) Coactivation of D1 and D2 dopamine receptors is required for long-term synaptic depression in the striatum. *Neurosci Lett* 142:95-99.
- Calabresi P, Maj R, Pisani A, Mercuri NB, Bernardi G (1992b) Long-term synaptic depression in the striatum: physiological and pharmacological characterization. *J Neurosci* 12:4224-4233.
- Calabresi P, Mercuri NB, Sancesario G, Bernardi G (1993) Electrophysiology of dopamine-denervated striatal neurons. Implications for Parkinson's disease. *Brain* 116 (Pt 2):433-452.
- Calabresi P, Picconi B, Tozzi A, Di Filippo M (2007) Dopamine-mediated regulation of corticostriatal synaptic plasticity. *Trends Neurosci* 30:211-219.
- Calabresi P, Picconi B, Tozzi A, Ghiglieri V, Di Filippo M (2014) Direct and indirect pathways of basal ganglia: a critical reappraisal. *Nat Neurosci* 17:1022-1030.
- Calabresi P, Pisani A, Mercuri NB, Bernardi G (1992c) Long-term Potentiation in the Striatum is Unmasked by Removing the Voltage-dependent Magnesium Block of NMDA Receptor Channels. *Eur J Neurosci* 4:929-935.
- Calabresi P, Pisani A, Mercuri NB, Bernardi G (1994) Post-receptor mechanisms underlying striatal long-term depression. *J Neurosci* 14:4871-4881.
- Calabresi P, Pisani A, Mercuri NB, Bernardi G (1996) The corticostriatal projection: from synaptic plasticity to dysfunctions of the basal ganglia. *Trends Neurosci* 19:19-24.

- Carroll RC, Beattie EC, Xia H, Luscher C, Altschuler Y, Nicoll RA, Malenka RC, von Zastrow M (1999) Dynamin-dependent endocytosis of ionotropic glutamate receptors. *Proc Natl Acad Sci U S A* 96:14112-14117.
- Cartmell J, Salhoff CR, Perry KW, Monn JA, Schoepp DD (2000) Dopamine and 5-HT turnover are increased by the mGlu2/3 receptor agonist LY379268 in rat medial prefrontal cortex, nucleus accumbens and striatum. *Brain Res* 887:378-384.
- Caunt CJ, Keyse SM (2013) Dual-specificity MAP kinase phosphatases (MKPs): shaping the outcome of MAP kinase signalling. *Febs J* 280:489-504.
- Celio MR, Heizmann CW (1981) Calcium-binding protein parvalbumin as a neuronal marker. *Nature* 293:300-302.
- Cenci MA (2007) Dopamine dysregulation of movement control in L-DOPA-induced dyskinesia. *Trends Neurosci* 30:236-243.
- Cenci MA (2014) Glutamatergic pathways as a target for the treatment of dyskinesias in Parkinson's disease. *Biochem Soc Trans* 42:600-604.
- Cenci MA, Campbell K, Wictorin K, Bjorklund A (1992) Striatal c-fos Induction by Cocaine or Apomorphine Occurs Preferentially in Output Neurons Projecting to the Substantia Nigra in the Rat. *Eur J Neurosci* 4:376-380.
- Cenci MA, Lee CS, Bjorklund A (1998) L-DOPA-induced dyskinesia in the rat is associated with striatal overexpression of prodynorphin- and glutamic acid decarboxylase mRNA. *Eur J Neurosci* 10:2694-2706.
- Cenci MA, Lundblad M (2006) Post- versus presynaptic plasticity in L-DOPA-induced dyskinesia. *J Neurochem* 99:381-392.
- Cenci MA, Ohlin KE, Rylander D (2009) Plastic effects of L-DOPA treatment in the basal ganglia and their relevance to the development of dyskinesia. *Parkinsonism Relat Disord* 15 Suppl 3:S59-63.
- Cenci MA, Whishaw IQ, Schallert T (2002) Animal models of neurological deficits: how relevant is the rat? *Nat Rev Neurosci* 3:574-579.
- Centonze D, Gubellini P, Picconi B, Calabresi P, Giacomini P, Bernardi G (1999) Unilateral dopamine denervation blocks corticostriatal LTP. *J Neurophysiol* 82:3575-3579.
- Cepeda C, Andre VM, Yamazaki I, Wu N, Kleiman-Weiner M, Levine MS (2008) Differential electrophysiological properties of dopamine D1 and D2 receptor-containing striatal medium-sized spiny neurons. *Eur J Neurosci* 27:671-682.
- Cepeda C, Hurst RS, Altemus KL, Flores-Hernandez J, Calvert CR, Jokel ES, Grandy DK, Low MJ, Rubinstein M, Ariano MA, Levine MS (2001) Facilitated glutamatergic transmission in the striatum of D2 dopamine receptor-deficient mice. *J Neurophysiol* 85:659-670.
- Charbonnier-Beaupel F, Malerbi M, Alcacer C, Tahiri K, Carpentier W, Wang C, Doring M, Xu D, Worley PF, Girault JA, Herve D, Corvol JC (2015) Gene Expression Analyses Identify Narp Contribution in the Development of L-DOPA-Induced Dyskinesia. *J Neurosci* 35:96-111.
- Charpier S, Deniau JM (1997) In vivo activity-dependent plasticity at cortico-striatal connections: evidence for physiological long-term potentiation. *Proc Natl Acad Sci U S A* 94:7036-7040.
- Chartier-Harlin MC, Kachergus J, Roumier C, Mouroux V, Douay X, Lincoln S, Levecque C, Larvor L, Andrieux J, Hulihan M, Waucquier N, Defebvre L, Amouyel P, Farrer M, Destee A (2004) Alpha-synuclein locus duplication as a cause of familial Parkinson's disease. *Lancet* 364:1167-1169.
- Chen H, Zhang SM, Hernan MA, Schwarzschild MA, Willett WC, Colditz GA, Speizer FE, Ascherio A (2003) Nonsteroidal anti-inflammatory drugs and the risk of Parkinson disease. *Arch Neurol* 60:1059-1064.
- Chen L, Feany MB (2005) Alpha-synuclein phosphorylation controls neurotoxicity and inclusion formation in a Drosophila model of Parkinson disease. *Nat Neurosci* 8:657-663.

- Chen N, Moshaver A, Raymond LA (1997) Differential sensitivity of recombinant N-methyl-D-aspartate receptor subtypes to zinc inhibition. *Mol Pharmacol* 51:1015-1023.
- Chen X, de Silva HA, Pettenati MJ, Rao PN, St George-Hyslop P, Roses AD, Xia Y, Horsburgh K, Ueda K, Saitoh T (1995) The human NACP/alpha-synuclein gene: chromosome assignment to 4q21.3-q22 and TaqI RFLP analysis. *Genomics* 26:425-427.
- Cheung P, Tanner KG, Cheung WL, Sassone-Corsi P, Denu JM, Allis CD (2000) Synergistic coupling of histone H3 phosphorylation and acetylation in response to epidermal growth factor stimulation. *Mol Cell* 5:905-915.
- Choi DW, Maulucci-Gedde M, Kriegstein AR (1987) Glutamate neurotoxicity in cortical cell culture. *J Neurosci* 7:357-368.
- Choi S, Lovinger DM (1997a) Decreased frequency but not amplitude of quantal synaptic responses associated with expression of corticostriatal long-term depression. *J Neurosci* 17:8613-8620.
- Choi S, Lovinger DM (1997b) Decreased probability of neurotransmitter release underlies striatal long-term depression and postnatal development of corticostriatal synapses. *Proc Natl Acad Sci U S A* 94:2665-2670.
- Chu Y, Le W, Kompoliti K, Jankovic J, Mufson EJ, Kordower JH (2006) Nurr1 in Parkinson's disease and related disorders. *J Comp Neurol* 494:495-514.
- Chung ES, Chung YC, Bok E, Baik HH, Park ES, Park JY, Yoon SH, Jin BK (2010a) Fluoxetine prevents LPS-induced degeneration of nigral dopaminergic neurons by inhibiting microglia-mediated oxidative stress. *Brain Res* 1363:143-150.
- Chung YC, Kim SR, Jin BK (2010b) Paroxetine prevents loss of nigrostriatal dopaminergic neurons by inhibiting brain inflammation and oxidative stress in an experimental model of Parkinson's disease. *J Immunol* 185:1230-1237.
- Chwang WB, Arthur JS, Schumacher A, Sweatt JD (2007) The nuclear kinase mitogen- and stress-activated protein kinase 1 regulates hippocampal chromatin remodeling in memory formation. *J Neurosci* 27:12732-12742.
- Clarke RJ, Glasgow NG, Johnson JW (2013) Mechanistic and structural determinants of NMDA receptor voltage-dependent gating and slow Mg²⁺ unblock. *J Neurosci* 33:4140-4150.
- Clarke RJ, Johnson JW (2006) NMDA receptor NR2 subunit dependence of the slow component of magnesium unblock. *J Neurosci* 26:5825-5834.
- Clarke RJ, Johnson JW (2008) Voltage-dependent gating of NR1/2B NMDA receptors. *J Physiol* 586:5727-5741.
- Collingridge GL, Isaac JT, Wang YT (2004) Receptor trafficking and synaptic plasticity. *Nat Rev Neurosci* 5:952-962.
- Collins LM, O'Keefe GW, Long-Smith CM, Wyatt SL, Sullivan AM, Toulouse A, Nolan YM (2013) Mitogen-activated protein kinase phosphatase (MKP)-1 as a neuroprotective agent: promotion of the morphological development of midbrain dopaminergic neurons. *Neuromolecular Med* 15:435-446.
- Conquet F, Bashir ZI, Davies CH, Daniel H, Ferraguti F, Bordi F, Franz-Bacon K, Reggiani A, Matarese V, Conde F, et al. (1994) Motor deficit and impairment of synaptic plasticity in mice lacking mGluR1. *Nature* 372:237-243.
- Constantinidis J, Bartholini G, Tissot R, Pletscher A (1968) Accumulation of dopamine in the parenchyma after decarboxylase inhibition in the capillaries of brain. *Experientia* 24:130-131.
- Corsini GU, Del Zompo M, Gessa GL, Mangoni A (1979) Therapeutic efficacy of apomorphine combined with an extracerebral inhibitor of dopamine receptors in Parkinson's disease. *Lancet* 1:954-956.
- Corti O, Lesage S, Brice A (2011) What genetics tells us about the causes and mechanisms of Parkinson's disease. *Physiol Rev* 91:1161-1218.

- Craiu A, Gaczynska M, Akopian T, Gramm CF, Fenteany G, Goldberg AL, Rock KL (1997) Lactacystin and clasto-lactacystin beta-lactone modify multiple proteasome beta-subunits and inhibit intracellular protein degradation and major histocompatibility complex class I antigen presentation. *J Biol Chem* 272:13437-13445.
- Crow T, Xue-Bian JJ, Siddiqi V, Kang Y, Neary JT (1998) Phosphorylation of mitogen-activated protein kinase by one-trial and multi-trial classical conditioning. *J Neurosci* 18:3480-3487.
- Cui G, Jun SB, Jin X, Pham MD, Vogel SS, Lovinger DM, Costa RM (2013) Concurrent activation of striatal direct and indirect pathways during action initiation. *Nature* 494:238-242.
- Curtius HC, Niederwieser A, Levine R, Muldner H (1984) Therapeutic efficacy of tetrahydrobiopterin in Parkinson's disease. *Adv Neurol* 40:463-466.
- da Costa CA, Masliah E, Checler F (2003) Beta-synuclein displays an antiapoptotic p53-dependent phenotype and protects neurons from 6-hydroxydopamine-induced caspase 3 activation: cross-talk with alpha-synuclein and implication for Parkinson's disease. *J Biol Chem* 278:37330-37335.
- Dalfo E, Ferrer I (2005) Alpha-synuclein binding to rab3a in multiple system atrophy. *Neurosci Lett* 380:170-175.
- Damier P, Hirsch EC, Agid Y, Graybiel AM (1999) The substantia nigra of the human brain. II. Patterns of loss of dopamine-containing neurons in Parkinson's disease. *Brain* 122 (Pt 8):1437-1448.
- Daniel SE, Hawkes CH (1992) Preliminary diagnosis of Parkinson's disease by olfactory bulb pathology. *Lancet* 340:186.
- Darmopil S, Martin AB, De Diego IR, Ares S, Moratalla R (2009) Genetic inactivation of dopamine D1 but not D2 receptors inhibits L-DOPA-induced dyskinesia and histone activation. *Biol Psychiatry* 66:603-613.
- Day M, Wang Z, Ding J, An X, Ingham CA, Shering AF, Wokosin D, Ilijic E, Sun Z, Sampson AR, Mugnaini E, Deutch AY, Sesack SR, Arbuthnott GW, Surmeier DJ (2006) Selective elimination of glutamatergic synapses on striatopallidal neurons in Parkinson disease models. *Nat Neurosci* 9:251-259.
- de Bartolomeis A, Fiore G (2004) Postsynaptic density scaffolding proteins at excitatory synapse and disorders of synaptic plasticity: implications for human behavior pathologies. *Int Rev Neurobiol* 59:221-254.
- de Lau LM, Breteler MM (2006) Epidemiology of Parkinson's disease. *Lancet Neurol* 5:525-535.
- de Rijk MC, Breteler MM, Graveland GA, Ott A, Grobbee DE, van der Meche FG, Hofman A (1995) Prevalence of Parkinson's disease in the elderly: the Rotterdam Study. *Neurology* 45:2143-2146.
- de Rijk MC, Tzourio C, Breteler MM, Dartigues JF, Amaducci L, Lopez-Pousa S, Manubens-Bertran JM, Alperovitch A, Rocca WA (1997) Prevalence of parkinsonism and Parkinson's disease in Europe: the EUROPARKINSON Collaborative Study. European Community Concerted Action on the Epidemiology of Parkinson's disease. *J Neurol Neurosurg Psychiatry* 62:10-15.
- Deak M, Clifton AD, Lucocq LM, Alessi DR (1998) Mitogen- and stress-activated protein kinase-1 (MSK1) is directly activated by MAPK and SAPK2/p38, and may mediate activation of CREB. *EMBO J* 17:4426-4441.
- Deas E, Plun-Favreau H, Gandhi S, Desmond H, Kjaer S, Loh SH, Renton AE, Harvey RJ, Whitworth AJ, Martins LM, Abramov AY, Wood NW (2011) PINK1 cleavage at position A103 by the mitochondrial protease PARL. *Hum Mol Genet* 20:867-879.
- Decressac M, Kadkhodaei B, Mattsson B, Laguna A, Perlmann T, Bjorklund A (2012) alpha-Synuclein-induced down-regulation of Nurr1 disrupts GDNF signaling in nigral dopamine neurons. *Sci Transl Med* 4:163ra156.

- Del Tredici K, Braak H (2012) Spinal cord lesions in sporadic Parkinson's disease. *Acta Neuropathol* 124:643-664.
- Del Tredici K, Rub U, De Vos RA, Bohl JR, Braak H (2002) Where does parkinson disease pathology begin in the brain? *J Neuropathol Exp Neurol* 61:413-426.
- DeMartino GN, Slaughter CA (1999) The proteasome, a novel protease regulated by multiple mechanisms. *J Biol Chem* 274:22123-22126.
- Desmond NL, Levy WB (1990) Morphological correlates of long-term potentiation imply the modification of existing synapses, not synaptogenesis, in the hippocampal dentate gyrus. *Synapse* 5:139-143.
- Deumens R, Blokland A, Prickaerts J (2002) Modeling Parkinson's disease in rats: an evaluation of 6-OHDA lesions of the nigrostriatal pathway. *Exp Neurol* 175:303-317.
- Dickson DW, Ruan D, Crystal H, Mark MH, Davies P, Kress Y, Yen SH (1991) Hippocampal degeneration differentiates diffuse Lewy body disease (DLBD) from Alzheimer's disease: light and electron microscopic immunocytochemistry of CA2-3 neurites specific to DLBD. *Neurology* 41:1402-1409.
- DiFiglia M, Sapp E, Chase KO, Davies SW, Bates GP, Vonsattel JP, Aronin N (1997) Aggregation of huntingtin in neuronal intranuclear inclusions and dystrophic neurites in brain. *Science* 277:1990-1993.
- Dipasquale B, Marini AM, Youle RJ (1991) Apoptosis and DNA degradation induced by 1-methyl-4-phenylpyridinium in neurons. *Biochem Biophys Res Commun* 181:1442-1448.
- Doble A (1999) The role of excitotoxicity in neurodegenerative disease: implications for therapy. *Pharmacol Ther* 81:163-221.
- Doty RL (2012) Olfactory dysfunction in Parkinson disease. *Nat Rev Neurol* 8:329-339.
- Dube L, Smith AD, Bolam JP (1988) Identification of synaptic terminals of thalamic or cortical origin in contact with distinct medium-size spiny neurons in the rat neostriatum. *J Comp Neurol* 267:455-471.
- Dunn KL, Espino PS, Drobic B, He S, Davie JR (2005) The Ras-MAPK signal transduction pathway, cancer and chromatin remodeling. *Biochem Cell Biol* 83:1-14.
- Duvoisin RC, Mytilineou C (1978) Where is L-DOPA decarboxylated in the striatum after 6-hydroxydopamine nigrotomy? *Brain Res* 152:369-373.
- Eadie MJ (1963) THE PATHOLOGY OF CERTAIN MEDULLARY NUCLEI IN PARKINSONISM. *Brain* 86:781-792.
- El-Agnaf OM, Jakes R, Curran MD, Wallace A (1998) Effects of the mutations Ala30 to Pro and Ala53 to Thr on the physical and morphological properties of alpha-synuclein protein implicated in Parkinson's disease. *FEBS Lett* 440:67-70.
- El Atifi-Borel M, Buggia-Prevot V, Platet N, Benabid AL, Berger F, Sgambato-Faure V (2009) De novo and long-term l-Dopa induce both common and distinct striatal gene profiles in the hemiparkinsonian rat. *Neurobiol Dis* 34:340-350.
- Elias S. IZ, Bergman H. (2008) Physiology of Parkinson's Disease. In: *Therapeutics of Parkinson's Disease and Other Movement Disorders* (Hallett, M. P., W., ed), p 501: John Wiley & Sons.
- Eliezer D, Kutluay E, Bussell R, Jr., Browne G (2001) Conformational properties of alpha-synuclein in its free and lipid-associated states. *J Mol Biol* 307:1061-1073.
- English JD, Sweatt JD (1996) Activation of p42 mitogen-activated protein kinase in hippocampal long term potentiation. *J Biol Chem* 271:24329-24332.
- Erreger K, Geballe MT, Kristensen A, Chen PE, Hansen KB, Lee CJ, Yuan H, Le P, Lyuboslavsky PN, Micale N, Jorgensen L, Clausen RP, Wyllie DJ, Snyder JP, Traynelis SF (2007) Subunit-specific agonist activity at NR2A-, NR2B-, NR2C-, and NR2D-containing N-methyl-D-aspartate glutamate receptors. *Mol Pharmacol* 72:907-920.
- Fahn S (2003) Description of Parkinson's disease as a clinical syndrome. *Ann N Y Acad Sci* 991:1-14.

- Fall PA, Axelson O, Fredriksson M, Hansson G, Lindvall B, Olsson JE, Granerus AK (1996) Age-standardized incidence and prevalence of Parkinson's disease in a Swedish community. *J Clin Epidemiol* 49:637-641.
- Fan J, Cowan CM, Zhang LY, Hayden MR, Raymond LA (2009) Interaction of postsynaptic density protein-95 with NMDA receptors influences excitotoxicity in the yeast artificial chromosome mouse model of Huntington's disease. *J Neurosci* 29:10928-10938.
- Fan J, Gladding CM, Wang L, Zhang LY, Kaufman AM, Milnerwood AJ, Raymond LA (2012) P38 MAPK is involved in enhanced NMDA receptor-dependent excitotoxicity in YAC transgenic mouse model of Huntington disease. *Neurobiol Dis* 45:999-1009.
- Farrer M, Kachergus J, Forno L, Lincoln S, Wang DS, Hulihan M, Maraganore D, Gwinn-Hardy K, Wszolek Z, Dickson D, Langston JW (2004) Comparison of kindreds with parkinsonism and alpha-synuclein genomic multiplications. *Ann Neurol* 55:174-179.
- Farrer MJ (2006) Genetics of Parkinson disease: paradigm shifts and future prospects. *Nat Rev Genet* 7:306-318.
- Fasano S, Bezard E, D'Antoni A, Francardo V, Indrigo M, Qin L, Dovero S, Cerovic M, Cenci MA, Brambilla R (2010) Inhibition of Ras-guanine nucleotide-releasing factor 1 (Ras-GRF1) signaling in the striatum reverts motor symptoms associated with L-dopa-induced dyskinesia. *Proc Natl Acad Sci U S A* 107:21824-21829.
- Fearnley JM, Lees AJ (1991) Ageing and Parkinson's disease: substantia nigra regional selectivity. *Brain* 114 (Pt 5):2283-2301.
- Fisone G, Bezard E (2011) Molecular mechanisms of L-DOPA-induced dyskinesia. *Int Rev Neurobiol* 98:95-122.
- Foley P, Riederer P (1999) Pathogenesis and preclinical course of Parkinson's disease. *J Neural Transm Suppl* 56:31-74.
- Forno LS (1969) Concentric hyalin intraneuronal inclusions of Lewy type in the brains of elderly persons (50 incidental cases): relationship to parkinsonism. *J Am Geriatr Soc* 17:557-575.
- Forno LS (1996) Neuropathology of Parkinson's disease. *J Neuropathol Exp Neurol* 55:259-272.
- Fortin DL, Troyer MD, Nakamura K, Kubo S, Anthony MD, Edwards RH (2004) Lipid rafts mediate the synaptic localization of alpha-synuclein. *J Neurosci* 24:6715-6723.
- Francardo V, Recchia A, Popovic N, Andersson D, Nissbrandt H, Cenci MA (2011) Impact of the lesion procedure on the profiles of motor impairment and molecular responsiveness to L-DOPA in the 6-hydroxydopamine mouse model of Parkinson's disease. *Neurobiol Dis* 42:327-340.
- Fuchs J, Nilsson C, Kachergus J, Munz M, Larsson EM, Schule B, Langston JW, Middleton FA, Ross OA, Hulihan M, Gasser T, Farrer MJ (2007) Phenotypic variation in a large Swedish pedigree due to SNCA duplication and triplication. *Neurology* 68:916-922.
- Fujiwara H, Hasegawa M, Dohmae N, Kawashima A, Masliah E, Goldberg MS, Shen J, Takio K, Iwatsubo T (2002) alpha-Synuclein is phosphorylated in synucleinopathy lesions. *Nat Cell Biol* 4:160-164.
- Galvan A, Wichmann T (2008) Pathophysiology of parkinsonism. *Clin Neurophysiol* 119:1459-1474.
- Galvin JE, Schuck TM, Lee VM, Trojanowski JQ (2001) Differential expression and distribution of alpha-, beta-, and gamma-synuclein in the developing human substantia nigra. *Exp Neurol* 168:347-355.
- Gandhi S, Wood-Kaczmar A, Yao Z, Plun-Favreau H, Deas E, Klupsch K, Downward J, Latchman DS, Tabrizi SJ, Wood NW, DuChen MR, Abramov AY (2009) PINK1-associated Parkinson's disease is caused by neuronal vulnerability to calcium-induced cell death. *Mol Cell* 33:627-638.
- Gaugler MN, Genc O, Bobela W, Mohanna S, Ardah MT, El-Agnaf OM, Cantoni M, Bensadoun JC, Schneckengburger R, Knott GW, Aebischer P, Schneider BL (2012) Nigrostriatal

- overabundance of alpha-synuclein leads to decreased vesicle density and deficits in dopamine release that correlate with reduced motor activity. *Acta Neuropathol* 123:653-669.
- Gautier CA, Kitada T, Shen J (2008) Loss of PINK1 causes mitochondrial functional defects and increased sensitivity to oxidative stress. *Proc Natl Acad Sci U S A* 105:11364-11369.
- Geisler S, Holmstrom KM, Skujat D, Fiesel FC, Rothfuss OC, Kahle PJ, Springer W (2010) PINK1/Parkin-mediated mitophagy is dependent on VDAC1 and p62/SQSTM1. *Nat Cell Biol* 12:119-131.
- George JM, Jin H, Woods WS, Clayton DF (1995) Characterization of a novel protein regulated during the critical period for song learning in the zebra finch. *Neuron* 15:361-372.
- Gerfen CR, Miyachi S, Paletzki R, Brown P (2002) D1 dopamine receptor supersensitivity in the dopamine-depleted striatum results from a switch in the regulation of ERK1/2/MAP kinase. *J Neurosci* 22:5042-5054.
- Ghiglieri V, Bageetta V, Pendolino V, Picconi B, Calabresi P (2012) Corticostriatal Plastic Changes in Experimental L-DOPA-Induced Dyskinesia. *Parkinsons Dis* 2012:358176.
- Ghosh D, Mondal M, Mohite GM, Singh PK, Ranjan P, Anoop A, Ghosh S, Jha NN, Kumar A, Maji SK (2013) The Parkinson's disease-associated H50Q mutation accelerates alpha-Synuclein aggregation in vitro. *Biochemistry* 52:6925-6927.
- Giasson BI, Duda JE, Forman MS, Lee VM, Trojanowski JQ (2001a) Prominent perikaryal expression of alpha- and beta-synuclein in neurons of dorsal root ganglion and in medullary neurons. *Exp Neurol* 172:354-362.
- Giasson BI, Murray IV, Trojanowski JQ, Lee VM (2001b) A hydrophobic stretch of 12 amino acid residues in the middle of alpha-synuclein is essential for filament assembly. *J Biol Chem* 276:2380-2386.
- Gibb WR, Lees AJ (1991) Anatomy, pigmentation, ventral and dorsal subpopulations of the substantia nigra, and differential cell death in Parkinson's disease. *J Neurol Neurosurg Psychiatry* 54:388-396.
- Giorgi M, D'Angelo V, Esposito Z, Nuccetelli V, Sorge R, Martorana A, Stefani A, Bernardi G, Sancesario G (2008) Lowered cAMP and cGMP signalling in the brain during levodopa-induced dyskinesias in hemiparkinsonian rats: new aspects in the pathogenetic mechanisms. *Eur J Neurosci* 28:941-950.
- Gispert S, Brehm N, Weil J, Seidel K, Rub U, Kern B, Walter M, Roeper J, Auburger G (2014a) Potentiation of neurotoxicity in double-mutant mice with Pink1 ablation and A53T-SNCA overexpression. *Hum Mol Genet*.
- Gispert S, Del Turco D, Garrett L, Chen A, Bernard DJ, Hamm-Clement J, Korf HW, Deller T, Braak H, Auburger G, Nussbaum RL (2003) Transgenic mice expressing mutant A53T human alpha-synuclein show neuronal dysfunction in the absence of aggregate formation. *Mol Cell Neurosci* 24:419-429.
- Gispert S, Kurz A, Brehm N, Rau K, Walter M, Riess O, Auburger G (2014b) Complexin-1 and Foxp1 Expression Changes Are Novel Brain Effects of Alpha-Synuclein Pathology. *Mol Neurobiol*.
- Gispert S, Ricciardi F, Kurz A, Azizov M, Hoepken HH, Becker D, Voos W, Leuner K, Muller WE, Kudin AP, Kunz WS, Zimmermann A, Roeper J, Wenzel D, Jendrach M, Garcia-Arencibia M, Fernandez-Ruiz J, Huber L, Rohrer H, Barrera M, Reichert AS, Rub U, Chen A, Nussbaum RL, Auburger G (2009) Parkinson phenotype in aged PINK1-deficient mice is accompanied by progressive mitochondrial dysfunction in absence of neurodegeneration. *PLoS One* 4:e5777.
- Glasgow NG, Siegler Retchless B, Johnson JW (2015) Molecular bases of NMDA receptor subtype-dependent properties. *J Physiol* 593:83-95.
- Glinka Y, Gassen M, Youdim MB (1997) Mechanism of 6-hydroxydopamine neurotoxicity. *J Neural Transm Suppl* 50:55-66.

- Gomes FC, Paulin D, Moura Neto V (1999) Glial fibrillary acidic protein (GFAP): modulation by growth factors and its implication in astrocyte differentiation. *Braz J Med Biol Res* 32:619-631.
- Gosal D, Ross OA, Toft M (2006) Parkinson's disease: the genetics of a heterogeneous disorder. *Eur J Neurol* 13:616-627.
- Graybiel AM, Moratalla R, Robertson HA (1990) Amphetamine and cocaine induce drug-specific activation of the c-fos gene in striosome-matrix compartments and limbic subdivisions of the striatum. *Proc Natl Acad Sci U S A* 87:6912-6916.
- Greenamyre JT, Eller RV, Zhang Z, Ovadia A, Kurlan R, Gash DM (1994) Antiparkinsonian effects of remacemide hydrochloride, a glutamate antagonist, in rodent and primate models of Parkinson's disease. *Ann Neurol* 35:655-661.
- Greger IH, Khatri L, Kong X, Ziff EB (2003) AMPA receptor tetramerization is mediated by Q/R editing. *Neuron* 40:763-774.
- Gubellini P, Picconi B, Bari M, Battista N, Calabresi P, Centonze D, Bernardi G, Finazzi-Agro A, Maccarrone M (2002) Experimental parkinsonism alters endocannabinoid degradation: implications for striatal glutamatergic transmission. *J Neurosci* 22:6900-6907.
- Gubellini P, Pisani A, Centonze D, Bernardi G, Calabresi P (2004) Metabotropic glutamate receptors and striatal synaptic plasticity: implications for neurological diseases. *Prog Neurobiol* 74:271-300.
- Gubellini P, Saulle E, Centonze D, Bonsi P, Pisani A, Bernardi G, Conquet F, Calabresi P (2001) Selective involvement of mGlu1 receptors in corticostriatal LTD. *Neuropharmacology* 40:839-846.
- Guzowski JF, Lyford GL, Stevenson GD, Houston FP, McGaugh JL, Worley PF, Barnes CA (2000) Inhibition of activity-dependent arc protein expression in the rat hippocampus impairs the maintenance of long-term potentiation and the consolidation of long-term memory. *J Neurosci* 20:3993-4001.
- Halliwell B, Jenner P (1998) Impaired clearance of oxidised proteins in neurodegenerative diseases. *Lancet* 351:1510.
- Hardebo JE, Owman C (1980) Barrier mechanisms for neurotransmitter monoamines and their precursors at the blood-brain interface. *Ann Neurol* 8:1-31.
- Hardie RJ, Lees AJ, Stern GM (1984) On-off fluctuations in Parkinson's disease. A clinical and neuropharmacological study. *Brain* 107 (Pt 2):487-506.
- Hardingham GE (2006) Pro-survival signalling from the NMDA receptor. *Biochem Soc Trans* 34:936-938.
- Hardingham GE, Bading H (2003) The Yin and Yang of NMDA receptor signalling. *Trends Neurosci* 26:81-89.
- Hasegawa M, Fujiwara H, Nonaka T, Wakabayashi K, Takahashi H, Lee VM, Trojanowski JQ, Mann D, Iwatsubo T (2002) Phosphorylated alpha-synuclein is ubiquitinated in alpha-synucleinopathy lesions. *J Biol Chem* 277:49071-49076.
- Hashimoto M, Bar-On P, Ho G, Takenouchi T, Rockenstein E, Crews L, Masliah E (2004) Beta-synuclein regulates Akt activity in neuronal cells. A possible mechanism for neuroprotection in Parkinson's disease. *J Biol Chem* 279:23622-23629.
- Hashimoto M, Hsu LJ, Xia Y, Takeda A, Sisk A, Sundsmo M, Masliah E (1999) Oxidative stress induces amyloid-like aggregate formation of NACP/alpha-synuclein in vitro. *Neuroreport* 10:717-721.
- Hashimoto M, Rockenstein E, Mante M, Mallory M, Masliah E (2001) beta-Synuclein inhibits alpha-synuclein aggregation: a possible role as an anti-parkinsonian factor. *Neuron* 32:213-223.

- Hatano Y, Li Y, Sato K, Asakawa S, Yamamura Y, Tomiyama H, Yoshino H, Asahina M, Kobayashi S, Hassin-Baer S, Lu CS, Ng AR, Rosales RL, Shimizu N, Toda T, Mizuno Y, Hattori N (2004) Novel PINK1 mutations in early-onset parkinsonism. *Ann Neurol* 56:424-427.
- Hawk JD, Abel T (2011) The role of NR4A transcription factors in memory formation. *Brain Res Bull* 85:21-29.
- He C, Klionsky DJ (2009) Regulation mechanisms and signaling pathways of autophagy. *Annu Rev Genet* 43:67-93.
- Hebb OD (1949) *The Organization of Behavior*. New York: Wiley.
- Hedrich K, Djarmati A, Schafer N, Hering R, Wellenbrock C, Weiss PH, Hilker R, Vieregge P, Ozelius LJ, Heutink P, Bonifati V, Schwinger E, Lang AE, Noth J, Bressman SB, Pramstaller PP, Riess O, Klein C (2004) DJ-1 (PARK7) mutations are less frequent than Parkin (PARK2) mutations in early-onset Parkinson disease. *Neurology* 62:389-394.
- Heiman M, Heilbut A, Francardo V, Kulicke R, Fenster RJ, Kolaczyk ED, Mesirov JP, Surmeier DJ, Cenci MA, Greengard P (2014) Molecular adaptations of striatal spiny projection neurons during levodopa-induced dyskinesia. *Proc Natl Acad Sci U S A* 111:4578-4583.
- Henning J, Koczan D, Glass A, Karopka T, Pahnke J, Rolfs A, Benecke R, Gimsa U (2007) Deep brain stimulation in a rat model modulates TH, CaMKIIa and Homer1 gene expression. *Eur J Neurosci* 25:239-250.
- Herrera DG, Robertson HA (1996) Activation of c-fos in the brain. *Prog Neurobiol* 50:83-107.
- Hetman M, Kharebava G (2006) Survival signaling pathways activated by NMDA receptors. *Curr Top Med Chem* 6:787-799.
- Heuer A, Smith GA, Lelos MJ, Lane EL, Dunnett SB (2012) Unilateral nigrostriatal 6-hydroxydopamine lesions in mice I: motor impairments identify extent of dopamine depletion at three different lesion sites. *Behav Brain Res* 228:30-43.
- Heximer SP, Watson N, Linder ME, Blumer KJ, Hepler JR (1997) RGS2/GOS8 is a selective inhibitor of Gqalpha function. *Proc Natl Acad Sci U S A* 94:14389-14393.
- Hirsch E, Graybiel AM, Agid YA (1988) Melanized dopaminergic neurons are differentially susceptible to degeneration in Parkinson's disease. *Nature* 334:345-348.
- Hisatsune C, Kuroda Y, Akagi T, Torashima T, Hirai H, Hashikawa T, Inoue T, Mikoshiba K (2006) Inositol 1,4,5-trisphosphate receptor type 1 in granule cells, not in Purkinje cells, regulates the dendritic morphology of Purkinje cells through brain-derived neurotrophic factor production. *J Neurosci* 26:10916-10924.
- Hoepken HH, Gispert S, Azizov M, Klinkenberg M, Ricciardi F, Kurz A, Morales-Gordo B, Bonin M, Riess O, Gasser T, Kogel D, Steinmetz H, Auburger G (2008) Parkinson patient fibroblasts show increased alpha-synuclein expression. *Exp Neurol* 212:307-313.
- Hoepken HH, Gispert S, Morales B, Wingerter O, Del Turco D, Mulsch A, Nussbaum RL, Muller K, Droese S, Brandt U, Deller T, Wirth B, Kudin AP, Kunz WS, Auburger G (2007) Mitochondrial dysfunction, peroxidation damage and changes in glutathione metabolism in PARK6. *Neurobiol Dis* 25:401-411.
- Hoffman-Zacharska D, Kozirowski D, Ross OA, Milewski M, Poznanski J, Jurek M, Wszolek ZK, Soto-Ortolaza A, Slawek J, Janik P, Jamrozik Z, Potulska-Chromik A, Jasinska-Myga B, Opala G, Krygowska-Wajs A, Czyzewski K, Dickson DW, Bal J, Friedman A (2013) Novel A18T and pA29S substitutions in alpha-synuclein may be associated with sporadic Parkinson's disease. *Parkinsonism Relat Disord* 19:1057-1060.
- Hokfelt T, Fuxe K, Goldstein M (1973) Immunohistochemical studies on monoamine-containing cell systems. *Brain Res* 62:461-469.
- Hoshi E, Tremblay L, Feger J, Carras PL, Strick PL (2005) The cerebellum communicates with the basal ganglia. *Nat Neurosci* 8:1491-1493.
- Huang CY, Tan TH (2012) DUSPs, to MAP kinases and beyond. *Cell Biosci* 2:24.

- Hughes AJ, Daniel SE, Kilford L, Lees AJ (1992) Accuracy of clinical diagnosis of idiopathic Parkinson's disease: a clinico-pathological study of 100 cases. *J Neurol Neurosurg Psychiatry* 55:181-184.
- Hunot S, Dugas N, Faucheux B, Hartmann A, Tardieu M, Debre P, Agid Y, Dugas B, Hirsch EC (1999) FcepsilonRII/CD23 is expressed in Parkinson's disease and induces, in vitro, production of nitric oxide and tumor necrosis factor-alpha in glial cells. *J Neurosci* 19:3440-3447.
- Hunt TW, Fields TA, Casey PJ, Peralta EG (1996) RGS10 is a selective activator of G alpha i GTPase activity. *Nature* 383:175-177.
- Huot P, Johnston TH, Koprach JB, Fox SH, Brotchie JM (2013) The pharmacology of L-DOPA-induced dyskinesia in Parkinson's disease. *Pharmacol Rev* 65:171-222.
- Hurd LB, 2nd, Eldred WD (1989) Localization of GABA- and GAD-like immunoreactivity in the turtle retina. *Vis Neurosci* 3:9-20.
- Ibanez P, Bonnet AM, Debarges B, Lohmann E, Tison F, Pollak P, Agid Y, Durr A, Brice A (2004) Causal relation between alpha-synuclein gene duplication and familial Parkinson's disease. *Lancet* 364:1169-1171.
- Ii K, Ito H, Tanaka K, Hirano A (1997) Immunocytochemical co-localization of the proteasome in ubiquitinated structures in neurodegenerative diseases and the elderly. *J Neuropathol Exp Neurol* 56:125-131.
- Ikonomidou C, Turski L (2002) Why did NMDA receptor antagonists fail clinical trials for stroke and traumatic brain injury? *Lancet Neurol* 1:383-386.
- Ingham CA, Hood SH, Arbuthnott GW (1989) Spine density on neostriatal neurones changes with 6-hydroxydopamine lesions and with age. *Brain Res* 503:334-338.
- Irizarry MC, Growdon W, Gomez-Isla T, Newell K, George JM, Clayton DF, Hyman BT (1998) Nigral and cortical Lewy bodies and dystrophic nigral neurites in Parkinson's disease and cortical Lewy body disease contain alpha-synuclein immunoreactivity. *J Neuropathol Exp Neurol* 57:334-337.
- Iwai A, Masliah E, Yoshimoto M, Ge N, Flanagan L, de Silva HA, Kittel A, Saitoh T (1995) The precursor protein of non-A beta component of Alzheimer's disease amyloid is a presynaptic protein of the central nervous system. *Neuron* 14:467-475.
- Jenner P (2003) Oxidative stress in Parkinson's disease. *Ann Neurol* 53 Suppl 3:S26-36; discussion S36-28.
- Jensen MB, Bhatia VK, Jao CC, Rasmussen JE, Pedersen SL, Jensen KJ, Langen R, Stamou D (2011) Membrane curvature sensing by amphipathic helices: a single liposome study using alpha-synuclein and annexin B12. *J Biol Chem* 286:42603-42614.
- Jensen PH, Hojrup P, Hager H, Nielsen MS, Jacobsen L, Olesen OF, Gliemann J, Jakes R (1997) Binding of A beta to alpha- and beta-synucleins: identification of segments in alpha-synuclein/NAC precursor that bind A beta and NAC. *Biochem J* 323 (Pt 2):539-546.
- Ji H, Liu YE, Jia T, Wang M, Liu J, Xiao G, Joseph BK, Rosen C, Shi YE (1997) Identification of a breast cancer-specific gene, BCSG1, by direct differential cDNA sequencing. *Cancer Res* 57:759-764.
- Jiang Y, Liu YE, Goldberg ID, Shi YE (2004) Gamma synuclein, a novel heat-shock protein-associated chaperone, stimulates ligand-dependent estrogen receptor alpha signaling and mammary tumorigenesis. *Cancer Res* 64:4539-4546.
- Jones N (2010) PINK1 targets dysfunctional mitochondria for autophagy in Parkinson disease. *Nat Rev Neurol* 6:181.
- Kageyama T, Nakamura M, Matsuo A, Yamasaki Y, Takakura Y, Hashida M, Kanai Y, Naito M, Tsuruo T, Minato N, Shimohama S (2000) The 4F2hc/LAT1 complex transports L-DOPA across the blood-brain barrier. *Brain Res* 879:115-121.
- Kahle PJ, Neumann M, Ozmen L, Muller V, Jacobsen H, Schindzielorz A, Okochi M, Leimer U, van Der Putten H, Probst A, Kremmer E, Kretschmar HA, Haass C (2000) Subcellular

- localization of wild-type and Parkinson's disease-associated mutant alpha -synuclein in human and transgenic mouse brain. *J Neurosci* 20:6365-6373.
- Kahn L, Alonso G, Robbe D, Bockaert J, Manzoni OJ (2001) Group 2 metabotropic glutamate receptors induced long term depression in mouse striatal slices. *Neurosci Lett* 316:178-182.
- Kandel E. R. SJH, Jessel T. M. (ed.) (1995) *Neurowissenschaften: Eine Einführung*. Heidelberg ; Berlin ; Oxford: Spektrum, Akad. Verl.
- Kapfhammer JP, Schwab ME (1994) Inverse patterns of myelination and GAP-43 expression in the adult CNS: neurite growth inhibitors as regulators of neuronal plasticity? *J Comp Neurol* 340:194-206.
- Kempster PA, Frankel JP, Stern GM, Lees AJ (1990) Comparison of motor response to apomorphine and levodopa in Parkinson's disease. *J Neurol Neurosurg Psychiatry* 53:1004-1007.
- Kerner JA, Standaert DG, Penney JB, Jr., Young AB, Landwehrmeyer GB (1997) Expression of group one metabotropic glutamate receptor subunit mRNAs in neurochemically identified neurons in the rat neostriatum, neocortex, and hippocampus. *Brain Res Mol Brain Res* 48:259-269.
- Khalaf O, Fauvet B, Oueslati A, Dikiy I, Mahul-Mellier AL, Ruggeri FS, Mbefo MK, Vercruyse F, Dietler G, Lee SJ, Eliezer D, Lashuel HA (2014) The H50Q mutation enhances alpha-synuclein aggregation, secretion, and toxicity. *J Biol Chem* 289:21856-21876.
- Kitada T, Asakawa S, Hattori N, Matsumine H, Yamamura Y, Minoshima S, Yokochi M, Mizuno Y, Shimizu N (1998) Mutations in the parkin gene cause autosomal recessive juvenile parkinsonism. *Nature* 392:605-608.
- Kitada T, Pisani A, Porter DR, Yamaguchi H, Tscherter A, Martella G, Bonsi P, Zhang C, Pothos EN, Shen J (2007) Impaired dopamine release and synaptic plasticity in the striatum of PINK1-deficient mice. *Proc Natl Acad Sci U S A* 104:11441-11446.
- Klein C, Westenberger A (2012) Genetics of Parkinson's disease. *Cold Spring Harb Perspect Med* 2:a008888.
- Klinkenberg M, Gispert S, Dominguez-Bautista JA, Braun I, Auburger G, Jendrach M (2012) Restriction of trophic factors and nutrients induces PARKIN expression. *Neurogenetics* 13:9-21.
- Kosaka K, Oyanagi S, Matsushita M, Hori A (1976) Presenile dementia with Alzheimer-, Pick- and Lewy-body changes. *Acta Neuropathol* 36:221-233.
- Koshimura K, Miwa S, Lee K, Fujiwara M, Watanabe Y (1990) Enhancement of dopamine release in vivo from the rat striatum by dialytic perfusion of 6R-L-erythro-5,6,7,8-tetrahydrobiopterin. *J Neurochem* 54:1391-1397.
- Koyano F, Okatsu K, Kosako H, Tamura Y, Go E, Kimura M, Kimura Y, Tsuchiya H, Yoshihara H, Hirokawa T, Endo T, Fon EA, Trempe JF, Saeki Y, Tanaka K, Matsuda N (2014) Ubiquitin is phosphorylated by PINK1 to activate parkin. *Nature* 510:162-166.
- Kreitzer AC, Malenka RC (2007) Endocannabinoid-mediated rescue of striatal LTD and motor deficits in Parkinson's disease models. *Nature* 445:643-647.
- Kruger R, Kuhn W, Muller T, Woitalla D, Graeber M, Kosel S, Przuntek H, Epplen JT, Schols L, Riess O (1998) Ala30Pro mutation in the gene encoding alpha-synuclein in Parkinson's disease. *Nat Genet* 18:106-108.
- Kuner T, Schoepfer R (1996) Multiple structural elements determine subunit specificity of Mg²⁺ block in NMDA receptor channels. *J Neurosci* 16:3549-3558.
- Kunikowska G, Jenner P (2001) 6-Hydroxydopamine-lesioning of the nigrostriatal pathway in rats alters basal ganglia mRNA for copper, zinc- and manganese-superoxide dismutase, but not glutathione peroxidase. *Brain Res* 922:51-64.

- Kurz A, Double KL, Lastres-Becker I, Tozzi A, Tantucci M, Bockhart V, Bonin M, Garcia-Arencibia M, Nuber S, Schlaudraff F, Liss B, Fernandez-Ruiz J, Gerlach M, Wullner U, Luddens H, Calabresi P, Auburger G, Gispert S (2010) A53T-alpha-synuclein overexpression impairs dopamine signaling and striatal synaptic plasticity in old mice. *PLoS One* 5:e11464.
- Kutsuwada T, Kashiwabuchi N, Mori H, Sakimura K, Kushiya E, Araki K, Meguro H, Masaki H, Kumanishi T, Arakawa M, et al. (1992) Molecular diversity of the NMDA receptor channel. *Nature* 358:36-41.
- Kuusisto E, Parkkinen L, Alafuzoff I (2003) Morphogenesis of Lewy bodies: dissimilar incorporation of alpha-synuclein, ubiquitin, and p62. *J Neuropathol Exp Neurol* 62:1241-1253.
- Kuusisto E, Salminen A, Alafuzoff I (2001) Ubiquitin-binding protein p62 is present in neuronal and glial inclusions in human tauopathies and synucleinopathies. *Neuroreport* 12:2085-2090.
- Kuzuhara S, Mori H, Izumiyama N, Yoshimura M, Ihara Y (1988) Lewy bodies are ubiquitinated. A light and electron microscopic immunocytochemical study. *Acta Neuropathol* 75:345-353.
- Laemmli UK (1970) Cleavage of structural proteins during the assembly of the head of bacteriophage T4. *Nature* 227:680-685.
- Lambolez B, Ropert N, Perrais D, Rossier J, Hestrin S (1996) Correlation between kinetics and RNA splicing of alpha-amino-3-hydroxy-5-methylisoxazole-4-propionic acid receptors in neocortical neurons. *Proc Natl Acad Sci U S A* 93:1797-1802.
- Lapper SR, Bolam JP (1992) Input from the frontal cortex and the parafascicular nucleus to cholinergic interneurons in the dorsal striatum of the rat. *Neuroscience* 51:533-545.
- Larsen KE, Schmitz Y, Troyer MD, Mosharov E, Dietrich P, Quazi AZ, Savalle M, Nemani V, Chaudhry FA, Edwards RH, Stefanis L, Sulzer D (2006) Alpha-synuclein overexpression in PC12 and chromaffin cells impairs catecholamine release by interfering with a late step in exocytosis. *J Neurosci* 26:11915-11922.
- Lashuel HA, Overk CR, Oueslati A, Masliah E (2013) The many faces of alpha-synuclein: from structure and toxicity to therapeutic target. *Nat Rev Neurosci* 14:38-48.
- Lavedan C (1998) The synuclein family. *Genome Res* 8:871-880.
- Lavedan C, Leroy E, Dehejia A, Buchholtz S, Dutra A, Nussbaum RL, Polymeropoulos MH (1998) Identification, localization and characterization of the human gamma-synuclein gene. *Hum Genet* 103:106-112.
- Lee CS, Cenci MA, Schulzer M, Bjorklund A (2000) Embryonic ventral mesencephalic grafts improve levodopa-induced dyskinesia in a rat model of Parkinson's disease. *Brain* 123 (Pt 7):1365-1379.
- Lees AJ (2007) Unresolved issues relating to the shaking palsy on the celebration of James Parkinson's 250th birthday. *Mov Disord* 22 Suppl 17:S327-334.
- Lees AJ, Selikhova M, Andrade LA, Duyckaerts C (2008) The black stuff and Konstantin Nikolaevich Tretiakoff. *Movement Disorders* 23:777-783.
- Leroux PD (1880) Contribution á l'étude des causes de la paralysie agitante. In: Imprimeur de la Faculté de Médecine Paris.
- Lewy HF (1912) Paralysis agitans. 1. Pathologische Anatomie. In: *Handbuch der Neurologie* (M., L., ed), pp 920-933 Berlin: Springer-Verlag.
- Li H, Kolluri SK, Gu J, Dawson MI, Cao X, Hobbs PD, Lin B, Chen G, Lu J, Lin F, Xie Z, Fontana JA, Reed JC, Zhang X (2000) Cytochrome c release and apoptosis induced by mitochondrial targeting of nuclear orphan receptor TR3. *Science* 289:1159-1164.
- Lin B, Kolluri SK, Lin F, Liu W, Han YH, Cao X, Dawson MI, Reed JC, Zhang XK (2004) Conversion of Bcl-2 from protector to killer by interaction with nuclear orphan receptor Nur77/TR3. *Cell* 116:527-540.
- Lin X, Parisiadou L, Sgobio C, Liu G, Yu J, Sun L, Shim H, Gu XL, Luo J, Long CX, Ding J, Mateo Y, Sullivan PH, Wu LG, Goldstein DS, Lovinger D, Cai H (2012) Conditional expression of Parkinson's disease-related mutant alpha-synuclein in the midbrain dopaminergic

- neurons causes progressive neurodegeneration and degradation of transcription factor nuclear receptor related 1. *J Neurosci* 32:9248-9264.
- Lindgren HS, Ohlin KE, Cenci MA (2009) Differential involvement of D1 and D2 dopamine receptors in L-DOPA-induced angiogenic activity in a rat model of Parkinson's disease. *Neuropsychopharmacology* 34:2477-2488.
- Lindgren HS, Rylander D, Ohlin KE, Lundblad M, Cenci MA (2007) The "motor complication syndrome" in rats with 6-OHDA lesions treated chronically with L-DOPA: relation to dose and route of administration. *Behav Brain Res* 177:150-159.
- Lipton SA, Kater SB (1989) Neurotransmitter regulation of neuronal outgrowth, plasticity and survival. *Trends Neurosci* 12:265-270.
- Lipton SA, Nakanishi N (1999) Shakespeare in love--with NMDA receptors? *Nat Med* 5:270-271.
- Livak KJ, Schmittgen TD (2001) Analysis of relative gene expression data using real-time quantitative PCR and the 2⁻(Delta Delta C(T)) Method. *Methods* 25:402-408.
- Lockhart PJ, Lincoln S, Hulihan M, Kachergus J, Wilkes K, Bisceglia G, Mash DC, Farrer MJ (2004) DJ-1 mutations are a rare cause of recessively inherited early onset parkinsonism mediated by loss of protein function. *J Med Genet* 41:e22.
- Lovinger DM, Tyler EC, Merritt A (1993) Short- and long-term synaptic depression in rat neostriatum. *J Neurophysiol* 70:1937-1949.
- Lucking CB, Durr A, Bonifati V, Vaughan J, De Michele G, Gasser T, Harhangi BS, Meco G, Deneffe P, Wood NW, Agid Y, Brice A (2000) Association between early-onset Parkinson's disease and mutations in the parkin gene. *N Engl J Med* 342:1560-1567.
- Luk KC, Song C, O'Brien P, Stieber A, Branch JR, Brunden KR, Trojanowski JQ, Lee VM (2009) Exogenous alpha-synuclein fibrils seed the formation of Lewy body-like intracellular inclusions in cultured cells. *Proc Natl Acad Sci U S A* 106:20051-20056.
- Lundblad M, Andersson M, Winkler C, Kirik D, Wierup N, Cenci MA (2002) Pharmacological validation of behavioural measures of akinesia and dyskinesia in a rat model of Parkinson's disease. *Eur J Neurosci* 15:120-132.
- Lundblad M, Decressac M, Mattsson B, Bjorklund A (2012) Impaired neurotransmission caused by overexpression of alpha-synuclein in nigral dopamine neurons. *Proc Natl Acad Sci U S A* 109:3213-3219.
- Lundblad M, Picconi B, Lindgren H, Cenci MA (2004) A model of L-DOPA-induced dyskinesia in 6-hydroxydopamine lesioned mice: relation to motor and cellular parameters of nigrostriatal function. *Neurobiol Dis* 16:110-123.
- Luscher C, Xia H, Beattie EC, Carroll RC, von Zastrow M, Malenka RC, Nicoll RA (1999) Role of AMPA receptor cycling in synaptic transmission and plasticity. *Neuron* 24:649-658.
- Manson A, Stirpe P, Schrag A (2012) Levodopa-induced-dyskinesias clinical features, incidence, risk factors, management and impact on quality of life. *J Parkinsons Dis* 2:189-198.
- Manson AJ, Turner K, Lees AJ (2002) Apomorphine monotherapy in the treatment of refractory motor complications of Parkinson's disease: long-term follow-up study of 64 patients. *Mov Disord* 17:1235-1241.
- Maraganore DM, de Andrade M, Elbaz A, Farrer MJ, Ioannidis JP, Kruger R, Rocca WA, Schneider NK, Lesnick TG, Lincoln SJ, Hulihan MM, Aasly JO, Ashizawa T, Chartier-Harlin MC, Checkoway H, Ferrarese C, Hadjigeorgiou G, Hattori N, Kawakami H, Lambert JC, Lynch T, Mellick GD, Papapetropoulos S, Parsian A, Quattrone A, Riess O, Tan EK, Van Broeckhoven C (2006) Collaborative analysis of alpha-synuclein gene promoter variability and Parkinson disease. *JAMA* 296:661-670.
- Maraganore DM, de Andrade M, Lesnick TG, Strain KJ, Farrer MJ, Rocca WA, Pant PV, Frazer KA, Cox DR, Ballinger DG (2005) High-resolution whole-genome association study of Parkinson disease. *Am J Hum Genet* 77:685-693.

- Marino MJ, Conn PJ (2002) Modulation of the basal ganglia by metabotropic glutamate receptors: potential for novel therapeutics. *Curr Drug Targets CNS Neurol Disord* 1:239-250.
- Maroteaux L, Campanelli JT, Scheller RH (1988) Synuclein: a neuron-specific protein localized to the nucleus and presynaptic nerve terminal. *J Neurosci* 8:2804-2815.
- Martignoni E, Pacchetti C, Godi L, Micieli G, Nappi G (1995) Autonomic disorders in Parkinson's disease. *J Neural Transm Suppl* 45:11-19.
- Martin LJ, Pan Y, Price AC, Sterling W, Copeland NG, Jenkins NA, Price DL, Lee MK (2006) Parkinson's disease alpha-synuclein transgenic mice develop neuronal mitochondrial degeneration and cell death. *J Neurosci* 26:41-50.
- Masliah E, Iwai A, Mallory M, Ueda K, Saitoh T (1996) Altered presynaptic protein NACP is associated with plaque formation and neurodegeneration in Alzheimer's disease. *Am J Pathol* 148:201-210.
- Masliah E, Rockenstein E, Veinbergs I, Mallory M, Hashimoto M, Takeda A, Sagara Y, Sisk A, Mucke L (2000) Dopaminergic loss and inclusion body formation in alpha-synuclein mice: implications for neurodegenerative disorders. *Science* 287:1265-1269.
- Massey PV, Johnson BE, Moulton PR, Auberson YP, Brown MW, Molnar E, Collingridge GL, Bashir ZI (2004) Differential roles of NR2A and NR2B-containing NMDA receptors in cortical long-term potentiation and long-term depression. *J Neurosci* 24:7821-7828.
- Mata IF, Lockhart PJ, Farrer MJ (2004) Parkin genetics: one model for Parkinson's disease. *Hum Mol Genet* 13 Spec No 1:R127-133.
- Matsuzaki M, Ellis-Davies GC, Nemoto T, Miyashita Y, Iino M, Kasai H (2001) Dendritic spine geometry is critical for AMPA receptor expression in hippocampal CA1 pyramidal neurons. *Nat Neurosci* 4:1086-1092.
- Maxwell MA, Muscat GE (2006) The NR4A subgroup: immediate early response genes with pleiotropic physiological roles. *Nucl Recept Signal* 4:e002.
- Mayeux R, Marder K, Cote LJ, Denaro J, Hemenegildo N, Mejia H, Tang MX, Lantigua R, Wilder D, Gurland B, et al. (1995) The frequency of idiopathic Parkinson's disease by age, ethnic group, and sex in northern Manhattan, 1988-1993. *Am J Epidemiol* 142:820-827.
- Mazzella L, Yahr MD, Marinelli L, Huang N, Moshier E, Di Rocco A (2005) Dyskinesias predict the onset of motor response fluctuations in patients with Parkinson's disease on L-dopa monotherapy. *Parkinsonism Relat Disord* 11:151-155.
- Mazzio EA, Reams RR, Soliman KF (2004) The role of oxidative stress, impaired glycolysis and mitochondrial respiratory redox failure in the cytotoxic effects of 6-hydroxydopamine in vitro. *Brain Res* 1004:29-44.
- McGeer PL, Itagaki S, Boyes BE, McGeer EG (1988) Reactive microglia are positive for HLA-DR in the substantia nigra of Parkinson's and Alzheimer's disease brains. *Neurology* 38:1285-1291.
- McGeer PL, McGeer EG, Suzuki JS (1977) Aging and extrapyramidal function. *Arch Neurol* 34:33-35.
- McLelland GL, Soubannier V, Chen CX, McBride HM, Fon EA (2014) Parkin and PINK1 function in a vesicular trafficking pathway regulating mitochondrial quality control. *EMBO J* 33:282-295.
- McNaught KS, Belizaire R, Isacson O, Jenner P, Olanow CW (2003) Altered proteasomal function in sporadic Parkinson's disease. *Exp Neurol* 179:38-46.
- McNaught KS, Lee M, Hyun DH, Jenner P (2001a) Glial cells and abnormal protein handling in the pathogenesis of Parkinson's disease. *Adv Neurol* 86:73-82.
- McNaught KS, Olanow CW, Halliwell B, Isacson O, Jenner P (2001b) Failure of the ubiquitin-proteasome system in Parkinson's disease. *Nat Rev Neurosci* 2:589-594.
- McNeill TH, Brown SA, Rafols JA, Shoulson I (1988) Atrophy of medium spiny I striatal dendrites in advanced Parkinson's disease. *Brain Res* 455:148-152.

- Mei Y, Zhang Y, Yamamoto K, Xie W, Mak TW, You H (2009) FOXO3a-dependent regulation of Pink1 (Park6) mediates survival signaling in response to cytokine deprivation. *Proc Natl Acad Sci U S A* 106:5153-5158.
- Meissner C, Lorenz H, Weihofen A, Selkoe DJ, Lemberg MK (2011) The mitochondrial intramembrane protease PARL cleaves human Pink1 to regulate Pink1 trafficking. *J Neurochem* 117:856-867.
- Michiorri S, Gelmetti V, Giarda E, Lombardi F, Romano F, Marongiu R, Nerini-Molteni S, Sale P, Vago R, Arena G, Torosantucci L, Cassina L, Russo MA, Dallapiccola B, Valente EM, Casari G (2010) The Parkinson-associated protein PINK1 interacts with Beclin1 and promotes autophagy. *Cell Death Differ* 17:962-974.
- Middleton ER, Rhoades E (2010) Effects of curvature and composition on alpha-synuclein binding to lipid vesicles. *Biophys J* 99:2279-2288.
- Millan MJ, Maiofiss L, Cussac D, Audinot V, Boutin JA, Newman-Tancredi A (2002) Differential actions of antiparkinson agents at multiple classes of monoaminergic receptor. I. A multivariate analysis of the binding profiles of 14 drugs at 21 native and cloned human receptor subtypes. *J Pharmacol Exp Ther* 303:791-804.
- Mjones H (1949) Paralysis Agitans. A clinical and genetic study. *Acta Psychiatr Neurol Scand* 54:1-195.
- Monyer H, Burnashev N, Laurie DJ, Sakmann B, Seeburg PH (1994) Developmental and regional expression in the rat brain and functional properties of four NMDA receptors. *Neuron* 12:529-540.
- Monyer H, Sprengel R, Schoepfer R, Herb A, Higuchi M, Lomeli H, Burnashev N, Sakmann B, Seeburg PH (1992) Heteromeric NMDA receptors: molecular and functional distinction of subtypes. *Science* 256:1217-1221.
- Morales M, Root DH (2014) Glutamate neurons within the midbrain dopamine regions. *Neuroscience* 282C:60-68.
- Moran LB, Croisier E, Duke DC, Kalaitzakis ME, Roncaroli F, Deprez M, Dexter DT, Pearce RK, Graeber MB (2007) Analysis of alpha-synuclein, dopamine and parkin pathways in neuropathologically confirmed parkinsonian nigra. *Acta Neuropathol* 113:253-263.
- Morrish PK, Sawle GV, Brooks DJ (1996) An [18F]dopa-PET and clinical study of the rate of progression in Parkinson's disease. *Brain* 119 (Pt 2):585-591.
- Moskovitz C, Moses H, 3rd, Klawans HL (1978) Levodopa-induced psychosis: a kindling phenomenon. *Am J Psychiatry* 135:669-675.
- Muenter MD, Forno LS, Hornykiewicz O, Kish SJ, Maraganore DM, Caselli RJ, Okazaki H, Howard FM, Jr., Snow BJ, Calne DB (1998) Hereditary form of parkinsonism--dementia. *Ann Neurol* 43:768-781.
- Murer MG, Moratalla R (2011) Striatal Signaling in L-DOPA-Induced Dyskinesia: Common Mechanisms with Drug Abuse and Long Term Memory Involving D1 Dopamine Receptor Stimulation. *Front Neuroanat* 5:51.
- Nadjar A, Gerfen CR, Bezard E (2009) Priming for l-dopa-induced dyskinesia in Parkinson's disease: a feature inherent to the treatment or the disease? *Prog Neurobiol* 87:1-9.
- Nakamura K, Nemani VM, Azarbal F, Skibinski G, Levy JM, Egami K, Munishkina L, Zhang J, Gardner B, Wakabayashi J, Sesaki H, Cheng Y, Finkbeiner S, Nussbaum RL, Masliah E, Edwards RH (2011) Direct membrane association drives mitochondrial fission by the Parkinson disease-associated protein alpha-synuclein. *J Biol Chem* 286:20710-20726.
- Nakanishi S, Nakajima Y, Masu M, Ueda Y, Nakahara K, Watanabe D, Yamaguchi S, Kawabata S, Okada M (1998) Glutamate receptors: brain function and signal transduction. *Brain Res Brain Res Rev* 26:230-235.
- Nalls MA, Pankratz N, Lill CM, Do CB, Hernandez DG, Saad M, DeStefano AL, Kara E, Bras J, Sharma M, Schulte C, Keller MF, Arepalli S, Letson C, Edsall C, Stefansson H, Liu X, Pliner H, Lee JH,

- Cheng R, International Parkinson's Disease Genomics C, Parkinson's Study Group Parkinson's Research: The Organized GI, andMe, GenePd, NeuroGenetics Research C, Hussman Institute of Human G, The Ashkenazi Jewish Dataset I, Cohorts for H, Aging Research in Genetic E, North American Brain Expression C, United Kingdom Brain Expression C, Greek Parkinson's Disease C, Alzheimer Genetic Analysis G, Ikram MA, Ioannidis JPA, Hadjigeorgiou GM, Bis JC, Martinez M, Perlmutter JS, Goate A, Marder K, Fiske B, Sutherland M, Xiromerisiou G, Myers RH, Clark LN, Stefansson K, Hardy JA, Heutink P, Chen H, Wood NW, Houlden H, Payami H, Brice A, Scott WK, Gasser T, Bertram L, Eriksson N, Foroud T, Singleton AB (2014) Large-scale meta-analysis of genome-wide association data identifies six new risk loci for Parkinson's disease. *Nat Genet* 46:989-993.
- Narendra DP, Jin SM, Tanaka A, Suen DF, Gautier CA, Shen J, Cookson MR, Youle RJ (2010) PINK1 is selectively stabilized on impaired mitochondria to activate Parkin. *PLoS Biol* 8:e1000298.
- Nausieda PA, Glantz R, Weber S, Baum R, Klawans HL (1984) Psychiatric complications of levodopa therapy of Parkinson's disease. *Adv Neurol* 40:271-277.
- Nemani VM, Lu W, Berge V, Nakamura K, Onoa B, Lee MK, Chaudhry FA, Nicoll RA, Edwards RH (2010) Increased expression of alpha-synuclein reduces neurotransmitter release by inhibiting synaptic vesicle reclustering after endocytosis. *Neuron* 65:66-79.
- Nishimune A, Isaac JT, Molnar E, Noel J, Nash SR, Tagaya M, Collingridge GL, Nakanishi S, Henley JM (1998) NSF binding to GluR2 regulates synaptic transmission. *Neuron* 21:87-97.
- Nitsch C, Riesenberger R (1995) Synaptic reorganisation in the rat striatum after dopaminergic deafferentation: an ultrastructural study using glutamate decarboxylase immunocytochemistry. *Synapse* 19:247-263.
- No H, Bang Y, Lim J, Kim SS, Choi HS, Choi HJ (2010) Involvement of induction and mitochondrial targeting of orphan nuclear receptor Nur77 in 6-OHDA-induced SH-SY5Y cell death. *Neurochem Int* 56:620-626.
- Nussbaum RL, Ellis CE (2003) Alzheimer's disease and Parkinson's disease. *N Engl J Med* 348:1356-1364.
- Nuytemans K, Theuns J, Cruts M, Van Broeckhoven C (2010) Genetic etiology of Parkinson disease associated with mutations in the SNCA, PARK2, PINK1, PARK7, and LRRK2 genes: a mutation update. *Hum Mutat* 31:763-780.
- Obeso JA, Olanow CW, Nutt JG (2000a) Levodopa motor complications in Parkinson's disease. *Trends Neurosci* 23:S2-7.
- Obeso JA, Rodriguez-Oroz M, Marin C, Alonso F, Zamarbide I, Lanciego JL, Rodriguez-Diaz M (2004) The origin of motor fluctuations in Parkinson's disease: importance of dopaminergic innervation and basal ganglia circuits. *Neurology* 62:S17-30.
- Obeso JA, Rodriguez-Oroz MC, Rodriguez M, Lanciego JL, Artieda J, Gonzalo N, Olanow CW (2000b) Pathophysiology of the basal ganglia in Parkinson's disease. *Trends Neurosci* 23:S8-19.
- Ohnishi YN, Ohnishi YH, Hokama M, Nomaru H, Yamazaki K, Tominaga Y, Sakumi K, Nestler EJ, Nakabeppu Y (2011) FosB is essential for the enhancement of stress tolerance and antagonizes locomotor sensitization by DeltaFosB. *Biol Psychiatry* 70:487-495.
- Ohtake H, Limprasert P, Fan Y, Onodera O, Kakita A, Takahashi H, Bonner LT, Tsuang DW, Murray IV, Lee VM, Trojanowski JQ, Ishikawa A, Idezuka J, Murata M, Toda T, Bird TD, Leverenz JB, Tsuji S, La Spada AR (2004) Beta-synuclein gene alterations in dementia with Lewy bodies. *Neurology* 63:805-811.
- Okazaki H, Lipkin LE, Aronson SM (1961) Diffuse intracytoplasmic ganglionic inclusions (Lewy type) associated with progressive dementia and quadriplegia in flexion. *J Neuropathol Exp Neurol* 20:237-244.
- Oldendorf WH, Szabo J (1976) Amino acid assignment to one of three blood-brain barrier amino acid carriers. *Am J Physiol* 230:94-98.

- Oliveras-Salva M, Macchi F, Coessens V, Deleersnijder A, Gerard M, Van der Perren A, Van den Haute C, Baekelandt V (2014) Alpha-synuclein-induced neurodegeneration is exacerbated in PINK1 knockout mice. *Neurobiol Aging* 35:2625-2636.
- Ottersen OP, Landsend AS (1997) Organization of glutamate receptors at the synapse. *Eur J Neurosci* 9:2219-2224.
- Owen AM (2004) Cognitive dysfunction in Parkinson's disease: the role of frontostriatal circuitry. *Neuroscientist* 10:525-537.
- Owen AM, James M, Leigh PN, Summers BA, Marsden CD, Quinn NP, Lange KW, Robbins TW (1992) Fronto-striatal cognitive deficits at different stages of Parkinson's disease. *Brain* 115 (Pt 6):1727-1751.
- Owens DM, Keyse SM (2007) Differential regulation of MAP kinase signalling by dual-specificity protein phosphatases. *Oncogene* 26:3203-3213.
- Ozansoy M, Basak AN (2013) The central theme of Parkinson's disease: alpha-synuclein. *Mol Neurobiol* 47:460-465.
- Pahapill PA, Lozano AM (2000) The pedunculopontine nucleus and Parkinson's disease. *Brain* 123 (Pt 9):1767-1783.
- Paille V, Henry V, Lescaudron L, Brachet P, Damier P (2007) Rat model of Parkinson's disease with bilateral motor abnormalities, reversible with levodopa, and dyskinesias. *Mov Disord* 22:533-539.
- Pallanck LJ (2010) Culling sick mitochondria from the herd. *J Cell Biol* 191:1225-1227.
- Pankiv S, Clausen TH, Lamark T, Brech A, Bruun JA, Outzen H, Overvatn A, Bjorkoy G, Johansen T (2007) p62/SQSTM1 binds directly to Atg8/LC3 to facilitate degradation of ubiquitinated protein aggregates by autophagy. *J Biol Chem* 282:24131-24145.
- Pankratz N, Beecham GW, DeStefano AL, Dawson TM, Doheny KF, Factor SA, Hamza TH, Hung AY, Hyman BT, Ivinson AJ, Krainc D, Latourelle JC, Clark LN, Marder K, Martin ER, Mayeux R, Ross OA, Scherzer CR, Simon DK, Tanner C, Vance JM, Wszolek ZK, Zabetian CP, Myers RH, Payami H, Scott WK, Foroud T (2012) Meta-analysis of Parkinson's disease: identification of a novel locus, RIT2. *Ann Neurol* 71:370-384.
- Paoletti P, Ascher P, Neyton J (1997) High-affinity zinc inhibition of NMDA NR1-NR2A receptors. *J Neurosci* 17:5711-5725.
- Parganlija D, Klinkenberg M, Dominguez-Bautista J, Hetzel M, Gispert S, Chimi MA, Droese S, Mai S, Brandt U, Auburger G, Jendrach M (2014) Loss of PINK1 impairs stress-induced autophagy and cell survival. *PLoS One* 9:e95288.
- Park JY, Lansbury PT, Jr. (2003) Beta-synuclein inhibits formation of alpha-synuclein protofibrils: a possible therapeutic strategy against Parkinson's disease. *Biochemistry* 42:3696-3700.
- Pasanen P, Myllykangas L, Siitonen M, Raunio A, Kaakkola S, Lyytinen J, Tienari PJ, Poyhonen M, Paetau A (2014) A novel alpha-synuclein mutation A53E associated with atypical multiple system atrophy and Parkinson's disease-type pathology. *Neurobiol Aging* 35:2180 e2181-2185.
- Paul ML, Currie RW, Robertson HA (1995) Priming of a D1 dopamine receptor behavioural response is dissociated from striatal immediate-early gene activity. *Neuroscience* 66:347-359.
- Paul ML, Graybiel AM, David JC, Robertson HA (1992) D1-like and D2-like dopamine receptors synergistically activate rotation and c-fos expression in the dopamine-depleted striatum in a rat model of Parkinson's disease. *J Neurosci* 12:3729-3742.
- Pavon N, Martin AB, Mendialdua A, Moratalla R (2006) ERK phosphorylation and FosB expression are associated with L-DOPA-induced dyskinesia in hemiparkinsonian mice. *Biol Psychiatry* 59:64-74.
- Payton JE, Perrin RJ, Woods WS, George JM (2004) Structural determinants of PLD2 inhibition by alpha-synuclein. *J Mol Biol* 337:1001-1009.

- Periquet M, Latouche M, Lohmann E, Rawal N, De Michele G, Ricard S, Teive H, Fraix V, Vidailhet M, Nicholl D, Barone P, Wood NW, Raskin S, Deleuze JF, Agid Y, Durr A, Brice A (2003) Parkin mutations are frequent in patients with isolated early-onset parkinsonism. *Brain* 126:1271-1278.
- Perry E, Walker M, Grace J, Perry R (1999) Acetylcholine in mind: a neurotransmitter correlate of consciousness? *Trends Neurosci* 22:273-280.
- Petit A, Kawarai T, Paitel E, Sanjo N, Maj M, Scheid M, Chen F, Gu Y, Hasegawa H, Salehi-Rad S, Wang L, Rogaeva E, Fraser P, Robinson B, St George-Hyslop P, Tandon A (2005) Wild-type PINK1 prevents basal and induced neuronal apoptosis, a protective effect abrogated by Parkinson disease-related mutations. *J Biol Chem* 280:34025-34032.
- Petralia RS, Wang YX, Hua F, Yi Z, Zhou A, Ge L, Stephenson FA, Wenthold RJ (2010) Organization of NMDA receptors at extrasynaptic locations. *Neuroscience* 167:68-87.
- Picconi B, Centonze D, Hakansson K, Bernardi G, Greengard P, Fisone G, Cenci MA, Calabresi P (2003) Loss of bidirectional striatal synaptic plasticity in L-DOPA-induced dyskinesia. *Nat Neurosci* 6:501-506.
- Picconi B, Gardoni F, Centonze D, Mauceri D, Cenci MA, Bernardi G, Calabresi P, Di Luca M (2004) Abnormal Ca²⁺-calmodulin-dependent protein kinase II function mediates synaptic and motor deficits in experimental parkinsonism. *J Neurosci* 24:5283-5291.
- Pickel VM, Chan J, Sesack SR (1992) Cellular basis for interactions between catecholaminergic afferents and neurons containing Leu-enkephalin-like immunoreactivity in rat caudate-putamen nuclei. *J Neurosci Res* 31:212-230.
- Pinna A, Bonaventura J, Farre D, Sanchez M, Simola N, Mallol J, Lluís C, Costa G, Baqi Y, Muller CE, Cortes A, McCormick P, Canela EI, Martínez-Pinilla E, Lanciego JL, Casado V, Armentero MT, Franco R (2014) L-DOPA disrupts adenosine A_{2A}-cannabinoid CB₁-dopamine D₂ receptor heteromer cross-talk in the striatum of hemiparkinsonian rats: biochemical and behavioral studies. *Exp Neurol* 253:180-191.
- Pisani A, Bonsi P, Catania MV, Giuffrida R, Morari M, Marti M, Centonze D, Bernardi G, Kingston AE, Calabresi P (2002) Metabotropic glutamate 2 receptors modulate synaptic inputs and calcium signals in striatal cholinergic interneurons. *J Neurosci* 22:6176-6185.
- Platt NJ, Gispert S, Auburger G, Cragg SJ (2012) Striatal dopamine transmission is subtly modified in human A53Talpha-synuclein overexpressing mice. *PLoS One* 7:e36397.
- Pollanen MS, Dickson DW, Bergeron C (1993) Pathology and biology of the Lewy body. *J Neuropathol Exp Neurol* 52:183-191.
- Polymeropoulos MH, Higgins JJ, Golbe LI, Johnson WG, Ide SE, Di Iorio G, Sanges G, Stenroos ES, Pho LT, Schaffer AA, Lazzarini AM, Nussbaum RL, Duvoisin RC (1996) Mapping of a gene for Parkinson's disease to chromosome 4q21-q23. *Science* 274:1197-1199.
- Polymeropoulos MH, Lavedan C, Leroy E, Ide SE, Dehejia A, Dutra A, Pike B, Root H, Rubenstein J, Boyer R, Stenroos ES, Chandrasekharappa S, Athanassiadou A, Papapetropoulos T, Johnson WG, Lazzarini AM, Duvoisin RC, Di Iorio G, Golbe LI, Nussbaum RL (1997) Mutation in the alpha-synuclein gene identified in families with Parkinson's disease. *Science* 276:2045-2047.
- Priestley T, Loughton P, Myers J, Le Bourdelles B, Kerby J, Whiting PJ (1995) Pharmacological properties of recombinant human N-methyl-D-aspartate receptors comprising NR1a/NR2A and NR1a/NR2B subunit assemblies expressed in permanently transfected mouse fibroblast cells. *Mol Pharmacol* 48:841-848.
- Proukakis C, Dudzik CG, Brier T, MacKay DS, Cooper JM, Millhauser GL, Houlden H, Schapira AH (2013) A novel alpha-synuclein missense mutation in Parkinson disease. *Neurology* 80:1062-1064.
- Putney JW, Jr., Bird GS (1993) The inositol phosphate-calcium signaling system in nonexcitable cells. *Endocr Rev* 14:610-631.

- Ramón y Cajal S (1893) Neue Darstellung vom histologischen Bau des Zentralnervensystems. Arch Anat Entwick 319-428.
- Richfield EK, Thiruchelvam MJ, Cory-Slechta DA, Wuertzer C, Gainetdinov RR, Caron MG, Di Monte DA, Federoff HJ (2002) Behavioral and neurochemical effects of wild-type and mutated human alpha-synuclein in transgenic mice. Exp Neurol 175:35-48.
- Rochet JC, Conway KA, Lansbury PT, Jr. (2000) Inhibition of fibrillization and accumulation of prefibrillar oligomers in mixtures of human and mouse alpha-synuclein. Biochemistry 39:10619-10626.
- Ronesi JA, Huber KM (2008) Homer interactions are necessary for metabotropic glutamate receptor-induced long-term depression and translational activation. J Neurosci 28:543-547.
- Rusakov DA, Kullmann DM (1998) Extrasynaptic glutamate diffusion in the hippocampus: ultrastructural constraints, uptake, and receptor activation. J Neurosci 18:3158-3170.
- Sachs C, Jonsson G (1975) Mechanisms of action of 6-hydroxydopamine. Biochem Pharmacol 24:1-8.
- Sakamoto K, Karelina K, Obrietan K (2011) CREB: a multifaceted regulator of neuronal plasticity and protection. J Neurochem 116:1-9.
- Sala C, Futai K, Yamamoto K, Worley PF, Hayashi Y, Sheng M (2003) Inhibition of dendritic spine morphogenesis and synaptic transmission by activity-inducible protein Homer1a. J Neurosci 23:6327-6337.
- Sanguedo FV, Dias FR, Bloise E, Cespedes IC, Giral-di-Guimaraes A, Samuels RI, Carey RJ, Carrera MP (2014) Increase in medial frontal cortex ERK activation following the induction of apomorphine sensitization. Pharmacol Biochem Behav 118:60-68.
- Santini E, Alcacer C, Cacciatore S, Heiman M, Herve D, Greengard P, Girault JA, Valjent E, Fisone G (2009) L-DOPA activates ERK signaling and phosphorylates histone H3 in the striatonigral medium spiny neurons of hemiparkinsonian mice. J Neurochem 108:621-633.
- Santini E, Valjent E, Usiello A, Carta M, Borgkvist A, Girault JA, Herve D, Greengard P, Fisone G (2007) Critical involvement of cAMP/DARPP-32 and extracellular signal-regulated protein kinase signaling in L-DOPA-induced dyskinesia. J Neurosci 27:6995-7005.
- Saper CB, Sorrentino DM, German DC, de Lacalle S (1991) Medullary catecholaminergic neurons in the normal human brain and in Parkinson's disease. Ann Neurol 29:577-584.
- Sato H, Arawaka S, Hara S, Fukushima S, Koga K, Koyama S, Kato T (2011) Authentically phosphorylated alpha-synuclein at Ser129 accelerates neurodegeneration in a rat model of familial Parkinson's disease. J Neurosci 31:16884-16894.
- Sato M, Suzuki K, Nakanishi S (2001) NMDA receptor stimulation and brain-derived neurotrophic factor upregulate homer 1a mRNA via the mitogen-activated protein kinase cascade in cultured cerebellar granule cells. J Neurosci 21:3797-3805.
- Scatton B, Javoy-Agid F, Rouquier L, Dubois B, Agid Y (1983) Reduction of cortical dopamine, noradrenaline, serotonin and their metabolites in Parkinson's disease. Brain Res 275:321-328.
- Schapira AH, Bezard E, Brotchie J, Calon F, Collingridge GL, Fergert B, Hengerer B, Hirsch E, Jenner P, Le Novere N, Obeso JA, Schwarzschild MA, Spampinato U, Davidai G (2006) Novel pharmacological targets for the treatment of Parkinson's disease. Nat Rev Drug Discov 5:845-854.
- Schapira AH, Olanow CW, Greenamyre JT, Bezard E (2014) Slowing of neurodegeneration in Parkinson's disease and Huntington's disease: future therapeutic perspectives. Lancet 384:545-555.
- Schneggenburger R (1996) Simultaneous measurement of Ca²⁺ influx and reversal potentials in recombinant N-methyl-D-aspartate receptor channels. Biophys J 70:2165-2174.

- Schnell E, Sizemore M, Karimzadegan S, Chen L, Bredt DS, Nicoll RA (2002) Direct interactions between PSD-95 and stargazin control synaptic AMPA receptor number. *Proc Natl Acad Sci U S A* 99:13902-13907.
- Schuster S, Nadjar A, Guo JT, Li Q, Ittrich C, Hengerer B, Bezard E (2008) The 3-hydroxy-3-methylglutaryl-CoA reductase inhibitor lovastatin reduces severity of L-DOPA-induced abnormal involuntary movements in experimental Parkinson's disease. *J Neurosci* 28:4311-4316.
- Schwab RS, Amador LV, Lettvin JY (1951) Apomorphine in Parkinson's disease. *Trans Am Neurol Assoc* 56:251-253.
- Scott D, Roy S (2012) alpha-Synuclein inhibits intersynaptic vesicle mobility and maintains recycling-pool homeostasis. *J Neurosci* 32:10129-10135.
- Scott DA, Tabarean I, Tang Y, Cartier A, Masliah E, Roy S (2010) A pathologic cascade leading to synaptic dysfunction in alpha-synuclein-induced neurodegeneration. *J Neurosci* 30:8083-8095.
- Sedelis M, Hofele K, Auburger GW, Morgan S, Huston JP, Schwarting RK (2000) MPTP susceptibility in the mouse: behavioral, neurochemical, and histological analysis of gender and strain differences. *Behav Genet* 30:171-182.
- Seidel K, Schols L, Nuber S, Petrasch-Parwez E, Gierga K, Wszolek Z, Dickson D, Gai WP, Bornemann A, Riess O, Rami A, Den Dunnen WF, Deller T, Rub U, Kruger R (2010) First appraisal of brain pathology owing to A30P mutant alpha-synuclein. *Ann Neurol* 67:684-689.
- Selkoe D, Dettmer U, Luth E, Kim N, Newman A, Bartels T (2014) Defining the native state of alpha-synuclein. *Neurodegener Dis* 13:114-117.
- Sgambato-Faure V, Buggia V, Gilbert F, Levesque D, Benabid AL, Berger F (2005) Coordinated and spatial upregulation of arc in striatonigral neurons correlates with L-dopa-induced behavioral sensitization in dyskinetic rats. *J Neuropathol Exp Neurol* 64:936-947.
- Sherman MY, Goldberg AL (2001) Cellular defenses against unfolded proteins: a cell biologist thinks about neurodegenerative diseases. *Neuron* 29:15-32.
- Shi G, Lee JR, Grimes DA, Racacho L, Ye D, Yang H, Ross OA, Farrer M, McQuibban GA, Bulman DE (2011) Functional alteration of PARL contributes to mitochondrial dysregulation in Parkinson's disease. *Hum Mol Genet* 20:1966-1974.
- Shibasaki Y, Baillie DA, St Clair D, Brookes AJ (1995) High-resolution mapping of SNCA encoding alpha-synuclein, the non-A beta component of Alzheimer's disease amyloid precursor, to human chromosome 4q21.3-->q22 by fluorescence in situ hybridization. *Cytogenet Cell Genet* 71:54-55.
- Shiraishi-Yamaguchi Y, Furuichi T (2007) The Homer family proteins. *Genome Biol* 8:206.
- Singleton AB, Farrer M, Johnson J, Singleton A, Hague S, Kachergus J, Hulihan M, Peuralinna T, Dutra A, Nussbaum R, Lincoln S, Crawley A, Hanson M, Maraganore D, Adler C, Cookson MR, Muentner M, Baptista M, Miller D, Blancato J, Hardy J, Gwinn-Hardy K (2003) alpha-Synuclein locus triplication causes Parkinson's disease. *Science* 302:841.
- Snyder H, Mensah K, Hsu C, Hashimoto M, Surgucheva IG, Festoff B, Surguchov A, Masliah E, Matouschek A, Wolozin B (2005) beta-Synuclein reduces proteasomal inhibition by alpha-synuclein but not gamma-synuclein. *J Biol Chem* 280:7562-7569.
- Sohal RS (2002) Oxidative stress hypothesis of aging. *Free Radic Biol Med* 33:573-574.
- Soloaga A, Thomson S, Wiggin GR, Rampersaud N, Dyson MH, Hazzalin CA, Mahadevan LC, Arthur JS (2003) MSK2 and MSK1 mediate the mitogen- and stress-induced phosphorylation of histone H3 and HMG-14. *EMBO J* 22:2788-2797.
- Sopher BL, Koszdin KL, McClain ME, Myrick SB, Martinez RA, Smith AC, La Spada AR (2001) Genomic organization, chromosome location, and expression analysis of mouse beta-

- synuclein, a candidate for involvement in neurodegeneration. *Cytogenet Cell Genet* 93:117-123.
- Spillantini MG, Divane A, Goedert M (1995) Assignment of human alpha-synuclein (SNCA) and beta-synuclein (SNCB) genes to chromosomes 4q21 and 5q35. *Genomics* 27:379-381.
- Spillantini MG, Schmidt ML, Lee VM, Trojanowski JQ, Jakes R, Goedert M (1997) Alpha-synuclein in Lewy bodies. *Nature* 388:839-840.
- St-Hilaire M, Bourhis E, Levesque D, Rouillard C (2006) Impaired behavioural and molecular adaptations to dopamine denervation and repeated L-DOPA treatment in Nur77-knockout mice. *Eur J Neurosci* 24:795-805.
- St-Hilaire M, Landry E, Levesque D, Rouillard C (2003) Denervation and repeated L-DOPA induce a coordinate expression of the transcription factor NGFI-B in striatal projection pathways in hemi-parkinsonian rats. *Neurobiol Dis* 14:98-109.
- Stephens B, Mueller AJ, Shering AF, Hood SH, Taggart P, Arbuthnott GW, Bell JE, Kilford L, Kingsbury AE, Daniel SE, Ingham CA (2005) Evidence of a breakdown of corticostriatal connections in Parkinson's disease. *Neuroscience* 132:741-754.
- Steward O, Wallace CS, Lyford GL, Worley PF (1998) Synaptic activation causes the mRNA for the IEG Arc to localize selectively near activated postsynaptic sites on dendrites. *Neuron* 21:741-751.
- Steward O, Worley P (2002) Local synthesis of proteins at synaptic sites on dendrites: role in synaptic plasticity and memory consolidation? *Neurobiol Learn Mem* 78:508-527.
- Steward O, Worley PF (2001) Selective targeting of newly synthesized Arc mRNA to active synapses requires NMDA receptor activation. *Neuron* 30:227-240.
- Subramaniam M, Althof D, Gispert S, Schwenk J, Auburger G, Kulik A, Fakler B, Roeper J (2014) Mutant alpha-synuclein enhances firing frequencies in dopamine substantia nigra neurons by oxidative impairment of A-type potassium channels. *J Neurosci* 34:13586-13599.
- Sun H, Charles CH, Lau LF, Tonks NK (1993) MKP-1 (3CH134), an immediate early gene product, is a dual specificity phosphatase that dephosphorylates MAP kinase in vivo. *Cell* 75:487-493.
- Sung KW, Choi S, Lovinger DM (2001) Activation of group I mGluRs is necessary for induction of long-term depression at striatal synapses. *J Neurophysiol* 86:2405-2412.
- Sung YH, Eliezer D (2007) Residual structure, backbone dynamics, and interactions within the synuclein family. *J Mol Biol* 372:689-707.
- Surguchov A (2013) Synucleins: are they two-edged swords? *J Neurosci Res* 91:161-166.
- Surmeier DJ, Graves SM, Shen W (2014) Dopaminergic modulation of striatal networks in health and Parkinson's disease. *Curr Opin Neurobiol* 29C:109-117.
- Swanson GT, Kamboj SK, Cull-Candy SG (1997) Single-channel properties of recombinant AMPA receptors depend on RNA editing, splice variation, and subunit composition. *J Neurosci* 17:58-69.
- Tallaksen-Greene SJ, Kaatz KW, Romano C, Albin RL (1998) Localization of mGluR1a-like immunoreactivity and mGluR5-like immunoreactivity in identified populations of striatal neurons. *Brain Res* 780:210-217.
- Tanaka A, Cleland MM, Xu S, Narendra DP, Suen DF, Karbowski M, Youle RJ (2010) Proteasome and p97 mediate mitophagy and degradation of mitofusins induced by Parkin. *J Cell Biol* 191:1367-1380.
- Tanaka H, Kannari K, Maeda T, Tomiyama M, Suda T, Matsunaga M (1999) Role of serotonergic neurons in L-DOPA-derived extracellular dopamine in the striatum of 6-OHDA-lesioned rats. *Neuroreport* 10:631-634.
- Tang K, Low MJ, Grandy DK, Lovinger DM (2001) Dopamine-dependent synaptic plasticity in striatum during in vivo development. *Proc Natl Acad Sci U S A* 98:1255-1260.
- Tanner CM, Goldman SM (1996) Epidemiology of Parkinson's disease. *Neurol Clin* 14:317-335.

- Tanzi G (1893) I fatti e le indizioni nell'odierna isologie del sistema nervoso. *Riv Sper Freniatr* 19:419-472.
- Tappe A, Kuner R (2006) Regulation of motor performance and striatal function by synaptic scaffolding proteins of the Homer1 family. *Proc Natl Acad Sci U S A* 103:774-779.
- Taschenberger G, Garrido M, Tereshchenko Y, Bahr M, Zweckstetter M, Kugler S (2012) Aggregation of alphaSynuclein promotes progressive in vivo neurotoxicity in adult rat dopaminergic neurons. *Acta neuropathologica* 123:671-683.
- Terry RD (2000) Do neuronal inclusions kill the cell? *J Neural Transm Suppl* 59:91-93.
- Testa CM, Friberg IK, Weiss SW, Standaert DG (1998) Immunohistochemical localization of metabotropic glutamate receptors mGluR1a and mGluR2/3 in the rat basal ganglia. *J Comp Neurol* 390:5-19.
- Testa CM, Standaert DG, Landwehrmeyer GB, Penney JB, Jr., Young AB (1995) Differential expression of mGluR5 metabotropic glutamate receptor mRNA by rat striatal neurons. *J Comp Neurol* 354:241-252.
- Testa CM, Standaert DG, Young AB, Penney JB, Jr. (1994) Metabotropic glutamate receptor mRNA expression in the basal ganglia of the rat. *J Neurosci* 14:3005-3018.
- Thomas B, Beal MF (2007) Parkinson's disease. *Hum Mol Genet* 16 Spec No. 2:R183-194.
- Thony B, Auerbach G, Blau N (2000) Tetrahydrobiopterin biosynthesis, regeneration and functions. *Biochem J* 347 Pt 1:1-16.
- Tison F, Dartigues JF, Dubes L, Zuber M, Alperovitch A, Henry P (1994) Prevalence of Parkinson's disease in the elderly: a population study in Gironde, France. *Acta Neurol Scand* 90:111-115.
- Todd AM, Staveley BE (2012) Expression of Pink1 with alpha-synuclein in the dopaminergic neurons of *Drosophila* leads to increases in both lifespan and healthspan. *Genet Mol Res* 11:1497-1502.
- Tofaris GK, Garcia Reitböck P, Humby T, Lambourne SL, O'Connell M, Ghetti B, Gossage H, Emson PC, Wilkinson LS, Goedert M, Spillantini MG (2006) Pathological changes in dopaminergic nerve cells of the substantia nigra and olfactory bulb in mice transgenic for truncated human alpha-synuclein(1-120): implications for Lewy body disorders. *J Neurosci* 26:3942-3950.
- Touchman JW, Dehejia A, Chiba-Falek O, Cabin DE, Schwartz JR, Orrison BM, Polymeropoulos MH, Nussbaum RL (2001) Human and mouse alpha-synuclein genes: comparative genomic sequence analysis and identification of a novel gene regulatory element. *Genome Res* 11:78-86.
- Tovar KR, Westbrook GL (1999) The incorporation of NMDA receptors with a distinct subunit composition at nascent hippocampal synapses in vitro. *J Neurosci* 19:4180-4188.
- Tozzi A, Costa C, Siliquini S, Tantucci M, Picconi B, Kurz A, Gispert S, Auburger G, Calabresi P (2012) Mechanisms underlying altered striatal synaptic plasticity in old A53T-alpha synuclein overexpressing mice. *Neurobiol Aging* 33:1792-1799.
- Traynelis SF, Burgess MF, Zheng F, Lyuboslavsky P, Powers JL (1998) Control of voltage-independent zinc inhibition of NMDA receptors by the NR1 subunit. *J Neurosci* 18:6163-6175.
- Traynelis SF, Hartley M, Heinemann SF (1995) Control of proton sensitivity of the NMDA receptor by RNA splicing and polyamines. *Science* 268:873-876.
- Traynelis SF, Wollmuth LP, McBain CJ, Menniti FS, Vance KM, Ogden KK, Hansen KB, Yuan H, Myers SJ, Dingledine R (2010) Glutamate receptor ion channels: structure, regulation, and function. *Pharmacol Rev* 62:405-496.
- Tsigelny IF, Bar-On P, Sharikov Y, Crews L, Hashimoto M, Miller MA, Keller SH, Platoshyn O, Yuan JX, Masliah E (2007) Dynamics of alpha-synuclein aggregation and inhibition of pore-like oligomer development by beta-synuclein. *Febs J* 274:1862-1877.

- Tu JC, Xiao B, Yuan JP, Lanahan AA, Leoffert K, Li M, Linden DJ, Worley PF (1998) Homer binds a novel proline-rich motif and links group 1 metabotropic glutamate receptors with IP3 receptors. *Neuron* 21:717-726.
- Turski L, Bressler K, Rettig KJ, Loschmann PA, Wachtel H (1991) Protection of substantia nigra from MPP+ neurotoxicity by N-methyl-D-aspartate antagonists. *Nature* 349:414-418.
- Tymianski M, Charlton MP, Carlen PL, Tator CH (1993) Source specificity of early calcium neurotoxicity in cultured embryonic spinal neurons. *J Neurosci* 13:2085-2104.
- Ueda K, Fukushima H, Masliah E, Xia Y, Iwai A, Yoshimoto M, Otero DA, Kondo J, Ihara Y, Saitoh T (1993) Molecular cloning of cDNA encoding an unrecognized component of amyloid in Alzheimer disease. *Proc Natl Acad Sci U S A* 90:11282-11286.
- Ulusoy A, Sahin G, Kirik D (2010) Presynaptic dopaminergic compartment determines the susceptibility to L-DOPA-induced dyskinesia in rats. *Proc Natl Acad Sci U S A* 107:13159-13164.
- Ungerstedt U (1971) Postsynaptic supersensitivity after 6-hydroxy-dopamine induced degeneration of the nigro-striatal dopamine system. *Acta Physiol Scand Suppl* 367:69-93.
- Uversky VN, Li J, Souillac P, Millett IS, Doniach S, Jakes R, Goedert M, Fink AL (2002) Biophysical properties of the synucleins and their propensities to fibrillate: inhibition of alpha-synuclein assembly by beta- and gamma-synucleins. *J Biol Chem* 277:11970-11978.
- Vadlamudi RK, Joung I, Strominger JL, Shin J (1996) p62, a phosphotyrosine-independent ligand of the SH2 domain of p56lck, belongs to a new class of ubiquitin-binding proteins. *J Biol Chem* 271:20235-20237.
- Valente EM, Abou-Sleiman PM, Caputo V, Muqit MM, Harvey K, Gispert S, Ali Z, Del Turco D, Bentivoglio AR, Healy DG, Albanese A, Nussbaum R, Gonzalez-Maldonado R, Deller T, Salvi S, Cortelli P, Gilks WP, Latchman DS, Harvey RJ, Dallapiccola B, Auburger G, Wood NW (2004) Hereditary early-onset Parkinson's disease caused by mutations in PINK1. *Science* 304:1158-1160.
- Valente EM, Bentivoglio AR, Dixon PH, Ferraris A, Ialongo T, Frontali M, Albanese A, Wood NW (2001) Localization of a novel locus for autosomal recessive early-onset parkinsonism, PARK6, on human chromosome 1p35-p36. *Am J Hum Genet* 68:895-900.
- Valente EM, Brancati F, Ferraris A, Graham EA, Davis MB, Breteler MM, Gasser T, Bonifati V, Bentivoglio AR, De Michele G, Durr A, Cortelli P, Wassilowsky D, Harhangi BS, Rawal N, Caputo V, Filla A, Meco G, Oostra BA, Brice A, Albanese A, Dallapiccola B, Wood NW (2002) PARK6-linked parkinsonism occurs in several European families. *Ann Neurol* 51:14-18.
- Vargas DL, Nascimbene C, Krishnan C, Zimmerman AW, Pardo CA (2005) Neuroglial activation and neuroinflammation in the brain of patients with autism. *Ann Neurol* 57:67-81.
- Varkey J, Mizuno N, Hegde BG, Cheng N, Steven AC, Langen R (2013) alpha-Synuclein oligomers with broken helical conformation form lipoprotein nanoparticles. *J Biol Chem* 288:17620-17630.
- Varney MA, Jachec C, Deal C, Hess SD, Daggett LP, Skvoretz R, Urcan M, Morrison JH, Moran T, Johnson EC, Velicelebi G (1996) Stable expression and characterization of recombinant human heteromeric N-methyl-D-aspartate receptor subtypes NMDAR1A/2A and NMDAR1A/2B in mammalian cells. *J Pharmacol Exp Ther* 279:367-378.
- Veyrac A, Besnard A, Caboche J, Davis S, Laroche S (2014) The transcription factor Zif268/Egr1, brain plasticity, and memory. *Prog Mol Biol Transl Sci* 122:89-129.
- Vicini S, Wang JF, Li JH, Zhu WJ, Wang YH, Luo JH, Wolfe BB, Grayson DR (1998) Functional and pharmacological differences between recombinant N-methyl-D-aspartate receptors. *J Neurophysiol* 79:555-566.

- Vingerhoets FJ, Snow BJ, Tetrad JW, Langston JW, Schulzer M, Calne DB (1994) Positron emission tomographic evidence for progression of human MPTP-induced dopaminergic lesions. *Ann Neurol* 36:765-770.
- Visanji NP (2014) Novel transgenic technology reveals several molecular adaptations and potential therapeutic targets in the direct pathway in levodopa-induced dyskinesia. *Mov Disord* 29:721.
- Vives-Bauza C, Przedborski S (2011) Mitophagy: the latest problem for Parkinson's disease. *Trends Mol Med* 17:158-165.
- Vives-Bauza C, Zhou C, Huang Y, Cui M, de Vries RL, Kim J, May J, Tocilescu MA, Liu W, Ko HS, Magrane J, Moore DJ, Dawson VL, Grailhe R, Dawson TM, Li C, Tieu K, Przedborski S (2010) PINK1-dependent recruitment of Parkin to mitochondria in mitophagy. *Proc Natl Acad Sci U S A* 107:378-383.
- Wade LA, Katzman R (1975) Synthetic amino acids and the nature of L-DOPA transport at the blood-brain barrier. *J Neurochem* 25:837-842.
- Wakabayashi K, Hayashi S, Ishikawa A, Hayashi T, Okuizumi K, Tanaka H, Tsuji S, Takahashi H (1998) Autosomal dominant diffuse Lewy body disease. *Acta Neuropathol* 96:207-210.
- Wakabayashi K, Tanji K, Mori F, Takahashi H (2007) The Lewy body in Parkinson's disease: molecules implicated in the formation and degradation of alpha-synuclein aggregates. *Neuropathology* 27:494-506.
- Wang S, Haynes C, Barany F, Ott J (2009) Genome-wide autozygosity mapping in human populations. *Genet Epidemiol* 33:172-180.
- Watson N, Linder ME, Druey KM, Kehrl JH, Blumer KJ (1996) RGS family members: GTPase-activating proteins for heterotrimeric G-protein alpha-subunits. *Nature* 383:172-175.
- Weihmuller FB, Ulas J, Nguyen L, Cotman CW, Marshall JF (1992) Elevated NMDA receptors in parkinsonian striatum. *Neuroreport* 3:977-980.
- Weinreb PH, Zhen W, Poon AW, Conway KA, Lansbury PT, Jr. (1996) NACP, a protein implicated in Alzheimer's disease and learning, is natively unfolded. *Biochemistry* 35:13709-13715.
- Westin JE, Vercaemmen L, Strome EM, Konradi C, Cenci MA (2007) Spatiotemporal pattern of striatal ERK1/2 phosphorylation in a rat model of L-DOPA-induced dyskinesia and the role of dopamine D1 receptors. *Biol Psychiatry* 62:800-810.
- Whitworth AJ, Lee JR, Ho VM, Flick R, Chowdhury R, McQuibban GA (2008) Rhomboid-7 and HtrA2/Omi act in a common pathway with the Parkinson's disease factors Pink1 and Parkin. *Dis Model Mech* 1:168-174; discussion 173.
- Whitworth AJ, Pallanck LJ (2009) The PINK1/Parkin pathway: a mitochondrial quality control system? *J Bioenerg Biomembr* 41:499-503.
- Williams GT, Lau LF (1993) Activation of the inducible orphan receptor gene nur77 by serum growth factors: dissociation of immediate-early and delayed-early responses. *Mol Cell Biol* 13:6124-6136.
- Williams K (1996) Separating dual effects of zinc at recombinant N-methyl-D-aspartate receptors. *Neurosci Lett* 215:9-12.
- Winkler C, Kirik D, Bjorklund A, Cenci MA (2002) L-DOPA-induced dyskinesia in the intrastriatal 6-hydroxydopamine model of parkinson's disease: relation to motor and cellular parameters of nigrostriatal function. *Neurobiol Dis* 10:165-186.
- Wolf HK, Buslei R, Schmidt-Kastner R, Schmidt-Kastner PK, Pietsch T, Wiestler OD, Blumcke I (1996) NeuN: a useful neuronal marker for diagnostic histopathology. *J Histochem Cytochem* 44:1167-1171.
- Wood-Kaczmar A, Gandhi S, Yao Z, Abramov AY, Miljan EA, Keen G, Stanyer L, Hargreaves I, Klupsch K, Deas E, Downward J, Mansfield L, Jat P, Taylor J, Heales S, Duchon MR, Latchman D, Tabrizi SJ, Wood NW (2008) PINK1 is necessary for long term survival and mitochondrial function in human dopaminergic neurons. *PLoS One* 3:e2455.

- Worley PF, Christy BA, Nakabeppu Y, Bhat RV, Cole AJ, Baraban JM (1991) Constitutive expression of zif268 in neocortex is regulated by synaptic activity. *Proc Natl Acad Sci U S A* 88:5106-5110.
- Wu JJ, Zhang L, Bennett AM (2005) The noncatalytic amino terminus of mitogen-activated protein kinase phosphatase 1 directs nuclear targeting and serum response element transcriptional regulation. *Mol Cell Biol* 25:4792-4803.
- Yamada H, Kuroki T, Nakahara T, Hashimoto K, Tsutsumi T, Hirano M, Maeda H (2007) The dopamine D1 receptor agonist, but not the D2 receptor agonist, induces gene expression of Homer 1a in rat striatum and nucleus accumbens. *Brain Res* 1131:88-96.
- Yang E, Zha J, Jockel J, Boise LH, Thompson CB, Korsmeyer SJ (1995) Bad, a heterodimeric partner for Bcl-XL and Bcl-2, displaces Bax and promotes cell death. *Cell* 80:285-291.
- Yavich L, Tanila H, Vepsalainen S, Jakala P (2004) Role of alpha-synuclein in presynaptic dopamine recruitment. *J Neurosci* 24:11165-11170.
- Ying SW, Futter M, Rosenblum K, Webber MJ, Hunt SP, Bliss TV, Bramham CR (2002) Brain-derived neurotrophic factor induces long-term potentiation in intact adult hippocampus: requirement for ERK activation coupled to CREB and upregulation of Arc synthesis. *J Neurosci* 22:1532-1540.
- Youle RJ, Narendra DP (2011) Mechanisms of mitophagy. *Nat Rev Mol Cell Biol* 12:9-14.
- Young ST, Porrino LJ, Iadarola MJ (1991) Cocaine induces striatal c-fos-immunoreactive proteins via dopaminergic D1 receptors. *Proc Natl Acad Sci U S A* 88:1291-1295.
- Yutsudo N, Kamada T, Kajitani K, Nomaru H, Katogi A, Ohnishi YH, Ohnishi YN, Takase K, Sakumi K, Shigeto H, Nakabeppu Y (2013) fosB-null mice display impaired adult hippocampal neurogenesis and spontaneous epilepsy with depressive behavior. *Neuropsychopharmacology* 38:895-906.
- Zaja-Milatovic S, Milatovic D, Schantz AM, Zhang J, Montine KS, Samii A, Deutch AY, Montine TJ (2005) Dendritic degeneration in neostriatal medium spiny neurons in Parkinson disease. *Neurology* 64:545-547.
- Zarranz JJ, Alegre J, Gomez-Esteban JC, Lezcano E, Ros R, Ampuero I, Vidal L, Hoenicka J, Rodriguez O, Atares B, Llorens V, Gomez Tortosa E, del Ser T, Munoz DG, de Yebenes JG (2004) The new mutation, E46K, of alpha-synuclein causes Parkinson and Lewy body dementia. *Ann Neurol* 55:164-173.
- Zhao JP, Constantine-Paton M (2007) NR2A^{-/-} mice lack long-term potentiation but retain NMDA receptor and L-type Ca²⁺ channel-dependent long-term depression in the juvenile superior colliculus. *J Neurosci* 27:13649-13654.
- Zhou C, Huang Y, Shao Y, May J, Prou D, Perier C, Dauer W, Schon EA, Przedborski S (2008) The kinase domain of mitochondrial PINK1 faces the cytoplasm. *Proc Natl Acad Sci U S A* 105:12022-12027.

9. ABBREVIATIONS

6-OHDA	6-hydroxydopamine
AADC	L-aromatic amino-acid decarboxylase
AD	Alzheimer's disease
AIMs	Abnormal involuntary movements
AMPA	α -amino-3-hydroxy-5-methyl-4-isoazolpropionacid
Arc	Activity regulated cytoskeletal-associated protein
ATP	Adenosine triphosphate
Bad	BCL2-associated agonist of cell death
BH4	Tetrahydrobiopterin
BSA	Bovine serum albumine
cAMP	Cyclic adenosine monophosphate
cDNA	Cyclic deoxyribonucleic acid
cFos	FBJ osteosarcoma oncogene
cGMP	Cyclic guanosine monophosphate
CM	Centromedian nucleus of the thalamus
D1 receptor	Dopamine receptor 1
D2 receptor	Dopamine receptor 2
DA	Dopamine
DNA	Desoxyribonucleic acid
Dusp	Dual specific phosphatase
Egr1	Early growth response 1
Egr2	Early growth response 2
ERK1/2	Extracellular signal-regulated kinases 1 and 2
Fos B	FBJ murine osteosarcoma viral oncogene homolog
Foxo3	Forkhead box O3
GIGYF2	GRB10-interacting GYF protein 2
GP	Entopeduncular nucleus
Gpe	Globus pallidus external
Gpi	Globus pallidus internal
Gria1	Glutamate receptor, ionotropic, AMPA1 (alpha 1)
Gria2	Glutamate receptor, iono-tropic, AMPA2 (alpha 2)
Gria3	Glutamate receptor, iono-tropic, AMPA3 (alpha 3)
Gria4	Glutamate receptor, iono-tropic, AMPA4 (alpha 4)
Grin1	Glutamate receptor, iono-tropic, NMDA1 (zeta 1)
Grin2a	Glutamate receptor, ionotropic, NMDA2A (epsilon 1)
Grin2b	Glutamate receptor, ionotropic, NMDA2B (epsilon 2)
Grin2c	Glutamate receptor, ionotropic, NMDA2C (epsilon 3)
Grin2d	Glutamate receptor, ionotropic, NMDA2D (epsilon 4)
Grin3a	Glutamate receptor ionotropic, NMDA3A
Grin3b	Glutamate receptor, ionotropic, NMDA3B
Grm1	Glutamate receptor, metabotropic 1
Grm2	Glutamate receptor, metabotropic 2

Grm3	Glutamate receptor, metabotropic 3
Grm4	Glutamate receptor, metabotropic 4
Grm5	Glutamate receptor, metabotropic 5
Grm6	Glutamate receptor, metabotropic 6
Grm7	Glutamate receptor, metabotropic 7
Grm8	Glutamate receptor, metabotropic 8
Homer1	Homer homolog 1 (Drosophila)
HPLC	High-performance liquid chromatography
IEG	Immediate early gene
IHC	Immunohistochemistry
IP3R (SCA15)	Inositol 1,4,5-trisphosphate receptor 1
JunB	Jun B proto-oncogene
L-DOPA	Levodopa
LID	Levodopa induced dyskinesia
LRRK2	Leucin-rich repeat kinase 2
LTD	Long-term depression
LTP	Long-term potentiation
MPP	Mitochondrial precursor protease
MSN	Medium spiny neuron
MTS	Mitochondrial target sequence
NAC	Non-amyloid- β component of AD amyloid plaques
NMDA	N-methyl-D-aspartate
NOR1 (Nr4A3)	Nuclear receptor subfamily 4, group A, member 3
Nur77 (Nr4A1)	Nuclear receptor subfamily 4, group A, member 1
Nurr1 (Nr4A2)	Nuclear receptor subfamily 4, group A, member 2
p62/SqSTM1	Sequestosome1
PBS	Phosphate buffered saline
Pcbd1	Pterin 4 alpha carbinolamine dehydratase/dimerization cofactor of hepatocyte nuclear factor
PCR	Polymerase chain reaction
PD	Parkinson's disease
PARL	Presenilin-associated rhomboid-like protein
PFA	Paraformaldehyde
PINK1	PTEN-induced kinase 1
PPN	Pedunculooptine nucleus
PrP	Prion protein promoter
Psd95 (Dlg4)	Discs, large homolog 4 (Drosophila)
qPCR	Quantitative Real-Time PCR
REM	Rapid eye movement
RGS2	Regulator of G-protein signaling 2
RNA	Ribonucleic acid
RT	Room temperature
SIM	Stereotypic involuntary movements
SNARE	Soluble N-ethylmaleimidensitive fusion factor attachment protein receptor
SNc	Substantia nigra pars compacta

SNCA	Alpha-synuclein
SNCB	Beta-synuclein
SNCG	Gamma-synuclein
SNr	Substantia nigra reticulata
STN	Subthalamic nucleus
Tac1	Tachykinin 1
Tbp	TATA box binding protein
TBS	Tris buffered saline
TH	Tyrosine hydroxylase
TM	Transmembrane region
UHCL1	ubiquitin COOH-terminal hydrolase 1
UPS	ubiquitin-proteasome system
VA	Ventral anterior nucleus of the thalamus
VL	Ventrolateral nucleus of the thalamus
VTA	Ventral tegmental area
WT	Wild-type

10. LIST OF TABLES AND FIGURES

10.1 List of Tables

Tab. 1 Overview of PD-related loci, referred to as PARK. Adapted from (Klein and Westenberger, 2012).	12
Tab. 2 Overview of results obtained in glutamate receptor subunit analysis of the striatum and midbrain of 6-month-old PrPmtA, A53T-SNCA + <i>Pink1KO</i> and <i>Pink1KO</i> mice using qPCR.	68
Tab. 3 Overview of results obtained in the analysis of the scaffolding proteins <i>Homer1</i> and <i>Psd95</i> in the striatum and midbrain of 6-month-old PrPmtA, A53T-SNCA + <i>Pink1KO</i> and <i>Pink1KO</i> mice using qPCR.	75
Tab. 4 Overview of results obtained in the analysis of immediate early genes and transcription factors in the striatum and midbrain of 6-month-old PrPmtA, A53T-SNCA + <i>Pink1KO</i> and <i>Pink1KO</i> mice using qPCR.	78
Tab. 5 Overview of results obtained in the pre- and postsynaptic analysis of additional candidate genes in 6-month-old PrPmtA, A53T-SNCA + <i>Pink1KO</i> and <i>Pink1KO</i> mice using qPCR.	84
Tab. 6 Overview of pre- and postsynaptic results obtained in the glutamate receptor subunit analysis of 3-month-old PrPmtA mice using qPCR.	88

10.2 List of Figures

Fig. 1 Illustration of the cardinal motor symptoms in Parkinson's disease.	2
Fig. 2 Anatomical structure of the basal ganglia circuitry adapted from Galvan and Wichmann, 2008.	4
Fig. 3 Illustration of the direct and indirect pathway in physiological conditions (a) and in Parkinson's disease (b).	5
Fig. 4 Illustration of Braak's staging system adapted from (Doty, 2012).	8
Fig. 5 Different maturation stages of substantia nigra Lewy bodies visualized by alpha-synuclein immunoreactivity.	9
Fig. 6 Illustration of the SNCA gene as well as the protein structure, adapted from (Corti et al., 2011).	14
Fig. 7 Illustration of the presynaptic function of SNCA in neurotransmission.	16
Fig. 8 Illustration of <i>PINK1</i> on transcript level and presentation of the functional protein domains.	19
Fig. 9 The PINK1/Parkin mitochondria quality control pathway.	20
Fig. 10 Overview of available drugs for PD motor and non-motor symptoms as well as exciting new drugs that are in development.	23
Fig. 11 Illustration of striatal LTP and LTD induction.	25
Fig. 12 Simplified cartoon of signaling pathways involved in synaptic plasticity.	27
Fig. 13 Experimental Design.	54
Fig. 14 Scheme of Western Blot organization.	59
Fig. 15 Striatal glutamate receptor subunit analysis in PrPmtA mice.	69
Fig. 16 Midbrain glutamate receptor analysis in PrPmtA mice.	70
Fig. 17 Striatal glutamate receptor analysis in A53T-SNCA + <i>Pink1</i> KO mice.	71
Fig. 18 Midbrain glutamate receptor analysis in A53T-SNCA + <i>Pink1</i> KO mice.	72
Fig. 19 Striatal glutamate receptor analysis in <i>Pink1</i> KO mice.	73
Fig. 20 Midbrain glutamate receptor analysis in <i>Pink1</i> KO mice.	74
Fig. 21 Striatal scaffolding protein analysis in PrPmtA mice.	75
Fig. 22 Striatal and midbrain analysis of scaffolding proteins in A53T-SNCA + <i>Pink1</i> KO mice.	76
Fig. 23 Striatal analysis of scaffolding proteins in <i>Pink1</i> KO mice.	77
Fig. 24 Striatal analysis of immediate early genes and transcription factors in PrPmtA mice.	79
Fig. 25 Midbrain analysis of immediate early genes and transcription factors in PrPmtA mice.	79

Fig. 26 Striatal analysis of immediate early genes and transcription factors in A53T-SNCA + <i>Pink1</i> KO mice.	80
Fig. 27 Midbrain analysis of immediate early genes and transcription factors in A53T-SNCA + <i>Pink1</i> KO mice.	81
Fig. 28 Striatal analysis of immediate early genes and transcription factors in <i>Pink1</i> KO mice.	82
Fig. 29 Midbrain analysis of immediate early genes and transcription factors in <i>Pink1</i> KO mice.	82
Fig. 30 Striatal analysis of additional candidates in PrPmtA mice.	85
Fig. 31 Midbrain analysis of additional candidates in PrPmtA mice.	86
Fig. 32 Striatal and midbrain analysis of additional candidates in A53T-SNCA + <i>Pink1</i> KO mice.	86
Fig. 33 Striatal analysis of the earliest effects in PrPmtA mice.	89
Fig. 34 Striatal analysis of the earliest effects in PrPmtA mice.	90
Fig. 35 Representative pictures of PrPmtA and WT mice after treatment with 5 mg/kg apomorphine.	92
Fig. 36 Quantitative analysis of stereotypic behavior within 100 min sessions following apomorphine treatment.	93
Fig. 37 Bright-field immunohistochemistry pictures of 18-month-old female PrPmtA and wild-type mice.	95
Fig. 38 Analysis of tyrosine hydroxylase optical density in the striatum and substantia nigra of 18-month-old female PrPmtA compared to wild-type mice.	96
Fig. 39 Apomorphine dependent phosphorylation of ERK1/2 30 min after treatment.	97
Fig. 40 Genotype dependent differences in apomorphine induced ERK1/2 phosphorylation 30 min after treatment.	98
Fig. 41 Apomorphine dependent phosphorylation of ERK1/2 100 min after treatment.	99
Fig. 42 Genotype dependent differences in apomorphine induced ERK1/2 phosphorylation 100 min after treatment.	99
Fig. 43 Representative bright-field microscopy pictures of phospho-histone H3 immunohistochemistry in the striatum of female 18-month-old PrPmtA and WT mice after vehicle or apomorphine treatment.	101
Fig. 44 Quantitative densitometric analysis of phospho-Histone H3 in striatal sections of 18-month-old female PrPmtA and wild-type mice after apomorphine treatment.	102
Fig. 45 Statistical analysis of qPCR data from striatum of wild-type and PrPmtA mice, 30 min after vehicle or apomorphine treatment.	104

Fig. 46 Statistical analysis of qPCR data from striatum of wild-type and PrPmtA mice 100 min after vehicle or apomorphine treatment.	105
Fig. 47 Statistical analysis of qPCR data from striatum of wild-type and PrPmtA mice 100 min after vehicle or apomorphine treatment.	106
Fig. 48 Statistical analysis of qPCR data from midbrain of wild-type and PrPmtA mice 100 min after vehicle or apomorphine treatment.	107
Fig. 49 Quantitative immunoblots and bar graphs of DUSP6.	109
Fig. 50 Representative pictures of hind limb paralysis in A53T-SNCA + <i>Pink1</i> KO mice.	110
Fig. 51 Bright-field microscopy pictures from immunohistochemistry in spinal cord of WT, <i>Pink1</i> KO, PrPmtA and double-mutant mice aged until 15-17 months.	112
Fig. 52 Representative bright-field microscopy picture of pSer129-SNCA immunoreactivity in midbrain of a paralyzed A53T-SNCA + <i>Pink1</i> KO double-mutant mouse.	113
Fig. 53 Bright-field microscopy pictures from immunohistochemistry in midbrain of WT, <i>Pink1</i> KO, PrPmtA and double-mutant mice.	115
Fig. 54 Representative bright-field microscopy pictures of pSer129-SNCA immunoreactivity in the thoracic and cervical spinal cord (A), the motor cortex (B) and the striatum of paralyzed double-mutant mice.	116
Fig. 55 Representative pictures showing double-immunofluorescence histology in paralyzed A53T-SNCA + <i>Pink1</i> KO mice.	117
Fig. 56 Representative pictures showing double-immunofluorescence histology in paralyzed A53T-SNCA + <i>Pink1</i> KO mice.	119
Fig. 57 Simplified cartoon of the main results obtained in project II. Highlighted are genotype dependent results obtained after apomorphine treatment. Abbreviations: DA: dopamine; Glut: glutamate MSN: medium spiny neuron; SNc: substantia nigra pars compacta	144

11. WRITTEN DECLARATION

ERKLÄRUNG

Ich erkläre hiermit, dass ich mich bisher keiner Doktorprüfung unterzogen habe.

Frankfurt am Main, den 11. 03. 2015
(Nadine Brehm)

Eidesstattliche Versicherung

Ich erkläre hiermit an Eides Statt, dass ich die vorgelegte Dissertation über

“The effects of alpha-synuclein gain-of-function on synaptic plasticity”

selbständig angefertigt und mich anderer Hilfsmittel als der in ihr angegebenen nicht bedient habe, insbesondere, dass alle Entlehnungen aus anderen Schriften mit Angabe der betreffenden Schrift gekennzeichnet sind.

Ich versichere, nicht die Hilfe einer kommerziellen Promotionsvermittlung in Anspruch genommen zu haben

Frankfurt am Main, den 11. 03. 2015
(Nadine Brehm)

